Studies of the Wnt/β-catenin signalling pathway in Chronic Myeloid Leukaemia.

Thesis submitted in accordance with the requirements of the University of Liverpool for the degree of Doctor in Philosophy by Rachael Fowler

August 2014

Table of Contents.

Thesis Declaration

The work presented in this thesis is my own work except for the following;

- GSK3β splice variant analysis by Dr L Wang.

- Optimisation of FTY720 and okadaic acid concentration and PP2A pathway antibodies by Dr Lucas.

- Part of the chronic phase data for PP2A, SET, CIP2A and c-Myc obtained from Dr C Lucas.

- High and low CIP2A protein level data provided by Dr Lucas.

- CIP2A siRNA methodology by Dr Lucas.

All of which has been produced in accordance with the University of Liverpool guidelines.

Acknowledgements

This thesis is dedicated to my Grandma, the late Louisa Ellen Williams. Without her love, support and encouragement growing up I would never have achieved so much. My inspiration to go into cancer research came through her own battle with this disease; to become part of the fight against cancer and to try to ensure that in the future others will not have to endure what she had to.

In order to undertake this study I was in receipt of funding provided by the Carol Shepherd Studentship. I wish to express my gratitude and thanks to the Trustees of this endowment for supporting me in Carol's name over the last three years of lab work. Thank you to Professor Clark, Dr Harris, and Dr Lucas for the opportunity to do this PhD. Additionally, I would like to thank both Bob and Joe for their help over the last 18 months in completing the PhD. Also to Lakis for his help and support as a mentor in the last few years.

Next, I would like to thank my parents, June and David, for being able to rely on their continued love and support especially through the PhD. Also thanks to Peter and Andrew for their brotherly encouragement. To Pete and Amanda (and Bear!) for putting me up for a month while I was writing up, and to Andrew and Chelsea for supporting me while you were home and providing a light at the end of the tunnel.

Liz, Athina, and Andrea, I don't think I would have made it through the last four years without having you all with me. Liz, I am so glad I had you to share the PhD experience

with; we got each other through it! From the much needed Costa breaks on hard days, to office chats – both scientific and non-scientific, and fighting laptop bags when things got that little bit too much! All three of you have been an amazing support – thank you! Also thank you to Liz and the rest of the McDonald clan for becoming my extended Liverpool family in the last three years of being up north!

To everyone else in the Haematology department (in particular Ali, Alix and Gemma) who helped me through the three years of lab work, I am really grateful for all the scientific and personal support you have given me. The tea breaks, and of course K-club, definitely made life in labs much more enjoyable! Thanks as well to John and Elinor for your western blotting wisdom! Also to everyone else in Liverpool who played a part in making the PhD experience more manageable; especially Holly and the rest of the girls, including Agnès, Áine, Ali, Alix, Fiazia, and Harriet, the nights out and after work pub trips all helped!

My thanks also goes to Kelly, I don't know what I would have done without our weekly Skype dates! Thank you for all the listening and advice you have given, especially during my PhD. Thanks also to Faye and Nicole who, alongside Kelly, have encouraged me, helped motivate me, and kept me focused on what is important. For that I cannot thank you all enough. Finally, thank you to Vanessa, Grant and everyone else at home that has supported me through the last four years. Special thanks to those who spent their evenings with me so I didn't go stir crazy at home!

Massive thanks to you all.

Abstract

The Wnt/β-catenin signalling pathway is involved in regulating cellular transcription of numerous target genes in chronic myeloid leukaemia (CML). A previous report using granulocyte-macrophage progenitors (GMPs) showed that elevated levels of unphosphorylated (active) β-catenin, alongside mis-splicing of glycogen synthase kinase 3β (GSK3β), correlated with disease progression. It was of interest to determine if using the more readily available peripheral blood mononuclear cells (MNCs) also showed any correlation with patient outcome when β-catenin and GSK3β were measured in this source material. Further investigation in these cells addressed GSK3β activity regulation, possible regulation of c-Myc degradation by GSK3β, and investigation of Wnt transcription factors in CML.

Results indicated that levels of β-catenin (and its phosphorylated variants) could not be used to distinguish patient treatment outcomes using CML MNCs. However the levels of BCR-ABL1 induced β-catenin-Tyr654 phosphorylation showed a significant decrease in patients in blast crisis compared to chronic phase (P=0.012), as did the levels of GSK3β – which demonstrated significantly decreased activity in blast crisis patients via a significant increase in Ser9 phosphorylation and a significant decrease in Tyr216 phosphorylation in blast crisis compared to chronic phase (P=0.026 and <0.001 respectively).

This decrease in GSK3β activity was not reflected by changes in the levels of β-catenin and, as such, this led to the question of whether alternative mechanisms were influencing regulation of GSK3β activity other than Wnt/β-catenin signalling. Results showed that protein phosphatase 2A (PP2A) was regulating the inhibition of GSK3β in CML. This is a dual mechanism with GSK3β also affecting PP2A inhibition.

GSK3β is known to have numerous substrates, which include c-Myc. Due to the role of c-Myc as an oncogene in CML and the role of GSK3β in c-Myc degradation, it was of interest to determine if the changes in GSK3β activity were reflected in the degradation of c-Myc. Results showed that neither GSK3β nor PP2A (also involved in the mechanism) were the rate limiting components of c-Myc degradation.

Analysis of the Wnt signalling pathway revealed up regulation of *WNT1, WNT8A, WNT9A* and *FZD7* mRNAs in chronic phase MNCs (P=0.011, 0.045, 0.037 and 0.037 respectively) - which was inconsistent with β-catenin findings. These unexpected results can be explained by internal regulation of the pathway by the negative regulator *NKD1*, which is also significantly higher in samples from chronic phase patients (P=0.013).

Finally, investigation into Wnt transcription factors showed that factors *TCF1, TCF4* and *LEF1* mRNA levels were significantly higher in blast crisis samples compared to chronic phase (P=0.001, 0.016, and 0.003 respectively). This suggests a possible mechanism for Wnt-independent activation of these transcription factors in the blast crisis phase of the disease.

In conclusion, it was determined that β-catenin levels cannot be used to either; distinguish between patient response cohorts, or be a factor of disease progression in CML MNCs. The activity of GSK3β is significantly down-regulated in blast crisis. PP2A is involved in this regulation. However when investigating c-Myc degradation, neither GSK3β nor PP2A act as the regulating factors in CML. There may be an internal regulation of the pathway by which *NKD1* prevents an upregulation of pathway activity via *WNT1, WNT8A, WNT9A* and *FZD7* reaching β-catenin (*CTNNB1*). Finally, the transcription factors mRNA expression is significantly upregulated in blast crisis, but they could be acting independently of the Wnt pathway.

Presentations

I presented this work at an invited oral presentation at the European School of

Haematology meeting on Chronic Myeloid Leukaemia in Estoril, Portugal in September

2013.

Abbreviations

6-FAM – 6-carboxyfluorescein

ABL1 - Abelson murine leukemia viral oncogene homolog 1

Allo-SCT – Allogeneic stem cell transplant

Akt –Protein kinase B

AML – Acute myeloid leukaemia

APC – Adenomatous polyposis coli

APS - Ammonium persulphate

ATF2 - Activating transcription factor 2

ATF7 - Activating transcription factor 7

ATP – Adenosine triphosphate

β-ARR1 - Beta-arrestin 1

BC – Blast crisis

BCL-2 – B-cell lymphoma 2

BCR - Breakpoint cluster region

BELA - Bosutinib efficacy and safety in chronic myeloid leukemia

BSA - Bovine serum albumin

CBP – CREB binding protein

CBY - Chibby

CCyR – Complete cytogenetic response

CER – Cerberus

CHR – Complete haematological response

CIP2A – Cancerous inhibitor of PP2A

CK1 – Casein Kinase 1

CN-AML – Cytogenetically normal acute myeloid leukaemia

CNL – Chronic neutrophilic leukaemia

CML – Chronic myeloid leukaemia

CP – Chronic phase

CREB - Cyclic adenosine monophosphate (cAMP)-response element-binding protein

Ct – Cycle threshold

DAS – Dasatinib

DASISION - Dasatinib versus imatinib study in treatment naive CML patients

ddH_2O – Double distilled water

DKK - Dickkopf

dNTP – Deoxyribonucleotide triphosphate

DMSO -Dimethyl sulphoxide

DPR – Dapper

DSH – Dishevelled

DSSB - Double strength SDS buffer

DTT - DL-Dithiothreitol

EDTA – Ethylenediaminetetraacetic acid

ENESTnd - Evaluating nilotinib efficacy and safety in clinical trials newly diagnosed patients

 ELN – European LeukemiaNet

ER - Endoplasmic reticulum

ERK – Extracellular signal regulated kinase

FACS – Fluorescence activated cell sorting

FCS - Foetal calf serum

FISH - Fluorescence in situ hybridisation

FZD – Frizzled

GAPDH – Glyceraldehyde 3-phosphate dehydrogenase

GBP – Glycogen synthase kinase binding protein

GDP – Guanosine diphosphate

GFP - Green fluorescent protein

GMP - Granulocyte-macrophage progenitors

GSK3β – Glycogen synthase kinase 3β

GTP – Guanosine triphosphate

HCl – Hydrochloric acid

HDAC - Histone deacetylase

hOCT1 - Human organic cation transporter 1

HRP – Horseradish peroxidase

HSC - Haematopoietic stem cells

HSPG – Heparan sulphate proteoglycan

HU – Hydroxyurea

ICAT - Inhibitor of β-catenin and TCF

IFNα - Interferon-α

IgG$_1$ – Immunoglobulin G subclass 1

IgG – Immunoglobulin G

ILK - Integrin-linked kinase

IM – Imatinib

IRIS - International randomised study of interferon-alpha plus cytarabine versus ST1571

JAK2 – Janus kinase 2

JNK – c-Jun N-terminal kinase

LEF - Lymphoid enhancer factor

LGS - Legless

LRP-5/6 - Low-density lipoprotein receptor-related proteins 5/6

LSC – Leukaemic stem cells

MAPK – Mitogen activated protein kinases

M-bcr - Major breakpoint cluster region

m-bcr - Minor breakpoint cluster region

MCL-1 - Induced myeloid leukaemia cell differentiation protein

MEK - Mitogen-activated protein kinase kinase

MGB – Minor groove binder

MNC - Mononuclear cells

MMR – Major molecular response

MTT - MTT 3-(4,5-dimethylthiazol-2-yl)-2,5-diphenyltetrazolium bromide

MW – Molecular weight

NaCl – Sodium chloride

NIL – Nilotinib

NLK - NEMO like kinase

NLS - Nuclear localisation signal

NP40 - Nonyl phenoxypolyethoxylethanol

p300 - E1A binding protein p300

p90Rsk – p90 ribosomal s6 kinase

PAOD - Peripheral artery occlusion disease

PBS - Phosphate buffered saline

PCR – Polymerase chain reaction

PDGF - Platelet-derived growth factor

Ph+ - Philadelphia positive

Ph- - Philadelphia negative

Ph^1 – Philadelphia Chromosome

PI - Propidium iodide

PI3K - Phosphatidylinositide 3-kinase

PKA - Protein kinase A

PP2A – Protein phosphatase 2A

PVDF - Polyvinylidene difluoride

PYGO - Pygopus

Pyk-2 – Protein tyrosine kinase 2

RAS – Rat sarcoma

RIPA – Radioimmunoprecipitation assay buffer

RLT – Red cell lysis buffer

RPMI 1640 - Roswell Park Memorial Institute 1640

RT-qPCR – Real time quantitative polymerase chain reaction

SDS – Sodium dodecyl sulphate

Ser - Serine

SET – I2PP2A

sFRPs - secreted Frizzled related proteins

SOST - Sclerostin

SRC – Sarcoma

SH1 – SRC homology domain 1

Stat5 - Signal transducer and activator of transcription 5

SWI/SNF - Switch/Sucrose non-fermentable

TBE - Tris/Borate/EDTA

TBS-T – Tris-buffered saline and tween 20

TCF - T-cell factor

TEMED – Tetramethylethylenediamine

Thr - Threonine

TKIs – Tyrosine kinase inhibitors

Tyr - Tyrosine

WIF - Wnt inhibitory protein

WHO – World Health Organisation

Wnt – Canonical Wnt signalling pathway

Chapter 1 - General Introduction

1.1 The history of CML

The first recognition of a disease entity consistent with what we now call 'Chronic Myeloid Leukaemia (CML)' took place in 1845 by John Hughes Bennett (Edinburgh) [1]. This was accompanied by a similar description five weeks later by Rudolf Virchow (Berlin), whereby both observed an enlargement of the spleen, liver and lymph nodes, along with a 'pus-like' substance in the veins [2, 3]. Both independently devised the phrases 'leucocythaemia' (Bennett) and 'Weisses Blut' (Virchow), which translate to 'white cell blood' and 'white blood' respectively [1, 3, 4]. Previous to Bennett's findings his colleague David Craigie (Glasgow) had two patients (in 1841, and 1844) whose symptoms were fever, splenomegaly and leukocytosis, which when Bennett performed an autopsy on the latter patient enabled him to submit his findings to the Edinburgh Medical and Surgical Journal.

In 1852 Bennett published a major review, which reported 37 cases [5]. Virchow also reported, in 1847, accounts of nine cases where an association was noted between the appearance of the blood and the occurrence of an abnormally enlarged spleen. He also observed that granular blood cells with irregular or divided nuclei were linked with splenomegaly [2, 6]. This was an astonishing feat when considering the limited resources available to him, in terms of both the efficiency of the microscopes of the day, and the lack of developed staining techniques.

In 1856, Virchow described the pathophysiology of the disease by noting the characteristics of leukaemia included elevated levels of 'colourless' cells alongside a decrease in red cells and alterations in the liver and spleen. Additionally he made the influential suggestion that there are two forms of chronic leukaemia; splenic and lymphatic [2]. Bennett and Virchow disagreed on the cause of death of the patients; Bennett concluded an infection was the cause, whereas Virchow believed it was a neoplastic disorder. The nomenclature of the disease was debated for many years [4].

In 1872, Ernst Neumann discovered the next important characteristic of CML; that it originates in the bone marrow. He identified that there was an additional form of leukaemia which he referred to as a 'myelogenous' leukaemia [4, 7]. Following this in 1878, Neumann additionally recognised that the anaemia which was observed in patients was due to disturbance in the marrow which he previously linked with leukaemia. This was acknowledged by Gowers in 1879 [2].

In 1879 Paul Ehrlich established methods for staining blood cells, making it easier to distinguish between the different forms of leukaemia [8]. This led to the observation that Virchow's 'splenic leukaemia' and Neumann's 'myelogenous leukaemia' were in fact observations of the same type, with both consisting of granular cells. This led to the 'splenic' nomenclature being dropped and the acknowledgement of two forms of chronic leukaemia; myelogenous and lymphatic [2].

1.1.1 Discovery of the Philadelphia Chromosome

A critical leap in the understanding of CML took place in Philadelphia in 1960. Nowell and Hungerford examined the blood of seven CML patients and identified a minute chromosome in the cells. Their findings were recognised worldwide, and the chromosome was entitled the 'Philadelphia chromosome' (Ph[1]) [4, 9].

In 1973, after improvements in cytogenetic techniques, Janet Rowley reported in nine CML patients that Ph[1] was part of a reciprocal translocation between chromosome 9 and chromosome 22 [10] (**Figure 1.1**). Following this, in the 1980s, it was recognised that a gene typically located on chromosome 9, known as *ABL1,* was translocated to the Ph[1] chromosome [11]. Studies were undertaken to determine the region on the *ABL1* gene at which the breakpoint was located. It was found to be in the first intron of the *ABL1* gene [12]. The breakpoint was more difficult to categorise on chromosome 22. In 1984, Groffen *et al.,* [13] discovered there were multiple breakpoints clustered into a region of 5.8-kb which they termed as the 'breakpoint cluster region (BCR)'. This region was later found to be part of a gene named accordingly as the *BCR* gene. Witte *et al.,* [14] found via the K562 cell line (the first cell line representative of myelogenous leukaemia that was derived from a 53 year old female patient in blast crisis) that the ABL1 protein was abnormally sized with increased enzymatic activity, implying that this abnormal ABL1 activity may be involved in the pathogenesis of CML. Using the idea that somehow BCR may influence the activity of ABL1, Eli Canaani [15] led a team of investigators who identified a *BCR-ABL1* fusion transcript in CML patient cells [4]. The discovery of this BCR-ABL1 fusion protein, which is formed by the coiled-coil domain located on the BCR protein fusing to the N-terminus of the ABL protein [16], was shown to generate a

constitutively active protein kinase involved in the activation of numerous signalling

pathways [17, 18], and was a crucial breakthrough in understanding the pathogenesis of

CML [2].

Figure 1.1 A diagram to show the reciprocal translocation which produces the Philadelphia Chromosome
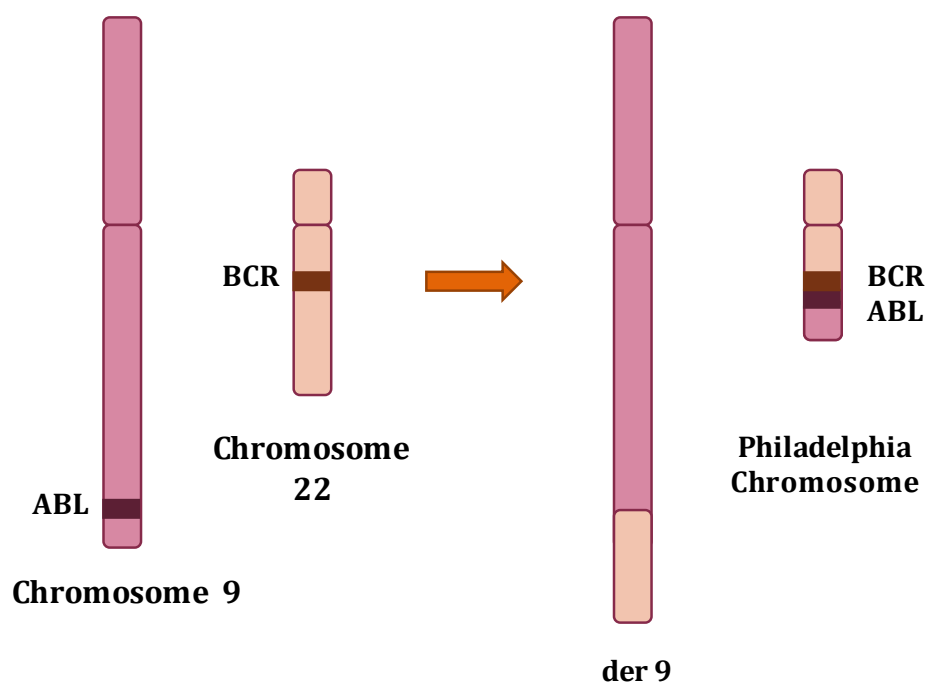
1.2 Molecular Pathogenesis

1.2.1 ABL1

ABL1 is a 145kDa modular protein with tyrosine kinase activity, which is ubiquitously expressed in the cell [19, 20]. At the N-terminus are three SRC-homology domains (SH1-SH3), which are integral to the function of the protein **(Figure 1.2)**. The tyrosine kinase function is situated in the SH1 domain. The SH2 and SH3 domains act by binding other proteins via the recognition of different sequences. The SH2 domain identifies phosphotyrosine residues, while the SH3 domain identifies proline-rich sequences [20]. Located on the last exon region of ABL1, three nuclear localisation signals (NLS) [19, 21], alongside one nuclear export signal (NES) [22] enable ABL1 to localise in both the nucleus and the cytoplasm.

Regulation of the function of ABL1 is important as without restraint multiple cellular functions are uncontrolled leading to adverse effects [19]. Abl1 null mice show elevated perinatal mortality, skeletal abnormalities and inferior immune function, signifying the importance of normal Abl1 function in the cell and in development [23]. In normal physiological conditions, a myristoyl group bound to the N-terminus of ABL1 is capable of binding several regions across the molecule, including a hydrophobic region on the SH1 domain, which leads to autoinhibition of the protein [20, 24]. This inhibition is reversed when Tyr412 is phosphorylated [19] which then allows access to the regulatory activation loop and phosphorylation of Tyr393 which was previously prevented by the conformation of the autoinhibited protein [20].

ABL1 is involved in many signalling pathways, and its subcellular localisation influences its impact on the cell. When located in the cytoplasm, it is connected to proliferation and cell survival. In contrast, ABL1 is located in the nucleus subsequent to cell cycle arrest and apoptosis via DNA damage. These functions prove that ABL1 is a fundamental protein involved in the maintenance of cell homeostasis [20].

1.2.2 BCR

The 160kDa BCR protein is ubiquitously expressed in the cell [25]and has various roles, however its true function still remains elusive. It is involved in cytoskeleton remodelling [20] via its regulatory effect on the Rho family GTPases [26]. Additionally, it may act as a tumour suppressor via its negative regulation of the RAS-ERK pathway [27], along with the Wnt/β-catenin pathway [28]. It is a multi-domain protein consisting of a coiled-coil domain on the N-terminus, allowing oligomerisation with other proteins. Adjacent to this is a serine/threonine kinase domain [20], followed by a dbl homology domain in the middle of the protein, which has homology with the guanine nucleotide dissociation-stimulating domain of the *DBL* oncogene product. Alongside the dbl homology domain is a pleckstrin homology domain. Both of these stimulate the exchange of guanidine diphosphate (GDP) on small GTPases of the Rho family [26]. Finally the C-terminus enables the GTPase activity of Rac to be switched on [20].

1.2.3 What is BCR-ABL1?

BCR-ABL1 is regarded as a crucial driving factor in the development of CML **(Section 1.1.1)** however the formation of *BCR-ABL1* is not limited to one transcript type **(Figure 1.2)**. *ABL1* has a breakpoint region mainly between exons 1a and 1b, however it can also occur downstream of exon 1a or upstream of exon 1b [17, 29]. *BCR* has three common breakpoint regions that give rise to different transcript types. The most prevalent isoform found in CML is the $p210^{BCR-ABL1}$ transcript, which has its breakpoint within a region known as the 'major breakpoint cluster region' (M-bcr) which covers the introns between exons e12-e16. Additionally in Ph+ acute lymphoblastic leukaemia and rare cases of CML, there is another region within *BCR* where a breakpoint can occur, known as the 'minor breakpoint cluster region' (m-bcr) found in the long intron between the exons e2' and e2. This produces a $p190^{BCR-ABL1}$ transcript [17, 29]. Finally the third transcript type, which is associated with chronic neutrophilic leukaemia (CNL), has a breakpoint located downstream of exon 19 (μ-bcr) which produces the $p230^{BCR-ABL1}$ transcript type [29-31].

Figure 1.2 Schematic of the most common BCR-ABL1 transcript types

[32]
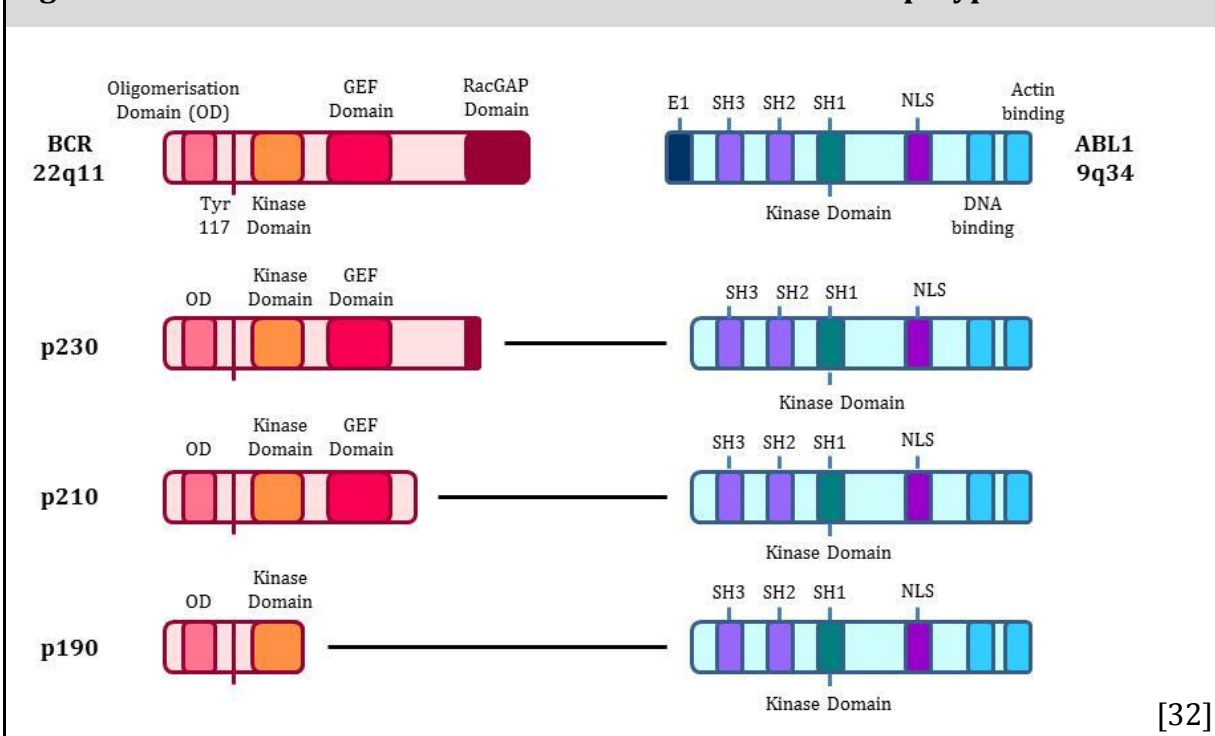
Although the *BCR-ABL1* transcript types described above are the most commonly found in CML, some patients who have the characteristics of the disease lack both the Ph[1] chromosome and the BCR-ABL1 fusion protein. These cases have been assigned as atypical CML [33], which is actually a different disease to true CML with a worse prognosis, and does not respond to tyrosine kinase inhibitors (TKIs). Additionally, 5% of true CML cases are BCR-ABL1 positive but Ph[1] negative. Expression of the p210[BCR-ABL1] transcript is found in these patients, and the disease characteristics are indistinguishable from Ph[1] positive CML. As a result these cases are currently believed to have cytogenetically invisible rearrangements of the chromosome [34].

1.3 CML in the Clinic

CML can be defined as a clonal myeloproliferative disease, affecting haematopoietic stem cells (HSCs). It is characterised by the amplification of myeloid proliferation leading to increased neutrophils and their immediate precursors in the peripheral blood, and by the increased cellularity of bone marrow resulting from expansion of the myeloid mass [35].

1.3.1 Epidemiology

The annual incidence of CML is 1.34 cases per 100,000 individuals [36], with a predominance of males over females in most series (1.69:1) [37]. The median age of disease onset is 60 years old [36]. However, the median age of patients recruited for trial studies is typically up to a decade younger [38]. The prevalence of CML in the population is currently rising due to the development of improved therapies TKIs , which are increasing survival rates [39].

1.3.2 Pathogenesis

There are limited contributing factors known to the pathogenesis of CML. Heyssel *et al.* [40] investigated the effect ionising radiation has on leukaemia development through analysing the disease prevalence in Hiroshima atomic bomb survivors. Results showed that the victims closest to the hypocentre of the explosion had massively increased incidence of leukaemia development compared to those further from the explosion site.

Those closest to the hypocentre at 0-999 meters had an annual incidence of 1,460 cases per million, while those furthest from the hypocentre at 2,000-10,000 meters had an annual incidence of 29 cases per million.

1.3.3 Diagnosis

At diagnosis, all patients should be analysed by both G-banded chromosome analysis of marrow cell metaphases to identify the presence of the Ph[1] chromosome, and qualitative polymerase chain reaction (PCR) to identify the *BCR-ABL1* transcript types. In addition, fluorescence in situ hybridisation (FISH) analysis can be undertaken in patients that are Ph[1] negative to identify variant and cryptic translocations [41]. From these tests a diagnosis can be made, and a treatment schedule put in place.

1.3.4 Clinical Features

Text book descriptions of CML often describe its course as a triphasic disease which develops through three clinical phases; chronic phase, accelerated phase, and blast crisis. However, in the era of the TKIs this may no longer be true, as few patients remain in accelerated phase for any length of time, with some bypassing it altogether. Patients who do progress can transform directly into blast crisis thus giving the appearance of a biphasic disorder of chronic phase and blast crisis. However, the vast majority of present day patients may remain in chronic phase indefinitely [42]. **Table 1.1** gives the European LeukaemiaNet (ELN) and World Health Organisation (WHO) definitions of the

clinical phases. Those patients in chronic phase do not meet any of the criteria stated for

accelerated phase and blast crisis [41].

Table 1.1 Definitions of the clinical CML phases		
CML Phase	**ELN Definition – Any of the following;**	**WHO Definition – Any of the following;**
Accelerated Phase	▪ 15-29% of blasts in the blood or bone marrow, or >30% of blasts plus promyelocytes in the blood or bone marrow with <30% blasts. ▪ ≥20% basophils in the blood. ▪ Persistent thrombocytopenia unrelated to treatment ($<100\times10^9$/L). ▪ Clonal chromosome abnormalities in Ph+ cells on treatment.	▪ 10-19% of blasts in the blood or bone marrow. ▪ ≥20% basophils in the blood. ▪ Persistent thrombocytopaenia unrelated to treatment ($<100\times10^9$/L), or thrombocytosis ($>1000\times10^9$/L) unresponsive to therapy. ▪ Increase in white blood cell count and spleen size which is unresponsive to therapy. ▪ Clonal chromosome abnormalities in Ph+ cells on treatment.
Blast Crisis	▪ ≥30% of blasts in the blood or bone marrow. ▪ Blast proliferation occurring outside the bone marrow, except for the spleen.	▪ ≥20% of blasts in the blood or bone marrow. ▪ Blast proliferation occurring outside the bone marrow. ▪ Clusters of blasts on bone marrow biopsy.

[41]

1.4 Response Definitions

1.4.1 Monitoring response to treatment

Monitoring a patient's response to treatment is important in determining subsequent treatment requirements. The hierarchy of treatment response is shown in **Table 1.2**. Complete haematological response (CHR) is the first target of treatment, while complete cytogenetic response (CCyR) reflects a deeper response. Major molecular response (MMR) indicates an even deeper response with a progression rate to blast crisis of <1% at 5 years.

Table 1.2 CML response definitions		
Response		**Definition**
Haematological	*Complete (CHR)* All of the following:	White blood cell (WBC) < 10x10^9/L <5% Basophils No myelocytes, promyelocytes, or myeloblasts within the WBCs A platelet count < 450x10^9/L A spleen that is nonpalpable
Cytogenetic	*Complete (CCyR):* *Partial:* *Minor:* *Minimal:* *None:*	No Ph+ metaphases (at least 20 examined) 1-35% Ph+ metaphases 36-65% Ph+ metaphases 66-95% Ph+ metaphases > 95% Ph+ metaphases
Molecular	*Major(MMR):* *MR^1* *MR^2* *MR^3* *MR^4* *MR$^{4.5}$* *MR^5*	Ratio of *BCR-ABL1 : ABL* of ≤0.1% Ratio of *BCR-ABL1 : ABL* of ≤10% Ratio of *BCR-ABL1 : ABL* of ≤1% As MMR Ratio of *BCR-ABL1 : ABL* of ≤0.01% or undetectable *BCR-ABL1* transcripts with >10,000 *ABL1* transcripts Ratio of *BCR-ABL1 : ABL* of ≤0.0032% or undetectable *BCR-ABL1* transcripts with >32,000 *ABL1* transcripts Ratio of *BCR-ABL1 : ABL* of ≤0.001%

[41, 43]

Note: *Complete molecular response* previously defined as undetectable *BCR-ABL1* mRNA transcripts by RT-qPCR in two consecutive blood samples of sufficient quality (sensitivity >10^4) has been replaced by *molecularly undetectable leukaemia* with specification of the number of the control gene transcript copies [41].

During treatment, real time quantitative PCR (RT-qPCR) is typically performed every three months until a MMR (assessed according to the international scale) is achieved, then subsequently every three to six months. In addition to, or instead of RT-qPCR, chromosome banding analysis of marrow cell metaphases may be carried out at three, six and twelve months until CCyR has been reached, then after every twelve months. In patients that fail treatment **(Section 1.4.2)** RT-qPCR, mutational analysis by conventional Sanger sequencing, and chromosome banding analysis of marrow cell metaphases should be performed. For those who progress into blast crisis immunophenotyping is carried out to define the blast lineage (myeloid or lymphoid). Finally, in those considered as 'warning' patients **(Section 1.4.2)** the molecular and cytogenetic tests are carried out more regularly and chromosome banding analysis of marrow cell metaphases is recommended in cases of myelodysplasia or clonal chromosome abnormalities in Ph- cells [41].

1.4.2 Treatment Response Definitions

In the 2013 update of the earlier 2006 and 2009 ELN recommendations, two categories of response to treatment are described; optimal, and failure **(Table 1.3)**. The cytogenetic and molecular criteria to meet these become more stringent with increasing time on treatment. They are dynamic, in that patients can move from one category to another. Optimal responders are patients who have the best long-term outcome as they

are achieving a response and therefore can safely remain on current treatment. Failure

patients are those whose chances of achieving a better response on current treatment

are very limited and should therefore switch therapy to reduce the risk of disease

progression and death. Finally, there is an intermediate category previously described

as 'sub-optimal' which has been re-categorised as 'warning' in the latest 2013

definitions [41]. This cohort includes patients who need to be more frequently

monitored to allow for appropriate therapy changes to reduce treatment failure [41].

Table 1.3 The requirements for patient categorisation as described by the ELN		
Treatment Response Definitions		
Optimal	*3 months*	*BCR-ABL1* ≤10% and/or Ph+ ≤35%
	6 months	*BCR-ABL1* <1% and/or Ph+ 0
	12 months	*BCR-ABL1* ≤0.1%
	>12months	*BCR-ABL1* ≤0.1%
Warning	*3 months*	*BCR-ABL1* >10% and/or Ph+ ≤36-95%
	6 months	*BCR-ABL1* 1-10% and/or Ph+ ≤1-35%
	12 months	*BCR-ABL1* >0.1-1%
	>12months	Clonal chromosome abnormalities in Ph- cells
Failure	*3 months*	No complete haematological response and/or Ph+ >95%
	6 months	*BCR-ABL1* >10% and/or Ph+ >35%
	12 months	*BCR-ABL1* >1% and/or Ph+ >0
	>12months	Loss of complete haematological response Loss of complete cytogenetic response Confirmed loss of major molecular response Mutations in the BCR-ABL1 kinase domain Clonal chromosome abnormalities in Ph+cells

[41]

Note: '*BCR-ABL1*' is shorthand for *BCR-ABL1/ABL1* ratio expressed as a percentage.

Inclusion of the warning cohort ('suboptimal' in earlier ELN definitions) of patients in

analysis within this thesis was not considered appropriate due to the group's

complexity in classification and treatment. Patients in the optimal and failure cohorts

are much better defined with treatment either being continued as it is, or switched, instead of a 'wait and see' strategy. The more precise cohort definitions also make it easier to determine which, if any, factors or biomarkers predict patient outcome. In contrast as the eventual outcome of warning patients is unknown and variable, it may be inaccurate to test them as a subset of patients, thus making it impossible to correlate levels with a treatment outcome that has not yet been achieved. It also must be taken into account that an additional reason why this cohort is complex is that there may be patient compliance issues which are hindering treatment response [44]. For these reasons warning patients will be removed from analysis in this thesis due to the difficulty in obtaining any conclusive data.

1.5 Treatment

1.5.1 Pre-Imatinib Era

The first definitive description of a treatment for CML was arsenic. Developed by Thomas Fowler in 1786, it was administered to a CML patient in 1865 by Lissauer [2]. In 1903 radiotherapy was introduced, and rapidly replaced arsenic. It proved to be extremely efficient at improving the patients' health by reducing spleen size, and decreasing the leukocyte count, leading to the concept of 'remission' being coined. However it soon became clear that CML becomes refractory to radiotherapy treatment [2].

It wasn't until after the Second World War when alkylating agents became available that treatment advances occurred. The first synthetic compounds used in the management of CML were the chemotherapeutic agents busulphan and hydroxyurea (HU) [42]. In a randomised trial, a comparison was made between the efficiency of busulphan and hydroxyurea in 441 CML patients [45]. Results from the trial showed that treatment with hydroxyurea displayed a statistically significant survival advantage (P=0.02) with the median survival for patients receiving hydroxyurea as a primary treatment being 5.6 years compared to 2.7 years with busulphan. In addition to this, hydroxyurea has fewer adverse side effects along with improved white blood cell counts after 18 and 24 months treatment (43% and 34%, vs. 11% and 16% for hydroxyurea vs. busulphan respectively) [45].

The development and introduction of interferon-α (IFNα) in the early 1980s gave CML patients a significantly increased survival advantage [46-48]. The UK Medical Research Council trial CML III reported an increase in median survival in patients treated with IFNα to 61 months compared with 41 months in patients treated with chemotherapy (busulphan or hydroxyurea) [48]. Additionally, long-term follow up (95-129 months) by the Italian cooperative study group showed 30% survival for patients treated with IFNα vs. 18% treated with conventional chemotherapy. Furthermore, the median survival for low risk patients was 104 months on IFNα vs. 64 months on chemotherapy [46]. Studies found that BCR-ABL1 is involved in regulating the sensitivity of CML cells to IFNα by inhibiting IFNα signalling and the response of the cells. This is achieved by accelerating the phosphorylation-dependent degradation of the IFNα receptor [49].

1.5.2 Stem Cell Transplant

Allogeneic stem cell transplant (allo-SCT) was the first curative treatment developed in the late 1970s [50]. Its use has diminished with the development of TKIs and fewer patients progressing to accelerated phase and blast crisis, but it is still an important treatment for patients with resistance to therapy, and for those who have previously progressed to blast crisis but have been restored to a second chronic phase [51].

Due to a majority of patients who now receive allo-SCT being patients who have previously failed treatment, it was investigated whether previous therapy influenced the patients outcome after allo-SCT. It was shown that prior treatment with imatinib

(see Section 1.5.3.1) had no effect on the success of allo-SCT, unless the patients on treatment had achieved a major cytogenetic remission, whereby these patients had significantly less hazard of mortality (p=0.03) [50].

Only a minority of patients can receive curative therapy from CML by stem cell transplantation, therefore it has been an important area within CML research to discover and develop drugs which increase patient survival [42]. As such the development of TKIs was a significant breakthrough in the treatment of CML.

1.5.3 Tyrosine Kinase Inhibitors (TKIs)

1.5.3.1 Imatinib

The discovery of the Ph[1] chromosome and the resultant BCR-ABL1 fusion protein has enabled the development of drugs which target this protein, revolutionising treatment. It is known that the BCR-ABL1 fusion protein actively increases the transformation of cells from non-leukaemic to a malignant phenotype via an increase in tyrosine kinase activity [52].

Imatinib mesylate (also known as STI571, or trade name Glivec), developed by Ciba-Geigy (now Novartis Pharmaceuticals), was the first TKI developed for the treatment of CML [53]. It functions by inhibiting the BCR-ABL fusion protein by competing for the occupation of the adenosine triphosphate (ATP) binding site of the tyrosine kinase

domain. Imatinib prevents ATP from binding, thus blocking the activation of the tyrosine kinase. This causes a reduction in the tyrosine kinase activity, consequently decreasing the clonal expansion of the leukaemic stem cells (LSCs) [53, 54] **(Figure 1.3)**.

The IRIS trial (International Randomised study of Interferon-alpha plus cytarabine versus ST1571) randomised treatment of 1106 newly diagnosed chronic phase CML patients on a 1:1 ratio. Patients either received 400mg of imatinib daily, or $5MU/m^2$ IFN-α daily continuously plus $20mg/m^2$ cytarabine daily for 10 days per month [55]. Results show that imatinib significantly improved outcome, where at 18 months 76.2% of patients treated with imatinib achieved a CCyR compared to 14.5% of patients treated with IFNα plus cytarabine [55, 56]. Also, only 3.3% of imatinib treated patients underwent disease progression to accelerated or blastic phase compared to 8.5% of patients who received IFNα plus cytarabine [55]. Imatinib consequently became universally accepted as the gold standard first line therapy for newly diagnosed chronic phase CML, and similar trials in accelerated phase and blast crisis showed advantages for imatinib treatment [55, 57].

Cellular responses to imatinib treatment in cells expressing the BCR-ABL1 protein include inhibition of proliferation, induction of apoptosis, and restriction of phosphorylation of substrates including BCR-ABL1 autophosphorylation [58].

Figure 1.3 A diagram to show the mechanism of action of imatinib on BCR-ABL1

Imatinib binds to the ATP binding site on BCR-ABL1 stabilising it in its inactive conformation. This prevents the autophosphorylation of BCR-ABL1 and subsequently phosphorylation of its substrates.
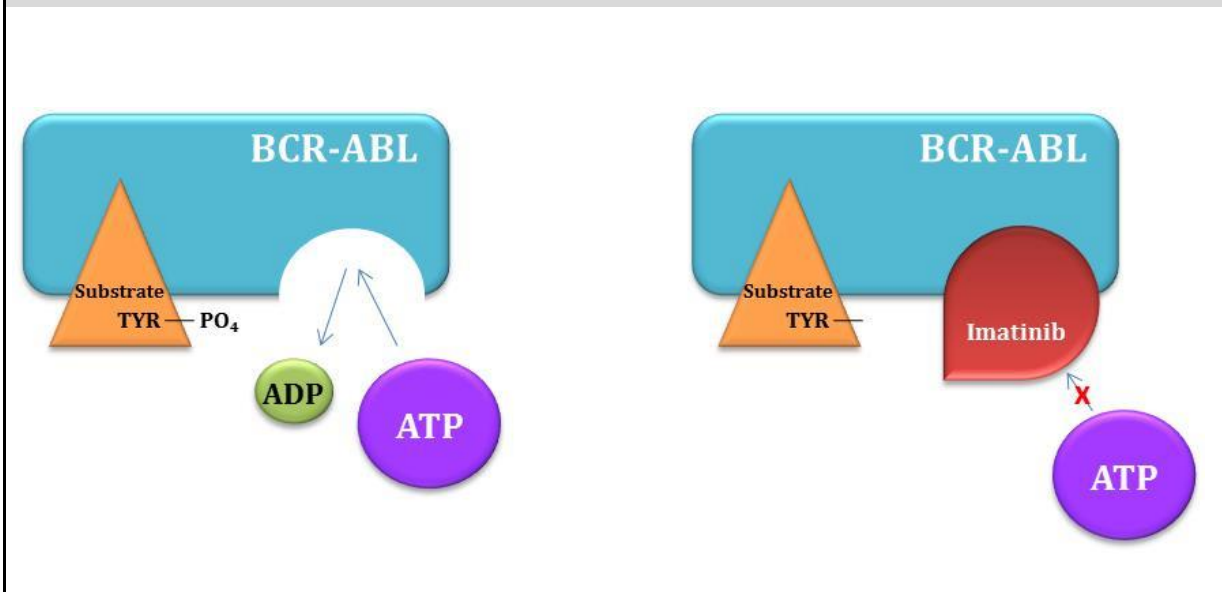
1.5.3.2 Imatinib resistance

More than one-third of patients either fail to achieve, or lose their initial response to imatinib and develop a resistance to the drug [59]. Resistance arises due to cells developing mechanisms to sustain sufficient levels of BCR-ABL1 signalling, or by cells becoming BCR-ABL1 independent. Mechanisms providing elevated levels of BCR-ABL1 include gene amplification, gene mutation and incomplete BCR-ABL1 inhibition [58]. Furthermore, there could be the development of a new genetic lesion which is independent of *BCR-ABL1*. The most prevalent mutations which confer resistance (85-90% of resistant cases) are located in the ABL1 kinase domain of the BCR-ABL1 protein, which prevents imatinib from binding and blocking the ATP binding site [53, 60]. These include the development of point mutations that arise within the kinase

domain, decreasing its sensitivity towards imatinib [61]. These change the conformation of ABL1 and impede the affinity of imatinib for the ATP binding site. Mutations can also occur in regulatory domains within the fusion protein, for example in the activation loop of the protein where a mutation stabilises the protein in its active conformation, impeding imatinib's ability to bind. Additionally, mutations can occur on contact residues preventing the formation of hydrogen bonds between imatinib and the protein, enhancing resistance [60], the P-loop which interferes with phosphate binding, and the hinge region preventing the formation of the ATP-binding cleft due to the loss of contact between the C- and N- terminal lobes of the kinase domain [61].

The first described and most well-known mutation in the BCR-ABL1 kinase domain is the T315I mutation, whereby the wild type threonine (T) amino acid is substituted by an isoleucine (I) at codon 315 on the ABL1 protein after a cytosine to thymine base pair substitution [62]. The T315 residue is located at the back of the ATP binding site, and is known as the 'gatekeeper position'. This location is the reason why this residue has a significant impact on imatinib resistance, as any changes in its properties lead to inhibition of the binding ability of imatinib and other TKIs. When the amino acid residue is a threonine, its hydroxymethylene side chain forms an essential hydrogen bond with imatinib. Conversely when a mutation occurs and the residue is subsequently changed to an isoleucine residue, the hydrogen bond with imatinib is unable to form. Furthermore, the conformation of the isoleucine residue stoichiometrically changes the ATP binding site so imatinib is no longer compatible, and hence BCR-ABL1 becomes imatinib resistant [61, 62].

In addition to resistance arising due to BCR-ABL1, the mechanism of drug uptake also has implications on resistance development. The uptake of imatinib is mediated by human organic cation transporter 1 (hOCT1) [63, 64]. Studies of hOCT1 showed that the uptake of imatinib was greater in KCL22 cells (cell line established from a 32 year old woman with Ph+ CML in blast crisis) which had high expression of hOCT1 compared to those with low expression (P=0.002). The levels of hOCT1 were also found to correlate with patient outcome, with patients who have high pre-treatment hOCT1 levels having a higher probability of achieving a CCyR (P=0.008), along with increased progression-free and overall survival rates (P=0.01 and 0.004 respectively) [64].

1.5.4 Second Generation TKIs

With the emergence of imatinib resistance, future therapies were developed to overcome the different mechanisms of resistance. These were named 'second generation' TKIs.

1.5.4.1 Nilotinib

Nilotinib (also known as AMN107, or trade name Tasigna) also developed by Novartis, acts similarly to imatinib by competitively inhibiting the ATP binding site of the tyrosine kinase domain of the BCR-ABL1 protein, stabilising it in its inactive conformation. However it is much more potent than imatinib by over 30-fold [65] due to an increased topological fit, and it has a much higher affinity for BCR-ABL1 of approximately 20 to 50 fold [66]. Furthermore, nilotinib has increased specificity with the ABL1 kinase domain

caused by a decrease in the number of hydrogen bonds between the drug and protein from six to four, limiting the contact points and restricting the proteins that nilotinib targets [67]. This increase in affinity and specificity enhances nilotinib's inhibitory action, enabling cytogenetic and molecular responses against most of the mutations which cause imatinib resistance[60]. Additionally, the uptake of nilotinib is not reliant on hOCT1 [68]. However, similarly to imatinib, the T315I mutation again confers resistance [69].

A trial was initiated to compare the efficiency of nilotinib treatment with imatinib, named the ENESTnd trial (Evaluating Nilotinib Efficacy and Safety in Clinical Trials Newly Diagnosed Patients [70]). 846 newly diagnosed chronic phase Ph+ patients were randomly allocated (1:1:1 ratio) to receive; 300mg nilotinib twice a day, 400mg nilotinib twice a day, or 400mg imatinib once a day [70]. The results from a three year follow up of the trial show nilotinib to be a significantly better treatment for CML than imatinib. It was shown that patients who received nilotinib (both 300mg and 400mg) achieved a significantly higher level of MMR (p<0.0001) than patients who received imatinib. In addition, significantly more patients who were allocated nilotinib achieved a deeper response of MR^4 and $MR^{4.5}$ (p<0.0001 for both). Alongside this, progression free survival was significantly higher in patients on 300 mg nilotinib treatment versus imatinib (p=0.0059) [71]. These findings indicate the superior efficacy of nilotinib compared to imatinib, and how nilotinib can overcome much of the resistance to imatinib (with the exception of a few mutations) suggesting nilotinib would be a good first line therapy in CML.

However, since being introduced there have been numerous reports of peripheral artery occlusion disease (PAOD) being observed in patients treated with nilotinib [72-75]. An initial study by Aichberger *et al.*, [72] found that three out of 24 CML cases treated with nilotinib developed PAOD. Furthermore, a subsequent study of 233 patients receiving nilotinib treatment showed 5% of these cases developed PAOD [73]. This discovery has resulted in the reconsideration of nilotinib when selecting therapy for the treatment of CML.

1.5.4.2 Dasatinib

Dasatinib (also known as BMS-354825, or trade name Sprycel) is another second generation TKI, developed by Bristol-Myers Squibb, which in the START-R trial (SRC/ABL tyrosine kinase inhibition activity research trial - randomised) was shown to be a more effective treatment for patients failing standard dose imatinib compared to dose escalation of imatinib [76]. Dasatinib is approximately 325-fold more potent than imatinib, and has the ability to be active against various imatinib-resistant BCR-ABL mutants. This is due to its ability to bind to BCR-ABL in both its active and inactive forms, whereas imatinib can only associate when BCR-ABL is inactive. Therefore imatinib is ineffective against BCR-ABL mutations which have destabilised its inactive form, whereas dasatinib is still effective against these changed conformations [77]. In addition, dasatinib is similar to nilotinib in that it does not rely upon hOCT1 for its uptake, making it an effective therapy for those patients with low hOCT1 levels [78]. There are however again some mutations where dasatinib is less effective, such as the missense mutation V299L and, as for the other TKIs T315I [79].

The clinical trial comparing imatinib to dasatinib was named DASISION (DASatinib versus Imatinib Study In treatment Naive CML patients) whereby 519 newly diagnosed Ph+ chronic phase CML patients were randomised treatment on a 1:1 ratio, receiving either 100mg dasatinib daily or 400mg imatinib daily [80]. Results from the trial showed that after a 24 month follow up, there was a significant increase in both CCyR (p=0.0002) and MMR (p<0.0001) in patients allocated dasatinib. The median time to achieve a MMR was 15 months on dasatinib vs. 36 months on imatinib, with 64% of patients receiving dasatinib achieving a MMR by 24 months compared to 46% of patients receiving imatinib [80]. There was also a non-significant trend to improved progression free survival with 3.5% of patients allocated dasatinib progressing to accelerated or blastic phase, compared to 5.8% of imatinib treated patients [80]. In addition to being effective in patients as a first line therapy, dasatinib is also an efficient treatment in imatinib-resistant or intolerant patients unable to achieve a MMR or CCyR. Furthermore, dasatinib was effective against accelerated or blast crisis CML patients, enabling the acquisition of a major haematological response. These responses were reached within 1-3 months and retained for a 1-5 year period [77]. These results again suggest dasatinib to be an effective therapy for the treatment of CML.

In addition to acting on BCR-ABL1, dasatinib has been shown to be an inhibitor of downstream cellular pathways involved in cell proliferation and apoptosis. These include Stat5, SRC and MAPK pathways, of which inhibition enhances dasatinib's antileukaemic properties [77].

1.5.4.3 Additional therapies

Further drug development has produced both bosutinib (another second generation TKI) and ponatinib (a third generation TKI). Bosutinib (also known as SKI-606, marketed by Pfizer with the trade name Bosulif) acts as a dual inhibitor by also inhibiting SRC more effectively than imatinib, but does not influence PDGF or c-KIT activity[81] . It has been shown to be an effective second line treatment for those patients who fail imatinib, dasatinib or nilotinib therapy; however as with the three previous TKIs it is ineffective against the T315I mutation. In patients who failed imatinib, bosutinib as a second line therapy resulted in 85% of patients achieving a CHR, 48% achieving a CCyR, and 35% achieving a MMR [82]. However in the Bosutinib Efficacy and safety in chronic myeloid LeukemiA (BELA) trial of first line bosutinib vs imatinib, results showed that CCyR response at 12 months treatment showed no significant difference between the drugs (P=0.601) [83]. The disadvantage of bosutinib therapy is the adverse side effects that accompany it. Common side effects include diarrhoea, nausea, and vomiting, with thrombocytopenia the most common grade 3/4 side effect [82, 83].

As all previous TKIs have been shown to be ineffective against the T315I mutation, ponatinib (also known as AP24534, or trade name Iclusig) was developed by ARIAD Pharmaceuticals for the treatment of patients with this previously incurable variation of the disease [84]. Results from the phase II trial showed that, in patients who were treated with ponatinib after failure on dasatinib or nilotinib, of those in chronic phase, 46% achieved a CCyR, 34% achieved a MMR, and no resistance to ponatinib occurred

via a single BCR-ABL1 mutation. Of those patients who received ponatinib in accelerated phase, 55% achieved a major haematological response and 39% achieved a major cytogenetic response. Finally, for patients in blast crisis who switched to ponatinib, 31% achieved a major haematological response, and 23% achieved a major cytogenetic response (as defined by the study) [84].

1.6 The Wnt/β-catenin Signalling Pathway

There are three pathways which are involved in intracellular signalling via the Wnt-protein ligand interactions. These are the β-catenin pathway, the planar cell polarity pathway, and the Wnt/Ca^{2+} pathway [85]. The Wnt/β-catenin signalling pathway is vital in a variety of signalling processes within embryonic development and tissue homeostasis, including; cell proliferation, cell polarity, and cell fate determination. Consequently when mutations arise within this pathway, they lead to human birth defects, cancer and other diseases as reviewed by Clevers *et al.,*[86].

1.6.1 Activation of the Wnt/β-catenin signalling pathway

1.6.1.1 Regulation of Wnt ligand binding

The regulation of Wnt signalling occurs through multiple mechanisms, summarised in **Figure 1.4**. Activation of the Wnt/β-catenin signalling pathway occurs through a family of secreted glycolipoproteins known as the WNT ligands. In humans these are made up of 19 different members [87]. Once these WNT ligands have been secreted, various binding partners control their activity. There is evidence indicating that heparan sulphate proteoglycans (HSPGs) function in stabilising and assisting the transport of WNT ligands [88]. The WNT ligands interact with two sets of co-receptors for efficient signalling: Frizzled (FZD) receptors, which are 7-transmembrane proteins that bind to WNT ligands via their cysteine-rich domains located on the N-terminus [89, 90], and low-density lipoprotein receptor-related proteins 5/6 (LRP-5/6) which are single-pass

transmembrane molecules [85, 91]. The FZD receptors are also normally associated with heterotrimeric G proteins, initiating intracellular signal transduction [89], while the importance of LRP-5/6 is emphasised by the binding of potent extracellular inhibitors WISE and Dickkopf (DKK) which inhibit Wnt/β-catenin signalling by blocking the formation of the LRP-5/6, FZD, and WNT ligand complex [88, 91].

In humans there are several *DKK* genes, of which *DKK1* is widely involved in Wnt/β-catenin signalling inhibition [92, 93]. DKK1 forms a complex with both LRP-5/6 and KREMEN and promotes LRP-5/6 internalisation, hence blocking Wnt/β-catenin signalling by making it unavailable for WNT ligand binding. KREMEN acts as a moderator of the inhibitory action of DKK as only specific KREMEN proteins enable DKK to inhibit Wnt/β-catenin signalling e.g. KREMEN2 [88, 92, 94]. The mechanism by which LRP-5/6 is internalised determines whether it is involved in normal Wnt/β-catenin signalling or whether it results in pathway inhibition by decreasing the accessibility of LRP-5/6 for WNT ligands. If internalisation of LRP-5/6 is via DKK-induced-CLATHRIN mediated internalisation, then this results in pathway inhibition. However, if internalisation is via CAVEOLIN-mediated LRP-5/6 internalisation, stimulated by WNT, then this results in normal Wnt/β-catenin signalling [95, 96]. In addition to DKK, other antagonists which act on LRP-5/6 include WISE/Sclerostin (SOST) proteins which act by preventing the interaction between LRP5/6 and WNT ligands[97, 98]. Inhibitors that bind to WNT ligands and block their interaction with the FZD receptor include Cerberus (CER) and FRZB-1 [85]. Furthermore, SHISA proteins prevent maturation of the FZD receptors and inhibit them from reaching the cell surface by confining them in the endoplasmic reticulum (ER) [99].

Wnt inhibitory factor (WIF) acts as an antagonist to the WNT ligands by directly binding to them [87]. In addition, the secreted Frizzled related proteins (sFRPs) have homology to the cysteine rich domains of the FZD family of WNT receptors [100] and consequently either compete with the FZD receptor for WNT ligand binding, or bind directly to FZD forming an inactive complex preventing binding of WNT ligands [101].

Figure 1.4 Regulation of WNT ligand binding
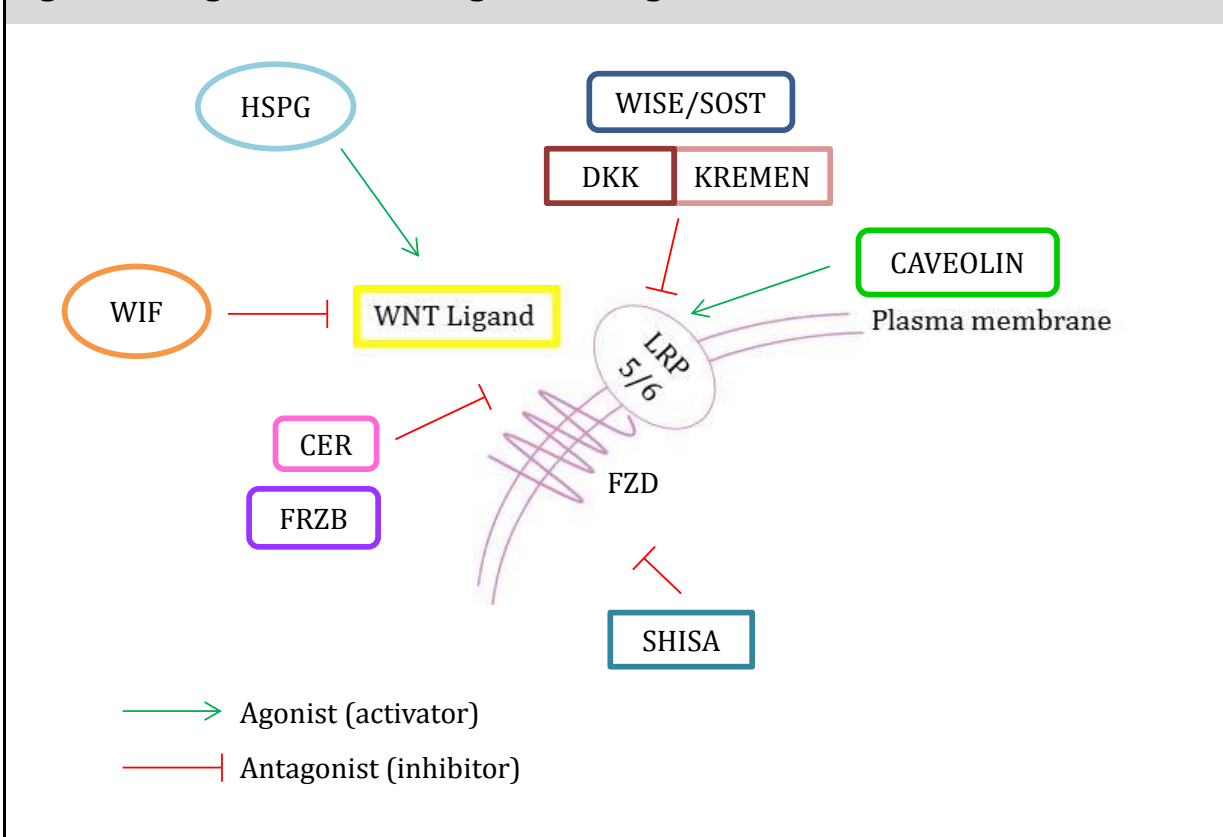
1.6.1.2 Transmission of the Wnt signal intracellularly

In the presence of WNT ligands, the receptors transduce a signal to Dishevelled (DSH) and AXIN, which consequently may interact through a sequence of amino acids known as the DIX domain [102]. DSH is phosphorylated [100], which is moderated by protein kinases including PAR1 [103], and binds to FZD intracellularly [85]. DSH functions by blocking the degradation of β-catenin via the recruitment of glycogen synthase kinase binding protein (GBP)/FRAT-1 [85]. GBP/FRAT-1 acts as the intermediate between DSH and a complex of proteins known as the 'destruction complex', enabling them to interact. The destruction complex is responsible for regulating the degradation of β-catenin through the phosphorylation status of β-catenin [104, 105]. When phosphorylated by this complex, β-catenin is degraded **(section 1.6.2)**, however inhibition of the destruction complex causes β-catenin to remain un-phosphorylated at these key sites [106] and is able to translocate to the nucleus **(section 1.6.1.3)**. FRAT-1 is reported to function by moderating the dissociation of glycogen synthase kinase 3β (GSK3β) from the degradation complex, consequently stabilising β-catenin by inhibiting the ability of GSK3β to phosphorylate β-catenin, subsequently preventing its degradation [107]. DSH can be also be regulated by FRODO to enhance Wnt/β-catenin signal transduction [108], β-arrestin 1 (β-ARR1) which binds to DSH and enhances its interaction with AXIN [109], and Dapper (DPR) which is involved in DSH degradation [110].

In addition to DSH regulating the transduction of the Wnt signal to the destruction complex to prevent phosphorylation of β-catenin, LRP-5/6 is involved in the

degradation of AXIN. The cytoplasmic tail of LRP-5/6 is known to contain a series of residues which can become phosphorylated subsequent to WNT ligand binding, which is mediated by GSK3β and casein kinase 1 (CK1) [95, 111, 112]. This phosphorylation creates a binding site for AXIN on LRP-5/6 enabling recruitment of AXIN to the plasma membrane and facilitating its degradation. This results in the disassembly of the destruction complex, rendering it incapable of marking β-catenin for degradation (see **Figure 1.5**) [111-113].

1.6.1.3 Translocation of β-catenin into the nucleus

Since β-catenin is not able to be phosphorylated by the destruction complex, it is unable to be degraded by the proteasome, and is instead stabilised in the cytoplasm. This increase in unphosphorylated β-catenin levels in the cytoplasm is the main characteristic which represents the activation of Wnt/β-catenin signalling [88]. The stabilised β-catenin is imported into the nucleus and binds to the transcription factors T-cell factor (TCF) and lymphoid enhancer factor (LEF) [114, 115]. The manner in which β-catenin is imported and retained in the nucleus involves various factors. It has been found that Wnt-induced activation of a Rac-JNK pathway by phosphorylation of β-catenin at Ser191 and Ser605 mediates the nuclear import of β-catenin [116]. AXIN and adenomatous polyposis coli (APC) have been reported to export β-catenin into the cytoplasm [117, 118], while BCL9 and the TCF factors import β-catenin into the nucleus [119]. However, there is evidence that these proteins work via retention instead of active transport [120]. More recently, Chibby (CBY) has been associated with nuclear export of β-catenin via association with protein 14-3-3, along with acting as an antagonist for TCF/LEF binding [121].

1.6.1.4 Regulation of transcriptional activation

Once in the nucleus, β-catenin can associate with the transcription factors TCF and LEF [114, 115] and activate the transcription of Wnt/β-catenin pathway target genes, which include *C-MYC* and *CYCLIN D1* (see **Figure 1.5**) [122, 123]. The interaction of β-catenin with the transcription factors TCF/LEF causes the displacement of transcriptional repressors and recruitment of additional transcriptional co-activators [95]. Co-activators include BRG-1 (also known as SMARCA4) which is involved in remodelling chromatin as part of the Switch/Sucrose non-fermentable (SWI/SNF) complex [124] and the histone acetylase CREB binding protein (CBP)/p300 which binds to the carboxy terminus of β-catenin and enhances transcriptional activation [125]. Additionally, Bc19/Legless (LGS) and Pygopus (PYGO) not only act to retain β-catenin in the nucleus, but also regulate the interaction between TCF/β-catenin complex and chromatin [119, 126-128]. Transcriptional repressors include inhibitor of β-catenin and TCF (ICAT) which acts as an antagonist of Wnt target gene transcription by inhibiting the association of β-catenin with TCF [129] and furthermore, it dissociates β-catenin, LEF and CBP/p300 complexes [130]. Without WNT ligands to activate the pathway, TCF itself can function as a repressor of transcription of Wnt target genes as it forms a complex with a molecule called GROUCHO [131]. When β-catenin is present, it is able to displace GROUCHO from TCF to activate transcription [132].

Figure 1.5 The process of β-catenin translocation to the nucleus

When WNT ligands are present they bind to the receptors Frizzled and LRP5/6 and cause the phosphorylation of the cytoplasmic tail of LRP.

This phosphorylation recruits AXIN to the membrane where it is degraded, disassembling the destruction complex.

Phosphorylation of DSH causes it to associate with FZD and recruit GBP/FRAT which prevent GSK3β from phosphorylating β-catenin.

Additionally the binding of WNT ligand causes phosphorylation of Dishevelled (DSH).

As β-catenin cannot be phosphorylated by GSK3β, this causes an increase in unphosphorylated β-catenin.

This unphosphorylated β-catenin translocates to the nucleus where it binds to TCF/LEF and transcriptional co-activators and activates transcription.

1.6.2 Inhibition of the Wnt/β-catenin signalling pathway

In the absence of WNT ligands, the destruction complex is able to target β-catenin for degradation by the proteasome. The destruction complex is made up of multiple proteins including AXIN, APC, and GSK3β [133, 134] which associate with β-catenin and regulate its phosphorylation at specific residues. Phosphorylation of β-catenin is a dual kinase mechanism which involves CK1 and GSK3β. Firstly, CK1α phosphorylates β-catenin on the N terminus at Ser45, which then facilitates the sequential phosphorylation of Thr41, Ser37 and Ser33 by GSK3β [104, 135, 136]. GSK3β is a vital component in the down regulation of β-catenin, consequently making it a potential tumour suppressor. It acts by phosphorylating multiple proteins involved in Wnt signalling [100], including AXIN [137] and APC (alongside CK1) enabling more β-catenin to associate with AXIN and APC, which in turn increases the amount of β-catenin that is phosphorylated and degraded [87, 104]. AXIN functions as a scaffold protein, and has specific binding sites for the other components of the destruction complex [138]. It is considered that AXIN acts as a limiting factor in Wnt/β-catenin signalling due to lower quantities of the molecule being present in the cells compared to the other components of the degradation complex. Increasing the concentration of AXIN in the cell reduced the half-life of β-catenin by 50%, unlike the other components of the destruction complex. This consequently means AXIN could be a key factor in regulating the stability of β-catenin in the cell [139] (See **Figure 1.6**). Phosphorylation at Ser37 and Ser33 by GSK3β enables the E3 ligase, beta-transducin repeat containing protein (β-TrCP), to recognise β-catenin as a target for ubiquitinated degradation by the proteasome [135, 140-142].

Figure 1.6 The process of β-catenin degradation

Without the presence of WNT ligands, β-catenin is able to associate with the destruction complex.

This allows phosphorylation of β-catenin on Ser45 by CK1.

Phosphorylation of β-catenin recruits the E3 ligase β-TrCP which ubiquitinates β-catenin

Phosphorylation by CK1 primes β-catenin on Ser33/37/Thr41 by GSK3β.

This ubiquitin tag targets β-catenin to the proteosome.

The proteosome acts to degrade β-catenin.
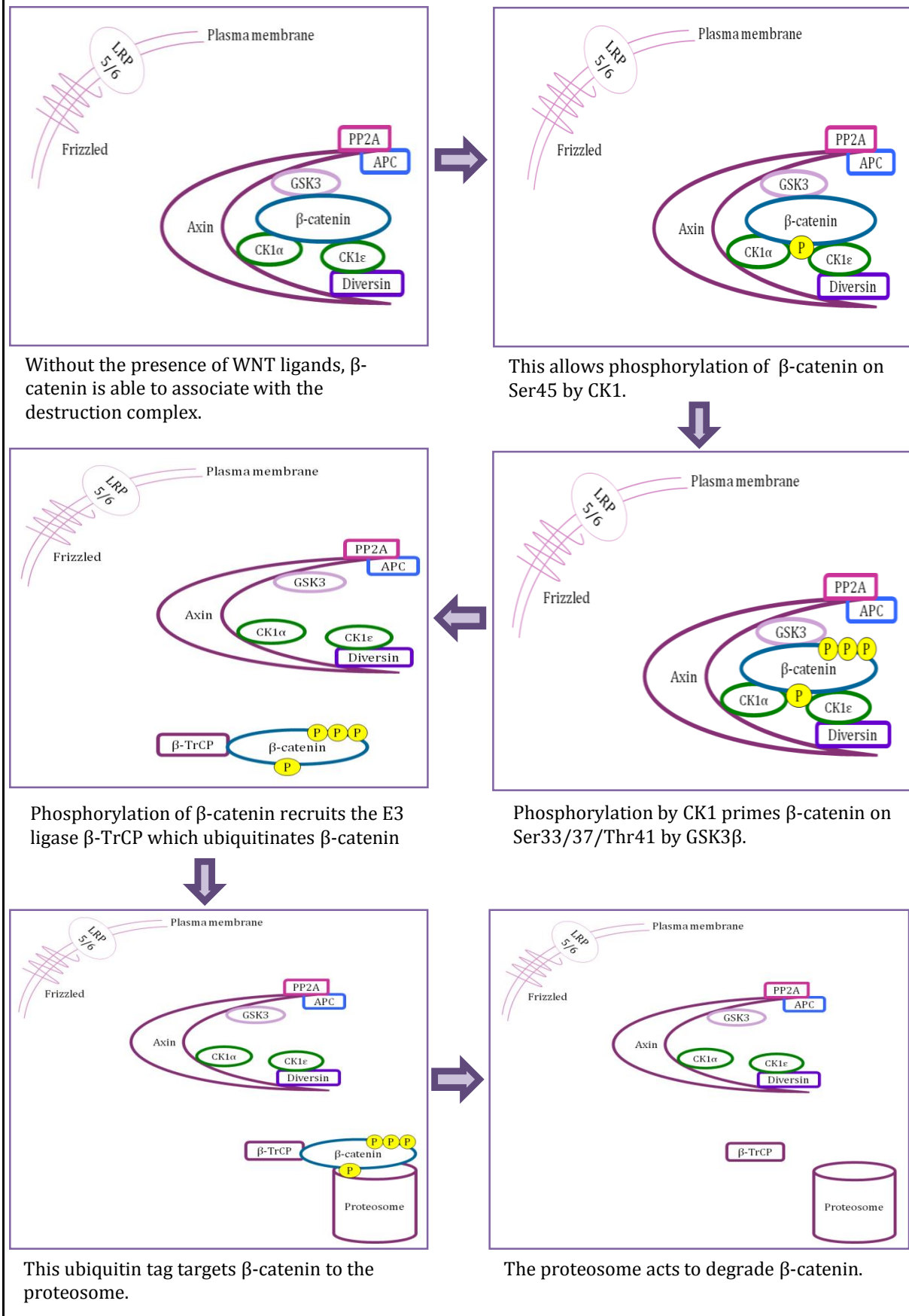
1.6.3 The Wnt/β-catenin Signalling Pathway in CML

Studies have shown that in CML, disease progression and relapse originate from an atypical population of LSCs. The development of these LSCs is via mutations which modify progenitor self-renewal, survival and differentiation[101]. Wnt/β-catenin signalling is crucial in maintaining the self-renewal of normal HSCs and when the signalling is disrupted, leukaemia consequently develops [143].

BCR acts as a tumour suppressor by inhibiting the expression of proliferation-promoting genes. It acts as a negative regulator of the Wnt/β-catenin signalling pathway by creating a complex with β-catenin, downregulating β-catenin/TCF-dependent transcription, which in turn negatively regulates the expression of various genes including *C-MYC*. Conversely, BCR-ABL1 has been shown to disrupt the BCR-β-catenin complex inhibiting the negative regulation BCR has on the Wnt/β-catenin pathway. This negative regulation can be reversed using imatinib [28].

The development of BCR-ABL1 has also been shown to have an adverse effect on Wnt signalling by phosphorylating specific tyrosine residues on β-catenin at Tyr86 and Tyr654 residues stabilising the protein. When β-catenin is phosphorylated on these residues by BCR-ABL1, it binds to the TCF4 transcription factor, enabling activation of transcription. Imatinib is able to reverse this effect by preventing the β-catenin/TCF-dependent transcription by retaining the unphosphorylated β-catenin in the cytoplasm increasing its binding affinity for the destruction complex [144].

BCR-ABL1 has also been speculated to inhibit antagonists of the pathway including sFRPs. It has been shown that DNA methylation of specific sites within the promoter region of genes has led to the reduction of sFRP which consequently constitutively activates Wnt signalling. This mechanism has been found to be involved in various forms of cancer specifically leukaemia. Within CML it has been found to be an uncommon event, but when it does arise it correlates with therapeutic resistance [145].

1.7 Beta-Catenin

Beta-catenin is a non-enzymatic 781 amino acid protein encoded by the *CTNNB1* gene which plays a crucial role in both cell adhesion and Wnt signalling. There are various parts of the β-catenin structure which play important roles in its functionality. These include helix C which may be involved in the recruitment of the transcriptional coactivators needed to enable β-catenin's activation of Wnt-responsive genes. Additionally, at the centre of the structure is a core made up of 12 armadillo repeats. This forms a positively charged domain which allows the binding of over 20 β-catenin binding partners, including TCF/LEF. This, along with the regulation of protein-protein interactions via its N- and C- terminal domains, gives β-catenin its ability to form multiprotein complexes. The N-terminus also functions in the degradation of β-catenin, as when it gets phosphorylated it is recognised by the β-TrCP ubiquitin ligase which ubiquitinates the protein allowing for it to associate and consequently be degraded by the proteasome [146] **(Figure 1.7)**.

Figure 1.7 Structure of β-catenin
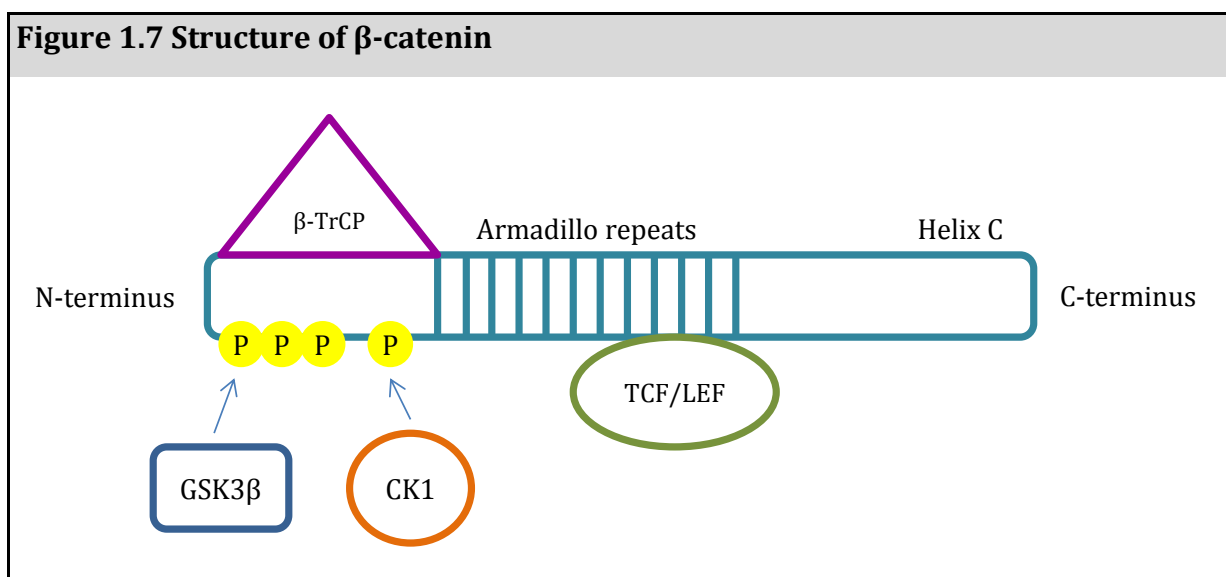
Beta-catenin is the central effector molecule of the Wnt signalling pathway and plays a key role in the transduction of the Wnt signal by transferring the signal from the cytoplasm into the nucleus, enabling the activation of gene transcription [87]. Under normal physiological conditions it is regulated by its phosphorylation status as this determines whether or not it will be degraded by the proteasome. It is primarily phosphorylated by CK1α on the N terminus at Ser45. This primes the protein and facilitates the phosphorylation of Thr41, Ser37 and Ser33 by GSK3β [104, 135, 136]. Phosphorylation at Ser37 and Ser33 on β-catenin are what initiates ubiquitination of β-catenin by βTrCP causing it to be degraded by the proteasome [135, 140-142].

In the absence of β-catenin phosphorylation, it is unable to be ubiquitinated by β-TrCP and hence is not degraded by the proteasome, instead being stabilised in the cytoplasm [100]. The stabilised unphosphorylated β-catenin is then imported into the nucleus **(Section 1.6.1.3)** and binds to the transcription factors TCF and LEF [114, 115]. This interaction of TCF/LEF with β-catenin causes the displacement of transcriptional repressors and, together with the recruitment of additional transcriptional co-activators initiates transcription [95] **(Section 1.6.1.4 and Figure1.5).**

Figure1.8 A diagram to show the complexes formed by β-catenin when it is either inactive and destined for degradation, or active and translocated to the nucleus to active transcription
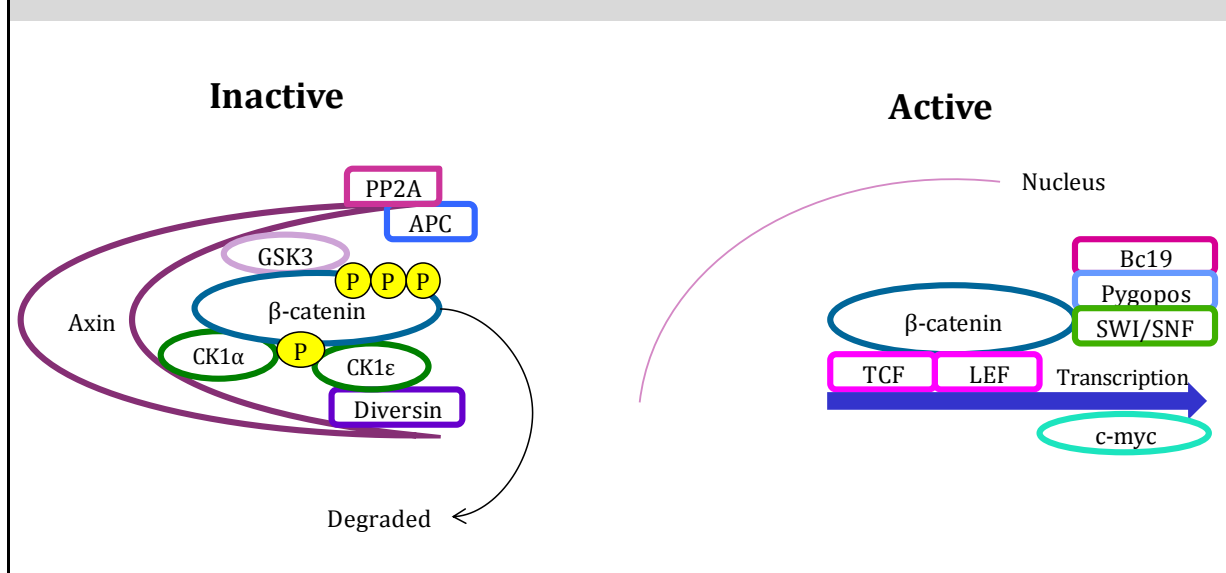
1.8.1 Beta-Catenin in CML

Alongside phosphorylation by CK1 and GSK3β, further phosphorylation on residues Ser552 [147], Ser675 [148], and Ser191 [116] of β-catenin have been reported to enhance its signalling capacity, but there is insufficient understanding as to whether the phosphorylation on these residues can modify β-catenin activity on their own [149]. Significantly to CML, BCR-ABL1 itself can physically interact with β-catenin and phosphorylate specific tyrosine residues on β-catenin at Tyr86 and Tyr654 residues which direct β-catenin to translocate to the nucleus and bind to the TCF4 transcription factor, enabling activation of transcription and consequently the acquisition of leukaemic stem cell (LSC) properties [144].

Investigation into β-catenin's role in CML has shown that the Wnt/β-catenin signalling pathway is involved in the maintenance of HSCs by being required for regulating their self-renewal capacity[143] [150]. But in addition to β-catenin being involved in HSC maintenance, it is also key for the preservation of LSCs. This was demonstrated by Hu *et al.*, [151]. They found that β-catenin was up-regulated 2.5 fold in LSCs in CML mice. Furthermore when primary CML mice LSCs were transferred to secondary mice, they were incapable of inducing CML when there was a deficiency in β-catenin. This signifies the importance of β-catenin in the survival and self-renewal of LSCs[151], implying that β-catenin is an important factor in the development of CML.

Previous to Hu *et al.*, Jamieson *et al.*, [150] found that in comparison to control cells there were elevated amounts of β-catenin present in CML patient myeloid progenitors in either accelerated phase or blast crisis, which subsequently normalised with imatinib treatment. Data showed a difference in active (unphosphorylated) β-catenin in HSC in comparison to granulocyte-macrophage progenitors (GMP), where in HSC there was no significant difference in levels of activated β-catenin between controls, patients with accelerated-phase CML and patients with blast crisis. In contrast in the GMPs there was a significant increase in activated β-catenin in patients with blast crisis and patients with imatinib resistant CML, in comparison to normal. To confirm these findings an activity assay (LEF/TCF-GFP reporter assay) was carried out and results substantiated what was previously shown with the HSC showing no significant difference between controls and the three phases of CML. In contrast, the GMPs again showed elevated levels of nuclear β-catenin via increased levels of GFP in blast crisis patients. In addition to looking at levels of β-catenin, the impact of these elevated levels was also assessed by

looking at the self-renewal capacity and proliferative potential. Results showed the re-plating capacity was higher in CML GMPs compared to normal GMPs, and by inducing the expression of β-catenin in normal GMPs their re-plating capacity was consequently elevated. In contrast transduction of AXIN, which acts as an inhibitor of β-catenin signalling, decreased the re-plating capacity of the cells. These results show the importance of β-catenin in the self-renewal of CML GMPs when patients are in blast crisis [150], however this work is yet to be confirmed by others.

1.8 Glycogen synthase kinase 3β (GSK3β)

A key component in the regulation of β-catenin is GSK3β which, as previously stated, phosphorylates β-catenin targeting it for degradation. GSK3β is a proline directed serine/threonine kinase which phosphorylates substrates which have previously been phosphorylated by a different kinase, 'priming' the substrate for subsequent phosphorylation by GSK3β. In regards to GSK3β phosphorylating β-catenin, this occurs by CK1 on Ser45 [135, 136]. GSK3β is an 832 amino acid protein which contains a DSH homologous domain in its C-terminus. Additionally, it has both an AXIN and β-catenin binding site which allow it to form a multi-protein complex with these two proteins [134].

GSK3β is a constitutively active kinase, which is regulated by its phosphorylation status. Inactivation of the kinase occurs by phosphorylation at Ser9. When this phosphorylation occurs it is thought to create a pseudosubstrate which interacts with the active site of GSK3β, blocking its ability to phosphorylate its target proteins [152]. This process of inhibition is competitive with levels of substrate competing with the levels of pseudosubstrate [152], however the phosphorylation of Ser9 is well recognised as the method of GSK3β inhibition with a direct correlation to a decrease in kinase activity [153]. Numerous kinases have the ability to phosphorylate GSK3β at this residue, including; protein kinase B (Akt), integrin-linked kinase (ILK), protein kinase A (PKA) and p90Rsk, amongst others. Akt was primarily shown to phosphorylate and inhibit GSK3β through Ser9 phosphorylation via the phosphatidylinositide 3-kinase (PI3K) pathway [154]. Additionally, two other phosphorylations that can occur on

GSK3β have been linked with an increase in this inhibitory phosphorylation on Ser9. These are; phosphorylation of Thr43, which occurs by extracellular signal regulated kinase (ERK) and correlates with inhibition, and phosphorylation of Ser389 and threonine 390 by p38 mitogen activated protein kinases (MAPK), both of which increase the ability of Ser9 phosphorylation of GSK3β and hence enhance inhibition of the kinase [153, 155].

Although GSK3β is constitutively active, it has been found that phosphorylation of Tyr216 has the ability to enhance the activity of this kinase. This occurs by the phosphorylation of Tyr216 altering the conformation of GSK3β's active site. When the Tyr216 residue is not phosphorylated, a side chain obstructs the base of the active site, reducing substrate binding ability to GSK3β. When the Tyr216 residue is phosphorylated, this acts by freeing up the active site allowing easier access by substrates, enhancing the activity of the kinase [152, 155, 156]. The method of phosphorylation on this site is uncertain; kinases including PYK-2 and FYN have been reported to be able to phosphorylate this residue, alongside MEK1/2 in mammalian fibroblasts [155]. However, it is also thought that there is a possibility of autophosphorylation being responsible for this increase in activity [155, 157]. Dephosphorylation of this site has been shown to correlate with a decrease in kinase activity, showing that although this site may not be required for GSK3β activity, it is significant in enhancing it [157]. Additionally, while inhibitors of GSK3β act by inducing inactivation by Ser9 phosphorylation, they do not have any effect on Tyr216 phosphorylation. This could be indicating that this inactivation of GSK3β is sufficient to override activation [157].

GSK3β is known to be involved in the degradation of numerous substrates other than β-catenin [152]. Others that are of interest to this study include MCL-1, and c-Myc. MCL-1 is a well-characterised member of the BCL-2 family [158] which has two isoforms; the longer isoform acts by inhibiting apoptosis and increasing cell survival (anti-apoptotic). In contrast the shorter isoform promotes apoptosis, inhibiting cell survival (pro-apoptotic). Down regulation of MCL-1 may be required for the instigation of the apoptosis cascade, therefore inhibiting its function may be an effective treatment in malignancies where MCL-1 is involved in inhibiting apoptosis [159]. Along with apoptosis, data suggest that MCL-1 can act to disrupt the association of β-catenin with the destruction complex in the cytoplasm. This is as a result of MCL-1 acting as a substrate for GSK3β, preventing GSK3β from phosphorylating and targeting β-catenin for degradation and hence active β-catenin accumulates in the nucleus [160].

In addition to β-catenin and MCL-1, C-MYC is also a target of GSK3β, and considering its role as an oncogene, could have major implications on cell homeostasis [161]. GSK3β is involved in the degradation of C-MYC through its phosphorylation on Thr58. This phosphorylation occurs once C-MYC has been stabilised by phosphorylation on Ser62 by ERK. Subsequent to both phosphorylation by ERK and GSK3β, PP2A acts to remove the Ser62 phosphorylation which then allows for ubiquitination and degradation via the proteasome [162]. This implicates GSK3β as an important mediator of C-MYC turnover independent of the Wnt/β-catenin signalling pathway.

1.8.1 GSK3β in CML

It is known that the Wnt/β-catenin pathway is activated when CML progenitors progress to myeloid blast crisis [150]. It was reported that, when patients progress from chronic phase and accelerated phase through to blast crisis, total GSK3β protein levels are significantly decreased and β-catenin transcriptional activity is elevated due to increased amounts of activated β-catenin [101].

Mutations in *GSK3β* give rise to splice isoforms which are deleted in exon 9, exon 11, or exon 9 and 11. Exon 9 and 11 deletions have been previously discovered in Parkinson's disease [163], however the truncated isoforms of exon 8 and 9 which have been found in CML progenitors have not previously been found elsewhere [101]. Due to overexpression of the full-length *GSK3β* causing a decrease in activated β-catenin, it was said that *GSK3β* mis-splicing is a significant event in the development of LSCs and that restoration of the splicing events may have a possible therapeutic benefit. Abrahamsson *et al.,* [101] proposed that the combination in CML of β-catenin stabilisation by BCR-ABL1 and the decrease of negative regulators of the Wnt pathway including AXIN2 may act by heightening the effects of mutated-*GSK3β* on the activation of β-catenin.

The mechanisms by which *GSK3β* splicing occur have yet to be determined. The expression of BCR-ABL1 in cord blood progenitors has particular relevance to CML development, which stimulates a rise in expression in genes implicated in alternative splicing. Changes in the splicing events can either inactivate tumour suppressors or

activate proteins which promote tumour development. Specific to CML the use of the splice isoforms in *GSK3β* can be used as an indicator of disease progression and as a therapeutic target for treatment of patients in advanced phase CML [101].

In addition to this, Reddiconto *et al*., [164] showed that CML progenitor cells contain an active pool of GSK3β marked by Tyr216 phosphorylation. They found that treating chronic phase CML progenitors with imatinib resulted in a dose dependent increase of Tyr216 phosphorylated GSK3β. Furthermore, it was suggested that BCR-ABL1 prevents the translocation of GSK3β into the nucleus and this was restored on imatinib treatment. The study showed that targeting GSK3β may have therapeutic benefits for patients by increasing the apoptotic effects of imatinib on CML stem cells.

1.9 PP2A

Protein phosphatase 2A (PP2A) is a serine/threonine protein phosphatase which is made up of various subunits. These consist of a core enzyme known as the 'A subunit', a catalytic subunit known as the 'C subunit' and regulatory subunits known as the 'B subunits' [165-167]. The B subunits contain four different families which contain 16 members overall. The regulatory sub-families are; B (PR55), B' (B56 or PR61), B'' (PR72), and B''' (PR93/PR110) [165, 167].

PP2A plays a role within multiple signalling pathways to regulate the function of activated kinases [167]. Of interest to this study, PP2A functions within the Wnt/β-catenin signalling pathway as part of the destruction complex, however it is reported to have multiple roles both parallel to, and downstream of, β-catenin [168]. As part of the destruction complex, the catalytic subunit of PP2A binds to AXIN through amino acids 632 and 836 [169], whilst the regulatory B' (B56) family of subunits associate with APC [170]. In response to a Wnt signal, dephosphorylation of AXIN through PP2A has shown to dissociate β-catenin from the destruction complex reducing its degradation [171]. In contrast dephosphorylation of APC through the B56 subunit of PP2A down-regulates β-catenin through enhancing its degradation [172]. PP2A has also been reported to act directly or indirectly on TCF3, one of the transcription factors of Wnt/β-catenin signalling, independently of β-catenin. This results in overexpression of the catalytic subunit of PP2A converting the function of TCF3 from a transcriptional repressor to a transcriptional activator [168].

1.9.1 PP2A in CML

Within CML, PP2A has also been reported to function as a tumour suppressor downstream of BCR-ABL1. Within blast crisis it has been shown that PP2A is down regulated [173]. Two mechanisms of inhibition have been reported to regulate PP2A via different inhibitory proteins; SET (also known as I2PP2A) [173-175] and cancerous inhibitor of PP2A (CIP2A) [176]. SET is a specific inhibitor of PP2A whose activity is elevated through BCR-ABL1 via Janus kinase 2 (JAK2) [177]. Its activity has been shown to increase with disease progression, which correlates with the down-regulation of PP2A activity in blast crisis [173]. The activity of PP2A is regulated through phosphorylation of Tyr307. This phosphorylation has been shown to be decreased with both down-regulation of SET and treatment with imatinib [173]. Similarly, CIP2A also regulates PP2A through the inhibitory phosphorylation on Tyr307 with down-regulation of CIP2A also decreasing inhibition of PP2A. CIP2A was also recognised as a predictive biomarker of disease progression, with elevated levels being found in diagnostic samples from chronic phase patients who later progressed to blast crisis [177].

1.10 TCF/LEF Transcription Factors

The TCF/LEF family of transcription factors consist of four members; TCF1, TCF3, TCF4, and LEF1. Their structure is made up of an N-terminal β-catenin binding domain and a C-terminal high mobility group DNA binding domain which binds proteins involved in regulating transcription [178]. These transcription factors function by binding to Wnt responsive elements within the promoter of target genes e.g. *CYCLIN D1* and *C-MYC*, activating their transcription [122, 123]. Their activity is enhanced and repressed by transcriptional co-activators including; CBP/p300, and transcriptional co-repressors such as GROUCHO **(See section 1.7)**. Nuclear β-catenin functions by displacing the co-repressors from TCF/LEF and permitting transcriptional activation[122]. Post translational modifications including phosphorylation, sumoylation, ubiquitination, and acetylation, also modify the potential of TCF/LEF transcription factors to interact with nuclear co-activators, repressors or DNA. An example of this is the phosphorylation of TCF/LEF by the activated NEMO like kinase (NLK)/Nemo, which is considered to reduce the binding affinity of the β-catenin/TCF/LEF complex with DNA, hence influencing transcriptional regulation of Wnt target genes [87, 95, 179, 180].

1.10.1 TCF/LEF in CML

There have been limited reports on TCF/LEF transcription factors in CML, however it has been found in acute myeloid leukaemia (AML) that the expression of *LEF1* correlates with a favourable prognosis. *LEF1* is known to be involved in normal haematopoiesis and leukaemogenesis independent of the Wnt/β-catenin signalling pathway. It has been found in cytogenetically normal AML (CN-AML) that an elevation

in *LEF1* levels correlated with better cytogenetic response rate, overall survival, event-free survival and relapse-free survival. Conversely, a decrease in *LEF1* levels correlated with higher blast counts and disease progression [123]. These results contradict what has previously been shown with elevated levels of *LEF1* inducing the development of myeloid and lymphoid leukaemias [181]. The reason for this discovery that *LEF1* correlates with better prognosis in CN-AML, considering increased Wnt signalling is regarded as bad, may be due to *LEF1* acting independently of the Wnt/β-catenin pathway either on its own or as part of a different cellular pathway. Further reports on *LEF1* acting within haematological malignancies show that mutations in *LEF1* take place in T-cell acute lymphoblastic leukaemia, and enhanced *LEF1* levels correlate with poor prognosis in B-cell acute lymphoblastic leukaemia[123]. This goes to show that different mechanisms of action exist.

The significant discovery that the TCF/LEF transcription factors can act independently of the Wnt/β-catenin signalling pathway has been seen recently in haematological malignancies [178]. Grumolato *et al.* [178] showed an increase in TCF/LEF transcriptional activity in the cell lines Ramos, K562 and Jurkat, as well as primary material from lymphoma tumours, which did not correlate with an increase in nuclear β-catenin levels. To determine if the TCF/LEF transcription factors were acting independently of β-catenin, *TCF1, LEF1* and *TCF4* were expressed in 293T cells which are known to not have an active Wnt pathway [182]. Results showed that both *TCF1* and *LEF1* still increased the level of TCF/LEF reporter activity; however this did not occur with *TCF4* expression. This was further supported by deletion of the β-catenin binding domain from *TCF1* having limited effects on the TCF/LEF activation which only

decreased slightly. Additionally, mutation of *TCF1* which obstructed β-catenin's binding ability had no effect on the transcriptional activity of *TCF1*. All this supports the theory that TCF1 can act independently of β-catenin and activate transcription [178]. Furthermore, Grumolato *et al.* [178]showed that the transcription factors ATF2 and ATF7 enhance both TCF1's and LEF1's transcriptional activity, measured by *AXIN2* expression, which decreased when ATF2 and ATF7 were suppressed by shRNA. This suggests a new method of transcriptional activation which is separate of β-catenin.

Aims

1) Determine if the levels of β-catenin and its phosphorylated forms in MNCs are predictive of clinical outcome in imatinib treated patients or differ in relation to patient treatment response groups.

2) Determine if BCR-ABL1 mediated β-catenin phosphorylation on Tyr654 correlates with disease progression.

3) Investigate phospho-GSK3β Tyr216 and phospho-GSK3β Ser9 to determine if GSK3β's activity differs in relation to patient outcome.

4) Examine what regulates GSK3β's activity in CML.

5) Determine if GSK3β activity correlates with c-Myc degradation.

6) Screen the Wnt pathway and analyse any of the genes which appear to be different between the response groups in a larger patient cohort.

7) Investigate the transcription factors involved in the Wnt pathway to see if they are differentially expressed in the different patient cohorts.

Chapter 2 - Materials and Methods

2.1 Patients

All patients included in this research were aged 18 or older at diagnosis and were

positive by metaphase cytogenetic analysis for the Philadelphia chromosome. Minimum

follow-up was 12 months. Healthy volunteers were all fit and well at the time of

donation and were 21 or more years of age. All healthy volunteer and patient samples

included in this study were given with informed consent in accordance with the

declaration of Helsinki. This work was approved by the Liverpool Central Committee of

the UK National Research Ethics Service.

2.2 Sample Collection and Preparation

2.2.1 Total leukocytes

Venous blood was collected and from this, erythrocytes were depleted using red cell

lysis buffer (0.1M ammonium chloride, 10mM sodium bicarbonate and 1.3mM

ethylenediaminetetraacetic acid (EDTA) (Sigma-Aldrich, Gillingham, Dorset)).

Approximately 5ml of venous blood was mixed with 40ml of lysis buffer for 5 minutes

then centrifuged at 770g for 10 minutes, washed with phosphate buffered saline (PBS),

centrifuged for a further 5 minutes and then leukocytes were pelleted. For RNA

extraction $5x10^6$ total leukocytes were resuspended in 600μl RLT buffer (Qiagen,

Crawley, West Sussex) containing 1% β-mercaptoethanol (Sigma-Aldrich) and stored at

-20°C for extraction at a later time point. Alternatively total leukocytes were used fresh as required.

2.2.2 MNC preparation

MNC were prepared from 20-30mls of peripheral blood collected into EDTA (Sigma-Aldrich). MNCs were separated by density-dependent centrifugation (Lymphoprep, density 1.077 ± 0.001 g/ml, Axis-Shield, Cambridge, Cambridgeshire), washed in Roswell Park Memorial Institute 1640 (RPMI 1640), and resuspended in RPMI 1640 containing 10% dimethyl sulphoxide (DMSO) (Sigma-Aldrich) and 10% foetal calf serum (FCS; BioSera, Ringmer, Sussex) at 4°C and cryopreserved in liquid nitrogen. When required, cells were thawed rapidly at 37°C until partially thawed and the DMSO was diluted to <1% at room temperature over a period of 30 minutes via dropwise addition of thawing media (RPMI/10% Heparin Sodium (1,000 IU/ml from Wockhardt UK Ltd, Wrexham, Wrexham County Borough) using 5mls per sample. After washing, cells were re-suspended at 2×10^6 /ml in 'culture medium' (RPMI 1640 containing 10% FCS, 1% L-glutamine and 2% penicillin / streptomycin; Invitrogen, Paisley, Renfrewshire), seeded into 6-well tissue culture plates (Becton Dickinson (BD), Oxford, Oxfordshire) and cultured under standard tissue culture conditions (5% CO_2 in air, 37°C, 100% humidity) overnight. MNC from normal healthy volunteers were freshly prepared and used immediately.

2.2.3 Preparation of CD34+ cells

Samples were enriched for CD34+ cells using the CliniMACS system (Miltenyi Biotec, Auburn, California, USA) according to the manufacturer's instructions. They were then resuspended in 10% DMSO/10% FCS/RPMI at 4°C and cryopreserved in liquid nitrogen. All CD34+ cells were collected at diagnosis and then labelled according to the patients' subsequent clinical outcome. In some experiments where purified CD34+ cell samples were not available, MNC were co-stained with CD34 antibody (BD), and FACS analysis was performed under gated conditions selected for CD34+ cells **(see Section 2.7)**.

2.2.4 Patient samples used

Table 2.1 shows a list of patients from which samples were used for experimental analysis, including their response, age at diagnosis, gender, white blood cell count and date of diagnosis.

Table 2.1 Patient samples used for experimental analysis

Patient ID	Response	Age at Diagnosis	Male/Female	White Blood Cell Count (x10^9/l)	Date of diagnosis
1	Failure	73	Male	477	16.09.05
2	Blast Crisis	58	Male	x	04.08.05
3	Optimal	59	Female	7.1	24.08.05
4	Optimal	35	Female	x	03.08.05
5	Optimal	56	Female	x	14.07.05
6	Failure	63	Female	10.5	04.08.05
9	Failure	49	Female	213	24.11.04
10	Failure	54	Female	3.5	27.07.05
13	Blast Crisis	24	Male	x	16.01.06
15	Optimal	59	Male	65.9	26.01.06
20	Blast Crisis	33	Male	384.1	14.02.06
28	Optimal	30	Female	58.2	04.04.06
29	Optimal	55	Male	33.8	12.04.06
30	Optimal	49	Male	168.7	03.05.06
32	Optimal	47	Female	85.9	01.06.06
33	Optimal	55	Male	x	01.08.06
34	Failure	33	Male	x	10.08.06
37	Blast Crisis	35	Male	4	21.08.06
39	Blast Crisis	55	Female	x	25.10.00
40	Optimal	38	Female	x	07.09.06
43	Failure	32	Female	x	12.02.03
44	Failure	48	Female	x	14.09.06
51	Blast Crisis	31	Female	x	23.03.05
52	Blast Crisis	59	Female	x	16.07.03
58	Optimal	39	Male	x	29.11.06
90	Failure	65	Male	2.6	03.05.06
107	Optimal	40	Male	78.4	07.03.07
108	Blast Crisis	57	Male	81.8	21.02.07
112	Blast Crisis	36	Female	8.9	14.03.07
113	Optimal	27	Female	x	04.04.07
115	Blast Crisis	24	Male	222	03.07.07
118	Optimal	55	Female	139.9	19.09.07
119	Optimal	66	Male	87.3	19.09.07
122	Optimal	47	Male	x	28.09.07
123	Failure	64	Male	x	27.09.07
124	Optimal	33	Male	119.2	02.10.07
130	Optimal	43	Female	75.9	28.01.08
204	Optimal	52	Female	182.9	09.07.08
206	Failure	43	Female	41	23.07.08
209	Optimal	46	Female	66.9	11.09.08
218	Optimal	23	Male	77.6	23.10.08
220	Blast Crisis	23	Male	542	30.10.08
236	Blast Crisis	48	Male	x	09.06.08

246	Optimal	29	Female	x	17.02.09
290	Failure	55	Female	11.1	24.04.09
291	Optimal	30	Female	x	25.02.09
293	Failure	25	Male	393.2	11.06.09
296	Failure	24	Male	476	22.06.09
313	Optimal	39	Male	x	10.08.09
316	Blast Crisis	38	Male	45.9	18.11.09
317	Blast Crisis	16	Male	x	04.06.08
321	Failure	42	Female	256.3	13.01.10
323	Failure	79	Male	68.9	04.02.10
324	Optimal	58	Female	37.3	17.03.10
337	Optimal	84	Female	259	25.05.10
366	Optimal	57	Female	405	08.09.10
371	Optimal	50	male	357.9	04.10.10
395	Failure	28	Female	x	21.02.11
414	Failure	68	Female	301.3	23.03.11
426	Blast Crisis	42	Male	x	13.05.11
467	Failure	57	Male	359.4	23.10.11
504	Blast Crisis	92	Female	22.3	16.05.12

2.3 Cell Culture

2.3.1 Maintenance of cells

Four human BCR-ABL1 positive CML cell lines, KCL22, KYO-1, LAMA84 and K562 were used as cell line models of CML and as controls in some experiments (donated by Prof Junia Melo from the LRF Leukaemia Unit, Hammersmith Hospital, London, UK). Cell lines were cultured under standard tissue culture conditions (37°C, 5% CO_2 in air, 100% humidity) at an approximate starting density of $3x10^5$/ml in culture medium (RPMI, 10% FCS, 1% L-glutamine and 2% penicillin and streptomycin, Invitrogen). Cultures were re-seeded into fresh media approximately every 3-4 days. Twenty-four hours prior to experimental use cell lines were resuspended in fresh culture medium to ensure optimal exponential growth prior to use.

2.3.3 *In vitro* cultures

In vitro studies of drugs were carried out on both cell lines and patient samples. Conditions for this were as follows; 2×10^6 cells per ml were cultured in RPMI-1640 supplemented media at 37°C for 24 hours with the drug concentrations shown in **Table 2.1**. Patient samples were used 24 hours subsequent to thawing.

Table 2.2 Concentrations of drugs/reagents used in *in vitro* cultures		
Drug/reagent	**Final Concentration**	**Company**
Imatinib	5μM	Novartis, Basel, Switzerland
Dasatinib	150nM	Bristol-Myers Squibb, NYC, New York, USA
Nilotinib	5μM	Novartis
FTY720	2.5μM	Millipore, Watford, Hertfordshire
Okadaic Acid	6nM	Sigma-Aldrich
SB216763	5μM	Sigma-Aldrich
Wnt3a	25ng	R&D Systems, Abingdon, Oxfordshire
WIF1	1.5μg	R&D Systems

2.4 Small interfering RNA

Small interfering RNA (siRNA) against various targets was carried out using Cell Line Nucleofector (TM) Kit V (Lonza/Amaxa Biosystems, Cambridge, Cambridgeshire) and the Amaxa machine (setting T-16). K562 cells were used for siRNA to knock down both GSK3β (Santa Cruz Biotechnology, Heidelberg, Germany) and CIP2A (Santa Cruz Biotechnology)(Table 2.2). Cells were firstly washed three times in PBS (pH 7.2) to remove any residual medium which may affect the siRNA process. 1×10^6 cells were then resuspended in 100μl nucleofector solution in an Eppendorf tube. 100nM of scrambled control siRNA (Santa Cruz Biotechnology), and test siRNAs (Table 2.2) were added separately to the re-suspended cells, and then these suspensions were transferred to Amaxa cuvettes. Electroporation was carried out using the Amaxa instrument. After nucleofection, 0.5ml of pre-warmed culture media was added to each vial using a soft pipette, and the cells were transferred to a 24 well plate (BD) containing another 0.5ml of pre-warmed culture medium. The cells were then incubated for 72 hours and the effects of siRNA measured by polymerase chain reaction (PCR), fluorescence activated cell sorting (FACS) and western blotting.

Table 2.3 siRNA used		
siRNA	**Catalogue Number**	**Company**
GSK3β	sc-355527	Santa Cruz Biotechnology
CIP2A	sc-77964	Santa Cruz Biotechnology
Control	sc-37007	Santa Cruz Biotechnology

2.5 Transient Transfection

The CIP2A-GFP transfection plasmid (PrecisionShuttle mammalian vector with C-terminal tGFP tag, 10µg, PS100010, Origene, Rockville, Maryland, USA) was used to transiently transfect CIP2A into K562 cells. A schematic of the plasmid can be seen in **Figure 2.1**. A GFP-only transfection plasmid was used as a control. Similar to siRNA, transient transfection was carried out using the Cell Line Nucleofector (TM) Kit V (Lonza/Amaxa Biosystems) and the Amaxa machine (setting T-16). Cells were washed three times in PBS (pH 7.2) to remove any residual media which may affect the transfection process. $2x10^6$ cells were then resuspended in 100µl nucleofector solution in an Eppendorf tube. 2µg/ml of the CIP2A-GFP (green fluorescent protein) tagged and GFP-only tagged plasmids were added to the re-suspended cells, and this suspension was transferred to an Amaxa cuvette. Electroporation was carried out using the Amaxa instrument. Following nucleofection, the cells were transferred to a 24 well plate containing 0.5ml of pre-warmed culture media. The cells were then incubated for 48 hours and the effects of the transfection measured by PCR, FACS and western blotting.

Prior to any analysis, the transfection efficiency was measured by GFP detection using fluorescence-cell analysis (FACScalibur, BD) and by propidium iodide (PI) (1µg/ml) staining for analysis of cell viability **(see Section 2.7.2)**.

Figure 2.1 A schematic of the cloning sites for the CIP2A-GFP tagged transfection plasmid
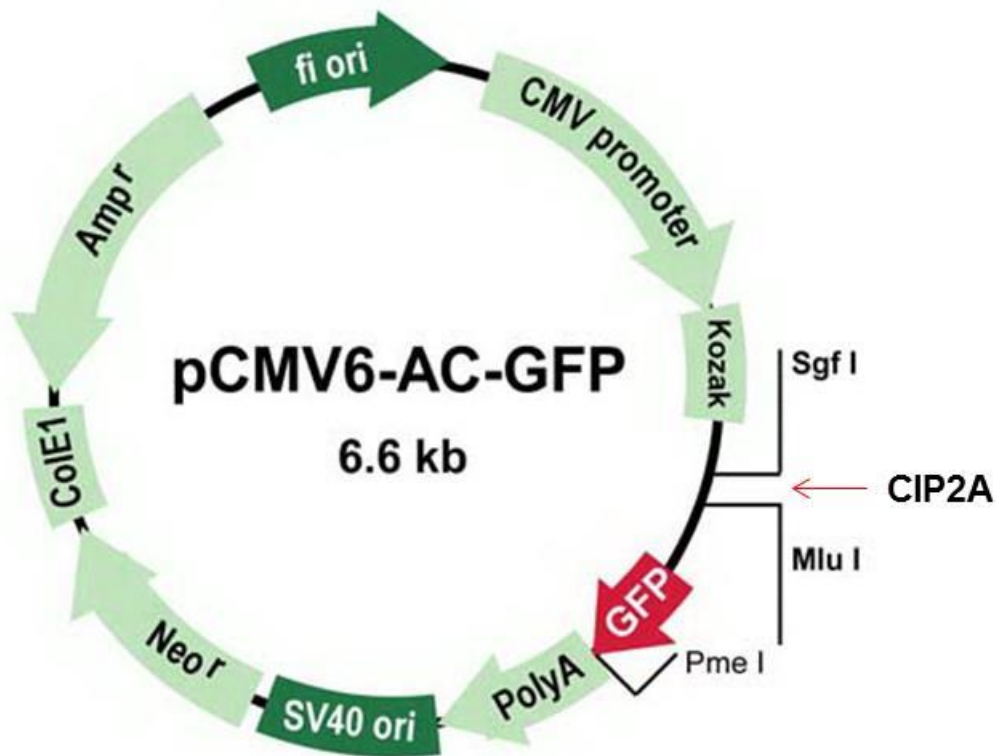
[183]

2.6 PCR Analysis

2.6.1 RNA extraction

RNA was extracted using RNeasy mini kit (Qiagen). Samples were thawed and transferred to a QIA shredder column sitting in a 2ml collection tube, and centrifuged at 14,000g for 2 minutes in a microcentrifuge. 600µl of 70% ethanol was added and mixed well with the flow through in the collection tube. 600µl of sample was added to an RNeasy mini spin column sitting in a 2ml collection tube and centrifuged for 15 seconds at 14,000g. The flow through was discarded. 700µl of kit RW1 buffer was added to the RNeasy column and left at room temperature for 5 minutes, followed by centrifugation at 14,000g for 5 minutes, and the flow through discarded. The RNeasy spin column was transferred to a new RNeasy collection tube. The RNeasy spin column was washed twice with 500µl kit RPE buffer and centrifuged at 14,000g for 15 seconds. The RNeasy spin column was transferred into a new 1.5ml collection tube, and then 40µl of RNase free water was added directly onto an RNeasy membrane and left at room temperature for 5 minutes. RNA was eluted by centrifuging for 2 minutes at 14,000g. RNA was stored at -70°C until used.

2.6.2 cDNA synthesis

cDNA was synthesised using the RNA prepared above. 30µl of RNA was incubated with 2µl (500ng/µl) of random hexamers (Promega, Southampton, Hampshire) at 70°C for 10 minutes then cooled on ice for 3 minutes. 16µl 5x reaction buffer (RT buffer), 8µl of 0.1M DL-Dithiothreitol (DTT) and 4µl of 10mM deoxyribonucleotide triphosphate

(dNTP) (SuperScript III Reverse Transcriptase kit, Invitrogen) was added to the sample and incubated for 5 minutes at 25°C for 10 minutes, then at 42°C for 60 minutes, and finally at 70°C for 15 minutes to stop the reaction. The cDNA was stored at -20°C until used.

2.6.3 Real time – quantitative Polymerase Chain Reaction (RT-qPCR)

Pre-designed TaqMan real time PCR assays (Life Technologies, Paisley, Renfrewshire) were used in a 96 well assay plate. Each assay consists of a forward and reverse primer at a final concentration of 900nM and a 6-carboxyfluorescein (6-FAM) dye-labelled TaqMan minor groove binder (MGB) probe at a final concentration of 250nM. The amount of cDNA was determined using the Nanodrop2000; 100ng of cDNA was used per 20μl reaction consisting of 4μl Distilled water, 10μl TaqMan gene expression master mix (Life Technologies), 1μl TaqMan gene expression assay **(Table 2.3)**, and 5μl of cDNA. Each sample was run in triplicate. After loading the reaction mixture, the plate was sealed. The real time PCR amplifications were performed using an ABI Prism 7900HT System with the following conditions specified by the manufacturer: 50°C for 2 minutes, 10 minutes at 95°C followed by 40 cycles of denaturation at 95°C for 15 seconds and annealing/extension at 60°C for 1 minute.

The relative expression level of a particular gene of a given sample was calculated by the comparative Ct method [184]. The comparative Ct method uses the $2^{-\Delta\Delta Ct}$ formula to achieve results for relative quantification, where $\Delta\Delta Ct$ is the normalised signal level in a sample relative to the normalised signal level in the calibrator sample. In this study a

pool of cDNA from six healthy volunteers was used as calibrator and all the samples were normalised to glyceraldehyde 3-phosphate dehydrogenase (*GAPDH*) endogenous control.

Table 2.4 Assay primers used for PCR		
Assay	**Product Code**	**Company**
CTNNB1 (β-catenin)	Hs00355049_m1	Life Technologies
GSK3β (long and short)	Hs01047719_m1	Life Technologies
GSK3β (long only)	Hs01053242_g1	Life Technologies
RT² Profiler PCR Array for the Human WNT Signalling Pathway	PAHS-043Z	Qiagen
WNT1	Hs01011247_m1	Life Technologies
WNT8A	Hs00230534_m1	Life Technologies
WNT9A	Hs00243321_m1	Life Technologies
FZD7	Hs00275833_s1	Life Technologies
NKD1	Hs00263894_m1	Life Technologies
APC	Hs01568269_m1	Life Technologies
TCF1	Hs00167041_m1	Life Technologies
TCF3	Hs00413032_m1	Life Technologies
TCF4	Hs00162613_m1	Life Technologies
LEF1	Hs01547250_m1	Life Technologies
C-MYC	Hs00153408_m1	Life Technologies
CYCLIN D1	Hs00765553_m1	Life Technologies
GAPDH	Hs99999905_m1	Life Technologies

2.6.4 Manual PCR

Forward and reverse primers were diluted in double distilled (dd) H_2O to give a mix containing 4μM concentration of each. A mastermix was made containing 10μl expression mix, 1μl primer mix and 4μl ddH_2O per sample, and then 15μl was pipetted into each required well of a 96 well PCR plate. 5μl of cDNA from each sample and controls were then added, and the plate was sealed with a cover. The plate was spun in a centrifuge, then the plate placed in the PCR block. The following PCR conditions were used to run the samples: 95°C for 5 minutes, followed by 40 cycles of 95°C for 15 seconds, 56°C for 20 seconds, and 60°C for 45 seconds, and then finally 72°C for 10 minutes.

The plate was then left at 4-8°C before running on a 2% agarose gel (agarose and Safeview Nucleic Acid Stain (NBS biologicals, Huntingdon, Cambridgeshire) in 150ml of 0.5M x Tris/Borate/EDTA (TBE). Agarose and TBE were first mixed and heated in a microwave until the agarose was completely dissolved. The gel was then poured into a mould with combs and left to set for approximately 30 minutes at room temperature. The gel was placed in a running tank, submerged in 0.5xTBE and the amplified samples (1:1 in running buffer) and any controls were loaded alongside a 50bp ladder. Finally the gel was run for approximately 60 minutes at 120V and the gel photographed.

2.7 FACS Analysis

Cells ($\sim 5 \times 10^5$) were fixed by resuspending in 500µl of 2% paraformaldehyde/PBS at pH 7.2 (VWR, Lutterworth, Leicestershire) for 10 minutes at 37°C. Cells were then centrifuged at 770g for 3 minutes. 500µl of 90% methanol (Fisher Scientific, Loughborough, Leicestershire) was added to the cell pellet and the cells were vortexed and then incubated at room temperature for 30 minutes. Cells were then thoroughly washed with 1ml incubation buffer containing PBS and 0.5% bovine serum albumin (BSA) (Sigma-Aldrich), and centrifuged at 770g for 3 minutes. Cells were resuspended in 25µl incubation buffer and appropriate antibodies were added **(Table 2.4)**. Cells were vortexed and incubated at room temperature for ≥45 minutes. Cells were then washed twice in incubation buffer and resuspended in 50µl incubation buffer containing 10µg/ml goat anti rabbit/mouse second layer Alexa Fluor 488 antibody (Invitrogen). Subsequently they were incubated at room temperature in the dark for at least 30 minutes, then washed twice in incubation buffer and analysed using flow cytometry (FACScalibur; BD), with Cellquest Pro software (BD) for data analysis. When analysing the data, events were gated on the live cell population, determined by forward and side scatter light properties, and antibody fluorescence was measured through this gate. The corresponding control value for each result was then subtracted to determine the protein level.

Table 2.5 Antibodies used for FACS analysis

Primary Antibody	Final Concentration	Control Antibody	Secondary Antibody
Total-β-catenin (Cell Signalling Technology (CST), Beverly, Massachusetts, USA)	0.032µg/ml	Rabbit IgG	Alexa Fluor 488 Rabbit
Unphosphorylated β-catenin (Millipore)	0.1µg/ml	Mouse IgG$_1$	Alexa Fluor 488 Mouse
Phospho-β-catenin (S45/T41) (CST)	0.4 µg/ml	Rabbit IgG	Alexa Fluor 488 Rabbit
Phospho-β-catenin (S33/37/T41) (CST)	0.4 µg/ml	Rabbit IgG	Alexa Fluor 488 Rabbit
Phospho-β-catenin (Tyr654) (Abcam, Cambridge, Cambrigeshire)	0.25µg/ml	Mouse IgG$_1$	Alexa Fluor 488 Mouse
C-MYC (CST)	20 µg/ml	Rabbit IgG	Alexa Fluor 488 Rabbit
C-MYC pT58 (Santa-Cruz Biotechnology (SCB), Dallas, Texas , USA)	0.25µg/ml	Rabbit IgG	Alexa Fluor 488 Rabbit
C-MYC pS62 (Abcam)	10 µg/ml	Rabbit IgG	Alexa Fluor 488 Rabbit
PP2A (Millipore)	100 µg/ml	Mouse IgG$_1$	Alexa Fluor 488 Mouse
PP2A pY307 (Abcam)	9 µg/ml	Rabbit IgG	Alexa Fluor 488 Rabbit
SET (I2PP2A) (SCB)	20 µg/ml	Rabbit IgG	Alexa Fluor 488 Rabbit
CIP2A (SCB)	16µg/ml	Mouse IgG$_1$	Alexa Fluor 488 Mouse
E2F1 (SCB)	0.5µg/ml	Rabbit IgG	Alexa Fluor 488 Rabbit
E2F1 pS364 (SCB)	0.5µg/ml	Rabbit IgG	Alexa Fluor 488 Rabbit

Mouse IgG$_1$ (BD, #349040)

Rabbit IgG (R&D Systems, #AB-105-C)

Alexa Fluor 488 Goat Anti-Mouse IgG (H+L) (Life Technologies, #A-11001)

Alexa Fluor 488 Goat Anti-Rabbit IgG (H+L) (Life Technologies, #A-11001)

2.7.1 CD34+ Staining.

For analysis of CD34+ cells in MNC preparations, standard FACS protocol was carried out with the addition of 0.1mg/ml of CD34+ conjugated antibody (BD) added at the same time as the secondary antibody. Cells were then gated on the CD34+ population on analysis.

2.7.2 Propidium Iodide (PI) Staining.

To analyse cell viability PI staining was used. Prior to the FACS experiment, 50µl of approximately $2x10^5$ cells were separated from each sample and transferred into a BD FACS tube. 50µl of PI (1µg/ml) was then added and the suspension was incubated on ice for 30 minutes. The cell death was then analysed by flow cytometry (FACScalibur, BD) with Cellquest Pro software (BD) for data analysis. From this the percentage viability of the cells was determined.

2.8 MTT Assay

The 'MTT reagent' was prepared by adding 1ml of PBS (pH 7.2) to 5mg of MTT (MTT 3-(4,5-dimethylthiazol-2-yl)-2,5-diphenyltetrazolium bromide) (Life Technologies) and vortexing. 100μl (approximately $2x10^5$ cells) of the treated cells were placed in triplicate in a 96 well flat bottomed plate. Additionally an empty well and a medium-only well were included on the plate to act as controls. 20μl of the MTT reagent was added to each well as required and left for 3 hours under standard cell culture conditions. 100μl of the MTT lysis buffer (0.01M HCl (hydrochloric acid), 10% of sodium dodecyl sulphate *(*SDS, Sigma-Aldrich)) was added to the appropriate wells and left overnight under standard cell culture conditions. The plate was then read on a spectrophotometer at a wavelength of 575nM to determine cellular proliferation.

2.9 Western Blotting

2.9.1 Lysate Preparation

Lysates were prepared using 1×10^7 cells incubated on ice. First, cells were washed in PBS before being pelleted by centrifugation for 5 minutes at 770g and a protease inhibitor mix added **(Table 2.5)** before addition of 10µl of lysis buffer per 1×10^6 cells **(Table 2.6)**. The mixture was vortexed before being sonicated (using a water sonicator at 4°C) 5 times at 30 second intervals with a 30 second break in between. The mixture was then spun down at 12000g for 5 minutes at 4°C and the supernatant was transferred into a fresh tube for subsequent protein determination **(see Section 2.9.3)**.

Table 2.6 Protease inhibitors used in lysate preparation	
Protease Inhibitors used	**Materials**
Protease inhibitor	1mg/ml Chymostatin; dissolved in DMSO 1mg/ml Leupeptin; dissolved in H_2O 1mg/ml Aprotonin; dissolved in H_2O 1mg/ml Pepstatin A; dissolved in DMSO 1mg/ml Antipain; dissolved in H_2O (all purchased from Sigma)
Phosphatase and protease inhibitors	Purchased from Roche (Basel, Switzerland)

Table 2.7 Lysis buffers used in lysate preparation

Lysis Buffer	Materials
SDS Lysis Buffer	1% SDS: 100µl of 10% SDS solution or 0.1g SDS 50mM Tris pH 6.8: 1.2ml of 0.5M Tris 5mM EDTA pH 6.8: 0.5ml of 0.1 EDTA 1ml of 10% Glycerol 7.2ml of H_2O
RIPA Lysis Buffer	100mls PBS 1% nonyl phenoxypolyethoxylethanol (NP40) 0.5% Sodium deoxycholate 0.1% SDS

2.9.2 Nuclear/Cytoplasmic Extraction

Nuclear extraction was carried out to separate the cytoplasmic and nuclear compartments of the cell to distinguish protein localisation. Two methods were tested which were as follows;

Method 1: Performed using a Nuclear Extract Kit (Active Motif, Kilkenny, Ireland) on ice. $2x10^7$ cells were spun down for 5 minutes at 770g. The supernatant was removed and the cells were washed twice with ice cold PBS/phosphatase inhibitors (1.6ml 10xPBS, 13.6ml ddH$_2$O, 0.8ml phosphatase inhibitors) in a pre-chilled 15ml conical tube. The samples were spun down and the supernatant was discarded and cell pellet was kept on ice to progress and prepare the cytoplasmic fraction.

Next the cells were gently resuspended in 500µl of 1x hypotonic buffer (100µl 10x hypotonic buffer, 0.9ml ddH$_2$O). The suspension was then transferred to a pre-chilled 1.5ml Eppendorf tube and incubated for 15 minutes on ice. 25µl of provided detergent was added and the suspension was vortexed for 10 seconds at maximum setting. Then the suspension was centrifuged for 30 seconds at 14000g in a microcentrifuge pre-cooled at 4°C. The supernatant which contains the cytoplasmic fraction was transferred into a pre-chilled Eppendorf tube and stored at -80°C until it was ready to be used. The cell pellet left was then used for nuclear fraction collection.

To get the nuclear fraction, the cell pellet was resuspended in 50µl of Complete Lysis Buffer (10µl 10mM DTT, 89µl lysis buffer AM1, 1µl protease inhibitor cocktail) and vortexed for 10 seconds at maximum setting. The suspension was incubated for 30 minutes on ice on a rocking platform set at 150rpm, before being vortexed for 30 seconds at maximum speed. The suspensions were spun down for 10 minutes at 14000g in a microentrifuge pre-cooled at 4°C and the supernatant which contains the nuclear fraction was transferred into a pre-chilled Eppendorf tube and stored at -80°C until it was ready to be used.

Method 2: Cells were pelleted by centrifugation before being resuspended in 100µl of pre-cooled cytoplasmic lysis buffer per 10^6 cells (1% Triton, 10mM Tris at pH7.4, 150mM NaCl, and protease inhibitors). The suspension was incubated on ice for 10 minutes and then spun at 4000g for 10 minutes at 4°C. The pellet obtained is the

nuclear compartment. The supernatant was removed as the cytoplasmic fraction and transferred into a separate Eppendorf tube. The nuclear pellet was then resuspended in 300µl of the cytoplasmic buffer to remove any residual cytoplasmic contamination and then spun again at 4000g for 10 minutes at 4°C. The supernatant was discarded and the pellet resuspended in 100µl of SDS lysis buffer per 10^6 cells. This was then sonicated as per the normal lysate protocol.

2.9.3 Protein Determination

Protein determination was performed according to manufacturer's recommendations (Bio-Rad, Hemel Hempstead, Hertfordshire). Firstly a set of standards were made to determine the unknown quantity of protein in the lysates. This was done using the required lysis buffer made to a stock of 10µg with 0.1% BSA in 10ml lysis buffer. The following dilutions were made to get the corresponding protein quantities **(Table 2.7)**.

Table 2.8 Protein determination standards		
Final Concentration (µg/ml)	**BSA Stock (10µg/ml)**	**1% Lysis Buffer**
0	(1000µl ddH$_2$0)	
0.5	50µl	950µl
1	100µl	900µl
1.5	150µl	850µl
2	200µl	800µl
2.5	250µl	750µl
3	300µl	700µl

A 96 well flat bottom plate was used loading 5µl of both the standards and lysates in triplicate to the wells. 25µl of the working reagent was then added (20µl of reagent S per ml of reagent A), followed by 200µl of reagent B, each as supplied in the kit. The plate was then left in the dark for 15 minutes, and read on a spectrophotometer at a wavelength of 670nM. The quantity of protein was then calculated using Microsoft Excel using the linear equation generated by the standards to convert the lysate's absorbance to protein quantity.

2.9.4 Gel Electrophoresis

Prior to loading, each sample was aliquoted with double strength SDS buffer (DSSB) before being heated for 5 minutes at 95°C. Simultaneously a polyacrylamide gel was set with a 12% resolving gel (3.5ml separating gel buffer, 7ml acrylamide, 3.5ml H_2O, 75µl 10% ammonium persulphate (APS, Sigma-Aldrich), 15µl tetramethylethylenediamine (TEMED)) and a 5% stacking gel (1.5ml stacking buffer, 1ml acrylamide, 3.5ml H_2O, 50µl 10% APS, 15µl TEMED). Samples were then loaded into the gels alongside a pre-stained protein ladder (Bio-Rad), which were then submerged in 1x electro buffer (25mM Tris, 192mM glycine, 0.1% SDS, diluted 1:10) and run at 35mA per gel for approximately 90 minutes.

2.9.5 Membrane Transfer

Subsequent to gel electrophoresis, the gel was removed from the running apparatus and the stacking gel was removed. A transfer cassette was then assembled according to manufacturer guidelines (Bio-Rad) which contained a layer of polyvinylidene difluoride

(PVDF, Bio-Rad) membrane soaked in 100% methanol. The cassette was placed in a transfer tank next to an ice pack and covered in transfer buffer (25nM Tris, 0.2M glycine) with due regard to electrode placement to ensure protein transfer to the membrane. The transfer was then carried out at 400mA for 60 minutes.

2.9.6 Antibody Incubation

When the membrane transfer was complete, the PVDF membrane was removed from the cassette and blocked in 5% ECL Prime blocking reagent (GE Healthcare, Little Chalfont, Buckinghamshire) made up in TBS-T (Tris 20mM, NaCl 150mM, Tween20 (0.1%), pH7.5) for 60 minutes at room temperature with rocking. The required antibodies **(see Table 2.8)** were then added directly to the milk and incubated for a minimum of 90 minutes at room temperature with rocking. Next the membrane was washed four times every 10 minutes in TBS-T. The appropriate secondary antibody was then added to the membrane (0.4µg/ml in 3% ECL Prime blocking milk in TBS-T) and incubated for a minimum of 30 minutes at room temperature with rocking. The membrane was then again washed four times every 10 minutes in TBS-T before being developed. ECL advance (GE Healthcare) was applied to the membrane for 1 minute, before membrane exposure and band visualisation using UNITEC Alliance 2.7 software.

Table 2.9 Antibodies used for western blot analysis

Primary Antibody	Concentration	Secondary Antibody	Molecular Weight (kDa)
Total-β-catenin (CST)	8ng/ml	Anti-rabbit IgG	92
Unphosphorylated β-catenin (Millipore)	1 µg/ml	Anti-mouse IgG	86
Phospho-β-catenin (S45/T41) (CST)	0.115 µg/ml	Anti-rabbit IgG	92
Phospho-β-catenin (Tyr654) (Abcam)	0.1 µg/ml	Anti-mouse IgG	86
Total GSK3β (BD)	0.25 µg/ml	Anti-mouse IgG	46
Phospho-GSK3α/β (Ser21/9) (CST)	0.3 µg/ml	Anti-rabbit IgG	α: 51 β: 46
Phospho-GSK3β (Tyr216) (Abcam)	1µg/ml	Anti-rabbit IgG	47
MCL-1 (SCB)	0.2 µg/ml	Anti-rabbit IgG	Long: 40 Short: 32
Anti-β-Actin (Sigma)	0.2 µg/ml	Anti-mouse IgG	42

Anti-mouse IgG, HRP-linked Antibody (CST, #7076)

Anti-rabbit IgG, HRP-linked Antibody (CST, #7074)

2.9.7 Membrane Stripping

Stripping buffer was made using 12.1g of 1M Tris, 10ml of 20% SDS, made up to 100ml with H_2O. 10ml of this was used per membrane to which 70µl β-mercaptoethanol was added. The ECL from previous exposure was washed off with 1xTBS-T and the membrane was added to a sealed bag with the stripping buffer and heated to 55°C for

10 minutes. The stripping buffer was then washed off with 1xTBS-T three times. The membrane was then cleared to be reprobed.

Monoclonal Anti-β-Actin antibody (Sigma) **(Table 2.8)** was used as a loading control on blots. The membrane was blocked in 5% ECL Prime blocking reagent (GE Healthcare) as per western protocol **(Section 2.9.6)**, and then incubated with the β-actin antibody at a 1:10,000 dilution for 1 hour at room temperature. After washing, the membrane was incubated with anti-mouse HRP (CST) for an hour at room temperature, washed again and then visualised as per western protocol **(Section 2.9.6)**.

2.10 Confocal Microscopy

Slides were prepared by coating in 10% poly-L-Lysine (Sigma) for 5 minutes. These were then allowed to dry at 37°C for 60 minutes. A circle of approximately $3cm^2$ was marked on the slide using a hydrophobic liquid blocker pen and allowed to dry for 30 minutes prior to adding the cells.

The cells were prepared as before for FACS analysis; cells ($\sim 5x10^5$) were fixed by resuspending in 500µl of 2% paraformaldehyde at pH 7.2 (VWR) for 10 minutes at 37℃. Cells were then centrifuged at 770g for 3 minutes. 500µl of 90% methanol (Fisher Scientific) was added to the cell pellet and the cells were vortexed and then incubated at room temperature for 30 minutes. Cells were then washed thoroughly with 1ml incubation buffer containing PBS and 0.5% BSA (Sigma-Aldrich), and centrifuged at 770g for 3 minutes. Cells were resuspended in 25µl incubation buffer and appropriate antibodies were added **(see Table 2.7)**. Cells were vortexed and incubated at room temperature for at least 45 minutes. Cells were then washed twice in incubation buffer and resuspended in 50µl incubation buffer containing 10µg/ml goat anti rabbit/mouse second Alexa Fluor 488 antibody (Invitrogen). Subsequently they were incubated at room temperature in the dark for at least 30 minutes, and then washed twice in incubation buffer. Finally the cells were resuspended in 50µl of incubation buffer and pipetted onto the appropriate slide. The slides were left in the dark overnight at 4°C for the cells to adhere to the slides. Before analysis 10µl of CyGel (BioStatus Limited, Shepshed, Leicestershire) was added to a cover slip and pressed firmly onto the slide to avoid air bubbles. The slides were then ready to be analysed by the Zeiss Confocal LSM

710. Images were analysed using Zen software and all images for each antibody were taken together using the same detector settings. The following settings were used for analysis; Plan-Apochromat 63x/1.4 oil DIC M27 objective was used with a 488 laser. Detector Ch1 was selected for use with a rainbow coarse spectrum and the 1024x1024 frame size.

Table 2.10 Antibodies used for Confocal Microscopy			
Primary Antibody	**Concentration**	**Control Antibody**	**Secondary Antibody**
Unphosphorylated β-catenin (Millipore)	0.1μg/ml	Mouse IgG_1	Alexa Fluor 488 Mouse
Phospho-β-catenin (S45/T41) (CST)	0.4 μg/ml	Rabbit IgG	Alexa Fluor 488 Rabbit
Phospho-β-catenin (S33/37/T41) (CST)	0.4 μg/ml	Rabbit IgG	Alexa Fluor 488 Rabbit
Phospho-β-catenin (Tyr654) (Abcam)	0.25μg/ml	Mouse IgG_1	Alexa Fluor 488 Mouse

Mouse IgG_1 (BD Biosciences, #349040)
Rabbit IgG (R&D Systems, #AB-105-C)
Alexa Fluor 488 Goat Anti-Mouse IgG (H+L) (Life Technologies, #A-11001)
Alexa Fluor 488 Goat Anti-Rabbit IgG (H+L) (Life Technologies, #A-11001)

2.11 Statistical Analysis

Two tests for statistical analysis were used. The student T-test using Microsoft Excel was used when testing two independent or paired groups of data which had a normal distribution. The Mann-Whitney u test using SPSS was used to test two independent samples that were not normally distributed. Bonferroni correction was used when comparing the various patient cohorts to allow for multiple comparisons.

Chapter 3 - The role of β-catenin in CML outcome

3.1 Introduction

Beta-catenin acts as an essential protein in the Wnt/β-catenin signalling pathway by playing a central role in the regulation of transcriptional activation. It has previously been described in CML that β-catenin is key in the preservation of LSCs by its involvement in self-renewal [151, 185].

Beta-catenin is a non-enzymatic protein whose activity in the Wnt/β-catenin signalling pathway is controlled by its phosphorylation status [105]. On interaction within a complex known as the 'destruction complex' its action is prevented, and β-catenin is targeted for destruction via the proteasome. The destruction complex consists of multiple proteins including Axin which acts as a scaffold protein, and CK1 and GSK3β which phosphorylate β-catenin. CK1 first 'primes' β-catenin by phosphorylation on Ser45, which then allows for phosphorylation on Thr41, Ser37 and Ser33 by GSK3β [135]. This series of phosphorylation events enables the ubiquitin ligase, β-TrCP, to recognise β-catenin as a target for ubiquitinated degradation by the proteasome [135]. When this destruction complex is disrupted/prevented, phosphorylation of β-catenin cannot occur, leaving β-catenin un-phosphorylated at these key sites [106]. The translocation of β-catenin into the nucleus can consequently occur, whereby it can

associate with the transcription factors TCF and LEF [114, 115]. As a result it can then activate the transcription of multiple genes including c-Myc and cyclin D1 [122, 123].

Other phosphorylation sites of β-catenin which are of high relevance to CML are on the tyrosine residues 86 and 654. These sites can be directly phosphorylated by BCR-ABL1 [186], stabilising β-catenin in its active conformation, and reducing the binding affinity of β-catenin to Axin preventing the action of the destruction complex. This allows for translocation into the nucleus and activation of transcription due to enhanced binding ability to the transcription factor TCF4. It has been shown that imatinib retains this form of β-catenin in the cytoplasm by increasing its binding affinity to Axin and subsequently enables the degradation of β-catenin [186].

A particularly interesting paper that investigated the role of β-catenin and its self-renewal capacity within CML was Jamieson *et al.,* [150]. They observed that the committed GMPs from CML patients who were either in blast crisis or who were resistant to imatinib had significantly increased levels of activated β-catenin in comparison to normal GMPs, and that these elevated levels of β-catenin correlated with the enhanced self-renewal capacity of the cells [150]. These results indicate that β-catenin may be important in CML progression and/or imatinib resistance by increased activity and consequent increased transcriptional activation.

The work of Jamieson *et al.*, [150] focussed on the levels of β-catenin in the GMP compartment. However, it was of interest to investigate if β-catenin levels are also

detectable in the later, more mature, MNCs as they are more readily available from the patient, easier to isolate, and less labour intensive and cheaper in terms of cost of purification. Furthermore, given that phosphorylation of β-catenin is needed for its degradation, it is important to also look at phosphorylated levels of β-catenin as these may indicate whether there is a fault in the degradation of β-catenin, which may be the reason for possible elevated levels. In addition to the phosphorylated forms which target β-catenin for degradation it is important for CML to look at BCR-ABL1 mediated β-catenin phosphorylation of Tyr654, to determine if BCR-ABL1 is having an effect on β-catenin turnover.

3.2 Aims

The aims of this chapter are;

1) To investigate whether β-catenin protein and/or mRNA expression levels can be predictive of clinical outcome in imatinib treated patients.

2) To determine if β-catenin phosphorylation status and degradation differ in relation to patient outcome.

3) To determine if BCR-ABL1 mediated β-catenin phosphorylation on Tyr654 correlates with disease progression.

4) To determine if high levels of β-catenin found in GMPs correlate with levels in MNC.

3.3 Optimisation of techniques

3.3.1 Optimisation of β-catenin (*CTNNB1*) mRNA analysis

3.3.1.1 Validation of the β-catenin primers by manual PCR

Manual PCR was performed **(Materials and Methods section 2.6.4)** to validate the primers being used for β-catenin detection. Patient samples were tested alongside a negative control (Neg Cont). Results showed that the primers were identifying the correct gene product with an amplicon length of 80Kb **(Figure 3.3.1)** and therefore were used in all further experimentation for the detection of β-catenin mRNA.

Figure 3.3.1 Validation of the β-catenin primers by manual PCR

Manual PCR was carried out using patient samples and a negative control to test whether the β-catenin primers are detecting the correct gene product. Results show a band at 80Kb in the patient samples indicating the accurate detection of β-catenin.
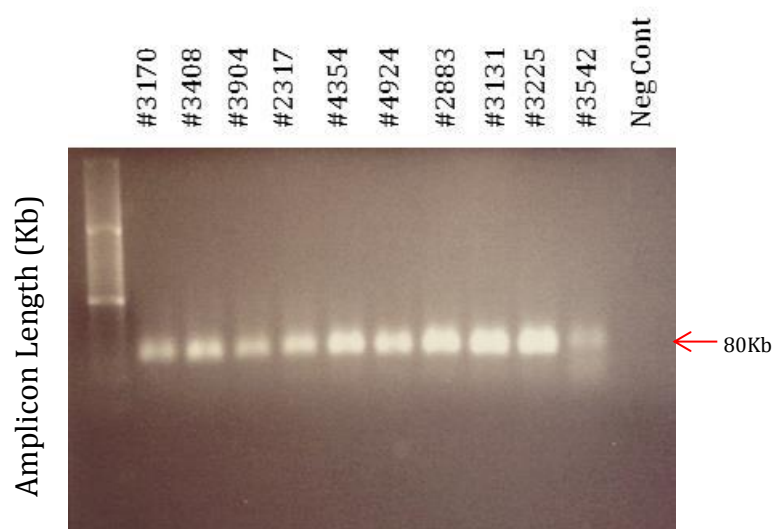
3.3.2 Optimisation of antibodies for the detection of β-catenin (CTNNB1) protein (using cell lines)

3.3.2.1 Optimisation of β–catenin antibodies by FACS

Cellular protein levels of β-catenin were determined using FACS **(Material and Methods section 2.7)**. Initially the CML cell lines were tested using 0.008μg/ml (concentration recommended by the company) of total β-catenin antibody **(Material and Methods, Table 2.4)** to determine which CML cell line had the highest β-catenin levels and could be used for further concentration optimisation experiments. Events were gated on the live cell population, as determined by forward and side scatter light properties, and antibody fluorescence was measured through this gate. The cell lines K562, LAMA-84, KCL-22, and KYO-1 were assessed **(Figure 3.3.2)**. Results show, as determined by the degree of fluorescence peak shift between test and control cells, that LAMA-84 cells have the highest β-catenin levels **(Figure 3.3.2 b)**.

Figure 3.3.2 Optimisation of the β-catenin FACS protocol in the CML cell lines; K562, LAMA-84, KCL-22 and KYO-1

A concentration of 0.008μg/ml of total β-catenin antibody was initially used to determine the optimum cell line to use for future concentration optimisation experiments. Results show this to be LAMA-84 cells.
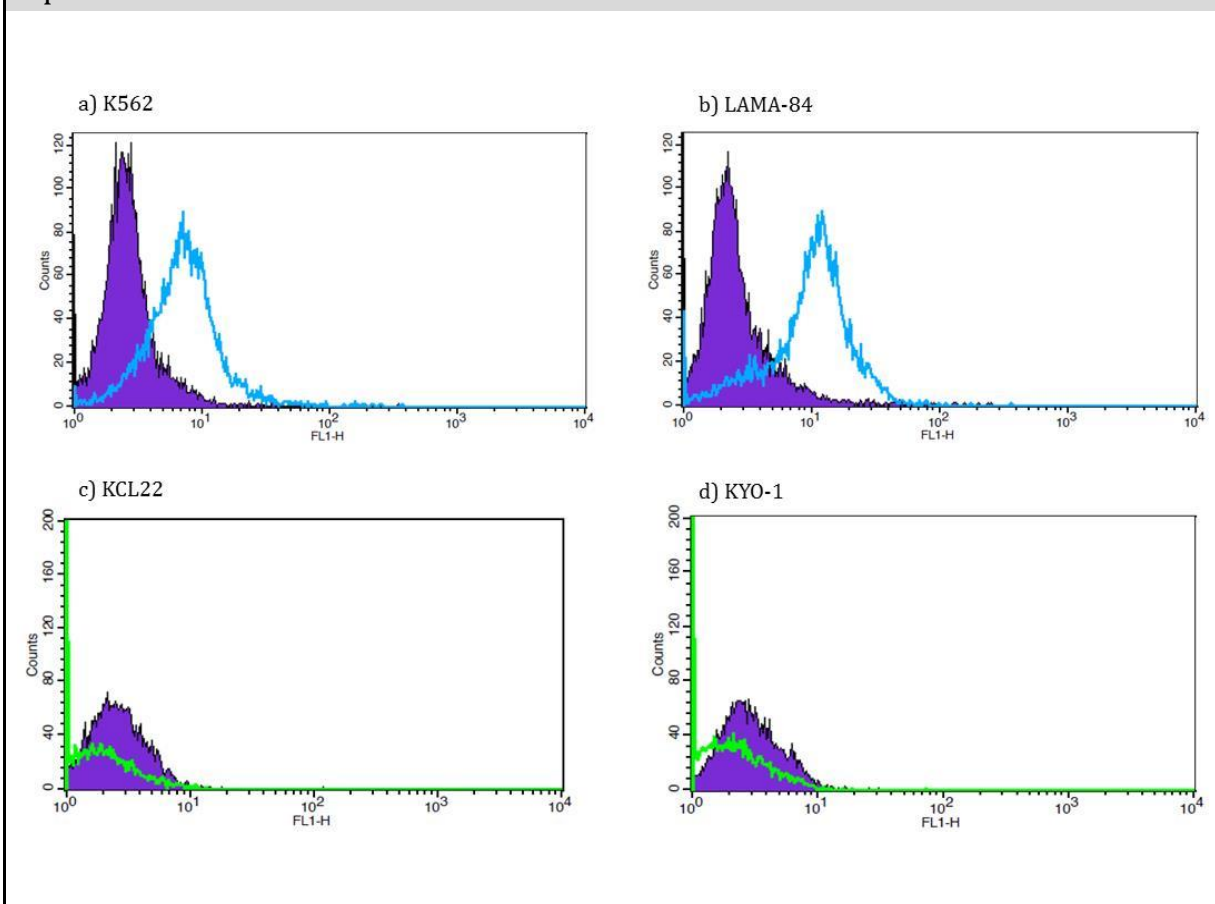
Using LAMA-84 cells, the optimum concentration of total β-catenin antibody was determined for subsequent use on primary material. **Figure 3.3.3A** shows that the optimum concentration, of those tested, for the total β-catenin antibody is 0.064μg/ml. However due to the expense of the antibody and the fact that there is still good peak separation at 0.032μg/ml, this concentration of antibody was used in all further experimentation.

In addition to testing total β-catenin, levels of unphosphorylated **(Figure 3.3.3 B)** and phosphorylated **(Figure 3.3.3 C and D)** forms of β-catenin were examined **(Material and Methods, Table 2.4)**. The unphosphorylated-β-catenin antibody binds β-catenin which is not phosphorylated on either Thr41 or Ser37, and targets the form of β-catenin which is considered to be 'active' [106] and can translocate to the nucleus to activate transcription. An initial dilution of 1:200 was made, and then six concentrations were tested. The results **(Figure 3.3.3B)** show that the optimum concentration, as determined by fluorescent peak shift, is a final concentration of 0.1µg/ml.

Phospho-β-catenin antibody (Ser45/Thr41) detects β-catenin phosphorylated on residues Ser45 (via the action of the kinase CK1) and Thr41 (via the action of GSK3β) and represents the form of β-catenin targeted for degradation by the proteasome [135]. **Figure 3.3.3C** indicates that the optimum antibody concentration to use for this antibody is a final concentration of 0.4µg/ml.

Finally, phospho-β-catenin antibody (Tyr654) was used to represent the form of β-catenin phosphorylated directly by BCR-ABL1, which functions by targeting β-catenin to the nucleus [186]. The optimum antibody concentration to proceed with was a final concentration of 0.5µg/ml **(Figure 3.3.3D)**. However, again due to the expense of the antibody and the fact there is still good peak separation at 0.25µg/ml, this concentration of antibody was used in all further experimentation.

Figure 3.3.3 Optimisation of β-catenin antibodies concentration in LAMA-84 cells

Antibodies optimised include:

A) Total β-catenin - optimum antibody concentration is 0.064μg/ml.

B) Unphosphorylated β-catenin - optimum antibody concentration to continue with is 0.1μg/ml.

C) Phospho-β-catenin(Ser45/Thr41) - optimum antibody concentration to use is 0.4μg/ml.

D) Phospho-β-catenin(Tyr654) - optimum antibody concentration is 0.5μg/ml.
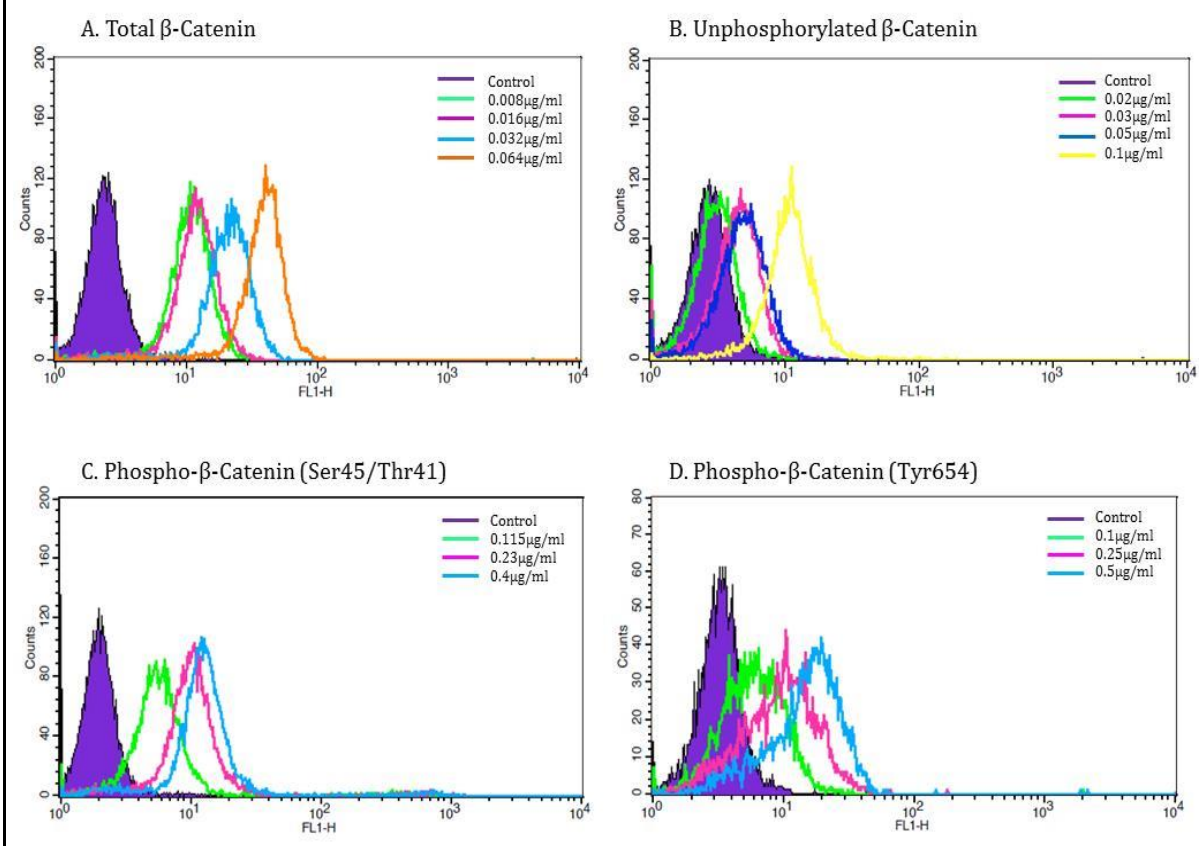
3.3.2.2 Optimisation of the western blotting technique with the β-catenin antibodies

The technique of western blotting **(Materials and Methods section 2.9)** was used to study the levels of β-catenin and its phosphorylated variants as confirmation of FACS derived data. The three CML cell lines K562, LAMA-84 and KCL22 were used, as was the colon cancer cell line HT-29, which is known to demonstrate over-expression of Wnt signalling [187, 188] which was included as a control. Multiple cell lysis buffers were also utilised during optimisation of signal detection e.g. SDS and RIPA lysis buffers. Three protein lysate concentrations were tested on loading; 10μg, 15μg and 20μg, and antibody dilutions from 1:4000 to 1:1000 were tried. Additionally, membranes were incubated overnight either at room temperature, to maximise the kinetics of the reaction, or at 4°C. Following initial experimentation further modifications were made to the preparation of lysates in order to enhance signal detection. These included using a water bath sonicator instead of a probe sonicator, meaning lysates were sonicated more efficiently. Also lysates were spun down following sonication and the supernatant was used to remove residual membrane contamination of the lysate which meant achieving a cleaner blot. In addition, when incubating the membrane with the antibodies, the antibody was added directly to the blocking buffer instead of diluting the blocking buffer in TBS-T before addition of the antibody. This again ensured a cleaner blot on development by decreasing background noise.

Figure 3.3.4 shows the results achieved via western blotting of whole cell lysates. Results show that although total-β-catenin and unphosphorylated β-catenin are readily detectable in HT29 cells, they are difficult to detect in the CML cell lines tested.

Phospho-β-catenin(Ser45/Thr41) was higher in the CML cell lines compared to HT-29 cells. Phospho-β-catenin(Tyr654) appeared to be absent from all cell lines, however it would not be predicted to be found in HT-29 cells, as Tyr654 phosphorylation of β-catenin is BCR-ABL1 dependent.

Figure 3.3.4 Optimisation of the β-catenin antibodies by western blotting in the CML cells lines K562, LAMA-84 and KCL22 alongside HT-29 colon cancer cells
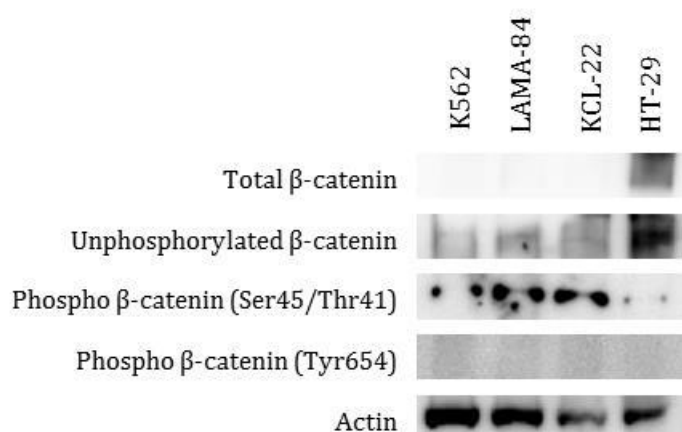
Overall, β-catenin did not prove to be easily detectable via western blot therefore it was decided to use another experimental technique and confocal microscopy was optimised.

3.3.2.3 Optimisation of the β-catenin antibodies using confocal microscopy

Protein levels of the various forms of β-catenin were also analysed by confocal microscopy. As the LAMA-84 cell line was shown to have the highest β-catenin protein levels via FACS analysis this cell line was used for confocal optimisation. The same antibody concentrations used for FACS analysis were used for confocal microscopy. Single slice images from different cells were used to show maximum signal and results show **(Figure 3.3.5)** all forms of β-catenin are detectable by confocal microscopy.

Key: Rainbow

Figure 3.3.5 The optimisation of β-catenin antibodies by confocal microscopy in LAMA-84 cells
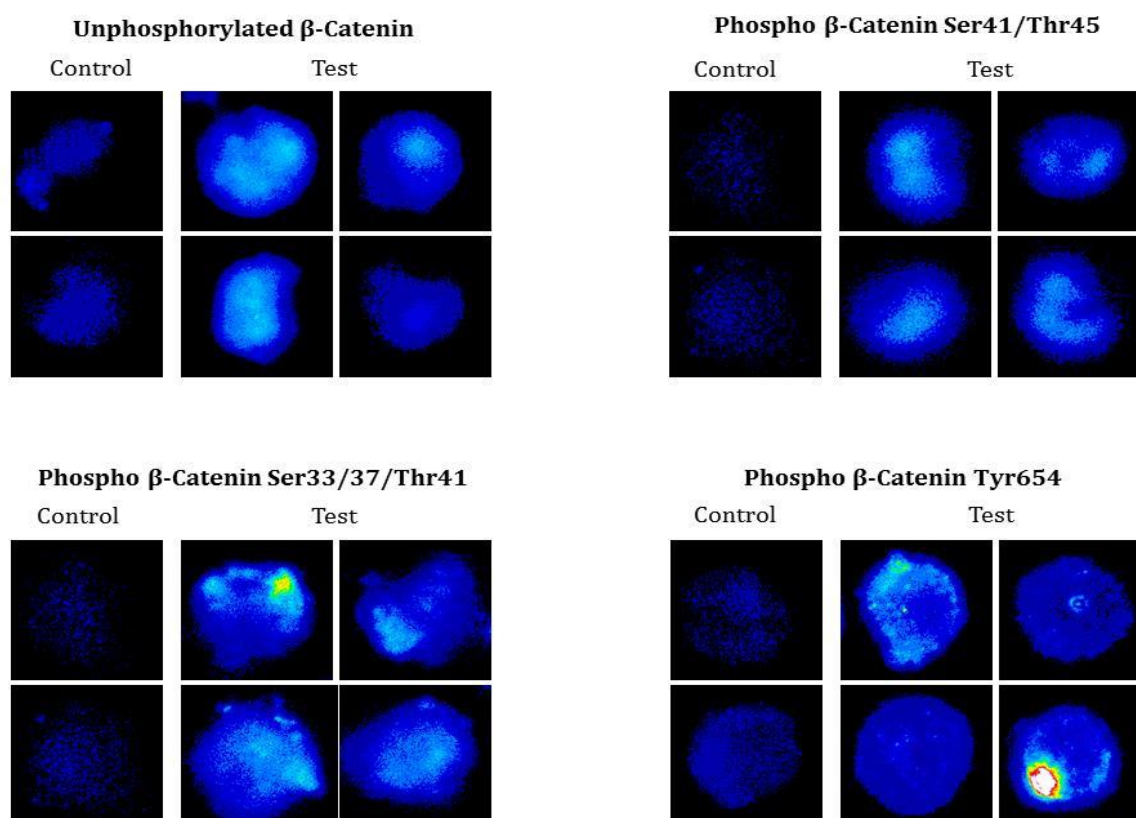
3.3.2.4 Optimisation of *in vitro* bortezomib treatment in cell lines

K562 and LAMA-84 cells were incubated *in vitro* with bortezomib for 24 and 48 hours using a range of concentrations (0.1μM, 1μM and 5μM) **(Materials and Methods section 2.3.3)**. Cellular viability following treatment was tested by propidium iodide (PI) exclusion, as determined by FACS analysis (N=3), and a MTT tetrazolium colourimetric assay **(Materials and Methods section 2.7 and 2.8)** to determine the drug's effect on cell proliferation (N=3) **(Figure 3.3.6)**. From results, it was decided to use 24 hours incubation for all further experiments.

Figure 3.3.6 The effects of bortezomib on cell viability measured by PI/FACS and MTT assay

Cells were incubated with bortezomib for 24 and 48 hours to test its effect on cell viability and cell proliferation. Results show incubation with 5μM of bortezomib for 24 hours was optimum (N=3).
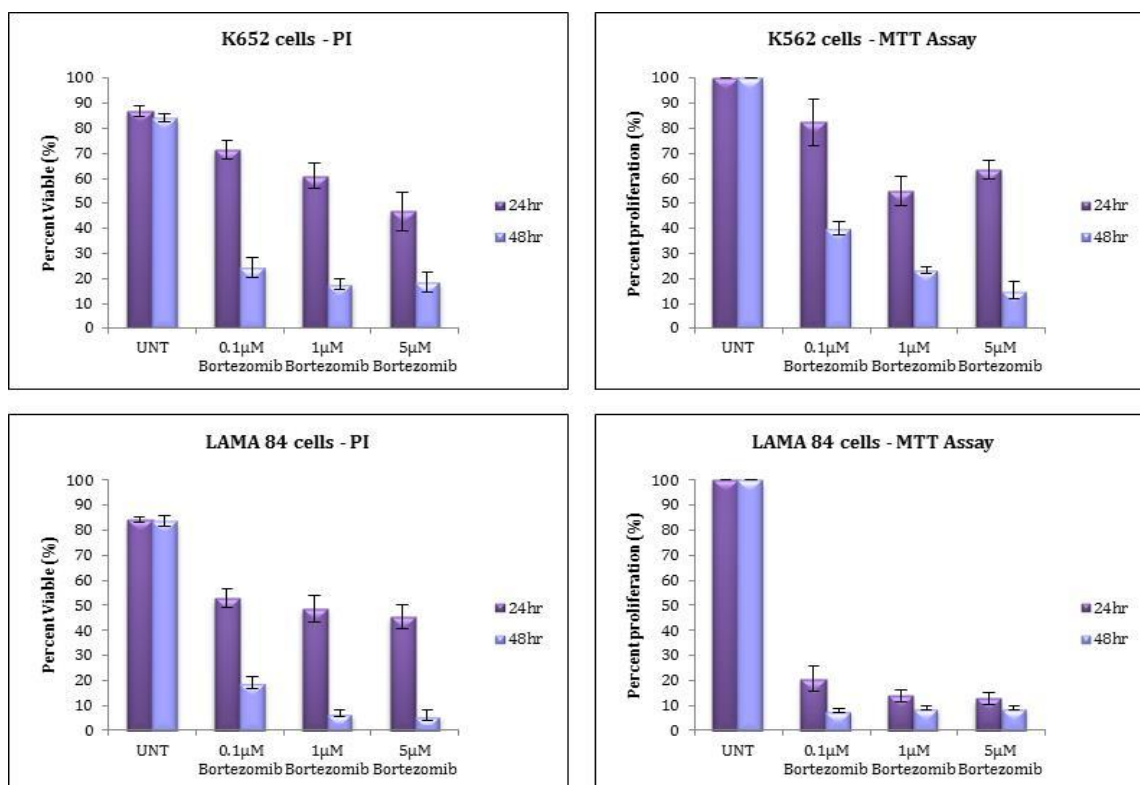
3.4 Results

Having optimised β-catenin detection in cell lines, the next stage was to detect and compare β-catenin and its phosphorylated variants in different clinical scenarios relevant to treatment outcomes in CML. Blood samples were taken from patients and the MNCs were extracted and frozen down to be stored in the Liverpool biobank **(Materials and Methods section 2.2.2)**. On use of this material, the samples were thawed and allowed to recover overnight before experimentation was carried out.

Patient samples were split into three patient outcome cohorts in line with the ELN definitions [41] (as described in **section 1.4.2**); optimal responders, failure patients and blast crisis patients. Patients who would be classified as 'sub-optimal' (ELN recommendations 2009 [43]) or warning (ELN recommendations 2013 [41]) were not included in analysis. For mRNA levels, patient material was available from both optimal responders and failure patients at diagnosis and 12 months, and from patients who subsequently transformed into blast crisis at diagnosis, 12 months and when they had transformed into blast crisis. For protein levels, patient material was available for both optimal responders and failure patients at both diagnosis and 12 months. However, for patients who subsequently transformed into blast crisis, material was only available from when they had transformed into the final stage of the disease due to limitations on resources at diagnosis.

3.4.1 Protein levels of β-catenin are elevated in primary CML material

To determine whether investigation into β-catenin levels was worthwhile, the protein levels of β-catenin and its phosphorylated forms were investigated in primary CML MNCs by FACS analysis **(Materials and Methods section 2.7)** and confocal microscopy **(Materials and Methods section 2.10)**. Due to the difficulty with optimising the western blot technique, this was not performed. Results showed that the levels of β-catenin and its phosphorylated forms are elevated in primary CML MNCs (representative images shown in **Figure 3.4.1**) therefore it was considered relevant to continue with this line of investigation to determine if there is a difference in β-catenin mRNA and protein levels between patient outcomes.

Figure 3.4.1 Protein levels of β-catenin are elevated in primary CML material

The levels of β-catenin were measured by FACS and confocal in primary CML material showed there is elevated levels of total β-catenin (A.) unphosphorylated β-catenin (B.) phospho-β-catenin (Ser45/Thr41) (C.) and phospho-β-catenin (Ser33/37/Thr41) (D.)
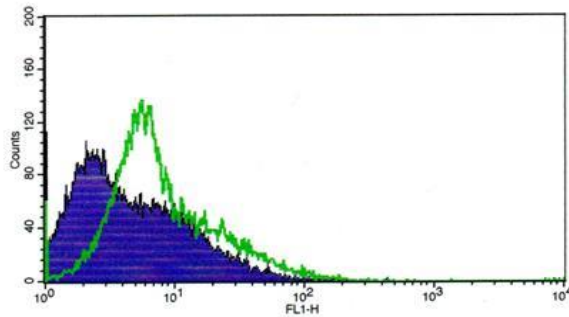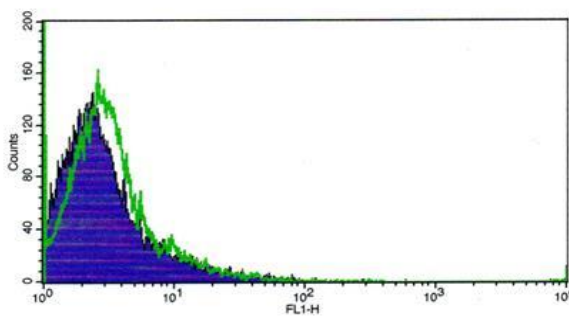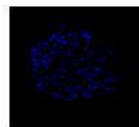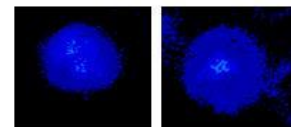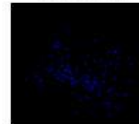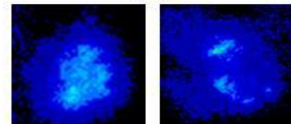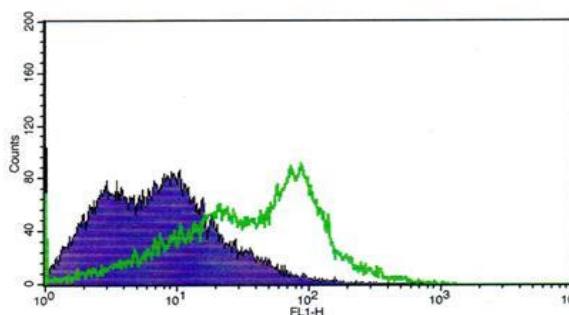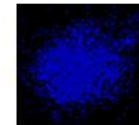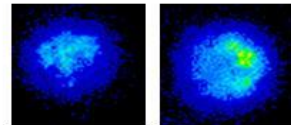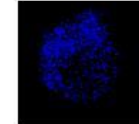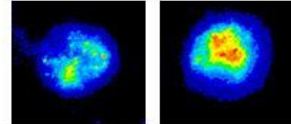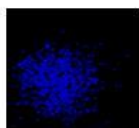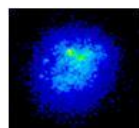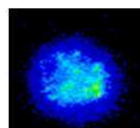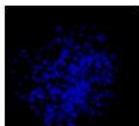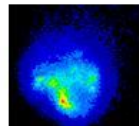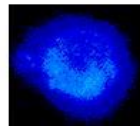
3.4.2 Comparison of β-catenin mRNA levels between different CML clinical groups

3.4.2.1 mRNA transcript levels of β-catenin demonstrate no correlation with predicting patient outcome

Initially, mRNA transcript levels of β-catenin were investigated in imatinib treated patients to determine if there was a difference between patient cohorts. Both diagnostic and 12 month samples were studied from each cohort, as well as samples from patients who had transformed into blast crisis. At diagnosis results showed that β-catenin expression was elevated in CML patients compared to healthy individuals. When comparing patient cohorts at initial diagnosis of chronic phase there was no distinguishable difference between the groups **(Figure 3.4.2)**. Beta-catenin levels appeared to be reduced after 12 months of standard imatinib treatment (400mg/day) to a level similar to that seen within healthy individual samples. This reduction could be anticipated as the leukaemic cell burden is replaced with non-leukaemic cells following treatment. Interestingly there is a reduction in β-catenin levels in optimal responders and failure patients after 12 months treatment. . This finding could be a reflection of altered morphology and cell make up after 12 months imatinib treatment. Notably, β-catenin mRNA levels of transforming patients initially reduce on imatinib treatment, but then rise again at transformation to levels similar to those found in those patients at initial diagnosis.

Figure 3.4.2 mRNA expression levels of β-catenin do not correlate with patient outcome in imatinib treated patients

mRNA expression levels of patient MNC samples were measured in optimal, failure and blast crisis patients at both diagnosis (N=19, 6 and 6 respectively) and 12 months (N=19, 6 and 5 respectively), and in addition when patients were in blast crisis (N=6). Levels were also measured in four healthy individual MNC samples as a comparator with patient results.

Results showed no correlation between mRNA expression at diagnosis and patient outcome to treatment. As expected, levels decrease after treatment, with the exception of blast crisis patients where the levels rise again at transformation into blast crisis.
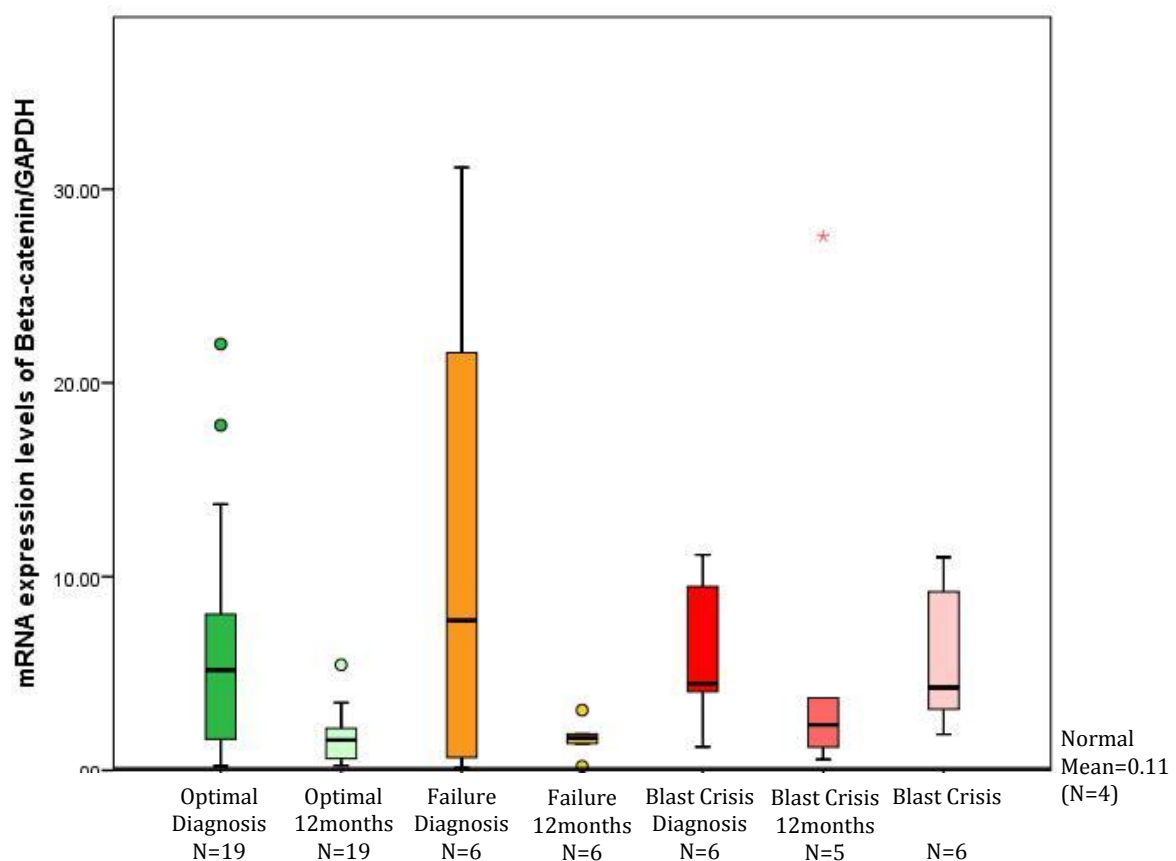
3.4.2.2 mRNA transcript levels of β-catenin demonstrate no correlation with patient progression

When comparing β-catenin mRNA levels between samples taken from patients in chronic phase and those actually in blast crisis, the data show no difference in the levels of β-catenin mRNA **(Figure 3.4.3)**. This indicates that mRNA expression of β-catenin does not change between disease stages, suggesting that protein levels may be more important in distinguishing between disease states in MNCs.

Figure 3.4.3 mRNA expression levels of β-catenin do not correlate with disease progression in imatinib treated patients

mRNA levels were stratified according to chronic phase (N=30) or blast crisis (N=6). Results showed there was no significant difference between the two groups indicating β-catenin mRNA levels do not alter at disease progression.
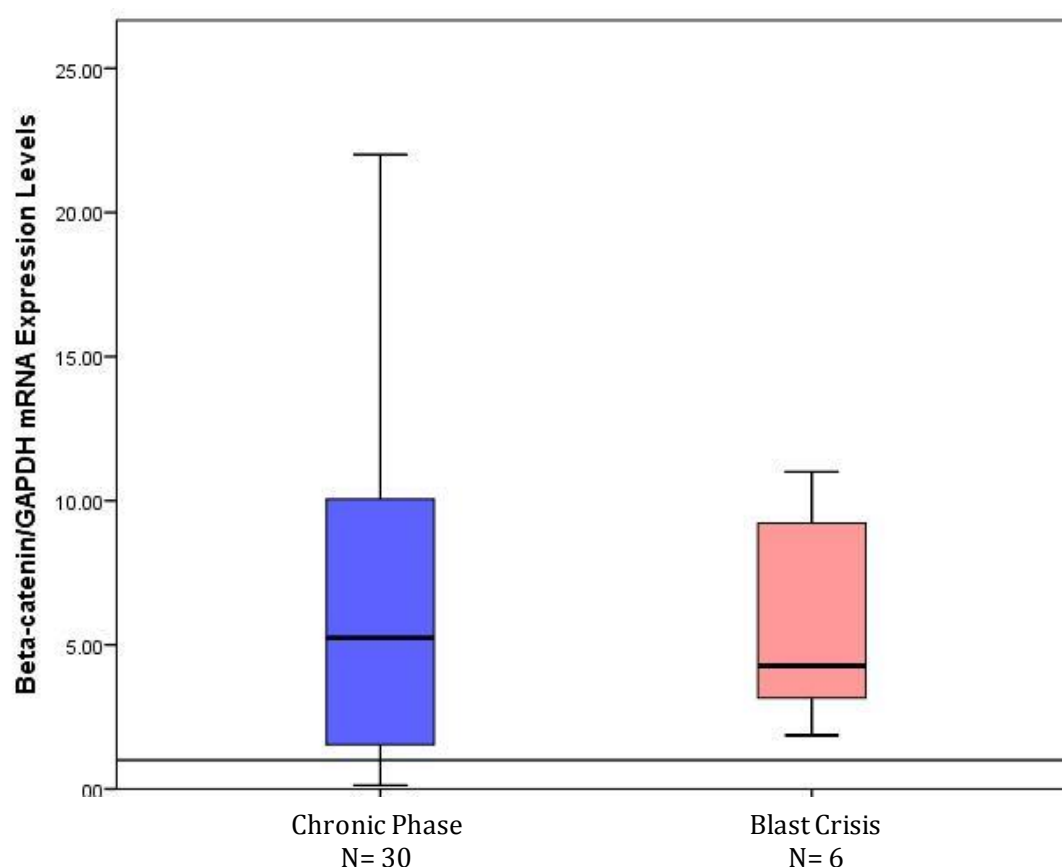
3.4.2.3 Imatinib decreases β-catenin mRNA expression *in vitro*

To investigate the effects that imatinib is having on the levels of β-catenin mRNA expression, LAMA-84 cells were cultured with imatinib for 24 hours **(Materials and Methods section 2.2.3)** and cDNA was extracted (N=3) **(Materials and Methods section 2.6.1 and 2.6.2)**. Results show that imatinib reduces the levels of β-catenin expression in vitro (P=0.069) **(Figure 3.4.4)** indicating that imatinib can act either directly or indirectly on β-catenin to alter its expression levels.

Figure 3.4.4 Imatinib reduces β-catenin mRNA levels *in vitro*

LAMA-84 cells were incubated with IM in vitro for 24 hours to determine the effect on β-catenin mRNA levels (N=3). Results show that IM reduces the expression of β-catenin in comparison to untreated (P=0.069).
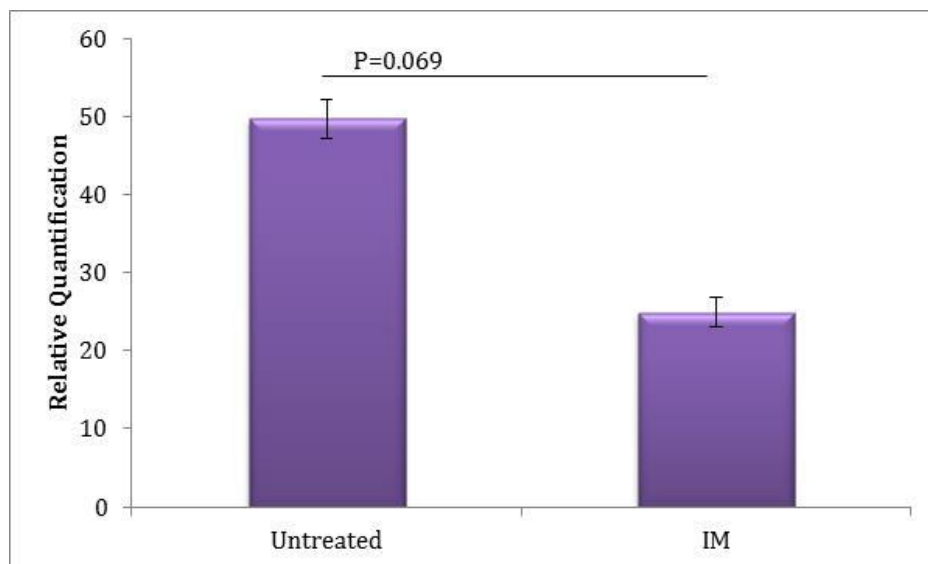
3.4.2.4 mRNA transcript levels of β-catenin in patients treated with dasatinib or nilotinib

The data of **Figures 3.4.2** and **3.4.3** were derived from patients receiving imatinib treatment. Subsequently, the levels of β-catenin expression were also studied in a group of patients who received either dasatinib or nilotinib from original diagnosis. As with imatinib treatment (P=0.006, **Figure 3.4.2**) β-catenin expression was significantly lower after 12 months of dasatinib and nilotinib treatment in the optimal responders (P=0.05 and 0.001 respectively) **(Figure 3.4.5)**. This adds to the premise that patients who respond well to treatment, irrespective of what type of drug they receive, have a significant reduction in their β-catenin levels, which could be due to changes in the constituent cell population. The decrease in β-catenin expression was not statistically significant in patients who failed dasatinib treatment (P=0.06, N=2), possibly due to the small cohort studied. No patients failed nilotinib treatment so trends in β-catenin expression between different response groups treated with these second generation drugs could not be assessed. Similarly no patients progressed to blast crisis when receiving either dasatinib or nilotinib.

Figure 3.4.5 mRNA expression levels of β-catenin in patients treated with the second generation TKIs dasatinib and nilotinib

The levels of β-catenin mRNA were determined in patients treated with either dasatinib or nilotinib. Results show that in the optimal responders β-catenin levels significantly reduced after 12months treatment (dasatinib P=0.05, nilotinib P=0.001). There was no significant difference between the optimal responders and failure patients at diagnosis who were treated with dasatinib. This could not be assessed in nilotinib treated patients as there were no patients who had failed treatment. Additionally, no patients transformed to blast crisis on either drug.
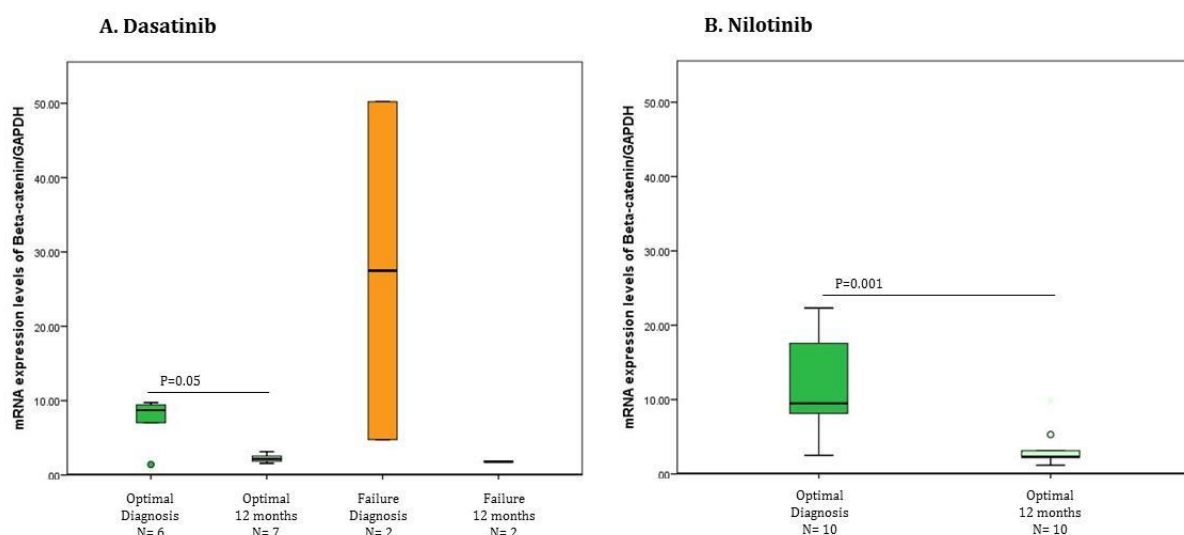
3.4.3 Comparison of β-catenin total protein levels between the different CML clinical groups

Following investigation of β-catenin mRNA expression levels and the observation that they have no value as either a prognostic marker for subsequent blast crisis or as an indicator of disease progression, the total β-catenin protein levels were next examined by FACS analysis **(Materials and Methods section 2.7)**. Events were gated on the live cell population, as determined by forward and side scatter light properties, and antibody fluorescence was measured in this gate.

3.4.3.1 Protein levels of total β-catenin demonstrate no correlation with predicting patient outcome or disease transformation

Total levels of β-catenin were initially investigated to determine if there was a change in overall levels of total β-catenin between patient cohorts. The results were analysed in accordance with patient outcome, with optimal response and failure patients being analysed at diagnosis and 12 months, and blast crisis patients being analysed when patients had transformed into blast crisis.

Figure 3.4.6 shows that in patients at diagnosis the levels of total β-catenin were higher than those observed in normal MNC, and did not alter significantly following 12 months of imatinib treatment. Interestingly, the total level of β-catenin protein in patients transformed into blast crisis was similar to healthy individuals. Overall, the results

indicate that total levels of β-catenin protein cannot be used to distinguish between different patient cohorts on imatinib treatment.

Figure 3.4.6 Protein levels of total β-catenin do not correlate with patient outcome in imatinib treated patients

Using MNC samples protein levels of total β-catenin were measured in optimal (N=7), and failure patients (N=7) at diagnosis and following 12 months of treatment (N=6 and 5 respectively). In addition samples taken when patients were in blast crisis (N=6) were also tested. Levels were also measured in MNC samples from healthy individuals (N=6). Results showed higher levels at both diagnosis and following 12 months imatinib treatment compared to healthy MNCs. The total level of β-catenin protein in patients transformed into blast crisis was similar to that in cells from healthy individuals.
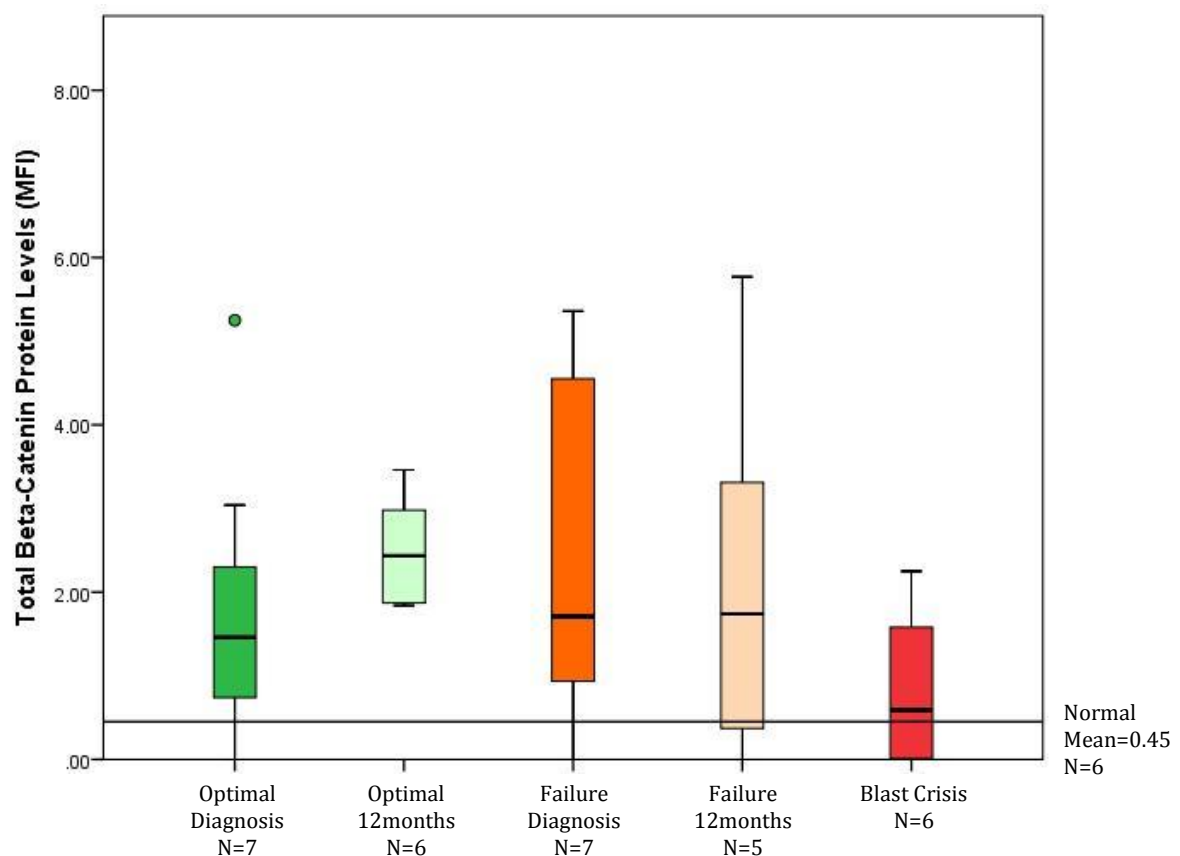
The data from the separate clinical cohorts were combined and re-stratified into chronic phase vs blast crisis to see if there was a difference in levels of total β-catenin at disease progression **(figure 3.4.7)**. Results showed the total β-catenin levels decreased in blast crisis compared to chronic phase diagnostic samples, however, this was not significant indicating that, along with mRNA levels of β-catenin, total β-catenin protein levels cannot be used to assess patient outcome or disease progression in CML.

Figure 3.4.7 Protein levels of total β-catenin do not correlate with disease progression in imatinib treated patients

Protein levels were re-stratified according to chronic phase (N=14) or blast crisis (N=6). Results showed a decrease in levels however this difference did not reach statistical significance.
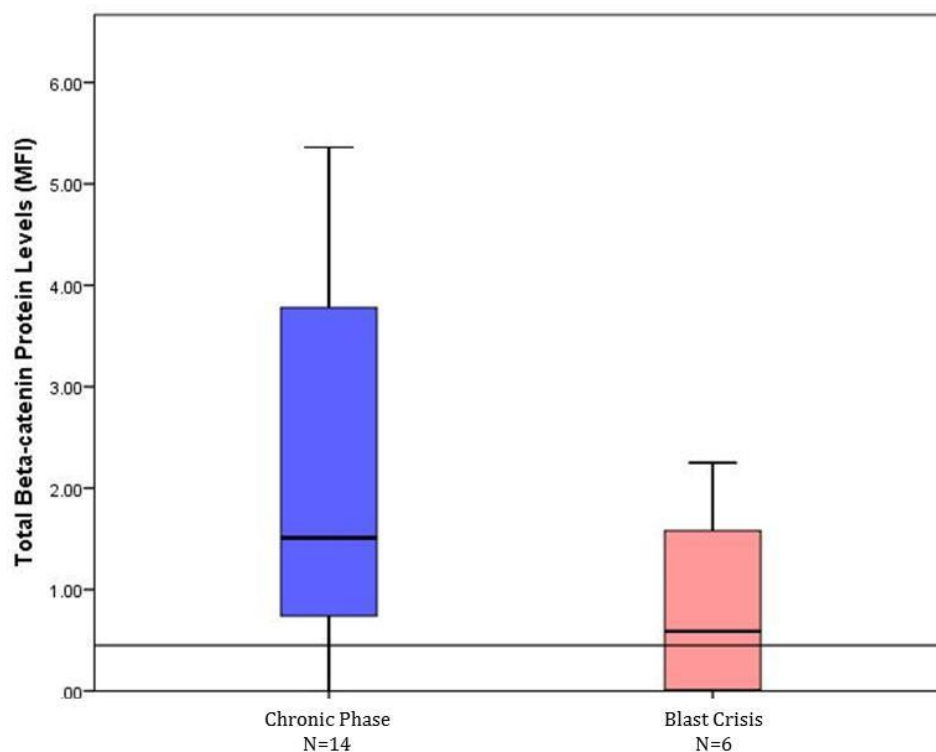
3.4.3.2 Imatinib reduces the level of total β-catenin protein *in vitro*

To examine the effects that imatinib is having on the levels of total β-catenin protein, LAMA-84 cells were cultured with the clinically achievable dose of 5μM imatinib for 24 hours **(Materials and Methods section 2.3.3)** and levels were measured by FACS analysis (N=3) **(Materials and Methods section 2.7)**. Results showed a significant reduction of total β-catenin levels with imatinib treatment (P=0.045) **(Figure 3.4.8)**. This shows that the reduction in β-catenin mRNA levels by imatinib **(Figure 3.4.4)** also translates to total protein levels. Why this decrease is not reflected in the patient samples on imatinib treatment it unknown **(Figure 3.4.6)**.

Figure 3.4.8 Imatinib reduces the level of total β-catenin *in vitro* in LAMA-84 cells

LAMA-84 cells were incubated with 5μM imatinib *in vitro* for 24 hours and measured by FACS to determine its effect on total β-catenin. Results show a reduction in levels on imatinib incubation (N=3).
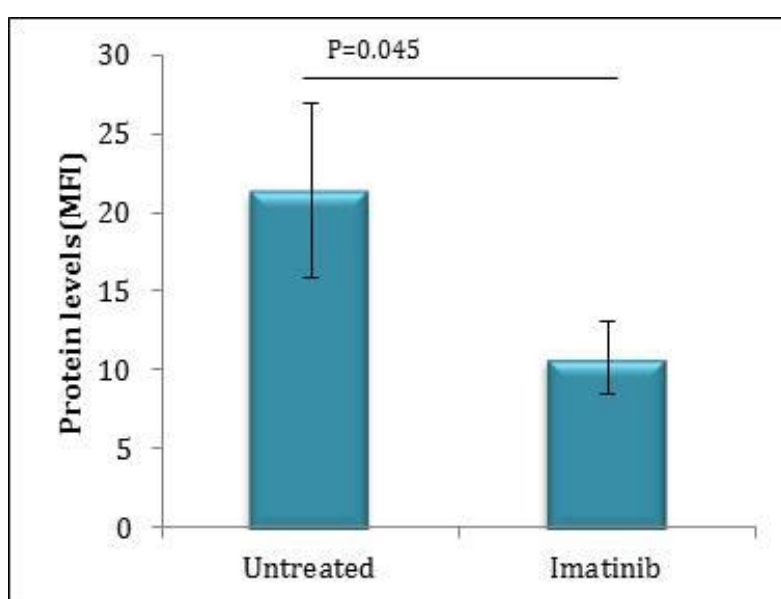
3.4.4 Does β-catenin protein phosphorylation status correlate with clinical outcome?

Beta-catenin activity is controlled by its phosphorylation status. When β-catenin is unphosphorylated it is unavailable for ubiquitination by βTrCP, and thus is free to enter the nucleus where it can initiate transcription. Conversely, phosphorylation of β-catenin by CK1α at Ser45 primes β-catenin for further phosphorylation by GSK3β at Thr41, Ser37 and Ser33 [104, 135, 136]. Specifically, the phosphorylation at Ser37 and Ser33 by GSK3β permits βTrCP to initiate ubiquitination leading to the degradation of β-catenin by the proteasome [135, 140-142].

The following variants were considered for further investigation and using commercially available antibodies specific to these forms.

1. Unphosphorylated β-catenin, which represents the 'active' form of β-catenin that can translocate into the nucleus from the cytoplasm and activate transcription.

2. Phospho-β-catenin (Ser45/Thr41), which is phosphorylated on Ser45 by CK1 and on Thr41 by GSK3β and is targeted for degradation by the proteasome. Without the phosphorylation on Ser45 by CK1, GSK3β cannot phosphorylate the subsequent sites.

3. Phospho-β-catenin (Ser33/37/Thr41), which is similar to phospho-β-catenin(Ser45/Thr41) whereby it is targeted for degradation by the proteasome, it is phosphorylated solely by GSK3β on all 3 residues subsequent to CK1 phosphorylation.

3.4.4.1 Protein levels of unphosphorylated β-catenin and phospho-β-catenin (Ser45/Thr41) demonstrate no correlation with predicting patient outcome but do alter at disease transformation

Phospho-β-catenin (Ser33/37/41) was removed from analysis when looking at patient samples due to the limited amount of cells available, and as it would be expected to show similar results to phospho-β-catenin (Ser45/Thr41). Patients analysed were the same as those examined for total β-catenin **(see Section 3.4.3.1)**.

The levels of unphosphorylated β-catenin were assessed **(Figure 3.4.9 A)** to represent the active form of β-catenin able to activate transcription [106]. Results for this form showed low levels in the optimal responders both pre and post 12 month imatinib treatment compared to failure patients, patients in blast crisis and levels from healthy donor MNCs. There was no statistically significant difference between any groups.

Figure 3.4.9 B shows the protein levels for the combined phosphorylation sites Ser45 (by CK1) and Thr41 (by GSK3β), representing the form of β-catenin targeted for degradation by the proteasome [135]. Low levels of phospho-β-catenin (Ser45/Thr41) were detected in MNC at diagnosis in both optimal responders and failure patients, and in patients transformed into blast crisis. However, there was no difference seen between patient cohorts. Following 12 months of imatinib treatment, levels were reduced to undetectable amounts, similar to levels seen in healthy MNCs. Phosphorylation of β-catenin at Ser45 and Thr41 indicates that the protein will be degraded. This could occur rapidly and hence may explain why only very low levels of the protein are detected.

Overall, the outcome from data shown in **Figure 3.4.9** is that both unphosphorylated β-catenin and phospho-β-catenin (Ser45/Thr41) protein levels cannot be used to differentiate between clinical outcomes in CML.

Figure 3.4.9 Protein levels of unphosphorylated β-catenin and phospho-β-catenin (Ser45/Thr41) do not correlate with patient outcome

Protein levels of unphosphorylated β-catenin and phospho-β-catenin (Ser45/Thr41) were measured in MNC cells in optimal and failure patients at both diagnosis (N=7 for both) and after 12 months imatinib treatment (N= 6 and 5 respectively) and when patients had transformed into blast crisis (N=6). Additionally levels were tested in six MNC samples from healthy donors. Results showed that neither unphosphorylated β-catenin, nor phospho-β-catenin (Ser45/Thr41) protein levels could be used to differentiate between clinical outcomes following imatinib treatment in CML.

A. Unphosphorylated β-catenin

B. Phospho-β-catenin (Ser45/Thr41)
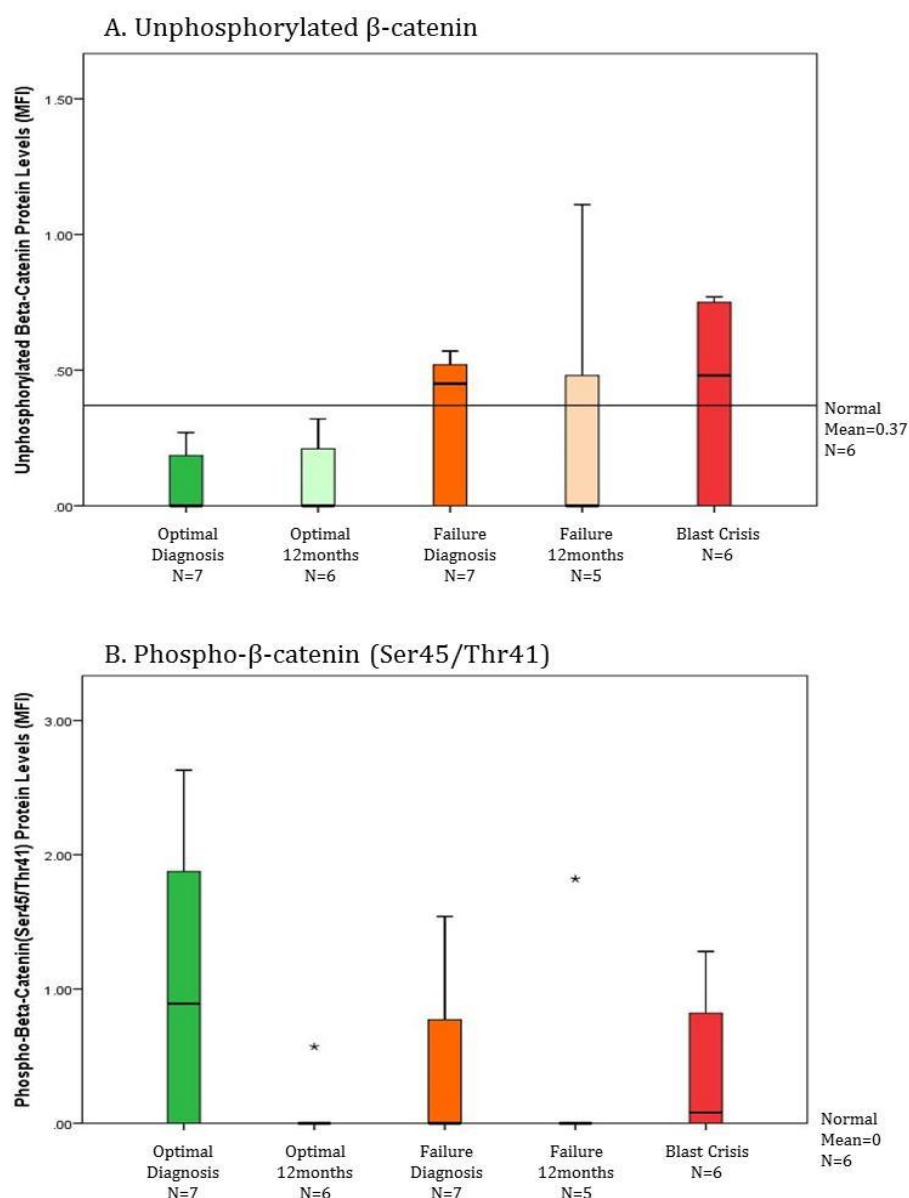
Stratification of the data into chronic phase vs blast crisis showed an expected trend of what would happen to the levels of β-catenin protein as patients progress into blast crisis **(see figure 3.4.10)**. Results showed an increase in unphosphorylated β-catenin in patients that have transformed into blast crisis **(see figure 3.4.10 A)**, which fits with what has previously been seen and with the hypothesis that unphosphorylated β-catenin acts to increase transcription in blast crisis [150]. In addition to this, there is a decrease in levels of phospho-β-catenin (Ser45/Thr41) at transformation into blast crisis **(see figure 3.4.10 B)**, which is also to be expected as a decrease in phospho-β-catenin (Ser45/Thr41) indicates a reduction in the levels of β-catenin being degraded by the proteasome. However, these results did not reach a statistical significance.

Figure 3.4.10 Beta-catenin protein levels stratified as chronic phase vs blast crisis fits the trend associated with CML

Re-stratification of the data into chronic phase (N=14) vs blast crisis (N=6) shows a trend towards an increase in unphosphorylated β-catenin (A) and a decrease in phospho-β-catenin (Ser45/Thr41) (B).
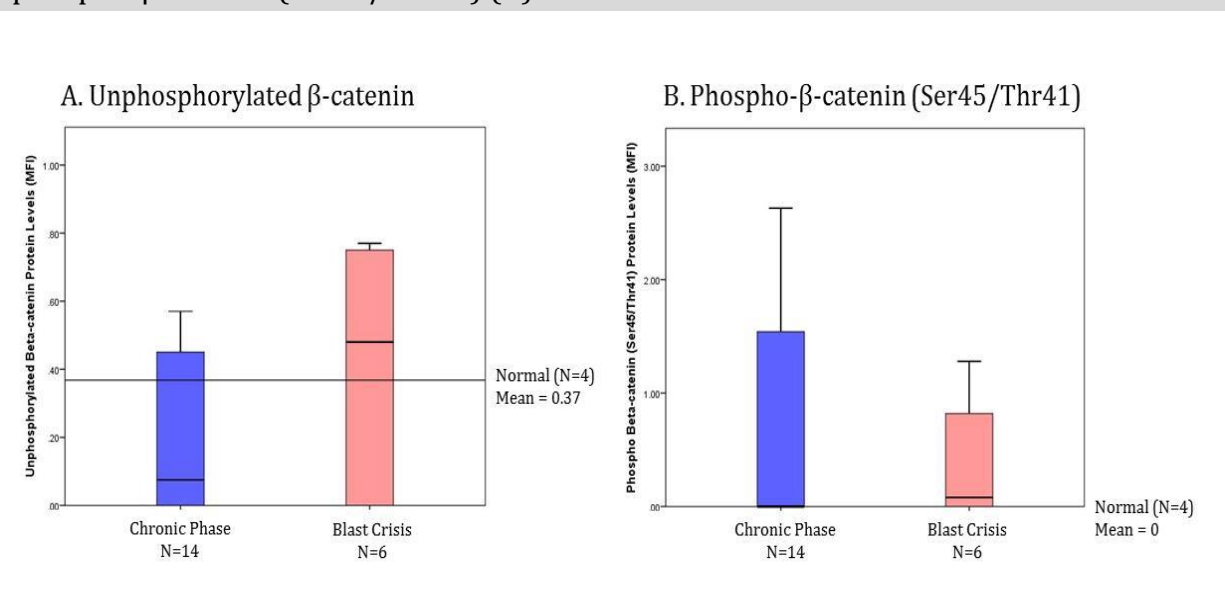
3.4.4.2 Imatinib reduces the level of unphosphorylated and phospho- β-catenin protein *in vitro*

Imatinib was tested *in vitro* on LAMA-84 cells to determine its effect on unphosphorylated β-catenin and the two phospho- forms. Cells were incubated with 5μM imatinib *in vitro* for 24 hours **(Materials and Methods section 2.3.3)** and levels were assessed by FACS analysis (N=3) **(Materials and Methods section 2.7)**. Results demonstrated a reduction in levels of all β-catenin forms with imatinib treatment **(Figure 3.4.11)**. These results appear to indicate that, instead of altering β-catenin function by either enhancing its activity or its degradation, imatinib acts by reducing all levels of β-catenin protein, possibly due to a reduction in the transcription of β-catenin **(Figure 3.4.4)**. The reduction seen for each form was not significant, possibly due to the small N number (N=3), however the reduction was greater for unphosphorylated β-catenin compared to the two phospho- forms (Ser45/Thr41 and Ser33/37/Thr41) (P=0.082, 0.218 and 0.164 respectively).

Figure 3.4.11 Imatinib reduces the levels of unphosphorylated and phospho β-catinin *in vitro* in LAMA-84 cells

LAMA-84 cells were incubated with 5µM imatinib *in vitro* for 24 hours and protein levels of β-catenin were measured by FACS analysis. Its effects on; A. unphosphorylated β-catenin, B. phospho-β-catenin (Ser45/Thr41), and C. phospho-β-catenin (Ser33/37/Thr41) were determined. Results show a reduction in all forms tested on imatinib treatment (N=3).
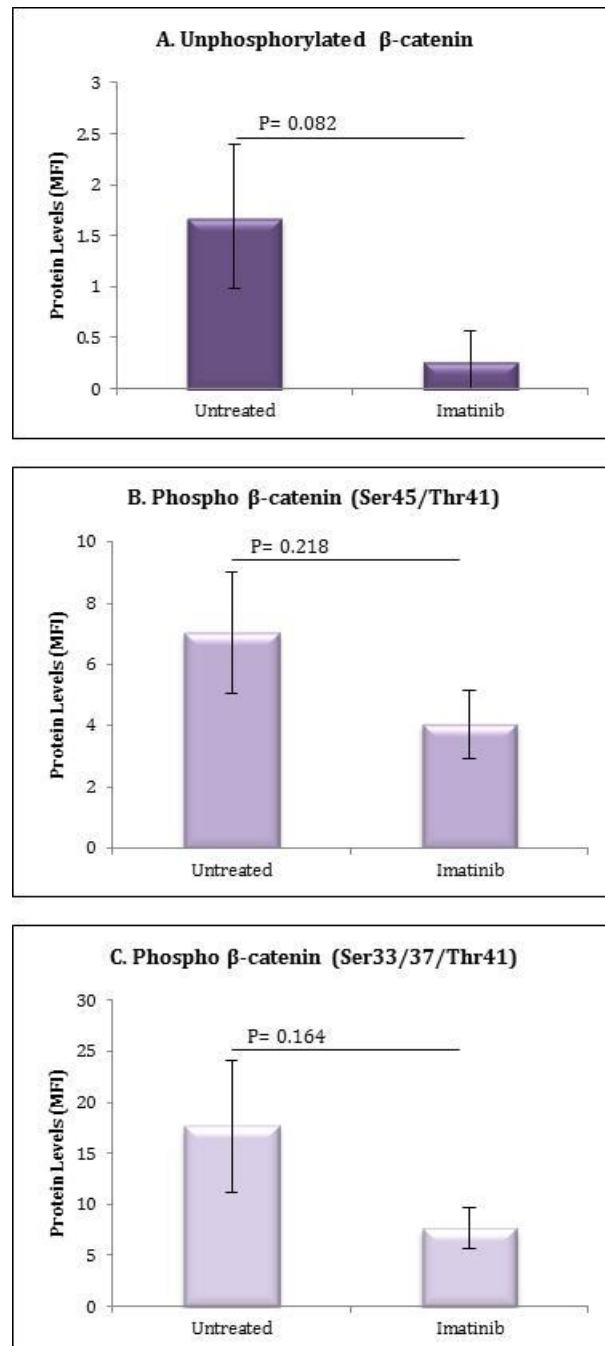
3.4.4.3 Subcellular localisation of the phospho- variants of β-catenin

It has previously been reported that the status of certain phosphorylation residues determines the sub-cellular localisation of β-catenin [100]. When β-catenin is unphosphorylated it translocates to the nucleus where it can initiate transcription. Phosphorylation on Ser45, Thr41, Ser33, and Ser37 localise β-catenin to the cytoplasm when it can be targeted by the proteasome. To test this, nuclear and cytoplasmic extractions were performed using K562 and LAMA-84 cells **(Materials and Methods section 2.9.2)**. These were then examined by western blotting **(Materials and Methods section 2.9)**.

Total β-catenin was tested at the same time as unphosphorylated β-catenin and phospho-β-catenin (Ser45/Thr41). Results showed that total β-catenin was located mainly in the cytoplasm, with less in the nucleus (**Figure 3.4.12**). Unphosphorylated β-catenin was found mainly in the nucleus, confirming that the absence of β-catenin phosphorylation causes it to translocate to the nucleus. Phospho-β-catenin (45/41) was also detected mainly in the nucleus. This is in contrast to what was anticipated, as this phosphorylation is a marker for degradation, which occurs in the cytoplasm. Therefore it is unexpected for this form to be able to bypass this and translocate into the nucleus. However, evidence was published which supports this finding, whereby β-catenin phosphorylated on Ser45/Thr41 can localise to the nucleus, unlike β-catenin phosphorylated on Ser33/37/Thr41 [149]. This therefore means that phospho-β-catenin (Ser45/Thr41) is not a good marker to use for β-catenin degraded by the proteasome.

Figure 3.4.12 Investigating the localisation of β-catenin by nuclear and cytoplasmic extraction

K562 and LAMA-84 cells were separated into their nuclear and cytoplasmic compartments and examined by western blotting alongside a whole cell lysate (WCL) to assess the localisation of the β-catenin variants. Results showed total β-catenin to be localised mainly in the cytoplasm with a small amount in the nucleus. Unphosphorylated β-catenin was found primarily in the nucleus, as was phospho-β-catenin (Ser45/Thr41).
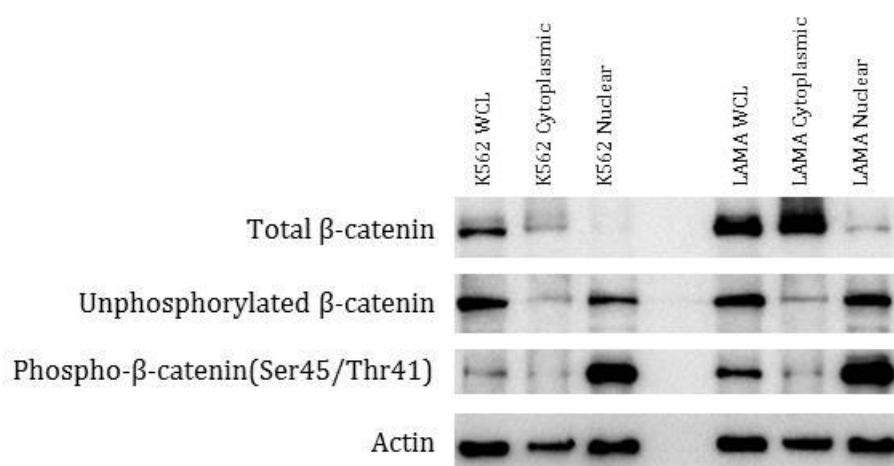
It was intended that this analysis of cellular localisation would be followed by looking at this in patient samples as confirmation of the FACS results; however, the technique makes heavy use of cell number ($2x10^7$ cells) which would have been a significant drain on the limited material available. Instead confocal microscopy was used **(Figures 3.4.13-15)**.

3.4.4.4 Analysis of β-catenin by confocal microscopy

Levels were analysed **(Materials and Methods section 2.10)** in optimal responders and failure patients at diagnosis, patients at diagnosis who subsequently transformed into blast crisis, and patients who have transformed into blast crisis. Samples from patients after 12 months imatinib treatment were eliminated from analysis as they were not providing any additional information due to replacement of the diagnostic leukaemic cell population by normal cells. Additionally, total β-catenin was excluded from analysis and replaced by phospho-β-catenin (Ser33/37/Thr41) to give a more accurate representation of β-catenin being degraded by the proteasome.

Results for unphosphorylated β-catenin **(Figure 3.4.13)** show low levels in the optimally responding patients, with a slight increase in the failures and those who have transformed into blast crisis. Interestingly, levels are elevated in diagnostic samples from patients who subsequently transform into blast crisis. This could suggest that an increase in unphosphorylated β-catenin could be predictive of blast crisis. Unfortunately this preliminary finding could not be confirmed due to the lack of availability of further cells from this cohort of patients.

Figure 3.4.14 shows results for phospho-β-catenin (Ser45/Thr41). Levels were elevated in the patients who had transformed into blast crisis. Additionally, there were also higher levels in the failure patients at diagnosis, while the optimal responders and

the patients at diagnosis who subsequently progress into blast crisis had lower levels of the protein.

Finally, the study of phospho-β-catenin (Ser33/37/Thr41) **(Figure 3.4.15)** showed that although there were slight elevations in the protein detected in one of the optimal responders (#209) and one of the patients at diagnosis who subsequently progressed into blast crisis (#115), there was no overall correlation between phospho-β-catenin (Ser33/37/Thr41) levels and patient outcome **(uncropped data shown in Appendix Figures 8.1-8.3)**.

Key:

Figure 3.4.13 Protein levels of unphosphorylated β-catenin visualised by confocal microscopy

Protein levels of unphosphorylated β-catenin were visualised in CML MNCs by confocal microscopy in two optimal responders (#130 and #209) and two failure patients (#296 and #308) at diagnosis, alongside two blast crisis patients at diagnosis (#115 and #13), and two cases after transformation of chronic phase into blast crisis (#20 and #13). Results show elevated levels of active β-catenin in blast crisis patients at diagnosis, alongside one of the blast crisis patients after transformation into blast crisis from chronic phase.
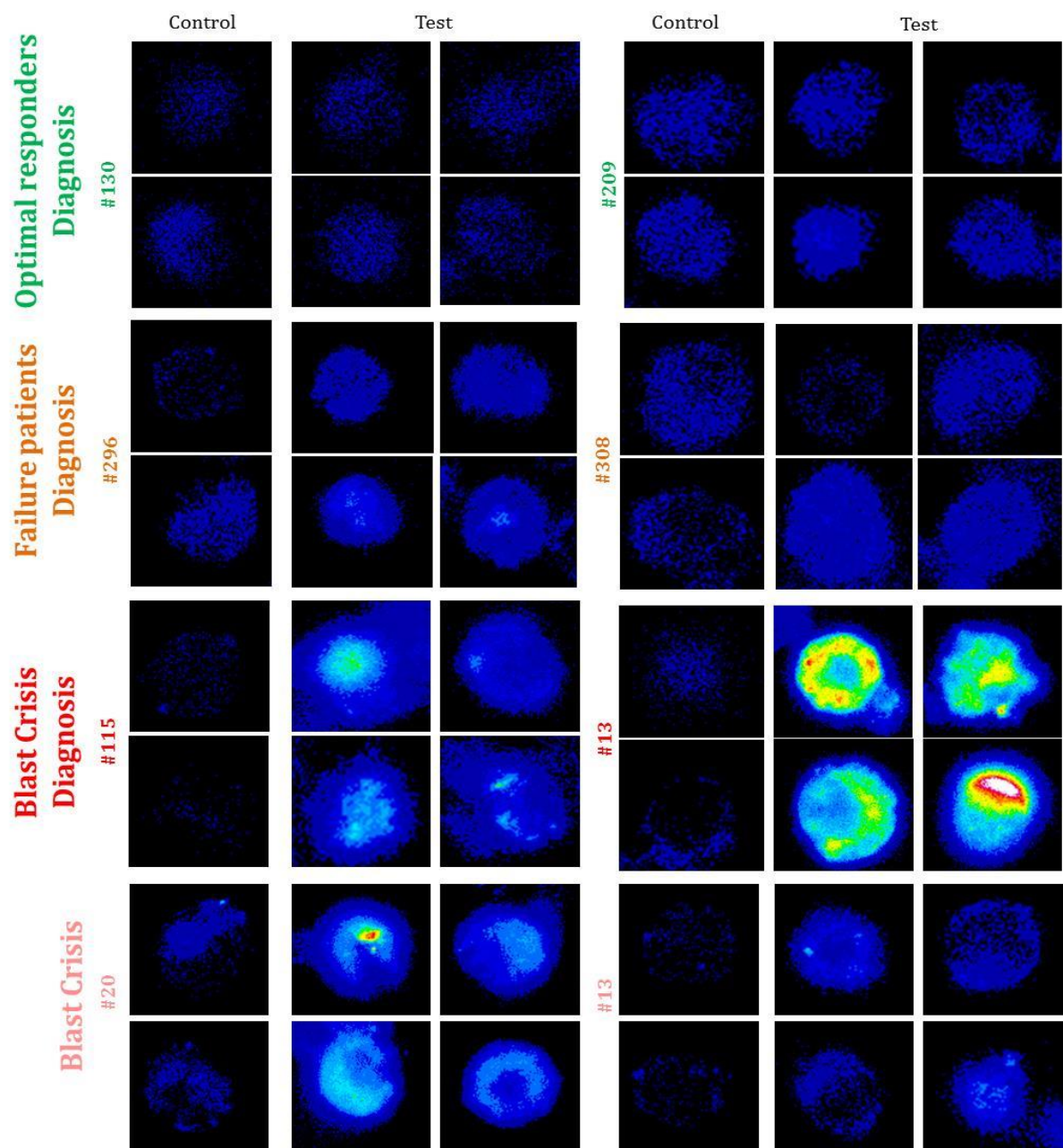
Figure 3.4.14 Protein levels of phospho-β-catenin (Ser45/Thr41) visualised by confocal microscopy

Protein levels of phospho-β-catenin (45/41) were visualised in CML MNCs by confocal microscopy, using the same samples as in Figure 3.4.11.
Results show much higher levels in the patients who have progressed to blast crisis. Additionally levels are elevated in one of the optimally responding patients and both failure patients.
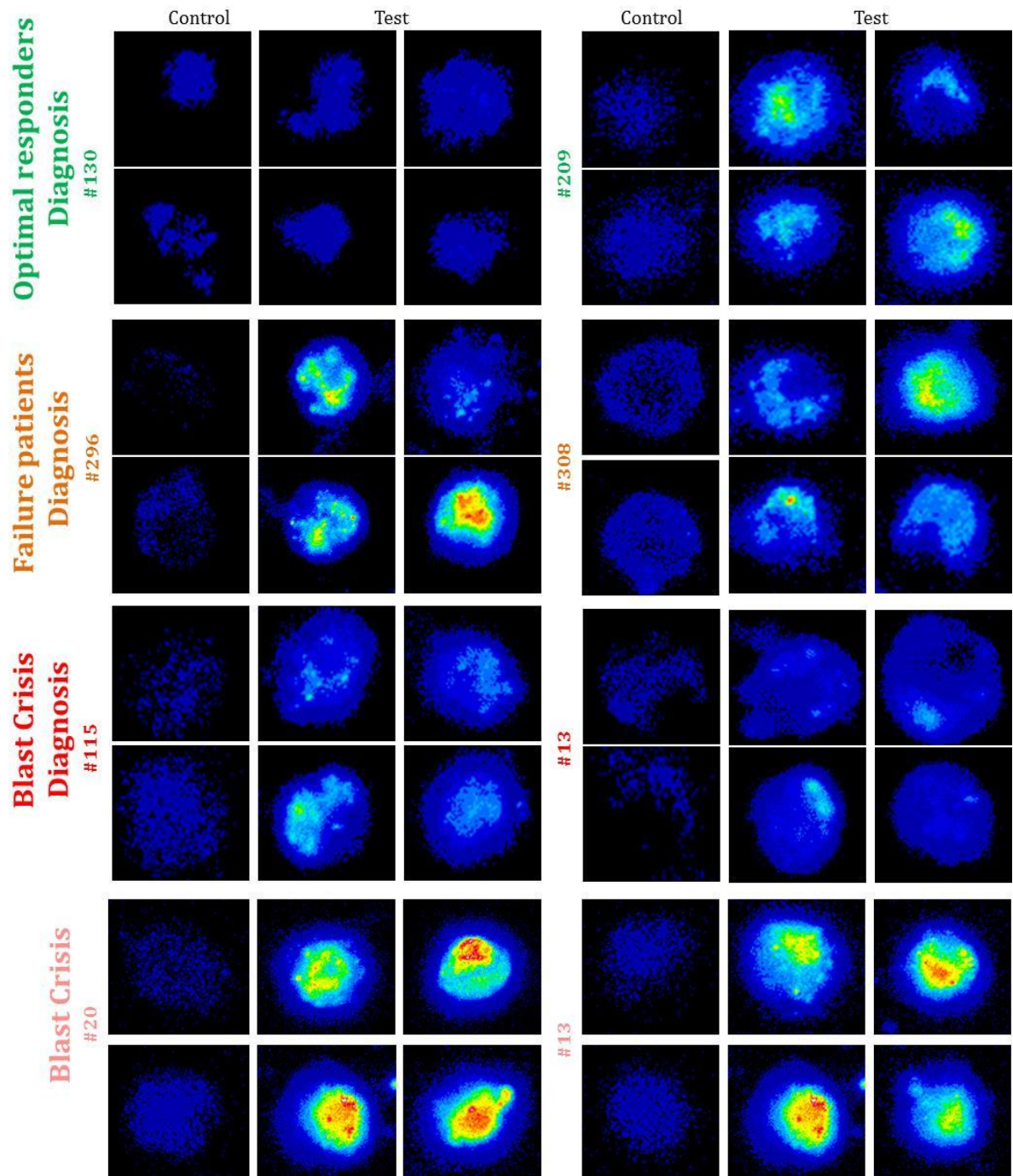
Figure 3.4.15 Protein levels of phospho-β-catenin (Ser33/37/Thr41) visualised by confocal microscopy

Protein levels of phospho-β-catenin (33/37/41) were visualised in CML MNCs by confocal microscopy, using the same samples as in Figure 3.4.11 and 3.4.12. Results show higher levels in one of the optimal and one of the blast crisis patients at diagnosis and in the blast crisis patients in blast crisis. This random distribution shows there is no correlation between phospho-β-catenin (33/37/41) levels and patient outcome.
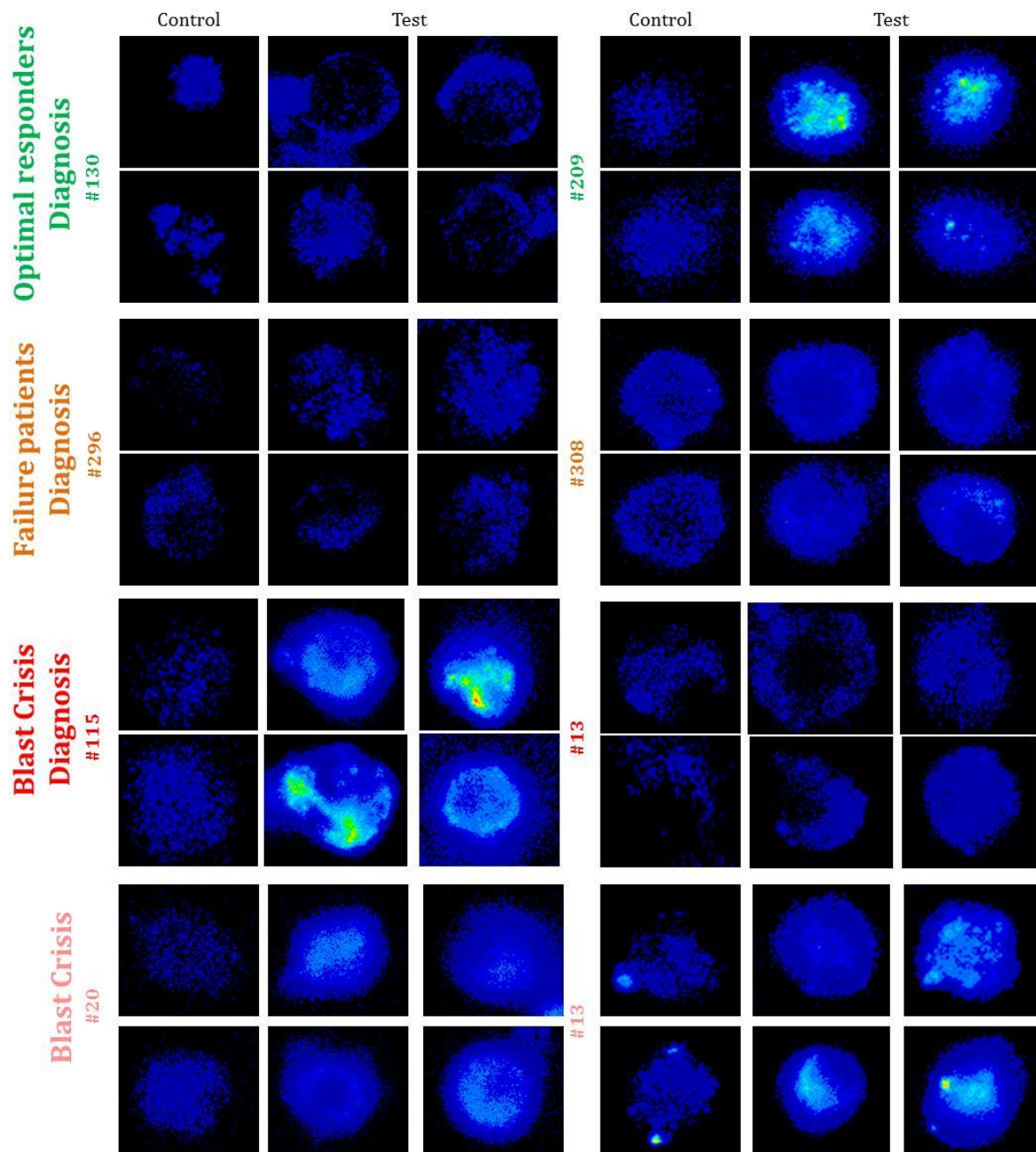
Next, the unphosphorylated β-catenin, representing the active form, and phospho-β-catenin(Ser33/37/Thr41), representing the form targeted for degradation, were examined to see how they inter-relate within an individual patient. From this, a relationship can be seen between expression levels in individual patients **(Figure 3.4.16)**. It appears that when levels of phospho-β-catenin (Ser33/37/Thr41) are elevated, the levels of unphosphorylated β-catenin are low, indicating when phosphorylated β-catenin is being degraded and is unable to activate transcription. This could be said for patient #209 which was a diagnostic sample from an optimal responder, and patient #13 when the patient had transformed into blast crisis. Conversely, when unphosphorylated β-catenin levels were higher, this correlated with low levels of phospho-β-catenin (Ser33/37/Thr41). This was seen in the chronic phase diagnostic sample from patient #13 (who later progressed to blast crisis). This shows that the mechanism by which β-catenin activity is regulated is active in CML, however it may not be involved in the progression of the disease.

Figure 3.4.16 The relationship between the various forms of β-catenin in individual patients

Unphosphorylated β-catenin and phospho-β-catenin (Ser33/37/Thr41) were examined within individual patients to see if there was a correlation between levels.
Results show that when levels of phospho-β-catenin (Ser33/37/Thr41) are elevated, the levels of unphosphorylated β-catenin are low (seen in patients #209 optimal responder at diagnosis, and #13 blast crisis). Also when unphosphorylated β-catenin levels were higher, this correlated with low levels of phospho-β-catenin (Ser33/37/Thr41) (seen in the diagnostic sample from patient #13 who later developed into blast crisis).
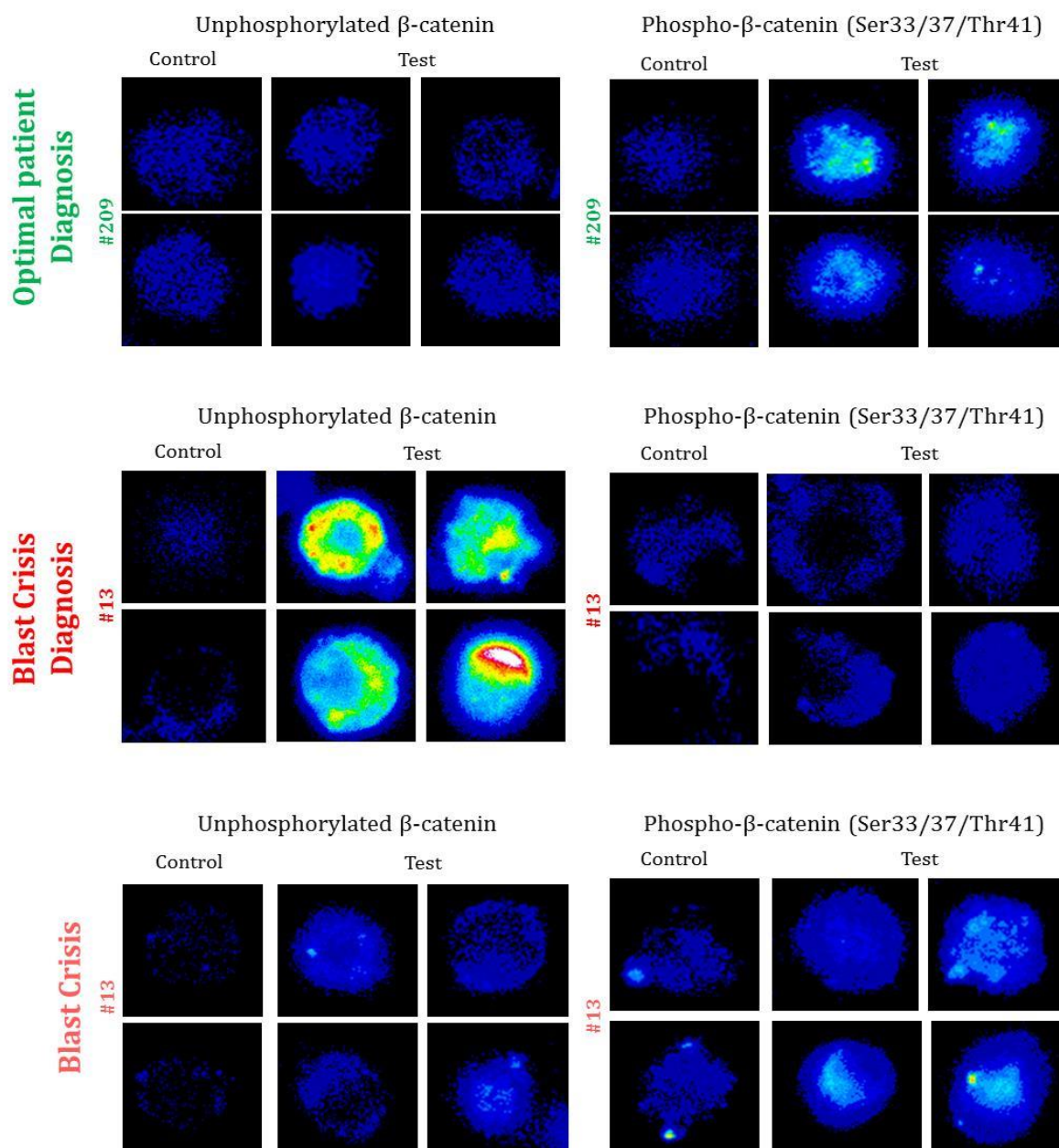
3.4.5 Why are the levels of β-catenin not correlating with disease outcome in CML MNCs?

As the results observed did not show a difference in the various forms of β-catenin between patient cohorts, it was hypothesised that β-catenin might be rapidly degraded by the proteasome. To investigate this, a proteasome inhibitor, bortezomib, was used to determine the effects on the levels of β-catenin when it is prevented from being degraded.

3.4.5.1 Inhibition of the proteasome leads to increased levels of β-catenin

The CML cell lines K562 and LAMA-84 were used to examine the effects of bortezomib on CML cells. The levels of β-catenin were measured by FACS analysis **(Materials and Methods section 2.7)** in untreated and 0.1μM, 1μM and 5μM bortezomib treated cells (data not shown) after 24 hours incubation **(optimised in section 3.3.2.4)** to determine the effects of proteasome inhibition on the levels of total β-catenin, unphosphorylated β-catenin, phospho-β-catenin (Ser45/Thr41), and phospho-β-catenin (Ser33/37/Thr41). Results showed that 5μM bortezomib displayed optimum results **(Figure 3.4.17)**. In both cell lines tested, levels of total β-catenin increased with bortezomib incubation. This trend was also seen for both unphosphorylated β-catenin and phospho-β-catenin (Ser45/Thr41). The increase in unphosphorylated β-catenin was significant in LAMA 84 cells (P=0.050). Results for phospho-β-catenin (Ser33/37/Thr41) show a decrease in levels with bortezomib incubation, which again reached statistical significance in the LAMA 84 cells (P=0.043). These data suggest that

under normal conditions, when the proteasome is not being inhibited, β-catenin is being

degraded by the cell.

Figure 3.4.17 The effects of the proteasome inhibitor bortezomib on the cellular levels of the various forms of β-catenin

The levels of β-catenin were measured by FACS in untreated (UNT) and 5μM bortezomib treated K562 (N=3) and LAMA-84 cells (N=3) after 24 hour incubation. Results show an increase total β-catenin, unphosphorylated β-catenin (P=0.050 in LAMA 84 cells), and phospho-β-catenin (Ser45/Thr41). Levels of phospho- β-catenin (Ser33/37/Thr41) decreased or bortezomib treatment (P=0.043 in LAMA 84 cells).
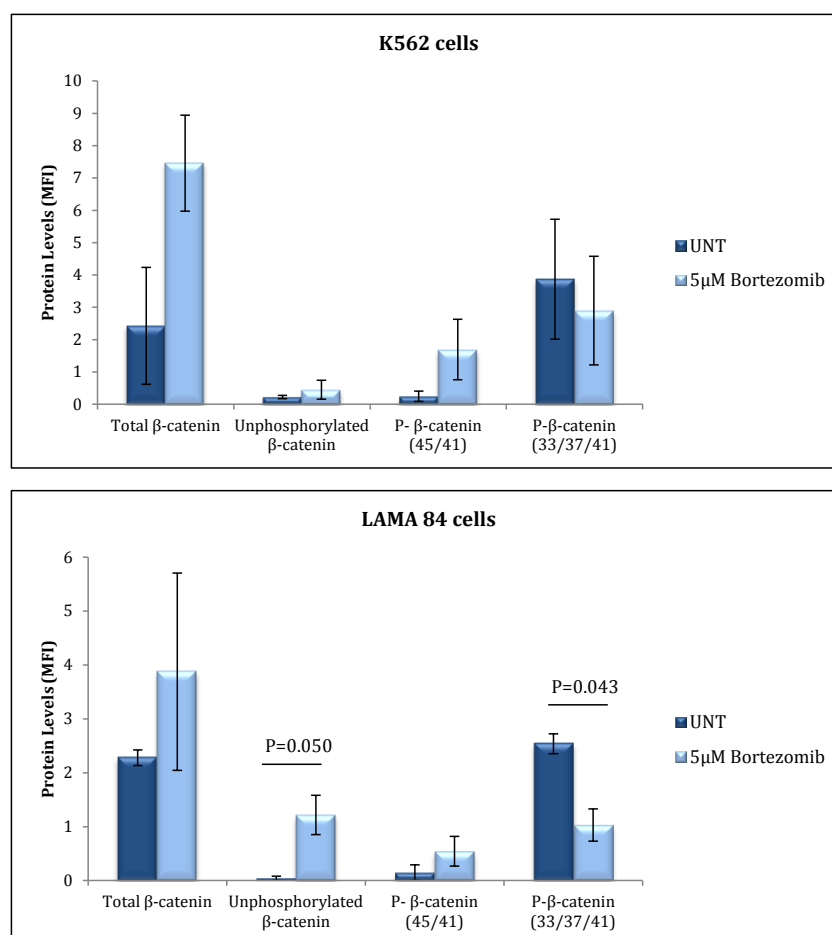
3.4.6 Does β-catenin phosphorylation by BCR-ABL1 have any correlation with disease progression?

Beta-catenin can also be phosphorylated by BCR-ABL1, amongst other kinases, on the residue Tyr654 [186]. This targets β-catenin to the nucleus where it can activate transcription. As BCR-ABL1 is considered a driving force in CML [17, 189], therefore it is of interest to see if BCR-ABL1 mediated β-catenin phosphorylation of Tyr654 is having an effect on β-catenin turnover in CML cells.

3.4.6.1 Protein levels of phospho-β-catenin (Tyr654) demonstrate no correlation with predicting patient outcome but do significantly change with disease transformation

Again, the results were analysed in accordance with patient outcome, with optimal response and failure patients being analysed at diagnosis and after 12 months imatinib treatment, and blast crisis patients being analysed when patients had transformed into blast crisis.

Analysed by FACS analysis **(Materials and Methods section 2.7)**, **Figure 3.4.18** indicates that there is no difference in Tyr654 between patient cohorts at diagnosis, consistent with the view that BCR-ABL1 activity is broadly similar across patients at initial diagnosis [190].Tyr654 levels decrease after 12 months of imatinib treatment; however this is to be expected as the BCR-ABL1 driven phosphorylation of β-catenin is removed as leukaemic cells are replaced with normal cells. Additionally, **Figure 3.4.18**

shows that when patients have transformed into blast crisis, there is no evidence of β-catenin being phosphorylated directly by BCR-ABL1, which is in line with the view that CML can become BCR-ABL1 independent at disease transformation [191].

Figure 3.4.18 Protein levels of phospho-β-catenin (Tyr654) do not correlate with patient outcome in imatinib treated patients

Protein levels of patient MNC samples were measured in optimal responders, and failure patients at both diagnosis (N=7) and after 12 months imatinib treatment (N=6 and 5 respectively), and in addition when patients were in blast crisis (N=6). Levels were also measured in 6 healthy donor MNC samples to compare with patients. Results showed no difference between patient cohorts at diagnosis and that levels decrease after 12 months of imatinib treatment. Levels found in patients transformed into blast crisis are lower than in healthy donors. .
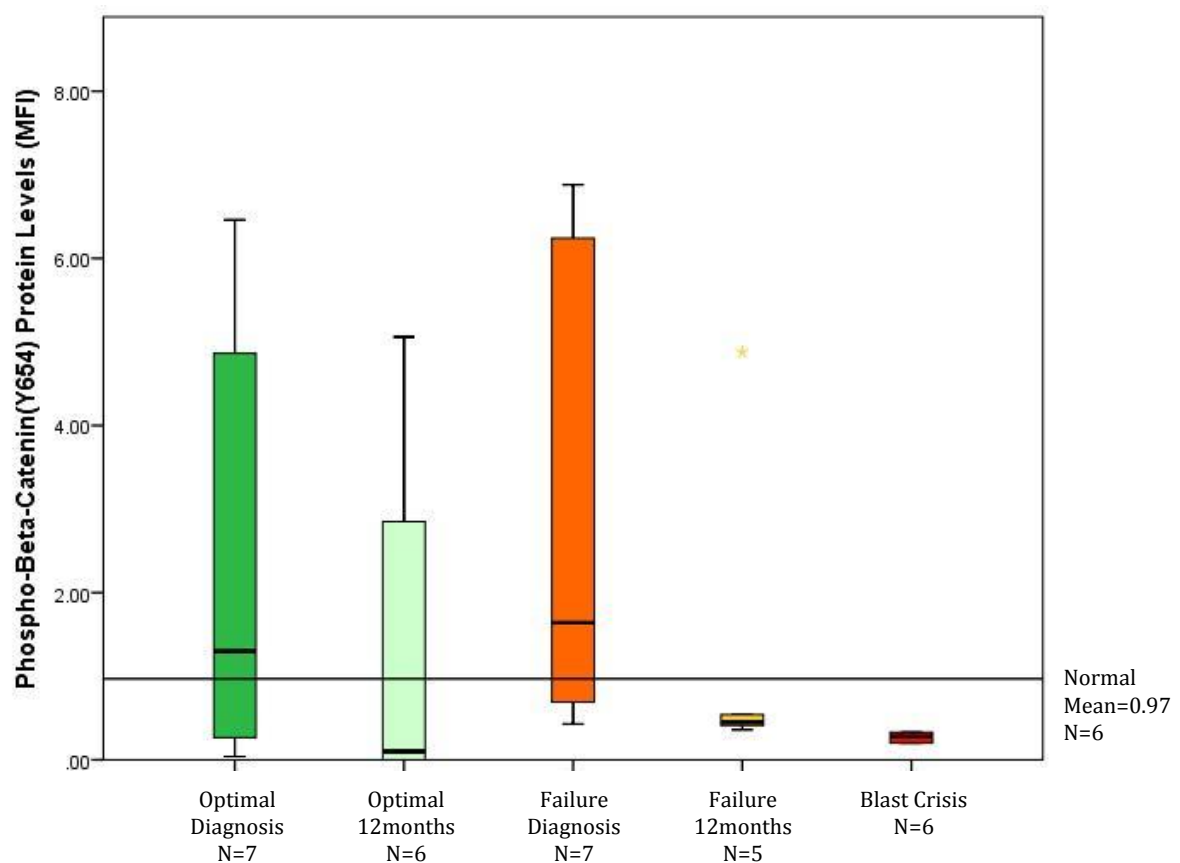
When the data were re-stratified into chronic phase vs blast crisis, levels of phospho-β-catenin (Tyr654) were significantly lower in patients transformed into blast crisis compared to chronic phase (p=0.012) **(Figure 3.4.19)**. Again, this is in line with the view that the disease can become BCR-ABL1 independent at disease transformation [191].

Figure 3.4.19 Phospho-β-catenin (Tyr654) protein levels are significantly lower in patients who have transformed into blast crisis compared to chronic phase

Re-stratification of the data into chronic phase (N=14) vs blast crisis (N=6) shows a significant decrease (P=0.012) in the levels of phospho-β-catenin (Tyr654) when patients had transformed into blast crisis.
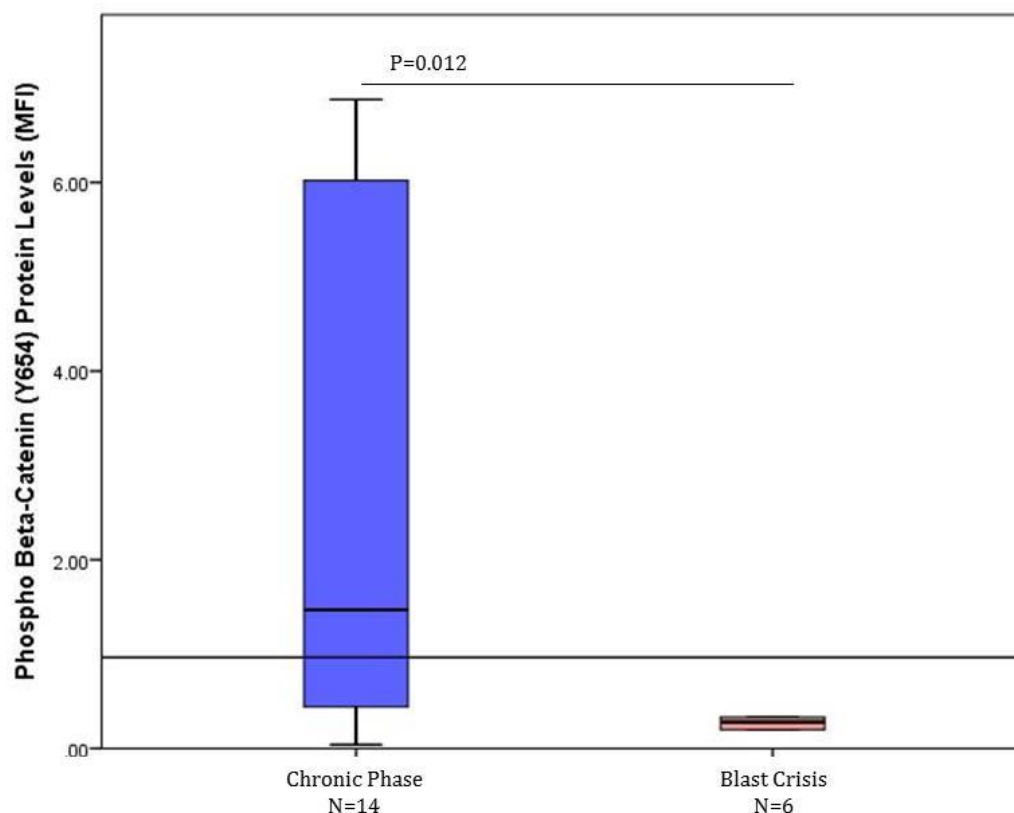
3.4.6.2 Imatinib significantly reduces the levels of phospho-β-catenin (Tyr654) *in vitro* in LAMA-84 cells

As before, LAMA-84 cells were incubated with 5µM imatinib *in vitro* for 24 hours and the levels of phospho-β-catenin (Tyr654) were measured by FACS to determine its effect **(Figure 3.4.20)**. Results showed a significant decrease in the levels of phospho-β-catenin (Tyr654) on imatinib incubation (P=0.024). This confirms what would be expected due to the direct inhibition of BCR-ABL1 by imatinib.

Figure 3.4.20 Imatinib significantly reduces the levels of phospho-β-catenin (Tyr654)

LAMA-84 cells were incubated *in vitro* for 24 hours with 5µM imatinib. Results show a significant reduction in phospho-β-catenin (Tyr654) levels (P=0.024) (N=3).
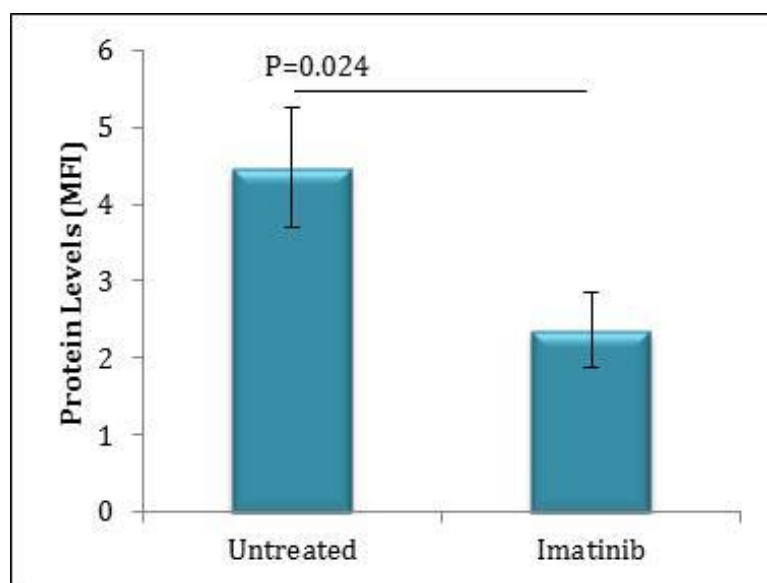
3.4.6.3 Subcellular localisation of phospho-β-catenin (Tyr654)

Phosphorylation of β-catenin on Tyr654 is reported to target β-catenin to the nucleus where it can activate transcription [186]. To test this, nuclear and cytoplasmic extractions were performed using K562 and LAMA-84 cells **(Materials and Methods section 2.9.2)**. These were then examined by western blotting **(Materials and Methods section 2.9)**. Results showed that there are slightly elevated levels of phospho-β-catenin (Tyr654) in the nucleus compared to the cytoplasm, re-confirming its role in targeting β-catenin to the nucleus **(Figure 3.4.21)**.

Figure 3.4.21 Investigating the localisation of phospho-β-catenin (Tyr654) by nuclear and cytoplasmic extraction

K562 and LAMA-84 cells were separated into their nuclear and cytoplasmic compartments using nuclear and cytoplasmic extraction. These compartments were then examined by western blotting to assess the localisation of the β-catenin variants. Results showed there are slightly higher levels of phospho-β-catenin (Tyr654) located in the nucleus.
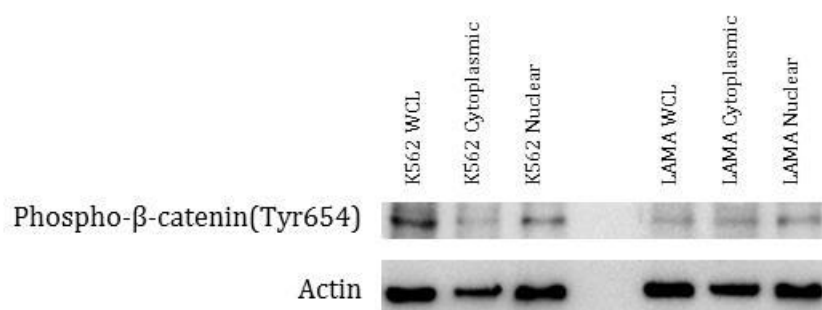
As in **section 3.4.4.3**, this method could not be extended to clinical samples as it uses an excess of cells which would deplete our store considerably. Confocal microscopy, which is much more economical on cell numbers was employed. Levels were analysed in optimal responders and failure patients at diagnosis, patients at diagnosis who subsequently transformed into blast crisis, and patients who were in blast crisis.

Results from confocal microscopy **(see Figure 3.4.22)** showed a similarity in levels of phospho-β-catenin (Tyr654) at diagnosis with a slight decrease in patients that have transformed into blast crisis. This concurs with the results from the FACS as they also suggest that BCR-ABL1 activity is broadly similar across patients at initial diagnosis. Additionally, with the reduction in phospho-β-catenin (Tyr654) in patients that have transformed into blast crisis, this fits with the view that CML can become BCR-ABL1 independent at disease transformation [191] **(uncropped data shown in Appendix Figures 8.4)**.

Figure 3.4.22 Protein levels of phospho-β-catenin (Tyr654) assessed by confocal microscopy

Protein levels of phospho-β-catenin (Tyr654) were visualised in MNC cells by confocal microscopy in optimal responders (#130 and #209) and failure patients (#296 and #308) at diagnosis and blast crisis patients at diagnosis (#115 and #13), and when patients had transformed into blast crisis (#20 and #13). Results show a similarity in levels between optimal responders, failure and blast crisis patients at diagnosis, and then a slight decrease in patients transformed into blast crisis.
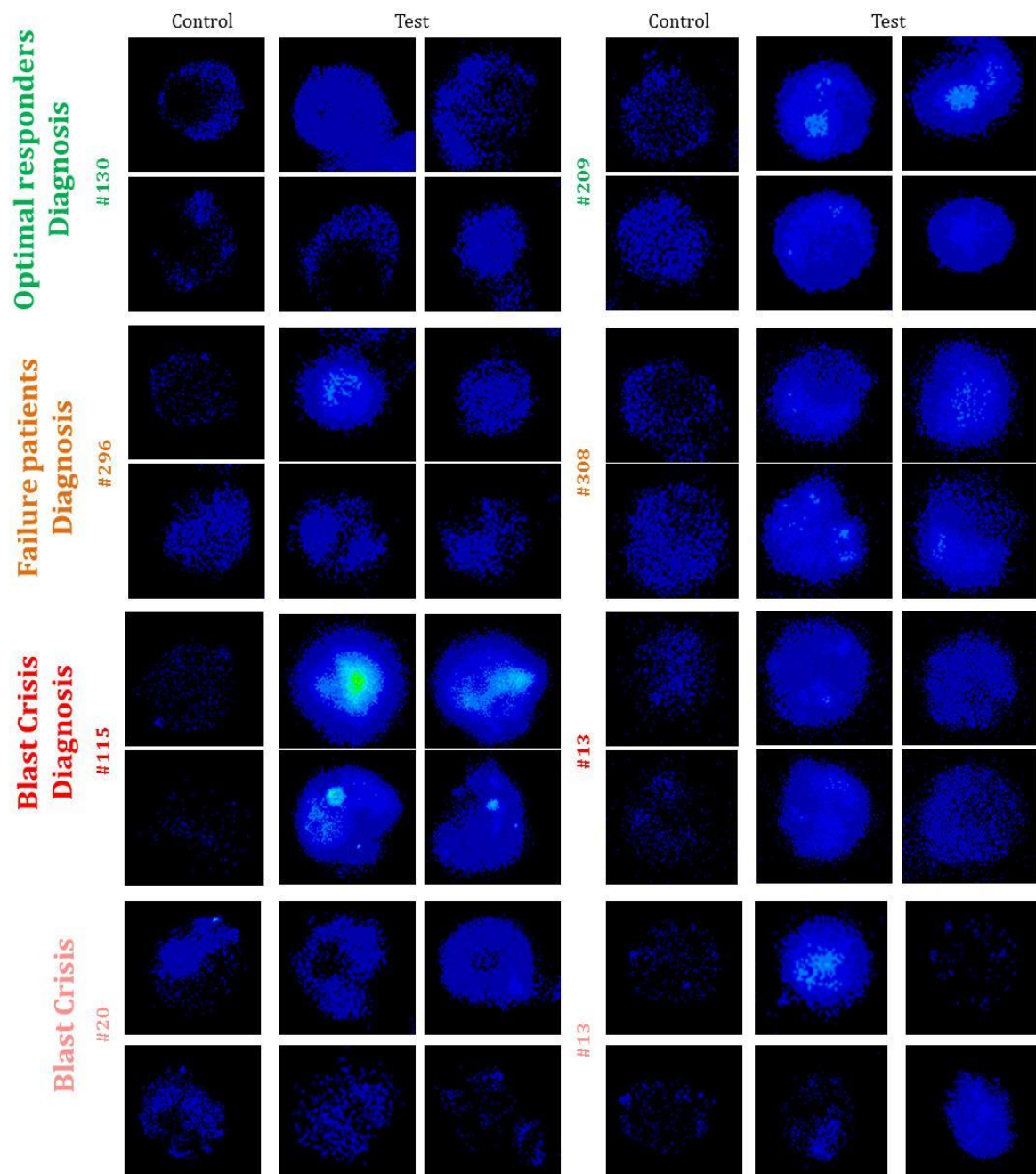
3.4.7 Do the levels of β-catenin found in MNCs correlate with levels in CD34+ cells?

CD34+ cells, obtained by selection from leukapheresis at original diagnosis **(see Methods section 2.2.3)**, were studied in optimal responders and failure patients. They were used as representative of the progenitor compartment to determine if there was a difference between a) MNC and CD34+ cells, and b) patient cohorts. CD34+ samples from patients at diagnosis who subsequently went into blast crisis were not available for analysis due to limitations on resources. This unfortunately limited the observations made in addressing this part of the study.

It was observed that the levels were significantly higher in the CD34+ cells compared to the MNCs **(Figure 3.4.23)** for phospho-β-catenin (Tyr654) in the optimal responders MNCs vs both the optimal responders and failure paitents CD34+ levels (P=0.044 and 0.050 respectively. This corresponds to higher expression of BCR-ABL1 in the more primitive CD34+ compartment [17]. However for the other β-catenin forms there was no significant difference between the patient cohorts. This could not be fully assessed due to the lack of samples available from the blast crisis patients. For the optimal responders and failure patients a similar trend was seen in both MNCs and CD34+ cells, but this did not achieve statistical significance.

Figure 3.4.23 Comparison of β-catenin levels between MNCs and CD34+ cells

Levels of the various forms of β-catenin were measured by FACS in matched MNCs and CD34+ cells from optimal responders and failure patients at diagnosis.

Results demonstrate that there are higher levels of all forms of β-catenin in the CD34+ cells, however this trend does not reach statistical significance, except for phospho-β-catenin (Tyr654) (P=0.044 in the optimal responders MNCs vs CD34+, and P=0.050 in the optimal responders MNCs vs failure patients CD34+).

A. Total β-catenin

B. Unphosphorylated β-catenin

C. Phospho-β-catenin (Ser45/Thr41)

D. Phospho-β-catenin (Tyr654)
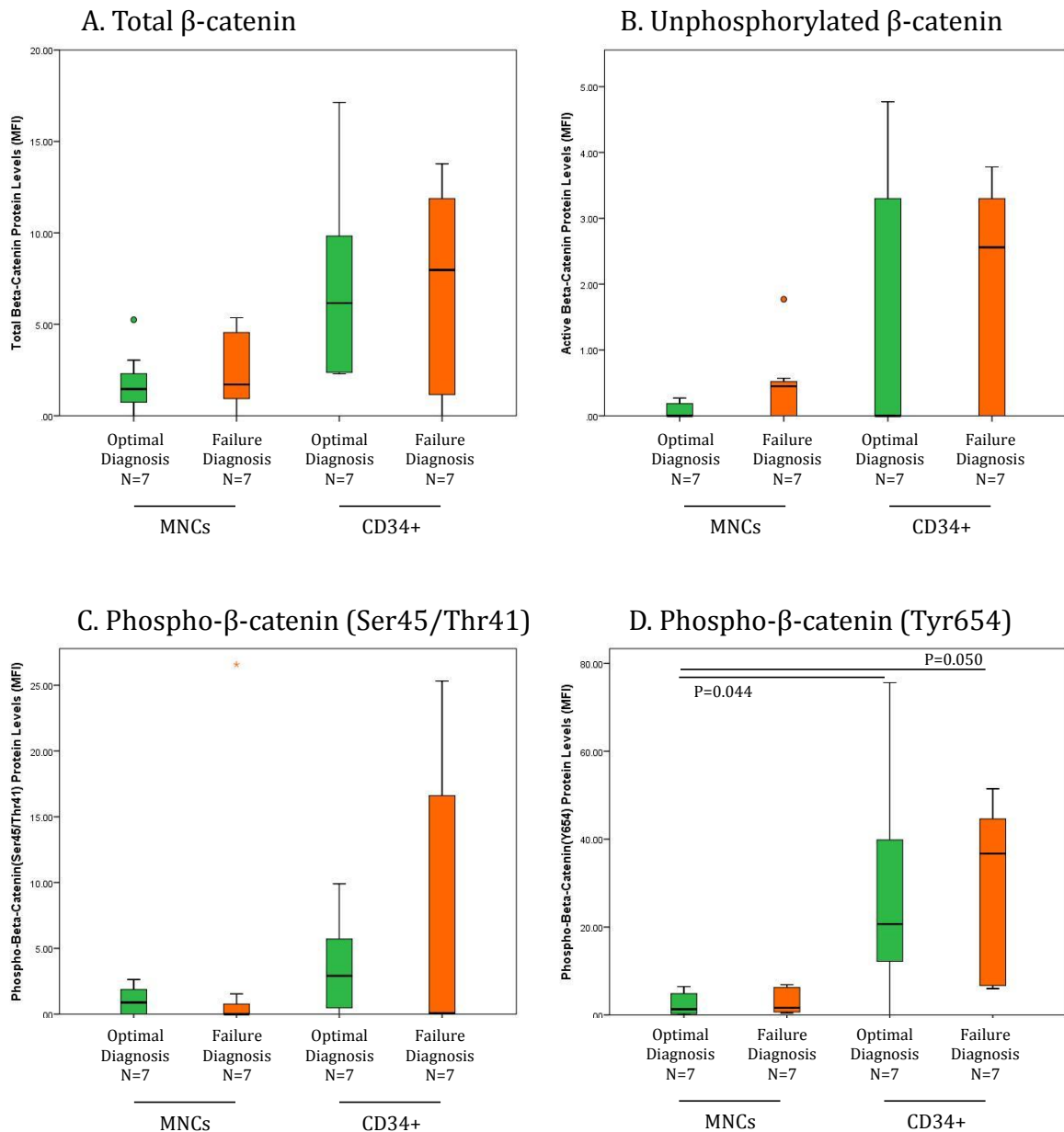
3.4.8 Is the Wnt pathway regulating the levels of β-catenin in CML MNCs?

3.4.8.1 The Wnt Pathway does not have the expected effects on β-catenin levels in CML cell lines

The Wnt pathway functions to regulate the activity of β-catenin which then translates to transcriptional activity [105]. Following on from the above experiments, which indicated that degradation by the proteasome may be an explanation why no change was seen between β-catenin levels in patient samples, the overall contribution of the Wnt pathway on β-catenin activity was measured. Cells were incubated with a Wnt pathway activator (WNT3A) and a Wnt pathway inhibitor (WIF1) [192] to see if modification of the Wnt pathway had an effect on the levels of β-catenin. On activation of the pathway with WNT3A, an increase in levels of unphosphorylated β-catenin would be expected. Conversely, with inhibition of the pathway by WIF1, an increase in the levels of phospho-β-catenin (Ser33/37/Thr41) would be expected.

LAMA-84 and HT-29 cells were incubated with 25ng WNT3A or 1.5µg WIF1 for 24 hours *in vitro* (N=3) **(Materials and Methods section 2.3.3)**. HT-29 cells were used as a control as they are known to have an active Wnt pathway [187, 188]. Levels were measured by FACS analysis **(Materials and Methods section 2.7)** and results show that in LAMA-84 cells both WNT3A and WIF1 do not have any effect on total β-catenin levels **(Figure 3.4.24 A)**. There is an elevation in unphosphorylated β-catenin levels with WNT3A incubation but this is not a significant change **(Figure 3.4.24 B)**. **Figure 3.4.24 C** shows that both WNT3A and WIF1 increase levels of phospho-β-catenin (Ser45/Thr41) compared to untreated levels. Finally, levels for phospho-β-catenin

(Ser33/37/Thr41) show a decrease with WNT3A, but no change in levels with WIF1 compared to untreated **(Figure 3.4.24 D)**. This could be indicating that β-catenin is being maximally degraded within CML MNCs; however these experiments on cell lines need to be further verified in patient samples.

Figure 3.4.24 The effects of WNT3A and WIF1 on the levels of β-catenin variants in LAMA-84 cells

The levels of β-catenin were measured by FACS in untreated, 25ng WNT3A, and 1.5µg WIF1 treated LAMA-84 cells (N=3) after 24 hour incubation. Results show A. total β-catenin, B. unphosphorylated β-catenin, C. phospho-β-catenin (Ser45/Thr41), and D. phospho-β-catenin (Ser33/37/Thr41) do not show the expected trend with either WNT3A or WIF1 treatment.
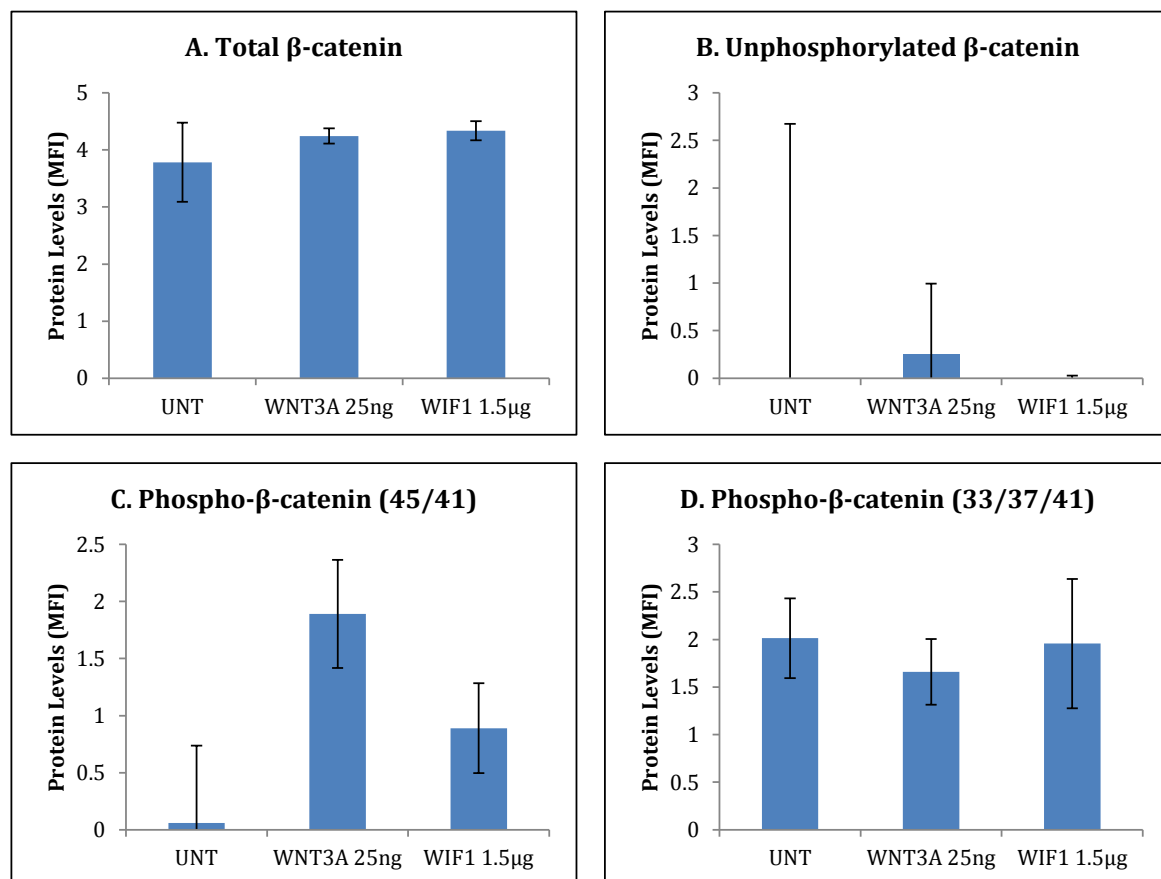
HT-29 cells were used as a control as they are known to have an active Wnt pathway [187, 188]. Results show that for total β-catenin, WNT3A does not change levels, while WIF1 causes an increase compared to untreated **(Figure 3.4.25 A)**. There is an elevation in unphosphorylated β-catenin levels with WNT3A incubation which was expected as the Wnt pathway is activated in these cells **(Figure 3.4.25 B)**. Phospho-β-catenin (Ser45/Thr41) levels decrease with both WNT3A and WIF1 incubation **(Figure 3.4.25 C)**. Finally, levels for phospho-β-catenin (Ser33/37/Thr41) **(Figure 3.4.25 D)** show a decrease with WNT3A as the pathway is activated and hence less β-catenin is degraded. In contrast, with WIF1 incubation there are significantly higher levels of phospho-β-catenin (Ser33/37/Thr41) than with WNT3A incubation (P=0.032), which correlates with inhibition of the pathway leading to increased degradation of β-catenin.

Figure 3.4.25 The effects of WNT3A and WIF1 on the levels of β-catenin variants in HT-29 cells

The levels of β-catenin were measured by FACS in untreated, 25ng WNT3A, and 1.5μg WIF1 treated LAMA-84 cells (N=3) after 24 hour incubation. Results show A. total β-catenin, B. unphosphorylated β-catenin, C. phospho-β-catenin (Ser45/Thr41), and D. phospho-β-catenin (Ser33/37/Thr41). WNT3A incubation increases levels of unphosphorylated β-catenin, while WIF1 incubation increases levels of phospho- β-catenin (Ser33/37/Thr41).
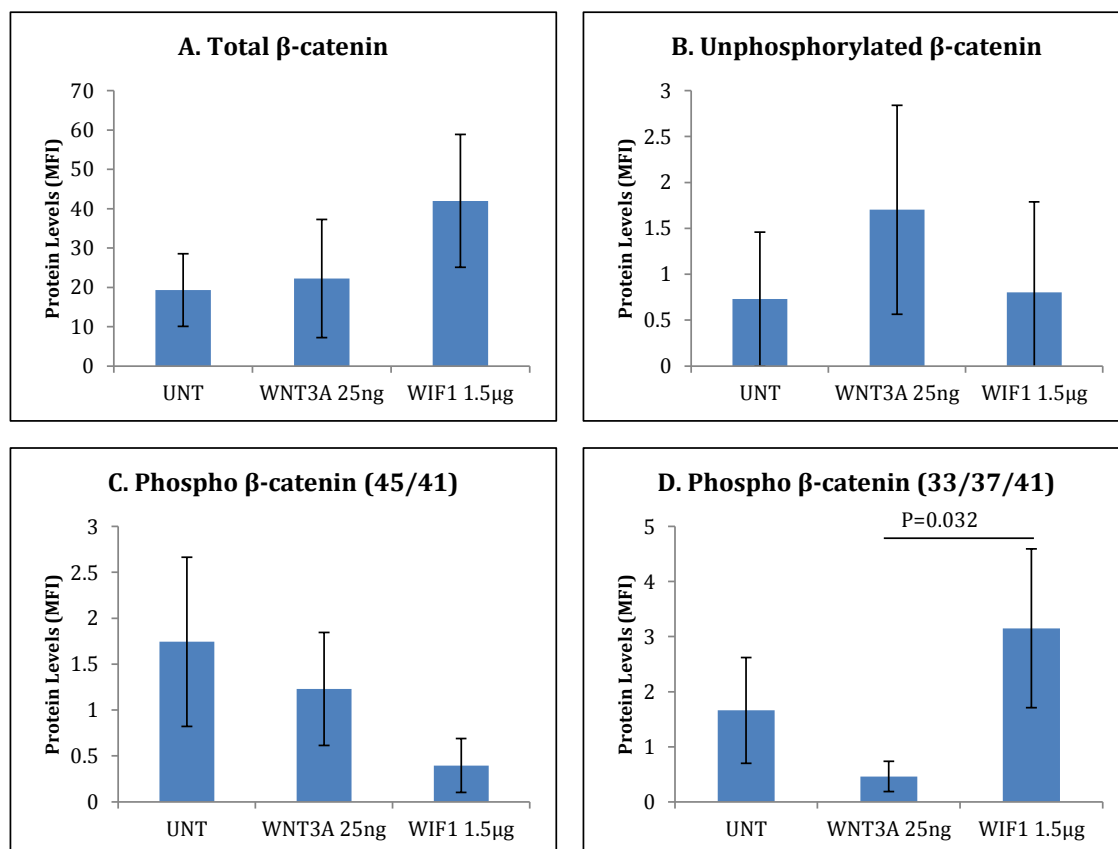
3.5 Main conclusions

Beta-catenin is a central component of the Wnt signalling pathway playing an essential role in mediating the activity of the pathway. Jamieson *et al.,* [150] previously showed an increase in unphosphorylated β-catenin in GMPs of those patients in blast crisis. As a consequence, the aim of this chapter was to pursue the study of β-catenin and its role within CML cells as previously described in **section 3.2**.

The main conclusions obtained from this chapter were the following;

1) After initial detection of elevated levels of β-catenin in primary CML MNCs, investigation into mRNA expression and total protein levels determined that these levels cannot be used to distinguish between different patient response cohorts and do not differentiate between stages of disease progression.

2) Analysis of 12 month samples showed a reduction in mRNA levels of β-catenin. However this reduction can be explained by the concept that after 12 months imatinib treatment leukaemic cells were replaced with normal cells. This was also seen in the second generation TKIs (dasatinib and nilotinib) with a significant reduction in β-catenin mRNA levels in the optimal responders after 12 months treatment (P=0.05 and 0.001 respectively).

3) Analysis of unphosphorylated β-catenin and phospho-β-catenin (Ser45/Thr41) was carried out to determine whether the activity and degradation of β-catenin differs in relation to patient outcome. Results showed levels to be similar between patient

cohorts. Re-stratification of the data into chronic phase vs blast crisis showed the expected trend with higher levels of unphosphorylated β-catenin in patients that have transformed into blast crisis. Additionally, phospho-β-catenin (Ser45/Thr41) levels decrease when patients have transformed into blast crisis. However, these results did not reach statistical significance, which could be because more differentiated cells are less dependent on β-catenin signalling for their survival [185]. This would then explain why the results found for GMPs by Jamieson *et al.*,[150] are not reproducible in MNCs.

4) Analysis of sub-cellular localisation confirmed that unphosphorylated β-catenin is found predominantly in the nucleus, however this was also found for phospho-β-catenin (Ser45/Thr41), opposite to what was anticipated with it being a marker for degradation in the cytoplasm. Maher *et al.* [149] also found this to be the case whereby β-catenin phosphorylated on Ser45/Thr41 can localise in the nucleus, unlike β-catenin phosphorylated on Ser33/37/Thr41. This therefore means that phospho-β-catenin (Ser45/Thr41) is not a good marker to use for β-catenin degradation by the proteasome.

5) Analysis by confocal microscopy alluded to a relationship between unphosphorylated β-catenin and the phospho-β-catenin forms in individual patients. This was shown by higher levels of unphosphorylated β-catenin correlating with low levels of phospho-β-catenin (both Ser45/Thr41 and Ser33/37/Thr41). Conversely, when the levels of phospho-β-catenin (again, both Ser45/Thr41 and Ser33/37/Thr41) were elevated, there were lower levels of unphosphorylated β-catenin. This indicates that regulation of β-catenin by its

phosphorylation status is still functioning in CML MNCs; however, the levels cannot be used to distinguish between patient cohorts.

6) Inhibition of the proteasome in CML cell lines using bortezomib corresponded with an increase in unphosphorylated β-catenin and a decrease in phospho-β-catenin (Ser33/37/Thr41) indicating that in CML cells, β-catenin is actively degraded by the cell. This could be why no difference in the levels of β-catenin is being detected between patient cohorts. To test this further, patient samples could be cultured *in vitro* with bortezomib to determine if the results seen in cell lines are replicated in patients.

7) Analysis of phospho-β-catenin (Tyr654) showed no difference between patient cohorts at diagnosis, consistent with the view that BCR-ABL1 activity is broadly similar across patients at initial diagnosis [190]. There are significantly lower levels of phospho-β-catenin (Tyr654) in blast crisis CML MNCs compared to chronic phase (p=0.012) which correlates with the premise that CML can become BCR-ABL1 independent at disease transformation [191].

8) CD34+ cells were used to represent the progenitor cell population and alongside MNCs, protein levels were assessed to answer the question of whether the high levels of β-catenin found in the more primitive cells correlate with levels in MNCs. Limitations to patient material meant that this part of the study could not be fully addressed. However, it was observed that the levels were higher in the CD34+ cells compared to the MNCs, significantly so for phospho-β-catenin (Tyr654) which had

higher levels in the optimal responders CD34+ cells (P=0.044). This corresponds to higher expression of BCR-ABL1 in the more primitive CD34+ compartment [17].

9) LAMA-84 cells cultured with WIF1 (Wnt pathway inhibitor) and WNT3A (Wnt pathway activator do not show the expected trend on β-catenin levels, suggesting that the Wnt pathway/β-catenin is not actively enhanced in CML MNCs.

Chapter 4 – Does glycogen synthase kinase 3β (GSK3β) have a role in CML?

4.1 Introduction

Glycogen synthase kinase 3β (GSK3β) is a constitutively active serine/threonine kinase which, within the Wnt signalling pathway, acts as a tumour suppressor by functioning as a key component in the degradation of β-catenin [105]. The activity of this kinase is itself controlled by its phosphorylation status with phosphorylation on Ser9 inhibiting its activity by forming a pseudosubstrate which blocks the active site of GSK3β [152]. Alternatively, phosphorylation at Tyr216 enhances the activity of GSK3β by altering its conformation, enabling substrate access to its active site **(Introduction section 1.9)** [152, 155, 156]. GSK3β substrates must be phosphorylated by another, different, kinase to 'prime' the substrate prior to phosphorylation by GSK3β [149].

The phosphorylation status of GSK3β is regulated by various kinases which are able to phosphorylate GSK3β at Ser9 to inhibit its activity. These include; Akt, ILK, PKA and p90Rsk [153, 155].The method of phosphorylation on Tyr216 is ambiguous with kinases including PYK-2, FYN, MEK1/2 and SRC-family kinases all being reported to be able to phosphorylate this residue [155, 164]. However, there is also a possibility of autophosphorylation being responsible for phosphorylation of GSK3β at this site [155, 157, 164].

Abrahamsson *et al.,* [101] have reported in CML that there is a decrease in GSK3β protein expression at disease progression as determined by FACS analysis. In these samples splice variants were discovered with mutations giving rise to splice isoforms in which exon 9, exon 11, or both are deleted. Exon 9 and 11 deletions have been previously discovered in Parkinson's disease [163], however the particular truncated isoforms of exon 8 and 9 which have been found in CML progenitors have not previously been reported. Due to overexpression of the full-length *GSK3β* causing a decrease in activated β-catenin, it can be said that *GSK3β* mis-splicing is a significant event in the development of LSCs and that restoration of the splicing events may have a possible therapeutic benefit [101]. The mechanisms which occur to induce this mis-splicing have yet to be determined. Changes in splicing events can either inactivate tumour suppressors or activate proteins which promote tumour development. In CML, assessment of the splice isoforms in *GSK3β* might be useful as an indicator of disease progression, and might also form a therapeutic target for treatment of patients in advanced phase CML [101].

In addition to mis-splicing of *GSK3β* having an impact on disease progression, GSK3β is also of interest as it has been shown to be crucial in the modulation of HSCs by controlling the decision between self-renewal and differentiation through both the Wnt and mTOR pathways, with Wnt stimulating self-renewal, and mTOR enhancing lineage commitment [193]. Furthermore, GSK3β has been reported to be involved in the maintenance and function of a quiescent HSC pool, independent of signalling pathways [164, 194].

SB216763, developed by GlaxoSmithKline (GSK), is an ATP-competitive inhibitor of GSK3β [195] which has been shown to reduce levels of Tyr216 phosphorylation of GSK3β in CML progenitor cells [164]. Additionally, it diminishes the levels of phosphorylated β-catenin targeted for degradation, while increasing the unphosphorylated levels[164]. The results obtained from this GSK3β inhibitor *in vitro* have encouraged the development of a GSK3β inhibitor to be used *in vivo* [164, 193, 194]. In addition to SB216763, another GSK3β inhibitor, CHIR-911, has been tested to determine its effects on HSC activity in vivo in mice transplanted with either mouse or human HSCs. Results found that the inhibitor increased haematopoietic repopulation by amplifying the yield of the progenitor population, as well as prolonging the survival of transplanted mice, indicating the value of GSK3β inhibition on the repopulation ability of HSCs [194].

As no difference was found in the levels of β-catenin forms between patient cohorts in the previous chapter, it was of interest to see if GSK3β was performing a role within CML. It would be expected that changes in GSK3β would be reflected in the levels of β-catenin. However, as GSK3β has been reported to function independently of the Wnt pathway [164], it may also have an effect on CML disease progression independent of β-catenin. Additionally, although it has been reported that there is a decrease in GSK3β protein expression, its phosphorylated forms and their impact on disease progression have not been previously investigated.

4.2 Aims

The aims of this chapter are;

1) To determine the effects of GSK3β inhibition by SB216763 on β-catenin levels, considering that there was no difference in the various forms of β-catenin between patient outcomes in the previous chapter.

2) To investigate whether the mRNA transcript levels of *GSK3β* can be predictive of clinical outcome in imatinib treated patients.

3) To look at phospho-GSK3β Tyr216 and phospho-GSK3β Ser9, to determine if GSK3β's activity differs in relation to patient outcome.

4) To investigate what regulates GSK3β's activity in CML.

5) To determine whether GSK3β activity correlates with C-MYC degradation.

4.3 Optimisation of techniques

All optimisation was performed on experimentation in cell lines prior to patient sample use.

4.3.1 Optimisation of the GSK3β antibodies by western blotting

Lysates were prepared from CML cell lines K562 and LAMA-84 and western blots were carried out **(Materials and Methods section 2.9)**. Initial antibody concentrations tested were taken from the supplied data sheet with final concentrations of phospho-GSK3β (Ser9) being 0.3µg/ml, phospho-GSK3β (Tyr216) being 1µg/ml and total GSK3β being 0.25µg/ml. A representative blot is shown in **Figure 4.3.1**.

Figure 4.3.1 Optimisation of the GSK3β antibodies

Antibodies were optimised for detection of GSK3β with a final concentration of phospho-GSK3β (Ser9) being 0.3µg/ml, phospho-GSK3β (Tyr216) being 1µg/ml and total GSK3β being 0.25µg/ml. The molecular weight for phospho-GSK3β (Ser9) and total GSK3β is 46kDa, and the molecular weight of phospho-GSK3β (Tyr216) is 47kDa. Both phospho-GSK3β (Ser9) and phospho-GSK3β (Tyr216) show a double band due to the additional detection of GSK3α. Actin was used as a loading control.
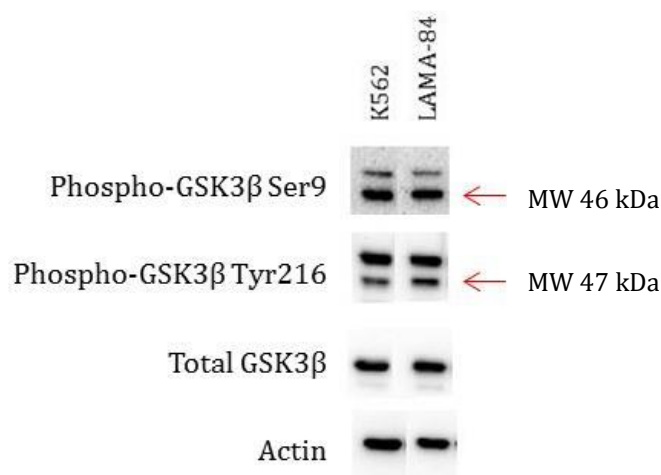
4.3.2 Optimisation of the GSK3β inhibitor SB216763 in K562 cells

The optimum concentration of the GSK3β inhibitor SB216763 was verified prior to experimentation. K562 cells were incubated with different concentrations of the inhibitor (2.5µM, 5µM, and 7.5µM) in vitro for 24 hours **(Materials and Methods section 2.3.3)**. Lysates were then prepared from the cultures and a western blot was carried out **(Materials and Methods section 2.9)**. The levels of phospho-GSK3β (Ser9), phospho-GSK3β (Tyr216), and total GSK3β were measured and results showed that 5µM SB216763 gave the optimum increase in phospho-GSK3β (Ser9) and decrease in phospho-GSK3β (Tyr216) **(Figure 4.3.2)**. This concentration was used for all further experimentation.

Figure 4.3.2 Optimisation of SB216763

K562 cells were incubated in vitro with SB216763 for 24 hours to determine which concentration is optimal. Results show that 5μM SB216763 showed optimal trade-off between increased levels of Ser9 phosphorylation and decreased levels of Tyr216 phosphorylation.
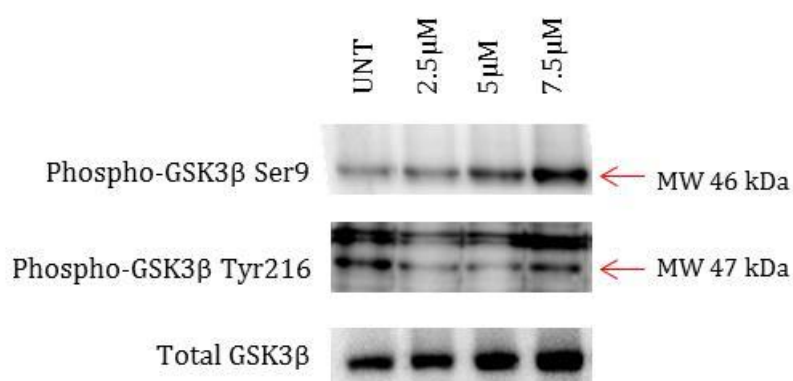
In addition to determining the optimum concentration of SB216763, K562 and LAMA-84 cells were incubated with 5μM SB216763 for 24 and 48 hours to ascertain whether incubation with the drug affects cellular proliferation and the viability of the cells. Cellular proliferation was measured by MTT assay (N=3) **(Materials and Methods section 2.8)** and the viability of the cells were tested by PI and FACS analysis (N=3) **(Materials and Methods section 2.7.2)**. Results showed **(Figure 4.3.3)** SB216763 has no effect on proliferation at 24 hours and increases it after 48 hours of culture. In addition it has no effect on cell viability at both 24 and 48 hours. It was decided that 24 hour incubation should be used for all further experimentation.

Figure 4.3.3 SB216763 has no effect on proliferation at 24 hours and increases it after 48 hours of culture. In addition it has no effect on cell viability at both 24 and 48 hours

Cells were incubated with SB216763 for 24 and 48 hours to test its effect on cell proliferation and viability. Results show SB216763 has no effect on proliferation at 24 hours but increases it after 48 hours of culture. It has no effect on cell viability at both 24 and 48 hours.
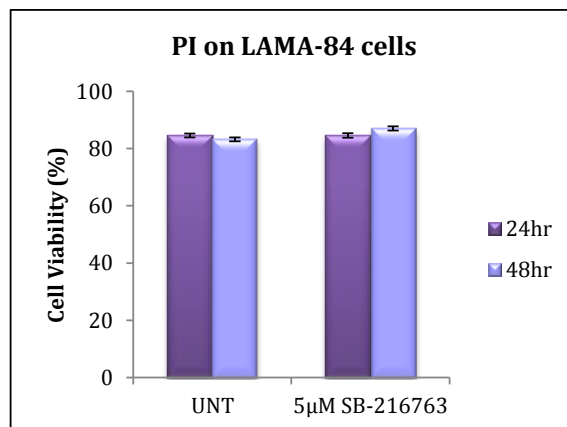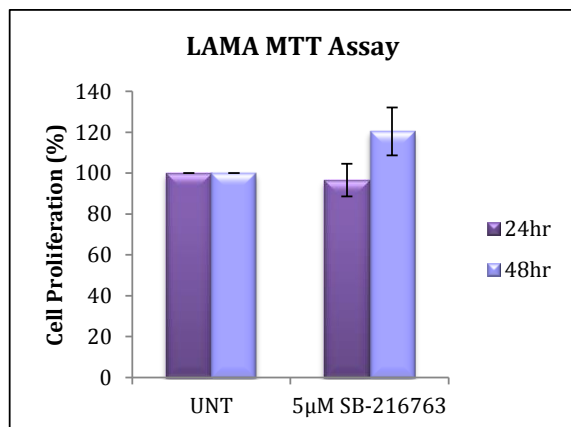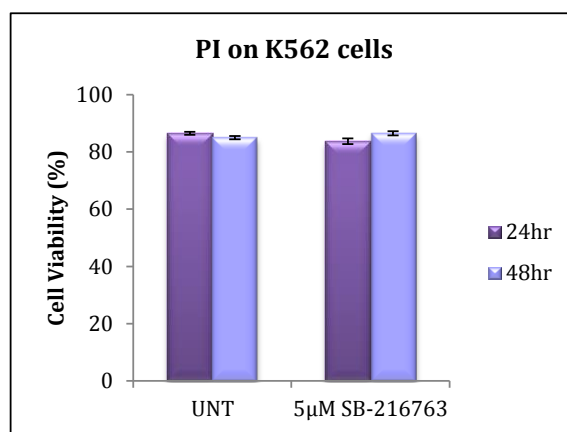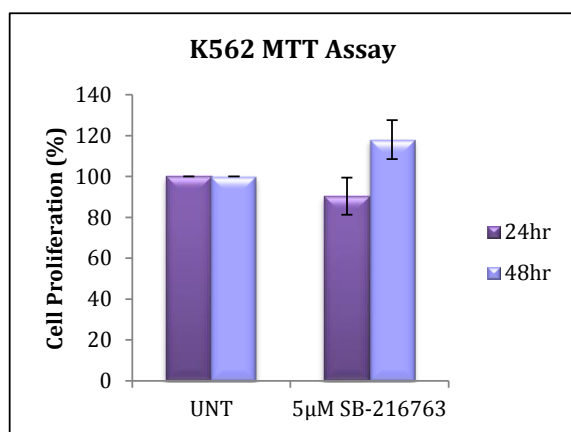
4.4 Results

4.4.1 Is GSK3β having an effect on the levels of β-catenin?

As a result of there being no significant difference found in the levels of β-catenin forms in correlation with patient outcome, it was relevant to determine the effects, if any, that GSK3β has on β-catenin levels. This was examined using the GSK3β inhibitor SB216763 to see if there were any changes in β-catenin forms when GSK3β activity was inhibited.

The levels of total β-catenin, unphosphorylated β-catenin, and phospho- β-catenin (Ser33/37/41) were measured to determine the effect inhibition of GSK3β has on the levels of β-catenin (N=3) **(Figure 4.4.2)**. Results showed that in both K562 and LAMA-84 cell lines there was a trend towards a decrease in total β-catenin levels on incubation with SB216763. Focussing on unphosphorylated β-catenin and phospho-β-catenin (Ser33/37/Thr41), results confirmed that inhibition of GSK3β has the predicted outcome on β-catenin levels, with unphosphorylated β-catenin increasing with inhibition of GSK3β, and phospho-β-catenin (Ser33/37/Thr41) decreasing. This shows that inhibition of GSK3β decreases the amount of β-catenin degraded, elevating unphosphorylated protein levels which can translocate to the nucleus and activate transcription. The differences in these levels are not significant, which could either be due to the small number of replicates, or may be indicative of why there was not a significant difference found in the levels of β-catenin in the previous chapter.

Figure 4.4.1 Inhibition of GSK3β increases the levels of unphosphorylated β-catenin and decreases the levels of phospho-β-catenin (Ser33/37/41)

K526 and LAMA-84 cells were incubated in vitro for 24 hours with 5µM SB216763 and FACS analysis was used to determine the effects this inhibitor has on β-catenin levels (N=3). Results show a trend towards a decrease in total β-catenin levels, an increase in unphosphorylated β-catenin levels, and a decrease in phospho-β-catenin (Ser33/37/Thr41) levels in both cell lines.
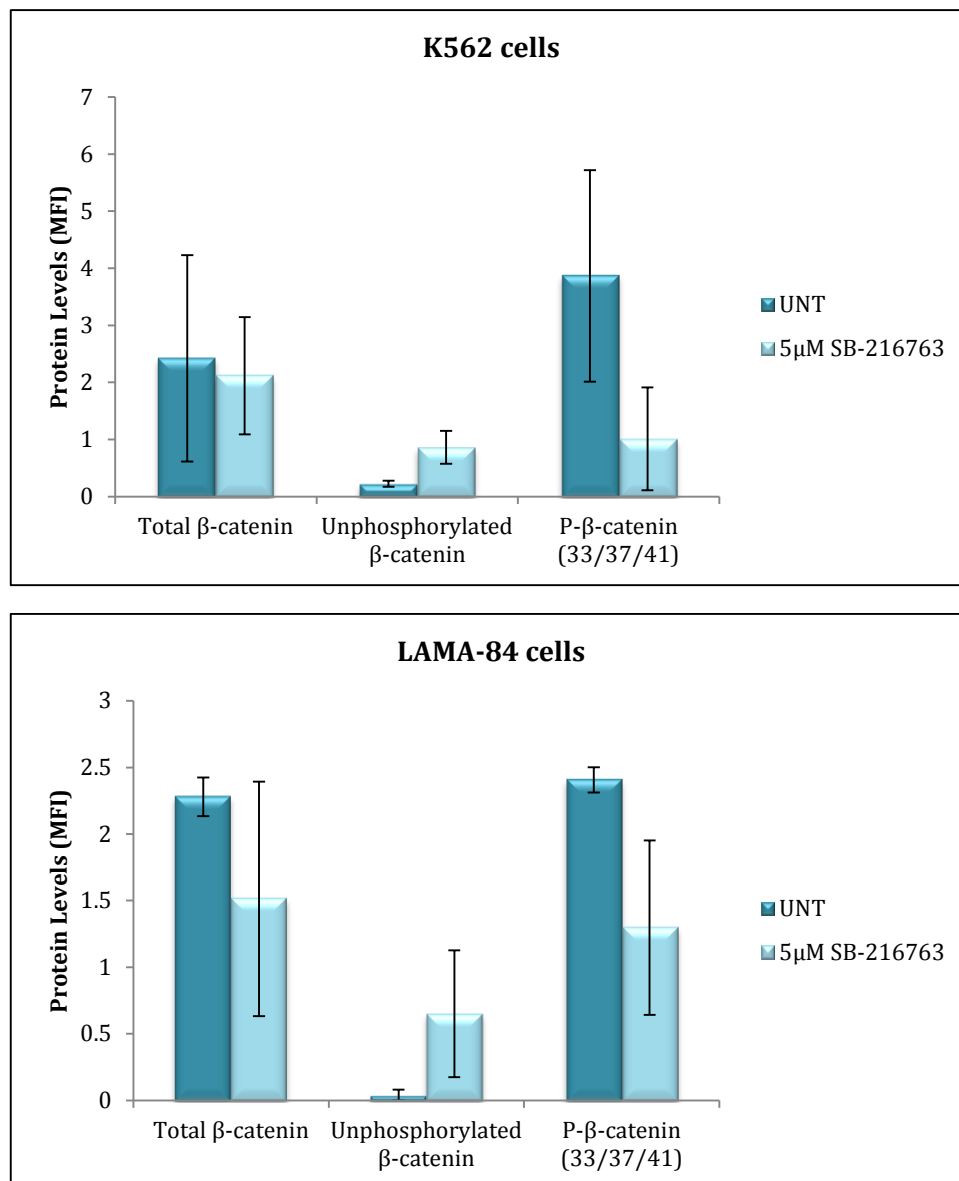
4.4.2 Comparison of GSK3β levels in the different CML patient cohorts

To analyse the difference in GSK3β between the various clinical groups, patient samples were again split into three patient outcome cohorts in line with the ELN definitions (as described in **section 1.4.2**); optimal responders, failure patients and blast crisis patients, exactly as was performed in the previous chapter. For mRNA levels, patient material was available to look at both optimal responders and failure patients at diagnosis, and patients who subsequently transformed into blast crisis at diagnosis, and patients when they had transformed into blast crisis. For protein levels, patient material was available for both optimal responders and failure patients at diagnosis. However, for patients who subsequently transform into blast crisis, material was only available from when they had transformed into the final stage of the disease and not at diagnosis.

4.4.2.1 *GSK3β* mRNA transcript levels are elevated in patients with poor prognosis

Similarly to the previous chapter, *GSK3β* mRNA transcript levels were first investigated to see if there was a difference between patient cohorts. As with previous findings, the decrease in levels shown in 12 month samples is likely due to the leukaemic cells being replaced with normal cells. These 12 month data were therefore eliminated from the study.

Two different primer sequences were used to examine the *GSK3β* transcript levels **(Materials and Methods, Table 2.3)**. Firstly, a primer sequence was used which detects both the long (normal) and short (spliced variant lacking exon 8 and 9) form of *GSK3β* by using primers within exons 1-2 found in both variants. Secondly, a primer sequence was used which detects only the long (normal) form of *GSK3β* by using primers within exons 8-9, which are deleted in the splice variant.

Results showed an increase in levels of *GSK3β* (long and short) transcript in diagnostic samples from patients who subsequently transformed into blast crisis (N=11), and in patients already in blast crisis (N=11), compared to optimal responders (N=14) and failure patients (N=12) at diagnosis. However, these observations were not statistically significant **(Figure 4.4.3)**.

Figure 4.4.3 mRNA transcript levels of all splice variants of *GSK3β* (long and short) show increasing levels of expression with worsened outcome

mRNA expression levels of the long and short transcript types of *GSK3β* were investigated in optimal, failure and blast crisis patients at both diagnosis (N=14, 12 and 11 respectively), and when patients were in blast crisis (N=11). Levels were also measured in 3 samples from healthy donors to compare with patients. Results showed an increase in levels of *GSK3β* mRNA in diagnostic samples from patients who subsequently transformed into blast crisis, and patients who are in blast crisis in comparison to optimal responders and failure patients at diagnosis. This observation was not statistically significant.
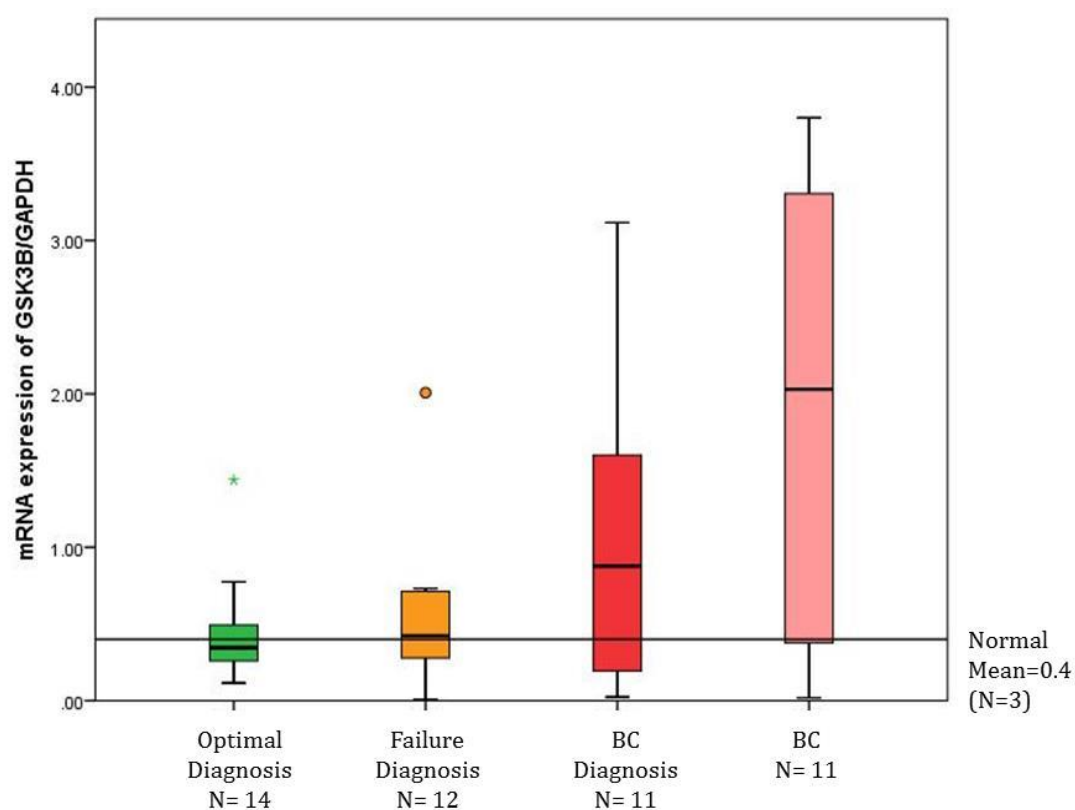
When looking at the long (normal) transcript type of *GSK3β* independently **(Figure 4.4.4)** levels were again higher in both the patients at diagnosis who subsequently transformed into blast crisis, and the patients already in blast crisis, compared to

optimal responders and failure patients. Again these observations were not statistically

significant..

Figure 4.4.4 mRNA transcript levels of long form *GSK3β* show significantly higher levels of expression with worsened outcome

mRNA expression levels of the long transcript type of *GSK3β* were investigated in the same cohort of patients as in Figure 4.4.3 Results showed levels of long form *GSK3β* were again higher in patients at diagnosis who subsequently transformed into blast crisis and patients in blast crisis compared to optimal responders at diagnosis and failure patients. These observations were not statistically significant.
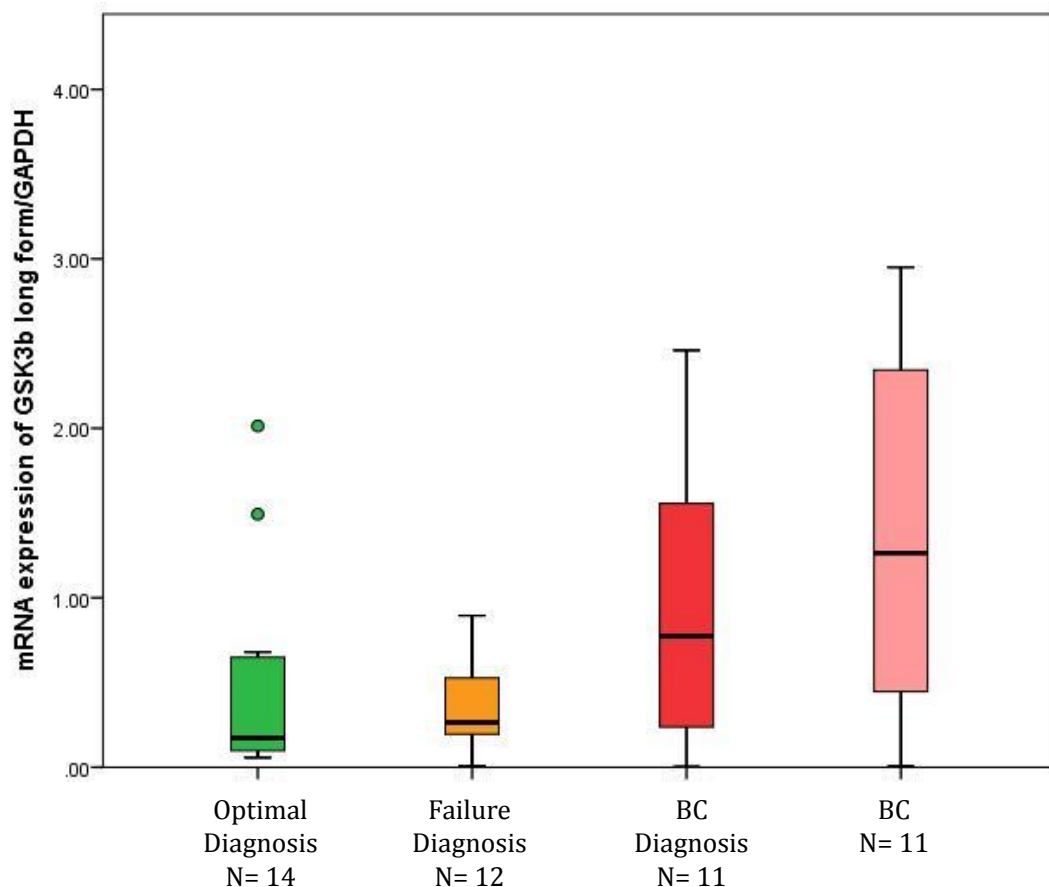
Splice variant analysis was performed by a Dr L Wang to look at the following transcript types of *GSK3β*; *GSK3β* with no deletion, *GSK3β* with exon 9 deletion, and *GSK3β* with exon 8 and 9 deletion, with regards to differences in splice variation between patient cohorts, however the results showed that the splice variants were found in all patient cohorts as well as healthy donors and the line of investigation was discarded.

Due to the role of GSK3β as a tumour suppressor, this may explain why its transcription is upregulated in blast crisis, in an attempt to balance the oncogenic potential of blast crisis cells. However, the activity of GSK3β is regulated through its phosphorylation status so this was investigated next to determine if there is a difference in GSK3β activity between patient outcomes.

4.4.2.2 GSK3β protein levels reveal that there are significantly decreased levels of GSK3β activity in patients who have transformed into blast crisis

The two phosphorylated forms of GSK3β which were of interest by their regulation on GSK3β activity were phospho- GSK3β Ser9 which inhibits GSK3β, and phospho-GSK3β Tyr216 which enhances GSK3β's activity. In addition, total GSK3β and levels of actin were used as controls.

Western blotting **(Materials and Methods section 2.9)** was used to analyse 31 CML samples. Optimal responders (N=13) and failure patients (N=10) were analysed at

diagnosis, and blast crisis samples were analysed when patients had transformed into blast crisis (N=8). Unfortunately, as before, samples from patients at diagnosis who subsequently transformed into blast crisis were not available for analysis. Due to the lack of samples available from this group it is not possible to determine if GSK3β could be a predictive biomarker. Analysis was carried out according to chronic phase vs blast crisis where chronic phase included optimal responders and failure patients at diagnosis (N=23), and blast crisis were the patients who had transformed (N=8). Levels were measured using antibodies against phospho-GSK3β Ser9 and phospho-GSK3β Tyr216. These were then calibrated to actin and total GSK3β. Densitometry was used to obtain quantitative data on the results so statistical analysis could be done using a Mann-Whitney u test to determine whether the difference is statistically significant. A common lysate of K562 cells was used to ensure consistency between different blots.

Results show **(Figure 4.4.6)** that there was a significant decrease in GSK3β activity demonstrated by opposing trends in Ser9 and Tyr216 phosphorylation. The results for phospho- GSK3β Ser9 **(Figure 4.4.6 A)**, showed elevated levels in those patients who had transformed into blast crisis compared to those in chronic phase (P=0.026). This reveals higher levels of GSK3β inhibition in those patients who have transformed into blast crisis. This finding was further substantiated by the results for phospho- GSK3β Tyr216 **(Figure 4.4.6 B)** which showed that there is significantly higher levels in the chronic phase patients compared to the patients who have transformed into blast crisis (P<0.001). The inhibition of GSK3β alongside a reduction in Tyr216 phosphorylation suggests a significant decrease in GSK3β activity in those patients who have transformed into blast crisis.

Figure 4.4.6 Protein levels of GSK3β indicate a significant decrease in GSK3β activity demonstrated by opposing trends in Ser9 and Tyr216 phosphorylation of GSK3β

Analysis was carried out according to chronic phase (N=23) vs blast crisis (N=8). Levels were measured via western blotting using antibodies against phospho-GSK3β Ser9 and phospho-GSK3β Tyr216. The results for phospho- GSK3β Ser9 showed increased levels in patients who had transformed into blast crisis compared to chronic phase (P=0.026).The results for phospho-GSK3β Tyr216 showed significantly higher levels in the chronic phase patients compared to patients in blast crisis (P<0.001). A representative blot is shown in C.
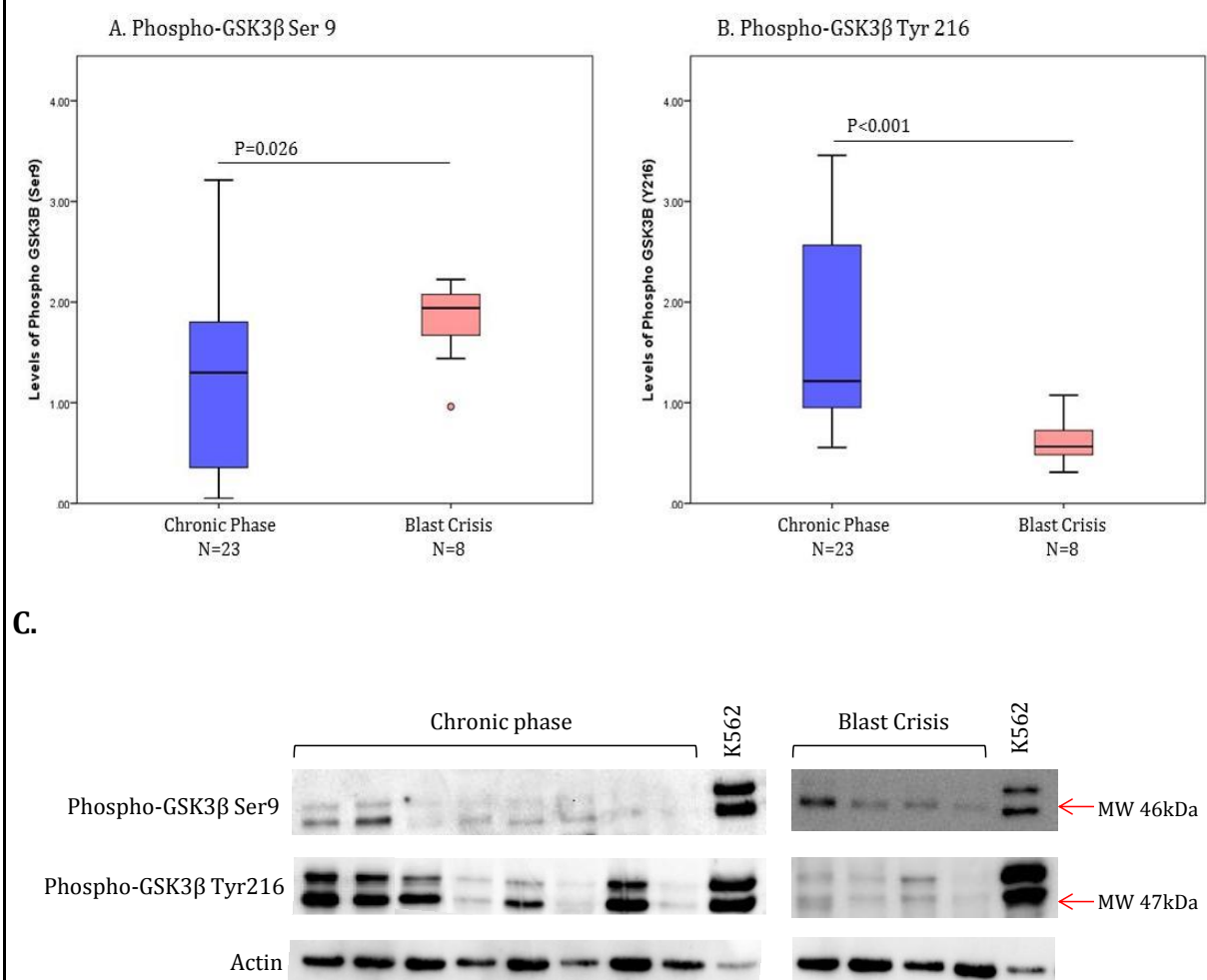
4.4.2.3 Confirming data using MCL-1 as a read out of GSK3β activity

MCL-1 is a member of the BCL-2 family [158]. There are two isoforms of MCL-1; the longer isoform acts by inhibiting apoptosis and increasing cell survival (anti-apoptotic), while the shorter isoform promotes apoptosis, inhibiting cell survival (pro-apoptotic) [159].

Along with apoptosis, data suggest that MCL-1 promotes the Wnt pathway by disrupting the association of β-catenin with the destruction complex in the cytoplasm. This is as a result of MCL-1 acting as a substrate for GSK3β, preventing GSK3β from phosphorylating and targeting β-catenin for degradation [160].

GSK3β is known to phosphorylate MCL-1 on serine 159 and initiate its degradation by the proteasome [196]. Therefore, MCL-1 was used as a read-out of GSK3β activity. As it was previously found that GSK3β activity significantly decreased in patients who had transformed into blast crisis, the levels of MCL-1 were measured by western blotting **(Materials and Methods section 2.9)** statistical analysis using a Mann-Whitney u test was carried out to see if the protein levels correlated with the results obtained for GSK3β. The two isoforms were detected by the antibody used; MCL-1 (MW 40kDa) represents the anti-apoptotic form, while MCL-1 (MW 32kDa) represents the pro-apoptotic form. Results showed that the levels of both isoforms of MCL-1 significantly increased in the patients who had transformed into blast crisis compared with chronic phase patients (P<0.001 for both isoforms of MCL-1) **(Figure 4.4.7)**. This supports the finding of decreased GSK3β activity in patients who have transformed into blast crisis as

it correlates with an increase in MCL-1 levels which may be due to a decrease in

phosphorylation, and thus degradation.

Figure 4.4.7 MCL-1 protein levels are significantly higher in patients who have transformed into blast crisis

Chronic phase (N=23) samples were compared to blast crisis (N=8) and levels of MCL-1 were measured via western blotting and calibrated to actin. Results showed that the levels of both isoforms of MCL-1 significantly increased in the patients who had transformed into blast crisis compared chronic phase (P<0.001 for both isoforms of MCL-1). A representative blot is shown in C.
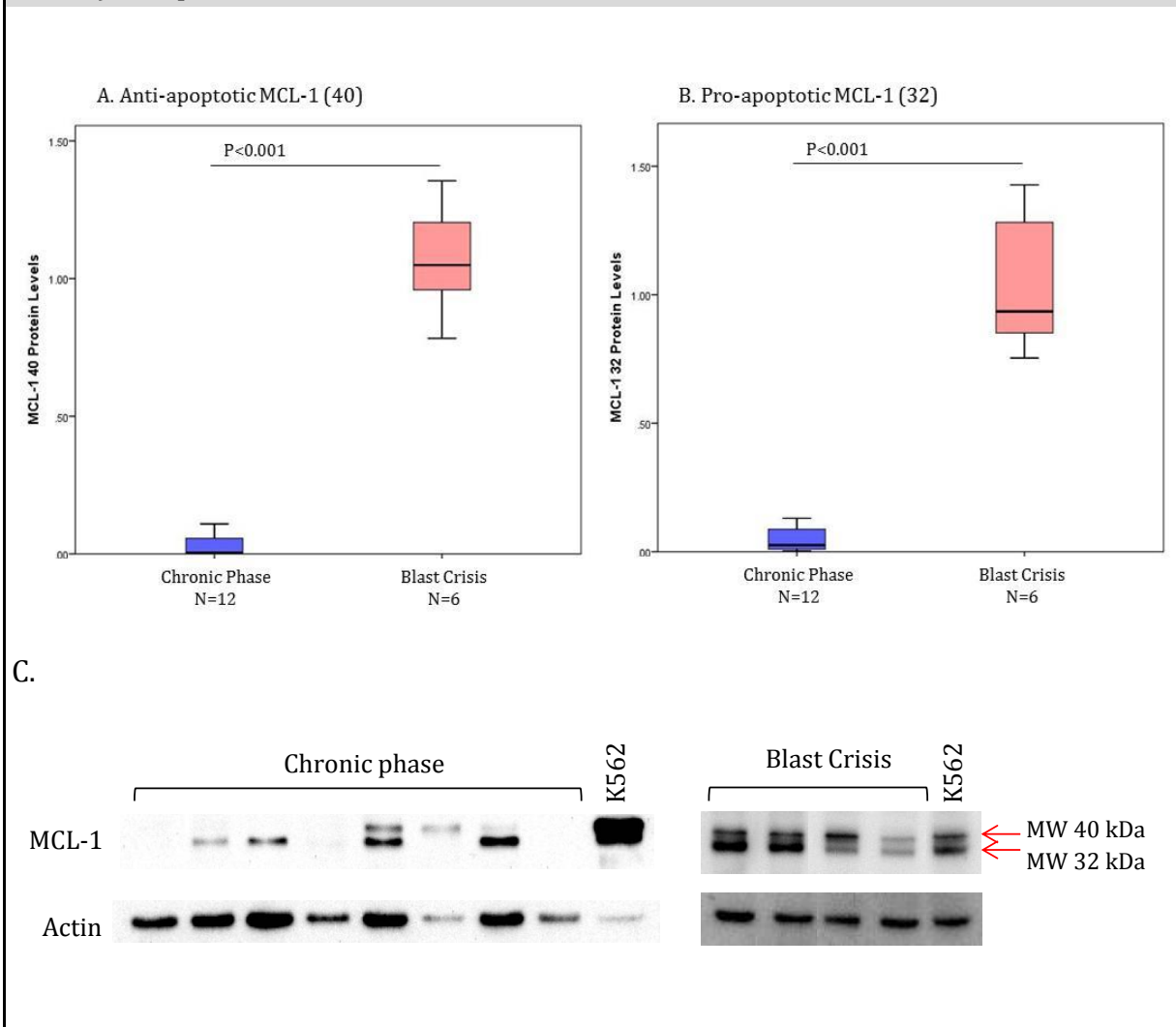
4.4.3 What regulates GSK3β activity?

Following the finding of a significant decrease in GSK3β activity in samples from patients who had transformed into blast crisis, the next question to ask is; what is regulating this activity?

4.4.3.1 The TKIs have no effect on GSK3β activity

Initially, the effect of the TKIs was investigated to determine if GSK3β activity was under the control of BCR-ABL1. K562 and LAMA-84 cells were treated with 5μM imatinib, 150nM dasatinib, and 5μM nilotinib for 24 hours *in vitro* **(Materials and Methods section 2.3.3)**, lysates were made and the levels of GSK3β were measured by western blot **(Materials and Methods section 2.9)**. These were compared to an untreated control to determine the effects of the TKIs on GSK3β (N=4). A representative blot is shown in **Figure 4.4.8**. Densitometry was used to obtain quantitative data on the results so statistical analysis could be done using a T-test to determine whether the difference is statistically significant. Results showed that for K562 cells, all three TKIs had no effect on the levels of phospho-GSK3β Ser9. This was also true for the LAMA-84 cells. Additionally, for both K562 and LAMA-84 cells there was a decrease in levels of phospho-GSK3β Tyr216 in the treated cells, especially with dasatinib and nilotinib treatment but these differences did not reach statistical significance.

Figure 4.4.8 TKIs have no effect on GSK3β levels

K562 and LAMA-84 cells were incubated with 5μM imatinib (IM), 150nM dasatinib (DAS), and 5μM nilotinib (NIL) for 24 hours *in vitro* and compared to an untreated control (UNT) (N=4). Results showed in K562 cells, all three TKIs had no effect on the levels of phospho-GSK3β Ser9 (MW 46kDa), which was also found for the LAMA-84 cells. In both cell lines the treated cells showed a decrease in levels of phospho-GSK3β Tyr216 (MW 47kDa), in particular DAS and NIL but these differences were not statistically significant.
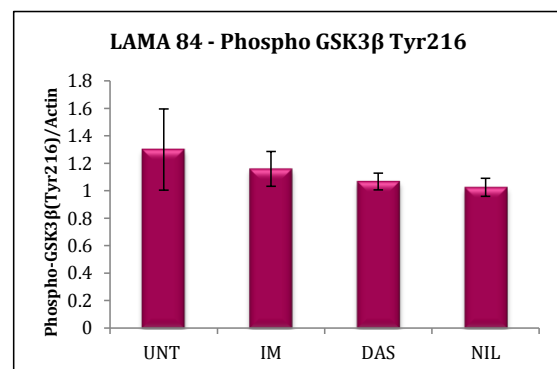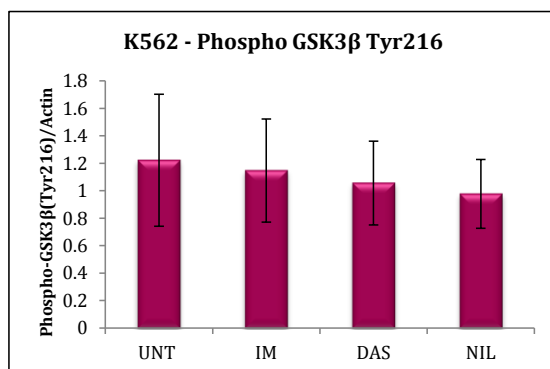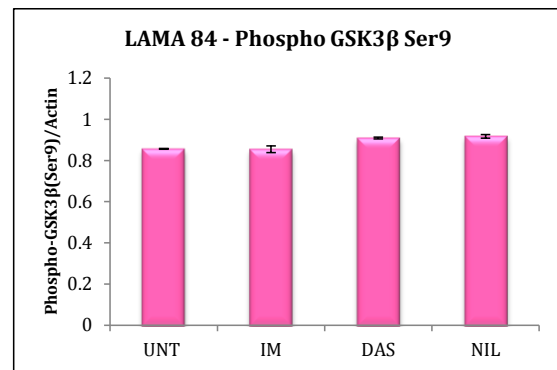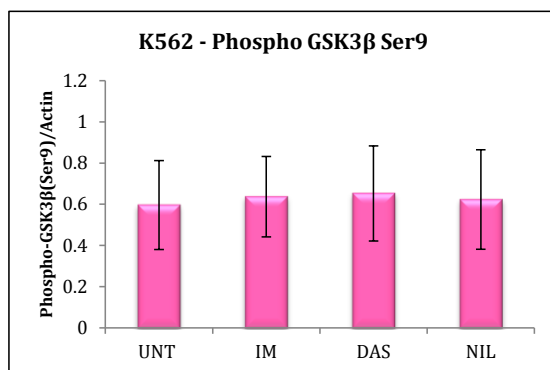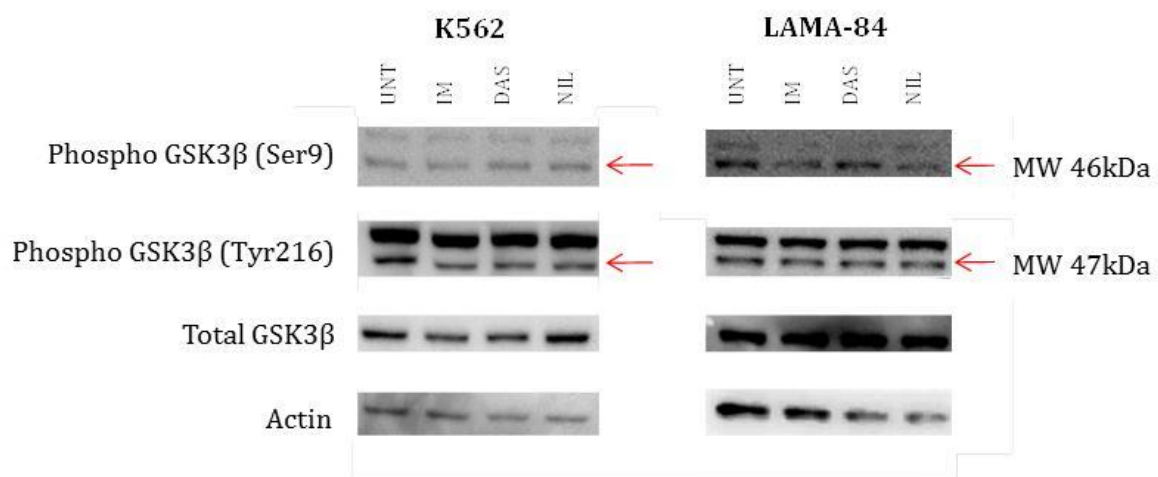
4.4.3.2 WNT3A acts to inhibit GSK3β by reducing Tyr216 phosphorylation, while WIF-1 has no effect on GSK3β levels

The significant decrease in GSK3β activity in patients who had transformed into blast crisis did not appear to be controlled by BCR-ABL1. Therefore it was of interest to see if the Wnt pathway was responsible for regulating the activity of GSK3β. To examine this, K562 and LAMA-84 cells were incubated with both WIF-1 which acts as a Wnt pathway inhibitor [192], and WNT-3A which functions as a Wnt pathway activator. Cells were incubated for 24 hours *in vitro* **(Materials and Methods section 2.3.3)**, lysates were made and the levels of GSK3β were measured by western blot compared to an untreated sample **(Materials and Methods section 2.9)**.

With inhibition of the pathway by WIF-1 it would be anticipated that there would be an increase in GSK3β activity shown by a decrease in Ser9 phosphorylation, and an increase in Tyr216 phosphorylation. Results show no change in GSK3β levels with WIF-1 treatment in a single experiment **(Figure 4.4.9).**

Figure 4.4.9 The *in vitro* effects of WIF-1 on CML cell lines K562 and LAMA-84

K562 and LAMA-84 cells were incubated with various concentrations of WIF-1 for 24hours *in vitro* and the levels of GSK3β were measured by western blot. Results show no change in GSK3β levels with increasing concentrations of WIF-1 (N=1).
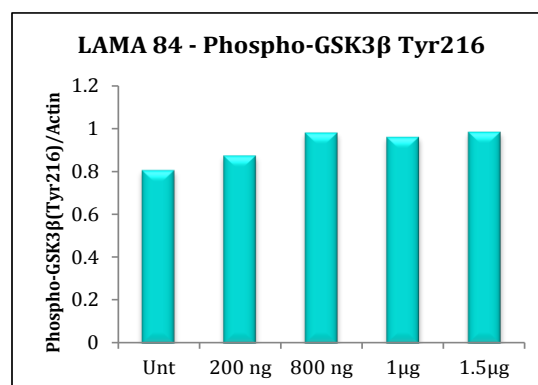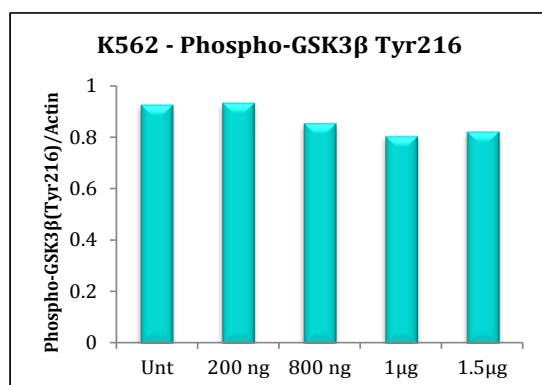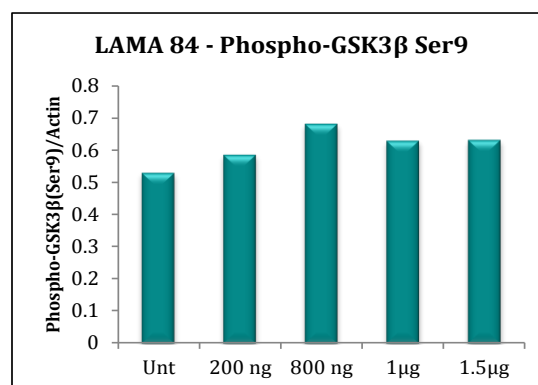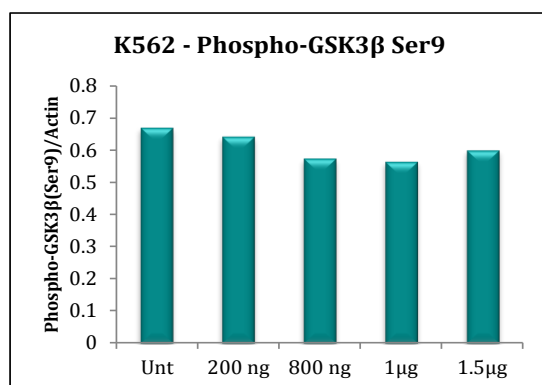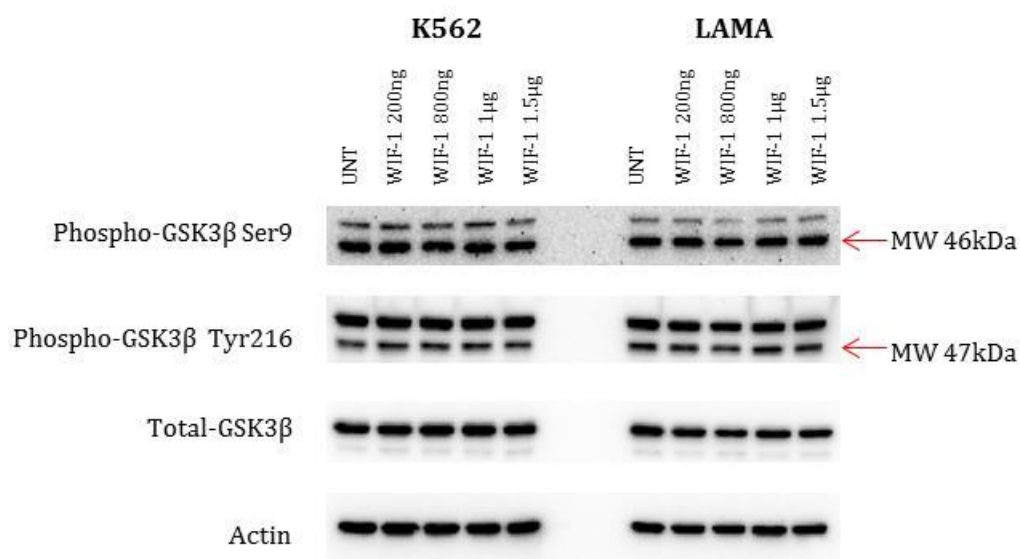
With activation of the pathway using WNT3A, it would be expected for GSK3β activity to decrease, shown by an increase in Ser9 phosphorylation, and reduction in Tyr216 phosphorylation. Results show no change in the levels of phospho GSK3β Ser9, however there is a dose dependent decrease in levels of phospho-GSK3β Tyr216 with increased concentrations of Wnt3A in both K562 and LAMA-84 cells **(Figure 4.4.10)**.

Figure 4.4.10 The *in vitro* effects of WNT-3A on CML cell lines K562 and LAMA-84

K562 and LAMA-84 cells were incubated with various concentrations of WNT-3A for 24hours *in vitro* and the levels of GSK3β were measured by western blot. Results show decreased levels of phospho-GSK3β Tyr216 (both K562 and LAMA-84 cells) with increased concentrations of Wnt3A (N=1).
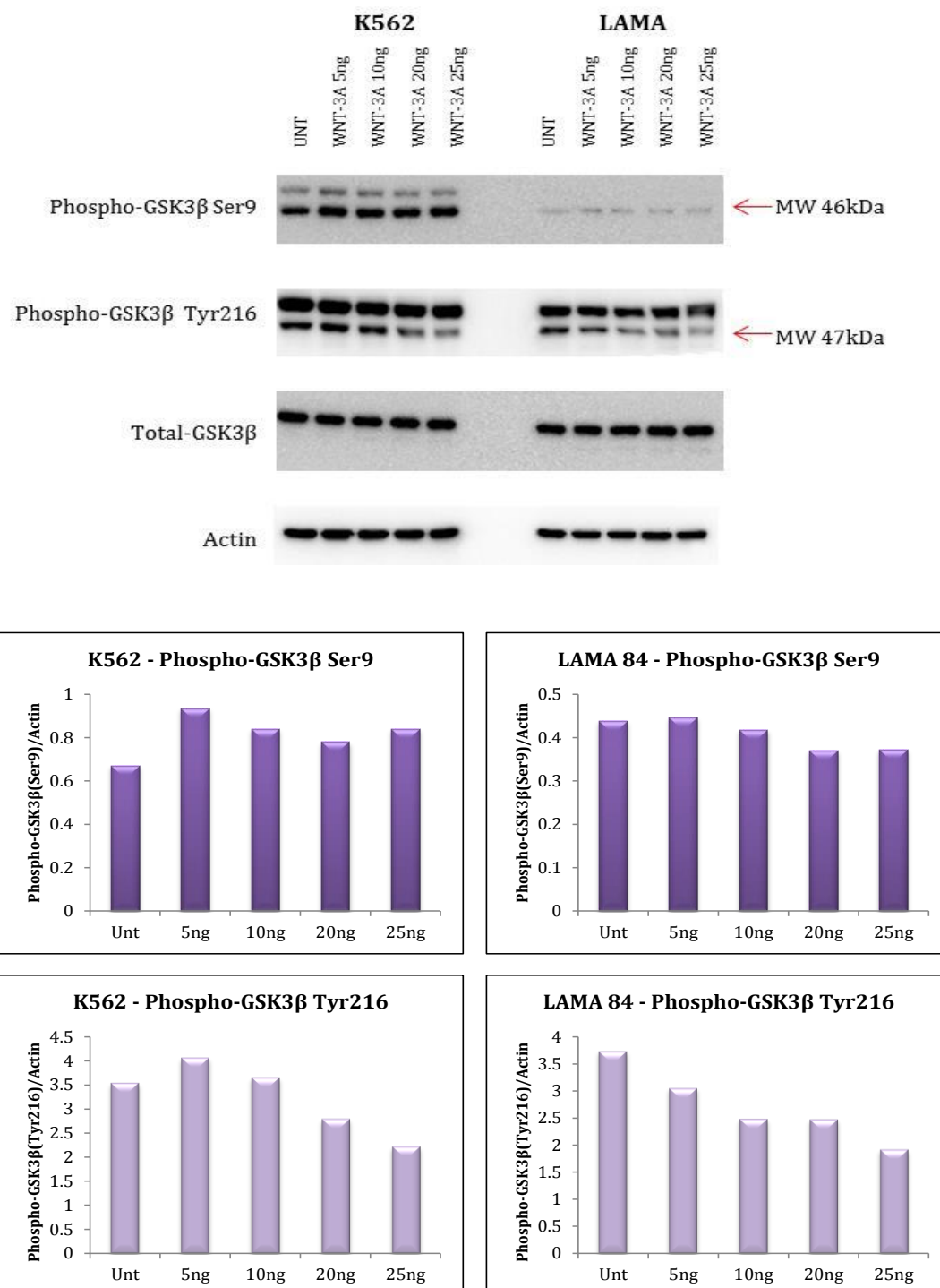
The combination of both WIF-1 having limited effect on GSK3β levels, alongside Wnt3A reducing activation suggests that the Wnt pathway may be maximally inhibited in these cells. This is a possible reason as to why there was no difference in the β-catenin levels between patient cohorts.

4.4.3.3 PP2A acts to regulate GSK3β activity

PP2A as a serine/threonine phosphatase is known to de-phosphorylate GSK3β on serine 9 [197] and therefore could be involved in the regulation of GSK3β by removing the inhibitory phosphorylation. Compounds have been developed which regulate the activity of PP2A including FTY720 which is known to activate PP2A, and okadaic acid which inhibits it. Consequently, K562 cells were incubated *in vitro* for 24 hours with 2.5μM FTY720 (FTY) and 6nM okadaic acid (OA) (previously optimised by Dr Lucas) **(Materials and Methods section 2.3.3)** and western blotting was used to see their effects on GSK3β levels and to determine whether PP2A is playing a role in regulating the activity of GSK3β (N=3) **(Materials and Methods section 2.9)**. **Figure 4.4.11** shows a representative blot and densitometry was used to obtain quantitative data for statistical analysis by a T-test to verify whether the difference is statistically significant.

Results show **(Figure 4.4.11)** that on incubation with FTY720 the levels of phospho-GSK3β Ser9 reduce compared to untreated (P=0.074). In contrast, incubation with OA increases the levels of Ser9 phosphorylation (P=0.053). This supports the view that PP2A is acting as a regulator of GSK3β activity in CML cells, as activation of PP2A via

FTY720 increases dephosphorylation of serine 9, while inhibition of PP2A by okadaic acid prevents GSK3β from being dephosphorylated by PP2A, resulting in the increased levels of serine 9 phosphorylation shown. Statistical analysis revealed that the difference did not reach statistical significance, which may be due to the small number of replicates, however a definite trend can be seen which correlates with the action of PP2A on GSK3β. Both compounds reduce tyrosine 216 phosphorylation, but not to a significant level.

Figure 4.4.11 GSK3β is activated on incubation with FTY720, and inhibited on incubation with okadaic acid suggesting GSK3β's activity could be controlled by PP2A

K562 cells were incubated *in vitro* for 24 hours with 2.5µM FTY720 (FTY) and 6nM okadaic acid (OA). Results show that on incubation with FTY, the levels of phospho-GSK3β (Ser9) reduce compared to untreated. In contrast, incubation with OA increases the levels of Ser9 phosphorylation. Both drugs appear to reduce Tyr216 phosphorylation but not significantly.
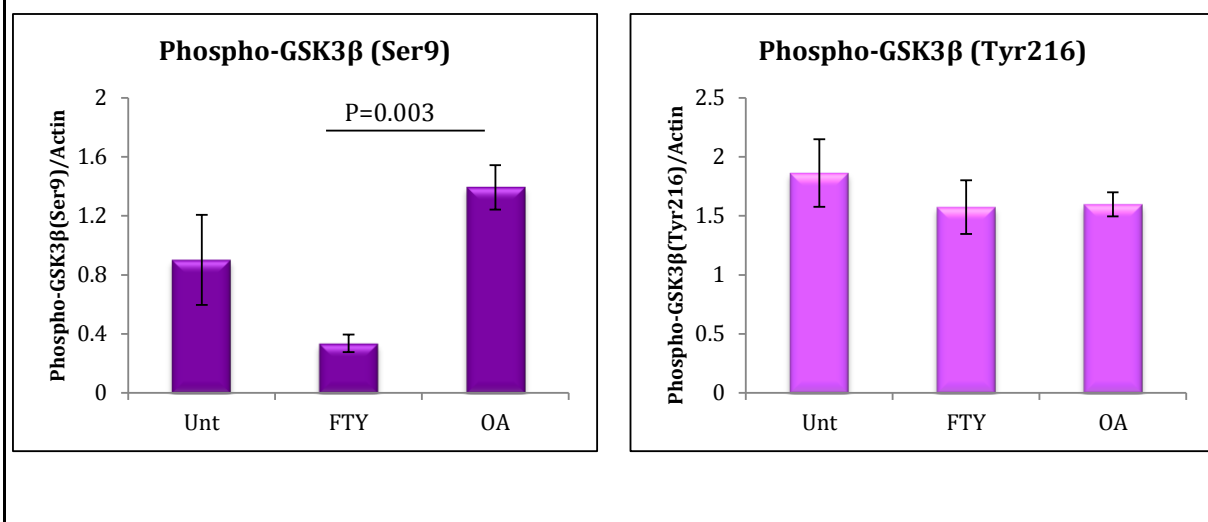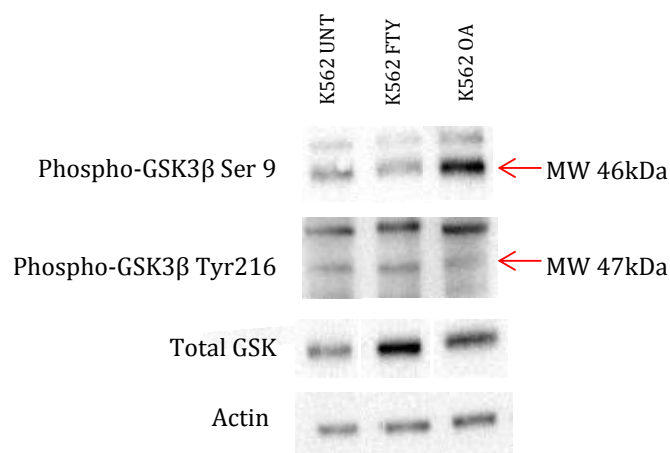
4.4.4 Is the decrease in GSK3β activity responsible for increased C-MYC levels in blast crisis?

GSK3β is not only involved in the degradation of β-catenin and MCL-1; phosphorylation by GSK3β is also involved in regulating the degradation of several other substrates [152]. One of these substrates which is of importance in malignancies is C-MYC. It has been shown in CML that C-MYC is involved in disease progression by the development of *C-MYC* knockout mice. While control mice developed blast crisis within five weeks, the mice with the *C-MYC* knockout did not develop the characteristics of CML [198]. The mechanism by which C-MYC degradation occurs can be seen in **Figure 4.4.12**. Initially, C-MYC is phosphorylated by ERK on Ser62 which primes C-MYC for phosphorylation on Thr58 by GSK3β. PP2A next has to dephosphorylate C-MYC on Ser62 to allow for the addition of a ubiquitin tail and degradation by the proteasome to occur [162]. Considering the decrease in GSK3β activity shown to occur in the patient samples in blast crisis, it was hypothesised that this would lead to a decrease in phosphorylation of C-MYC on Thr58 which in turn would reduce the degradation of C-MYC in blast crisis.

Figure 4.4.12 Mechanism of C-MYC degradation
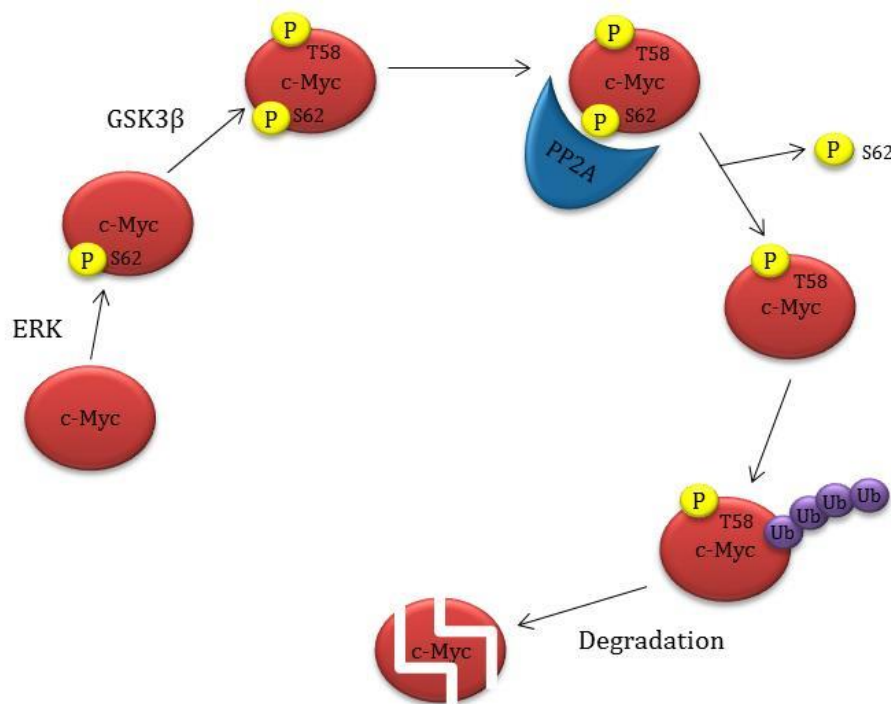
[162]

As previously shown there is a significant decrease in GSK3β activity in blast crisis compared to chronic phase represented by a significant decrease in Tyr216 phosphorylation **(Figure 4.4.13 A)** and a significant increase in Ser9 phosphorylation **(Figure 4.4.13 B)**. The levels of total C-MYC were measured by FACS analysis **(Materials and Methods section 2.7)** and results showed significantly higher levels of total C-MYC in blast crisis patients compared to chronic phase (P=0.024) **(Figure 4.4.13 C)**, suggesting there is a defect in the degradation of C-MYC in blast crisis. The levels of phospho C-MYC (Thr58) were next measured to determine if the decrease in GSK3β activity correlated with a decrease in C-MYC phosphorylation and hence a decrease in

degradation. Results showed **(Figure 4.4.13 D)** there was no difference in the levels of Thr58 phosphorylation of C-MYC in chronic phase patients compared to blast crisis, indicating that the phosphorylation of C-MYC by GSK3β is not controlling the degradation of C-MYC.

PP2A is also crucial in the degradation of C-MYC as without removal of the serine 62 phosphorylation C-MYC cannot be ubiquitinated and hence degraded. Consequently, PP2A levels were measured and results showed that there were significantly higher levels of PP2A in the blast crisis patients compared to chronic phase **(see Figure 4.4.13 E)**. This is opposite to what would be expected as higher levels of PP2A would correlate with increased removal of the Ser62 phosphorylation, allowing C-MYC to be degraded. To determine if PP2A is active and able to dephosphorylate C-MYC, or inactive and unable to dephosphorylate C-MYC, inactive PP2A was investigated by measuring the levels of phospho-PP2A (Tyr307). Results showed a non-significant elevation in the levels of phospho-PP2A (Tyr307) in the blast crisis cohort compared to chronic phase **(see Figure 4.4.13 F)**. This suggests the significantly higher levels of PP2A found in the blast crisis patients is active and able to dephosphorylate C-MYC at Ser62. These data demonstrate that PP2A, along with GSK3β is not controlling the degradation of C-MYC.

Figure 4.4.13 Neither GSK3β or PP2A are the controlling factors of C-MYC degradation.

Results previously showed there is a significant decrease in GSK3β activity in blast crisis through Tyr216 $P<0.001$(A) and Ser9 $P=0.026$ (B) phosphorylation. Additionally there is a significant increase in total c-Myc levels in blast crisis $P=0.024$ (C) however there is no difference between Thr58 phosphorylation of c-Myc (D). Results for PP2A levels show there are significantly higher levels of total PP2A in blast crisis $P=0.013$ (E), with increased levels of inactive PP2A (Tyr307) however this difference is not significant (F).
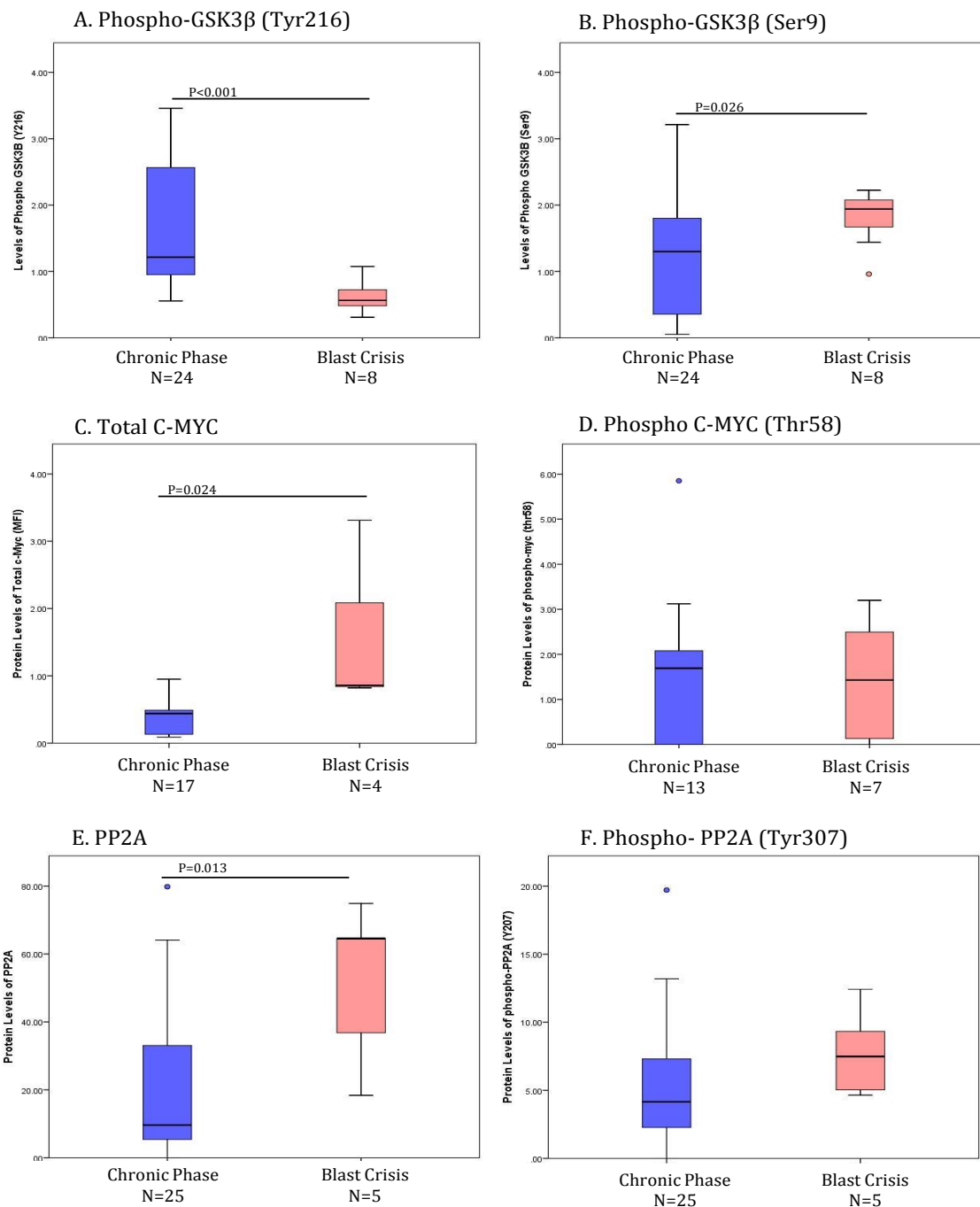
4.5 Main conclusions

GSK3β is an important regulator of multiple cellular functions[199]. It is fundamental in the regulation of the Wnt signalling pathway, and has more recently become of interest independently of signalling pathways as a component involved in the maintenance and function of a quiescent HSC pool [164, 194]. Due to no difference being found in the various forms of β-catenin between patient outcomes in the previous chapter, it was of interest to investigate whether GSK3β is still playing a role in CML. The main conclusions drawn from this chapter are;

1. GSK3β has the predicted outcome on β-catenin levels. SB216763 was used to inhibit GSK3β to determine its effects on β-catenin. Results showed unphosphorylated β-catenin (active) increasing with inhibition of GSK3β, while phospho-β-catenin (Ser33/37/Thr41) decreased with inhibition indicating GSK3β is still effective at regulating the degradation of β-catenin.

2. *GSK3β* mRNA transcript levels are elevated in patients with poor prognosis for both the normal and spliced variant (exons 8 and 9) transcript type and for the normal-only transcript type.

3. GSK3β activity is significantly reduced in patients who have transformed into blast crisis compared to chronic phase. This was demonstrated by opposing trends in Ser9 and Tyr216 phosphorylation. Elevated levels of phospho- GSK3β Ser9 were found in those patients who had transformed into blast crisis compared to those in chronic phase (P=0.026), which correlated to lower levels of phospho- GSK3β

Tyr216 in the patients who have transformed into blast crisis compared to the chronic phase patients (P<0.001). This result was corroborated by MCL-1 levels being significantly higher in patients in blast crisis (P<0.001 for both forms), confirming that GSK3β's activity is impaired and therefore it cannot act to phosphorylate and degrade MCL-1.

4. GSK3β activity is not under the control of BCR-ABL1 in CML.

5. WNT3A reduces GSK3β activity in CML cell lines, while WIF-1 has limited effects on GSK3β levels. Results showed with WNT3A treatment *in vitro* that there was a dose dependent decrease in levels of phospho-GSK3β Tyr216 with increased concentrations of Wnt3A in both cell lines. This in combination with limited effects with WIF-1 treatment may suggest that the Wnt pathway could be maximally inhibited in these cells.

6. PP2A is involved in the regulation of GSK3β activity in CML cells, by controlling its inhibition. Incubation with the PP2A activator (FTY720) causes a reduction in the levels of phospho-GSK3β serine 9. In contrast, incubation with the PP2A inhibitor (okadaic acid) increases the levels of serine 9 phosphorylation.

7.   Neither GSK3β nor PP2A are controlling the rate of C-MYC degradation. Results showed that there was no difference in the GSK3β dependent Thr58 phosphorylation on C-MYC in chronic phase patients compared to blast crisis. Additionally, analysis of PP2A levels showed that there were significantly higher levels of PP2A in blast crisis in combination with the levels of inactive PP2A being

elevated but not significantly higher in blast crisis. This is opposite to what would be expected if PP2A was regulating C-MYC degradation. Instead, the E3 ubiquitin ligase FBXW7, responsible for the ubiquitination of C-MYC, could be controlling the level at which C-MYC is degraded [198, 200, 201].

Chapter 5 – Is GSK3β involved in the PP2A pathway?

5.1 Introduction

The activity of GSK3β can be regulated by PP2A via the dephosphorylation of Ser9 alleviating inhibition of GSK3β [197]. This was demonstrated in the previous chapter with inhibition of PP2A increasing Ser9 phosphorylation, and activation of PP2A reducing serine 9 phosphorylation of GSK3β.

The relationship between GSK3β and PP2A is known to be reciprocal, with GSK3β also acting indirectly to regulate PP2A activity, via the inhibitory phosphorylation on Tyr307 [202, 203]. As GSK3β is a serine /threonine kinase, it cannot act on this regulatory domain itself, but it regulates protein tyrosine phosphatase 1B (PTP1B) which in turn regulates Tyr307 phosphorylation, and consequently the inhibition of PP2A. It was found that a decrease in GSK3β activity decreases the phosphorylation of PP2A, while activation of GSK3β increased levels of phospho-PP2A (Tyr307). This occurs by inhibition of GSK3β increasing PTP1B and enabling the dephosphorylation of PP2A to occur, while activation of GSK3β decreases PTP1B which prevents PTP1B dephosphorylating PP2A at Tyr307. Knocking out PTP1B by siRNA increased Tyr307 phosphorylation that was previously suppressed by GSK3β inhibition. GSK3β can act to regulate PTP1B by either its transcription or its phosphorylation status [202].

PP2A is known to play an important role in CML due to it being a recipient of BCR-ABL1 regulation. BCR-ABL1 acts to inhibit PP2A preventing its tumour suppressive characteristics by inhibiting the ability of PP2A to auto-dephosphorylate itself on Tyr307. BCR-ABL1 appears to regulate the activity of PP2A via two mechanisms **(see Figure 5.1.1).** Firstly, via a mechanism including SET, whereby BCR-ABL1 kinase activity increases SET expression, which then enables SET to inactivate PP2A directly. A decrease in SET expression, by inhibition of BCR-ABL1 via imatinib treatment, correlated with a reduction in PP2A inhibition via Tyr307 phosphorylation. SET was found to be elevated in CML blast crisis which subsequently correlated with inactivation of PP2A [175]. Secondly via CIP2A which has been shown to co-localise with PP2A reducing its phosphatase activity [204]. Elevated levels of CIP2A were found in those patients at diagnosis who are destined to progress to blast crisis in comparison to optimal responders and failure patients at diagnosis, with 100% of patients with high levels of CIP2A transforming to blast crisis within 21 months. CIP2A may therefore be a useful biomarker of disease progression. Lucas *et al.,* [176] also showed that high levels of CIP2A correlated with high levels of phospho-PP2A (Tyr307), and when CIP2A was knocked out by siRNA, this resulted in a decrease in phospho-PP2A (Tyr307) indicating that when CIP2A levels are reduced PP2A is able to remain in its active conformation.

Figure 5.1.1 Mechanism of PP2A regulation
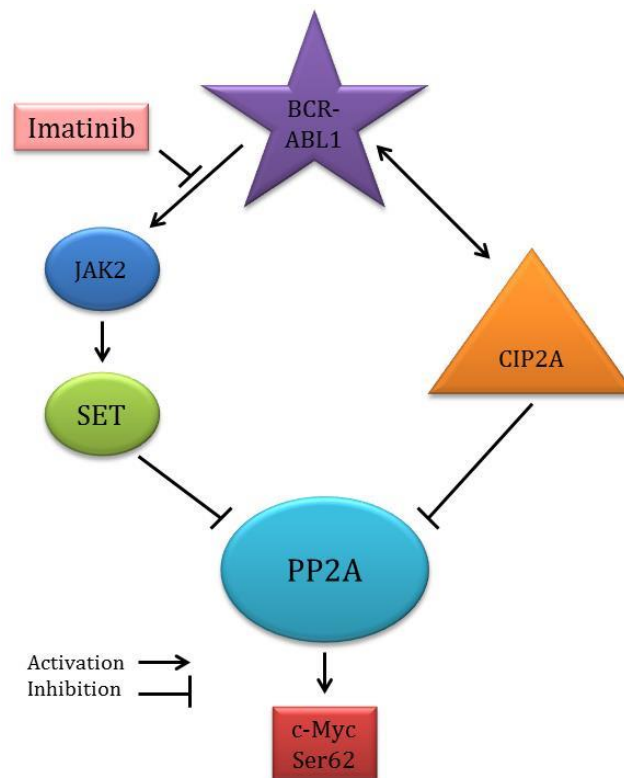
Lucas *et al.*, [176]

Activation of PP2A promoted inactivation and subsequently degradation of BCR-ABL1 via the tyrosine phosphatase SHP-1 dephosphorylating BCR-ABL1, indicating a two way mechanism by which PP2A is also able to regulate BCR-ABL1 activity [173, 175]. Additionally, PTP1B has been linked to dephosphorylation of BCR-ABL1 in K562 cells. This shows PP2A to be a useful therapeutic target via activation of its phosphatase activity [175].

In addition CIP2A and PP2A are known to be involved in a feedback mechanism with E2F1, whereby increased levels of E2F1 result in an increase in CIP2A, this then transposes to inactivate PP2A, which then stabilises E2F1 as it is unable to

dephosphorylate E2F1 on Ser364 [205]. E2F1 is also known to correlate with increased levels of active β-catenin in human liver cancer [206, 207] possibly linking the PP2A and Wnt/β-catenin pathways even further.

Considering the reciprocal regulatory relationship between PP2A and GSK3β, and the significant decrease in GSK3β activity found in blast crisis patients in the previous chapter it was of interest to understand the relationship between GSK3β and the PP2A pathway in CML.

5.2 Aims

The aims of this chapter are to;

1. Determine if there is any correlation between PP2A, CIP2A or SET and GSK3β in patients.

2. Investigate whether GSK3β inhibition has any effect on the PP2A and CIP2A pathway.

3. Investigate whether CIP2A regulation affects GSK3β and β-catenin levels.

5.3 Optimisation of techniques

The optimisation of GSK3β antibodies was shown in the previous chapter **(see Chapter 4 – Optimisation of techniques Figure 4.3.1)** as were the conditions for SB216763 treatment **(see Chapter 4 – Optimisation of techniques Figure 4.3.2)**. Antibody optimisation conditions for the various members of the PP2A pathway were performed by Dr Lucas.

5.3.1 Optimisation of GSK3β siRNA

K562 cells were used to test the protocol conditions for GSK3β as stated by Santa Cruz Biotechnology to determine if they sufficiently suppressed GSK3β in my hands. 10μM of both the control siRNA and the GSK3β siRNA was used per $1x10^6$ cells **(Materials and Methods section 2.4)**. Lysates were prepared from the cultures and western blotting was used to measure the effect on GSK3β levels **(Materials and Methods section 2.9)**. As can be seen in **Figure 5.3.1**, results showed that 10μM of the GSK3β siRNA sufficiently suppressed the expression of all forms of GSK3β compared to the untreated and control siRNA. This was therefore the concentration used for all further experimentation.

Figure 5.3.1 Optimisation of GSK3β siRNA in K562 cells

The levels of phospho-GSK3β (Ser9), phospho-GSK3β (Tyr216), and total GSK3β were measured by western blot in untreated (UNT), control siRNA, and GSK3β siRNA treated cells. Results show a decrease in all forms of GSK3β in GSK3β siRNA treated cells compared to control siRNA and untreated cells.
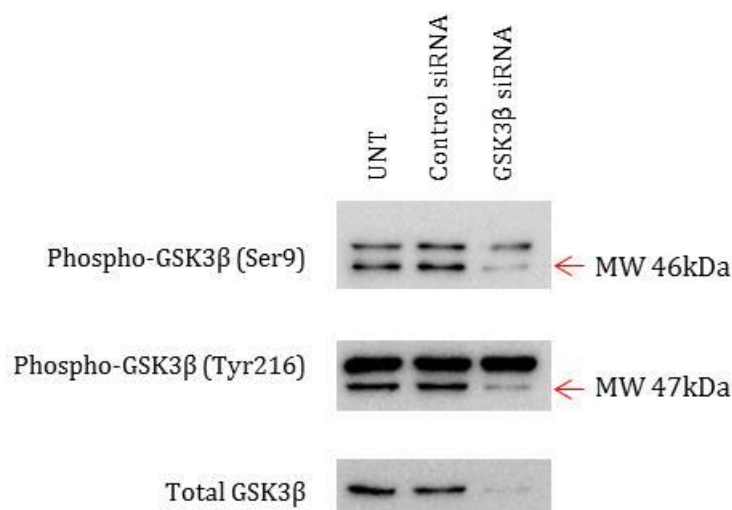
5.3.2 Optimisation of CIP2A transfection

K562 cells were used for transient CIP2A transfection to temporarily increase CIP2A levels within the cell. Cells were either untreated, GFP transfected, or CIP2A-GFP transfected **(Materials and Methods section 2.5)**. The transfection efficiency was analysed after 24 hours by both FACS analysis by gating on GFP positive cells, and by microscopy to determine if the plasmid vector had been incorporated into the K562 cells sufficiently. Using GFP detection by FACS, results showed that the control and CIP2A plasmid had been successfully incorporated into the cells with ≥70% transfection

efficiency **(Figure 5.3.2)**. This was also seen via microscopy **(Figure 5.3.3)**. PI was also

used to ensure the vector was not affecting the viability of the cells. Results showed that

≥80% of the cells were viable subsequent to transfection **(Figure 5.3.2)**.

Figure 5.3.2 Transfection efficiency of CIP2A transient transfection by FACS (GFP detection and PI)

The efficiency of transfection was measured by GFP detection (A.) and results for both GFP-only transfection, and CIP2A-GFP transfection was ≥70% (N=3).
PI was also tested (B.) to ensure the transfection was not affecting cell viability. The percentage of live cells was ≥80% (N=3).

A. GFP dectection
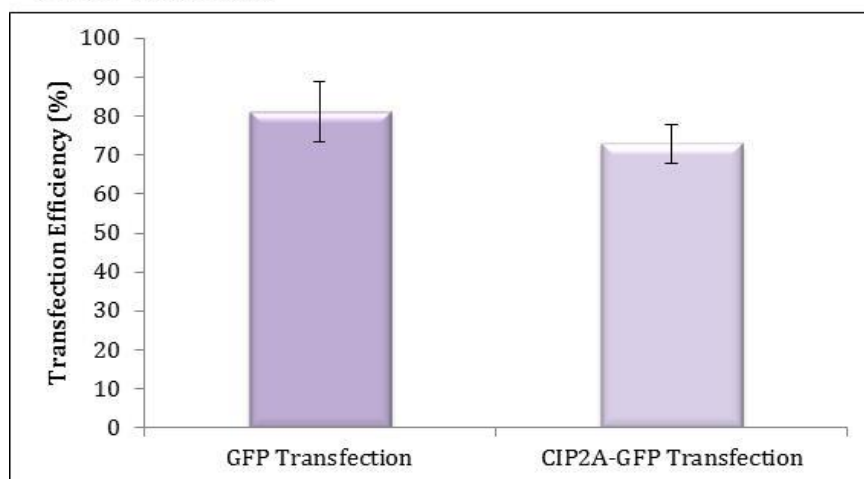
B. PI
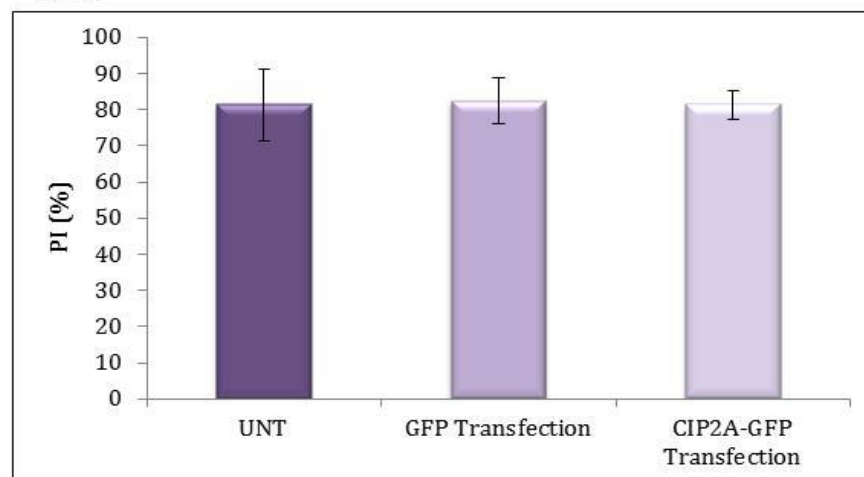
Figure 5.3.3 Transfection efficiency of CIP2A transient transfection by microscopy

K562 cells were visualised under a light microscope to determine if transfection had been successful by observing the presence of GFP fluorescence. Results showed that both GFP-only and CIP2A-GFP transfection had been incorporated successfully into the cells.
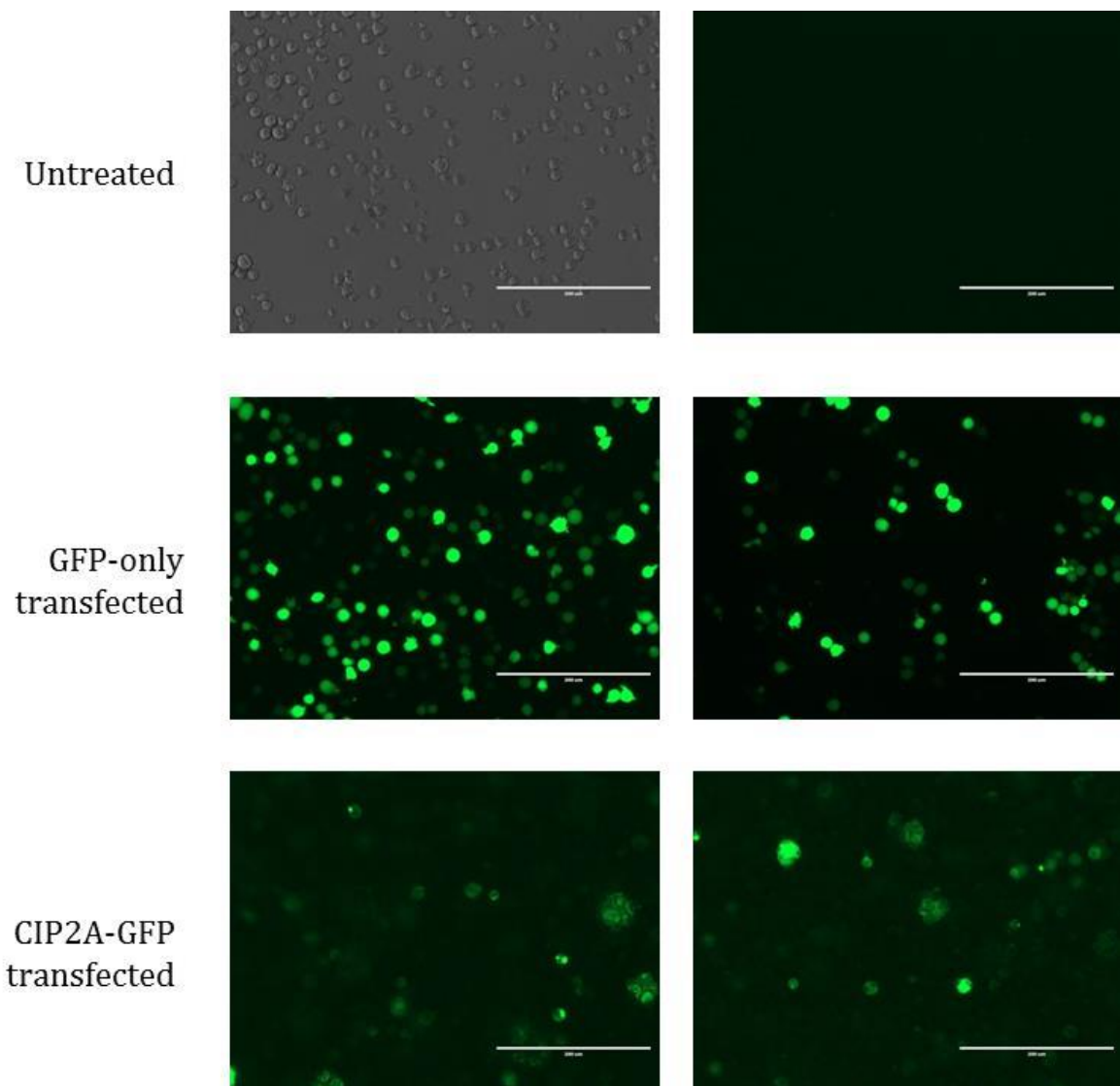
CIP2A levels were measured by FACS to test whether the transient transfection had

successfully increased the levels of CIP2A by gating on GFP positive cells (N=3) **(Figure**

5.3.4). Results showed that there are significantly higher levels of CIP2A in the CIP2A-

GFP transfected cells compared to the GFP-only transfected cells (P=0.05).

Figure 5.3.4 Optimisation of CIP2A transfection in K562 cells

CIP2A levels were measured in GFP positive K562 cells to determine whether CIP2A-GFP transfection had effectively increased levels of CIP2A (N=3). Results show significantly higher levels in comparison to the GFP-only transfected cells (P=0.05).
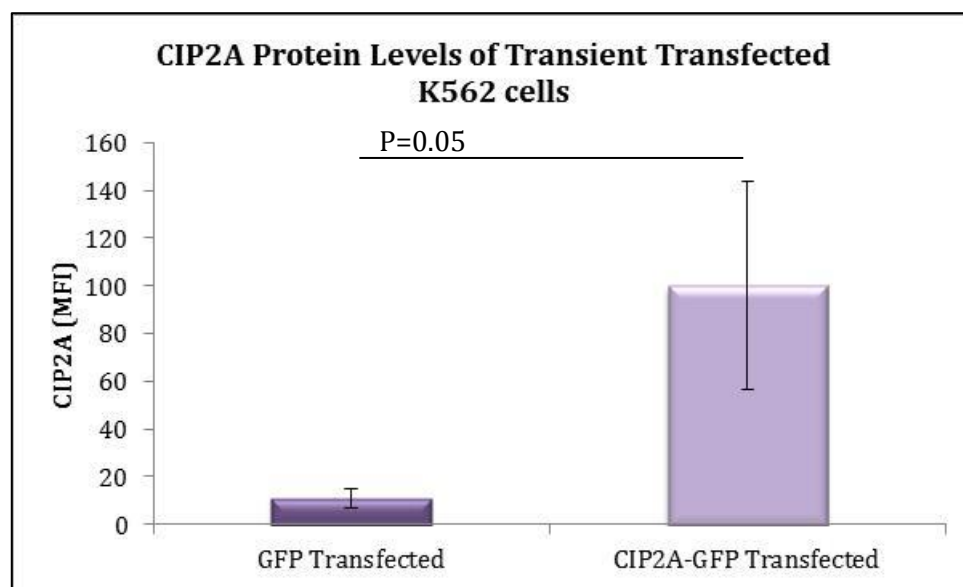
5.4 Results

5.4.1 Is there any correlation between GSK3β and PP2A/CIP2A/SET?

5.4.1.1 A decrease in GSK3β activity correlates with an increase in inactive PP2A

It was previously found that patients in blast crisis had significantly reduced GSK3β activity compared to patients in chronic phase **(Chapter 4 – Results section 4.4.2.2)**. Additionally, it was demonstrated that PP2A can regulate the activity of GSK3β in CML cells **(Chapter 4 – Results section 4.4.3.3).** Therefore, it was of interest to determine whether the levels of PP2A correlate with the levels of GSK3β. It is hypothesised that an increase in GSK3β inhibition could either a) cause an increase in PTP1B and subsequent dephosphorylation of PP2A on Tyr307, or b) correspond with higher levels of phospho-PP2A Tyr307 (inactive) in those patients with high levels of GSK3β inhibition as PP2A would not be dephosphorylating Ser9 of GSK3β. Lucas *et al.*, [176] previously showed that the level of phospho-PP2A Tyr307 is significantly higher in blast crisis MNCs compared to normal MNCs (P=0.004). Therefore, it was of interest to see whether, in matched patient samples, GSK3β levels correlated with PP2A levels to give an indication of the relationship between GSK3β and PP2A in CML cells.

Levels of total PP2A and phospho-PP2A (Tyr307) were examined by FACS analysis **(see Methods section 2.7)** in patient samples matched to those also measured for GSK3β levels. Results show that levels of total PP2A do not change between chronic phase and blast crisis. The proportion of inactive PP2A is higher in blast crisis than in chronic

phase, but not to a statistically significant level. The higher levels of phospho-PP2A Tyr307 seen in the blast crisis patients are indicative that PP2A is regulating GSK3β by preventing the dephosphorylation of serine 9. The reason as to why the difference in phospho-PP2A Tyr307 levels is not significant may be due to a feedback mechanism whereby in blast crisis phospho-PP2A Tyr307 is unable to dephosphorylate GSK3β on serine 9 increasing its inhibition which consequently increases PTP1B and dephosphorylates PP2A on Tyr307 **(Figure 5.4.2)**.

Figure 5.4.1 Inactive PP2A is higher in blast crisis patients

Levels of total PP2A and phospho-PP2A (Tyr307) were measured in chronic phase patients (N=11) and patients who had transformed into blast crisis (N=4). Results show no difference between the cohorts for total PP2A (A.). There are elevated levels of phospho-PP2A (Tyr307) in blast crisis patients but the difference is not statistically significant (P=0.226).
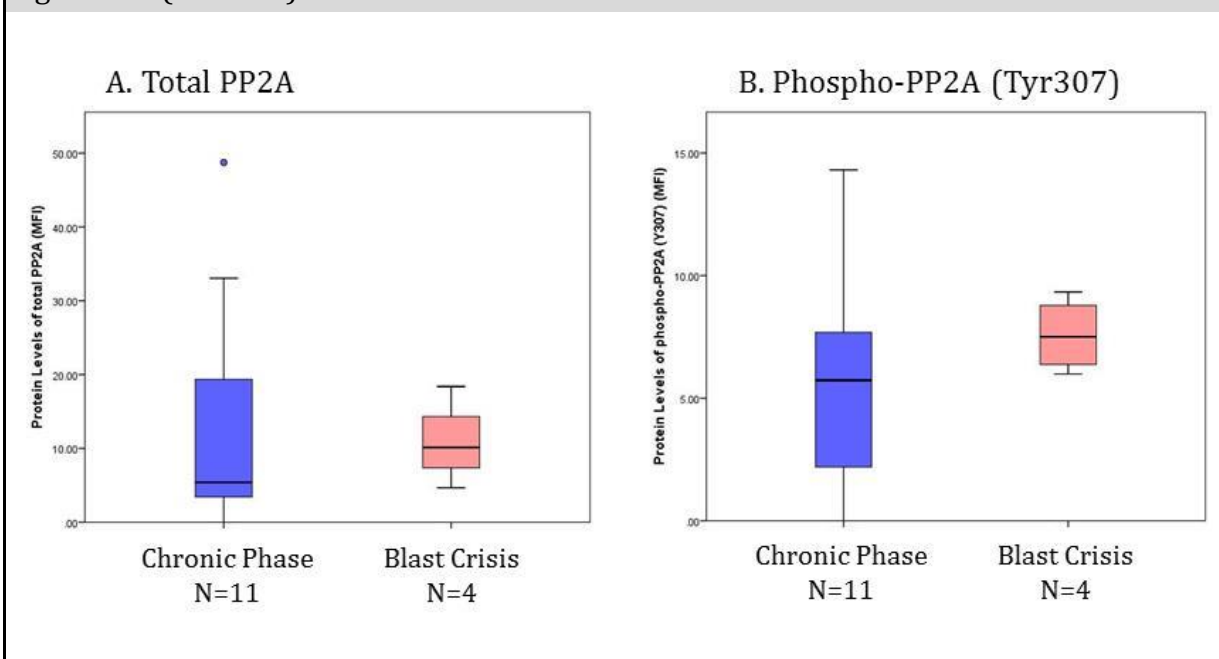
Figure 5.4.2 Feedback mechanism of PP2A and GSK3β

Inhibited PP2A (phospho PP2A Tyr307) prevents the dephosphorylation of the inhibitory Ser9 phosphorylation on GSK3β. This inhibition of GSK3β increases the levels of PTP1B which then dephosphorylates PP2A at Tyr307.
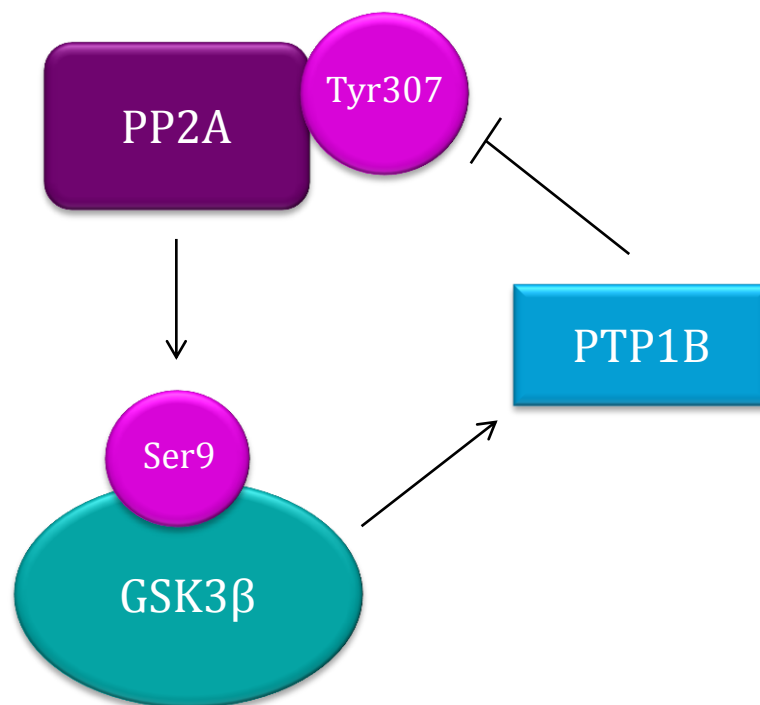
5.4.1.2 A decrease in GSK3β activity correlates with an increase in SET

As for levels of PP2A, SET protein levels were examined by FACS analysis **(Materials and Methods section 2.7)** in matched patient samples to those measured for GSK3β levels. Results show **(Figure 5.4.3)** that there are increased levels of SET in the blast crisis patients compared to chronic phase (P=0.078), correlating with levels of phospho-PP2A (Tyr307) being higher in this cohort of patients. This provides evidence that, in patients who have transformed into blast crisis, an increase in SET levels increases the inhibition of PP2A which, in turn, can prevent the dephosphorylation of GSK3β on Ser9 increasing inhibition of GSK3β activity.

Figure 5.4.3 SET protein levels are higher in blast crisis patients compared to chronic phase

Levels of SET were measured in chronic phase (N=11) and blast crisis (N=4) patients. Results show that SET levels are elevated in patients in blast crisis (P=0.078).
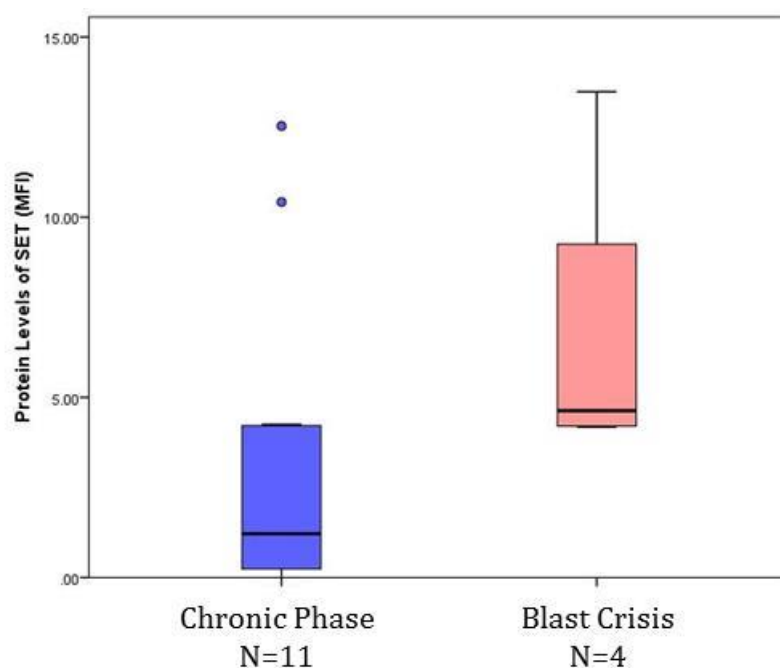
5.4.1.3 A decrease in GSK3β activity does not correlate with a change in CIP2A levels.

As before, CIP2A protein expression was examined by FACS analysis **(Materials and Methods section 2.7)** in patient samples matched to those measured for GSK3β levels. Results show that levels of CIP2A protein do not change between chronic phase and blast crisis **(Figure 5.4.4)**. This indicates that CIP2A does not correlate with the activity of GSK3β when stratified by patient outcomes. However, CIP2A has been recognised as a predictive biomarker for CML by Lucas *et al.*, [176] and therefore patient outcome can be stratified according to either high or low CIP2A protein expression levels. The data were subsequently revised based on this division **(see Section 5.4.1.4)**.

Figure 5.4.4 There is no difference in CIP2A levels between chronic phase and blast crisis

Levels of CIP2A were measured in chronic phase patients (N=14) and patients who had transformed into blast crisis (N=6). Results show no difference between the cohorts (P=1.00).
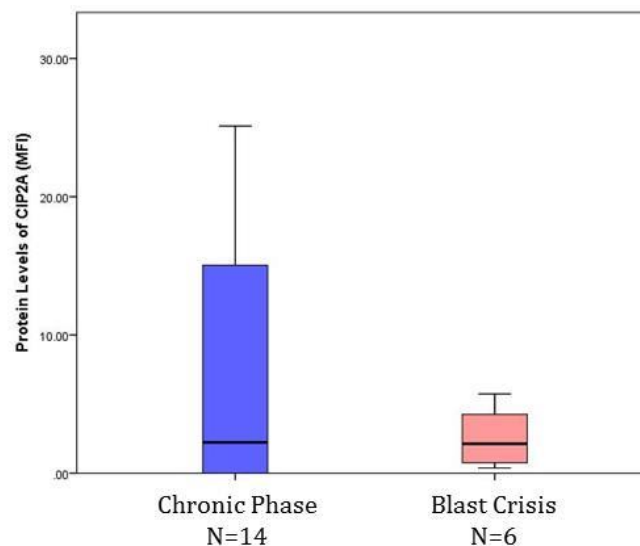
5.4.1.4 GSK3β levels are lower overall in the high CIP2A patients

When re-stratifying the levels of GSK3β with CIP2A, the patient data were paired and then separated according to their CIP2A levels with high CIP2A having a MFI>7 and low CIP2A having a MFI<7 (as previously defined by Lucas *et al.*, [176]) to determine what happens to the levels of phospho-GSK3β (Ser9) and phospho-GSK3β (Tyr216). Results show **(Figure 5.4.5)** that both forms of phospho-GSK3β are lower in the patients with high CIP2A compared to low CIP2A, indicating that CIP2A may promote the degradation of GSK3β. These results however do not reach statistical significance.

Figure 5.4.5 Both forms of GSK3β are reduced in patients with high CIP2A levels

Patients were split into low CIP2A (N=16) and high CIP2A (N=4) and the levels of phospho-GSK3β (Ser9), and phospho-GSK3β (Tyr216) were analysed. Results show both forms of phospho-GSK3β are lower in the patients with high CIP2A (Ser9 P=0.104, Tyr216 P=0.310).
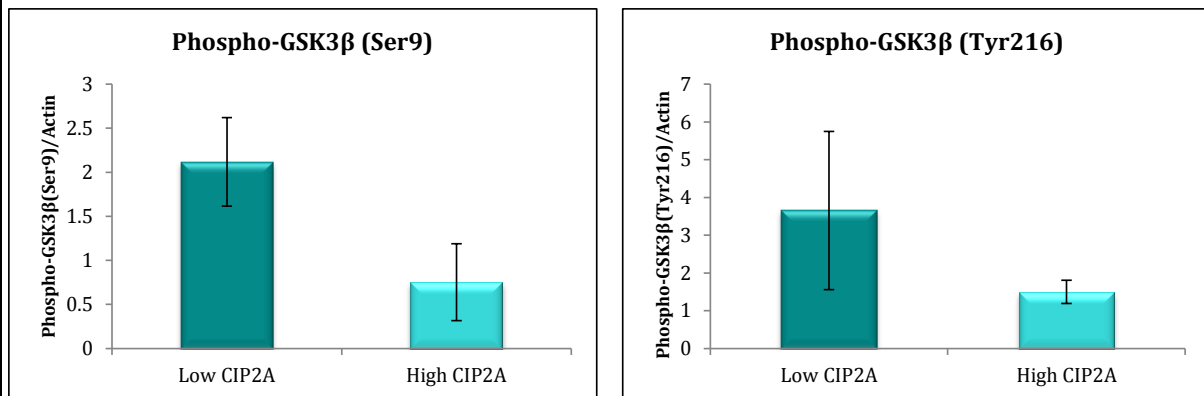
5.4.2 Does inhibition of GSK3β affect the PP2A pathway?

Due to the two-way regulatory relationship between GSK3β and PP2A, it was of interest to see whether inhibition of GSK3β had any effect on PP2A, CIP2A, SET and BCR-ABL1 activity. The levels of c-Myc were also analysed as GSK3β and PP2A are involved in c-Myc degradation (even though they may not be rate-limiting components) to see if there is any impact on c-Myc degradation with altering levels of GSK3β.

It would be predicted that inhibition of GSK3β would lead to a decrease in the levels of phospho-PP2A (Tyr307) enabling the phosphatase activity of PP2A to occur. In theory, this could lead to a decrease in BCR-ABL1 activity as PP2A could act to inactivate and degrade BCR-ABL1 [173, 175]; this would in turn reduce levels of both SET and CIP2A.

5.4.2.1 Inhibition of GSK3β using SB216763 decreases inhibition of PP2A and up regulates CIP2A and SET

SB216763 is an ATP-competitive inhibitor of GSK3β which was selected for use over lithium chloride (LiCl) as LiCl does not selectively inhibit GSK3β complicating data interpretation [195]. K562 cells were incubated with SB216763 *in vitro* for 24 hours **(Materials and Methods section 2.3.3)** and then analysed by FACS analysis (N=6) **(Materials and Methods section 2.7)**. Results show **(Figure 5.4.6)** that inhibition of GSK3β by incubation with 5μM SB216763 in K562 cells reduces the levels of phospho-PP2A (Tyr307) as well as total levels of PP2A. This fits with inhibition of GSK3β acting

to activate PP2A through a reduction in its inhibitory phosphorylation via PTP1B. The levels of CIP2A and SET protein increase, alongside BCR-ABL1 activity (p-CrKL/CrKL ratio), which is opposite to what would be predicted; potentially suggesting a feedback mechanism within the malignancy whereby a down regulation in inactive PP2A (Tyr307) triggers an increase in the PP2A inhibitors CIP2A and SET, to restore inhibition of PP2A in the malignant cells.

Additionally inhibition of GSK3β resulted in a decrease in phospho C-MYC (Thr 58) **(Figure 5.4.6)** which confirms expectations as GSK3β phosphorylates C-MYC directly on this site. Inhibition has no effect on Ser62 phosphorylation of C-MYC and slightly increases total levels of C-MYC.

Figure 5.4.6 Inhibition of GSK3β using SB216763

K562 cells were incubated *in vitro* with SB216763 for 24 hours. Levels of the various PP2A pathway components were then measured by FACS analysis (N=6). Results show the trend that inhibition of GSK3β decreases total and inactive (Tyr307) PP2A levels, increases CIP2A, and SET levels, as well as BCR-ABL1 activity (p-CrKL/CrKL ratio), and increases total C-MYC levels, decreases phospho C-MYC (Thr58), and has no effect on serine 62 phosphorylation of C-MYC.
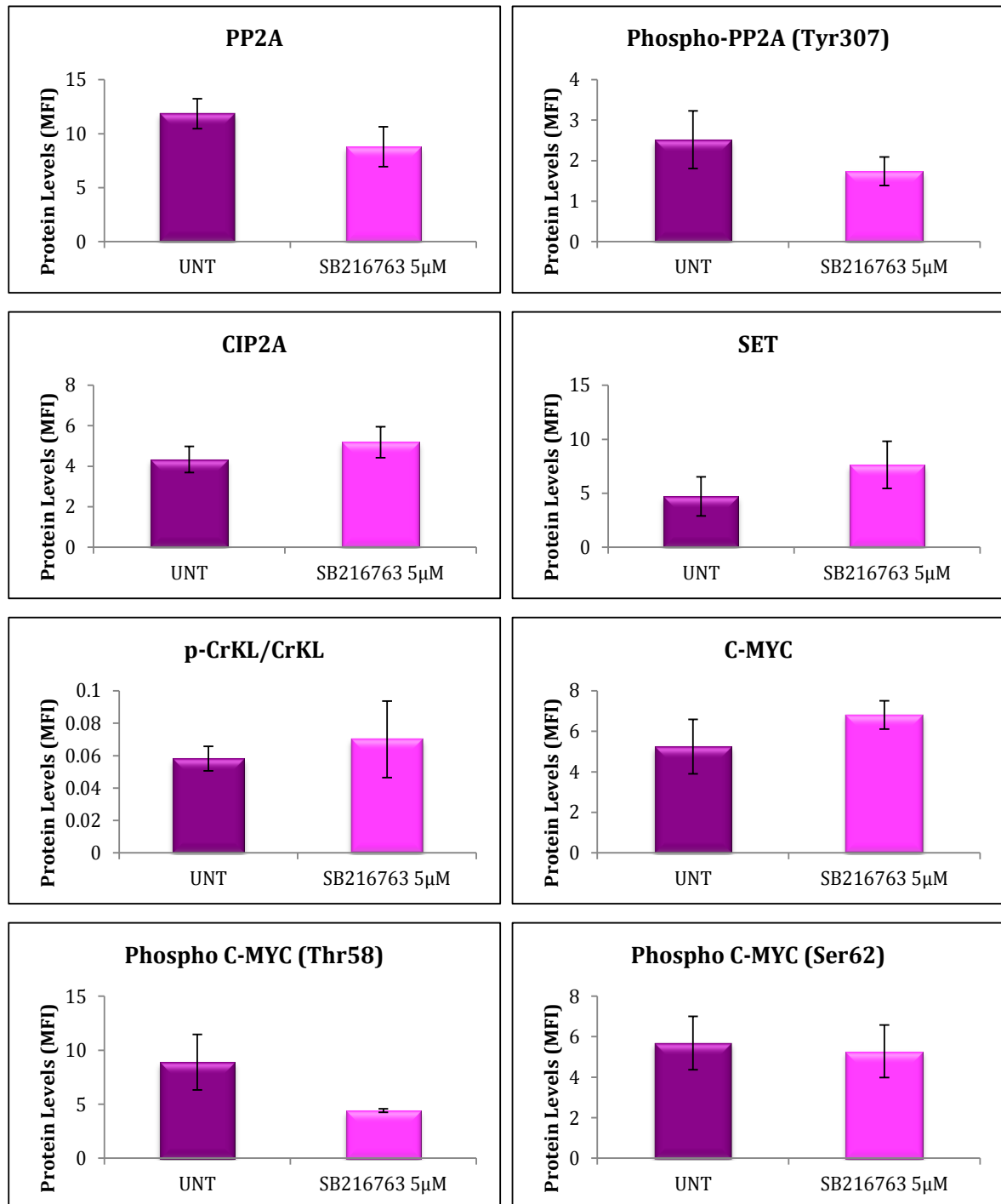
5.4.2.2 Inhibition of GSK3β using siRNA

GSK3β inhibition by siRNA was again measured by FACS analysis (N=4) **(Materials and Methods section 2.4 and 2.7)**, however, results had the opposite effect on the PP2A pathway as was seen with SB216763 mediated GSK3β inhibition **(Figure 5.4.7)**. Knocking out GSK3β reduced total levels of PP2A, similar to the effect seen with SB216763 inhibition, however in contrast the levels of inhibitory phospho-PP2A (Tyr307) increased with the knockdown of GSK3β. The opposite results to that with SB216763 incubation were also found with CIP2A and SET, with both their levels decreasing with GSK3β knockdown, together with decreased BCR-ABL1 activity (p-CrKL/CrKL ratio). This shows that inhibition of GSK3β through ATP competition has a different impact on the substrates of GSK3β compared to down-regulation of the protein. This difference can be explained as inhibition of GSK3β by SB216763 increases Ser9 phosphorylation **(Chapter 4, Figure 4.3.2)**, which in turn would decrease levels of phospho-PP2A Tyr307 seen in **Figure 5.4.6**. However, knockdown of GSK3β reduces Ser9 phosphorylation **(Figure 5.3.1)**, which consequently would increase levels of Tyr307 **(Figure 5.4.7)** as GSK3β cannot increase levels of PTP1B which therefore prevents PTP1B from dephosphorylating PP2A at Tyr307. Again the results for CIP2A, SET and BCR-ABL1 activity (p-CrKL/CrKL ratio) are opposite to what would be predicted, implying that PP2A may not be acting to down-regulate BCR-ABL1 activity in CML.

The results on C-MYC levels corroborated what was seen with SB216763, with phospho C-MYC (Thr58) levels decreasing with GSK3β knockdown, while there was no effect

seen on the levels of phospho C-MYC (Ser62) and total C-MYC. The fact that both forms of GSK3β inhibition have no effect on total C-MYC levels further emphasises that GSK3β is not the rate limiting component of C-MYC degradation **(Chapter 4 - Results section 4.4.4)**.

Figure 5.4.7 Inhibition of GSK3β using siRNA

GSK3β was knocked out in K562 cells using siRNA. Levels of the various PP2A pathway components were then measured by FACS analysis (N=4). Results show the trend that inhibition of GSK3β by siRNA decreases total PP2A but increases inactive (Tyr307) PP2A levels, decreases CIP2A, and SET levels, as well as BCR-ABL1 activity (p-CrKL/CrKL), and decreases phospho C-MYC (Thr58), while having no effect on total C-MYC and Ser62 phosphorylation of C-MYC.
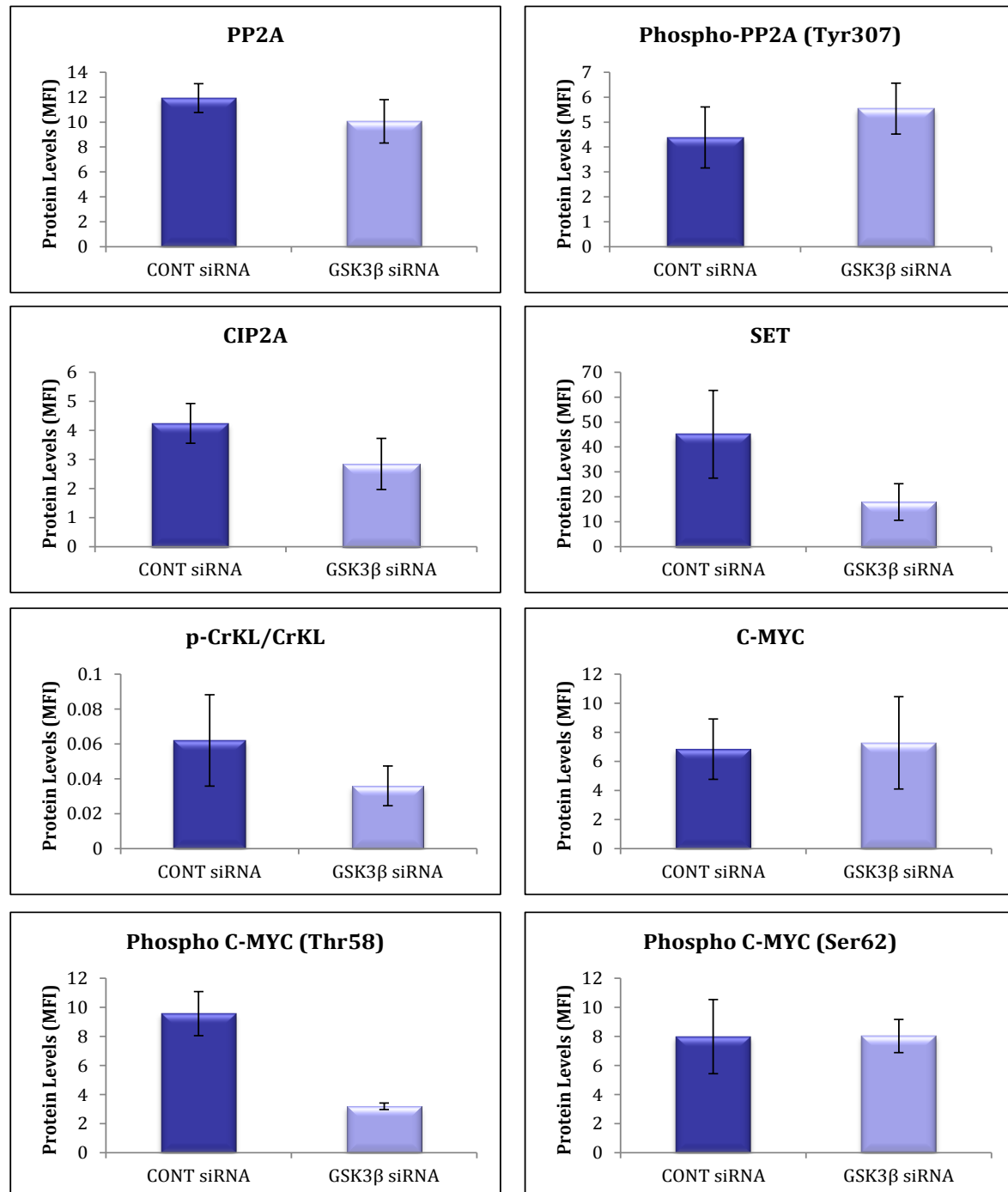
5.4.3 Does regulation of CIP2A affect GSK3β?

Considering the dynamic relationship between PP2A and GSK3β which could be impacted by the regulation of CIP2A on PP2A activity, alongside results in patient samples showing high levels of CIP2A correlated with reduced forms of GSK3β, the next line of investigation was to manipulate the levels of CIP2A to see if this had an impact on GSK3β.

5.4.3.1 Knocking out CIP2A reduces GSK3β

CIP2A siRNA methodology was previously optimised by Dr Lucas. 10μM of both a control and CIP2A siRNA was used **(Materials and Methods section 2.4)** and lysates were prepared from the cultures. Levels of GSK3β were measured by western blotting **(Materials and Methods section 2.9)** to determine if knocking out CIP2A has any effect of GSK3β levels (N=3). Results show that a reduction in CIP2A gives rise to a decrease in all forms of GSK3β **(Figure 5.4.8)**. These results contradict what was seen in patients with high CIP2A correlating with low GSK3β, however, the decrease in CIP2A via siRNA knockdown would increase active levels of PP2A which would subsequently be able to dephosphorylate GSK3β at Ser9, represented by the decrease in phospho-GSK3β Ser9 seen.

Figure 5.4.8 Inhibition of CIP2A by siRNA reduces GSK3β levels

K562 cells were treated with control siRNA (10μM) and CIP2A siRNA (10μM). GSK3β levels were analysed using western blotting and results show that knocking out CIP2A results in a reduction of all forms of GSK3β (N=3).
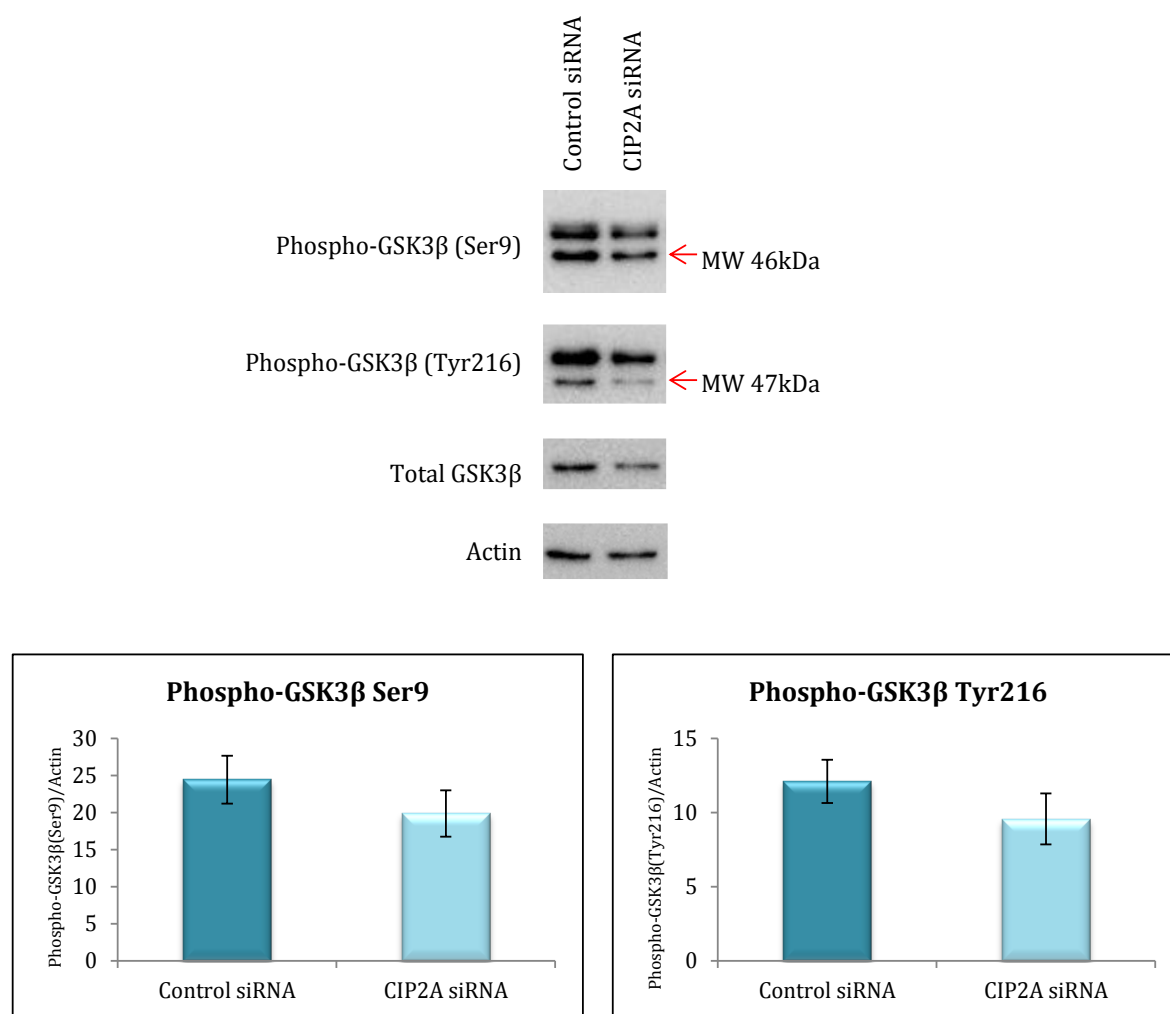
5.4.3.2 Transfecting in CIP2A increases GSK3β

Next, transient CIP2A transfection was used to increase the CIP2A levels, **(Materials and Methods section 2.5)** lysates were prepared from the cultures and western blots were carried out (N=3) **(Materials and Methods section 2.9)**. **Figure 5.4.9** shows that an increase in CIP2A levels results in an increase in both phospho-GSK3β (Ser9), and

phospho-GSK3β (Tyr216). This would be as a result of an increase in CIP2A elevating

the levels of inactive PP2A (Tyr307), which would then increase the levels of Ser9

phosphorylation of GSK3β as PP2A would not be able to dephosphorylate this residue.

Figure 5.4.9 Transient transfection of CIP2A increases levels of GSK3β

K562 cells were transiently transfected with GFP-only and CIP2A-GFP to increase levels of CIP2A and compared to an untreated control (UNT). Levels of GSK3β were then analysed by western blotting (N=3). Results show that both phospho-GSK3β (Ser9) and phospho-GSK3β (Tyr216) increase in CIP2A-GFP transfected cells.
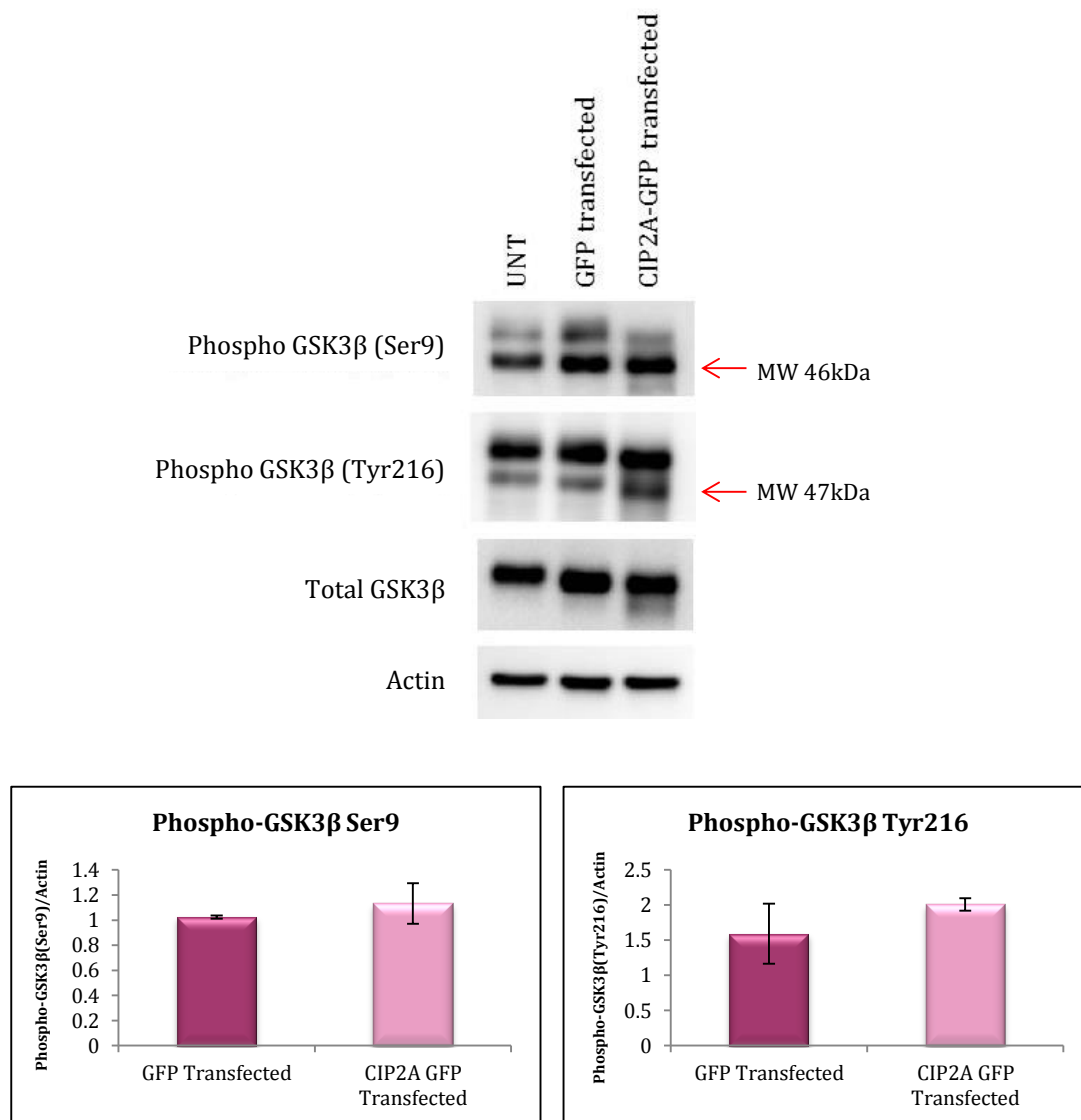
Neither siRNA knockdown nor transfectional upregulation of CIP2A showed a significant effect on the levels of GSK3β, which may indicate that the effect of CIP2A on PP2A is reduced in translation to GSK3β levels.

5.4.4 Does regulation of CIP2A affect β-catenin?

CIP2A is involved in the regulation of two components which are known to interact with β-catenin; PP2A and E2F1. Specifically, the PP2A isoforms B55α and B56γ have been reported to regulate the phosphorylation status of β-catenin. The B55α isoform of PP2A has been shown to directly interact with β-catenin, as well as Axin, and regulate the phosphorylation status of β-catenin by dephosphorylating residues Ser552 and Ser675 which can also activate β-catenin [208]. Alternatively B56γ acts as part of the destruction complex via association with both APC [170] and Axin [209] and correlates with degradation of β-catenin [170, 175, 209]. Additionally, E2F1 has been reported to correlate with increased levels of unphosphorylated β-catenin [206, 207]. Since CIP2A is known to regulate both of these factors it was of interest to see if regulation of CIP2A had an impact on β-catenin levels.

5.4.4.1 Unphosphorylated β-catenin is higher in patients with high CIP2A

Levels of β-catenin and CIP2A protein were investigated by FACS analysis **(see Methods section 2.7)** in patient samples that were separated in accordance to their CIP2A protein expression levels using a cut off of MFI > or <7 as previously determined

by Lucas *et al.,* [176]. Results showed **(Figure 5.4.10)** that high CIP2A levels correlated

with increased levels of unphosphorylated β-catenin. This could be either a direct effect,

or an indirect effect via PP2A or E2F1.

Figure 5.4.10 High CIP2A levels correlate with increased levels of active β-catenin in patient samples

Levels of β-catenin and CIP2A protein were analysed in patient samples and separated in high and low CIP2A levels. Results showed a correlation of high CIP2A levels with increased levels of unphosphorylated β-catenin expression.
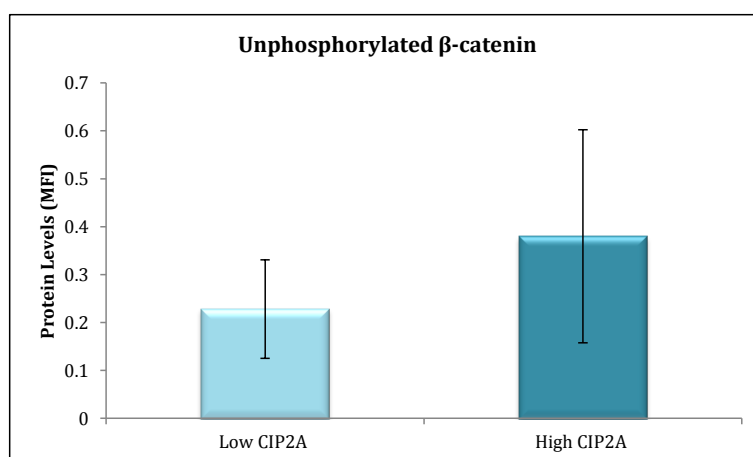
5.4.4.2 CIP2A transfection increases unphosphorylated β-catenin at the same time as reducing phospho-β-catenin (Ser33/37/Thr41) targeted for degradation

Transient CIP2A transfection was used to increase CIP2A levels temporarily **(Materials**

and Methods section 2.5) and β-catenin levels were measured by FACS analysis

(Methods section 2.7) to determine if CIP2A was having a direct effect on β-catenin

levels. Results showed that increased CIP2A generated an increase in unphosphorylated

β-catenin **(Figure 5.4.11 B.)**, which correlated with a decrease in phospho-β-catenin (Ser33/37/Thr41) **(Figure 5.4.11 D.)** that is targeted for degradation. Additionally increasing CIP2A expression increased both phospho-β-catenin (Ser45/Thr41) **(Figure 5.4.11 C.)** and phospho-β-catenin (Tyr654) **(Figure 5.4.11 E.)**, while it reduced the overall expression of total β-catenin **(Figure 5.4.11 A.)**. This increase in unphosphorylated β-catenin, which correlates with a decrease in phospho-β-catenin (Ser33/37/Thr41), shows that with elevation of CIP2A β-catenin is active in the cell and hence can activate transcription of its target genes. The differences did not reach statistical significance which could either be due to the N number (N=3) or may be due to the effect of CIP2A on β-catenin being an indirect effect which may reduce its impact on the levels of β-catenin.

Figure 5.4.11 Transfection of CIP2A results in an increase in active β-catenin and decreases levels targeted for degradation

K562 cells were transiently transfected with GFP-only and CIP2A-GFP to increase levels of CIP2A. Levels of β-catenin were then investigated by FACS analysis (N=3). Results show that levels of total-β-catenin (A.) and phospho-β-catenin (Ser33/37/Thr41) (D.) decrease in CIP2A-GFP transfected cells compared to GFP-only transfected. Increasing CIP2A expression also increases unphosphorylated β-catenin (B.), phospho-β-catenin (Ser45/Thr41) (C.), and phospho-β-catenin (Tyr654) (E.).
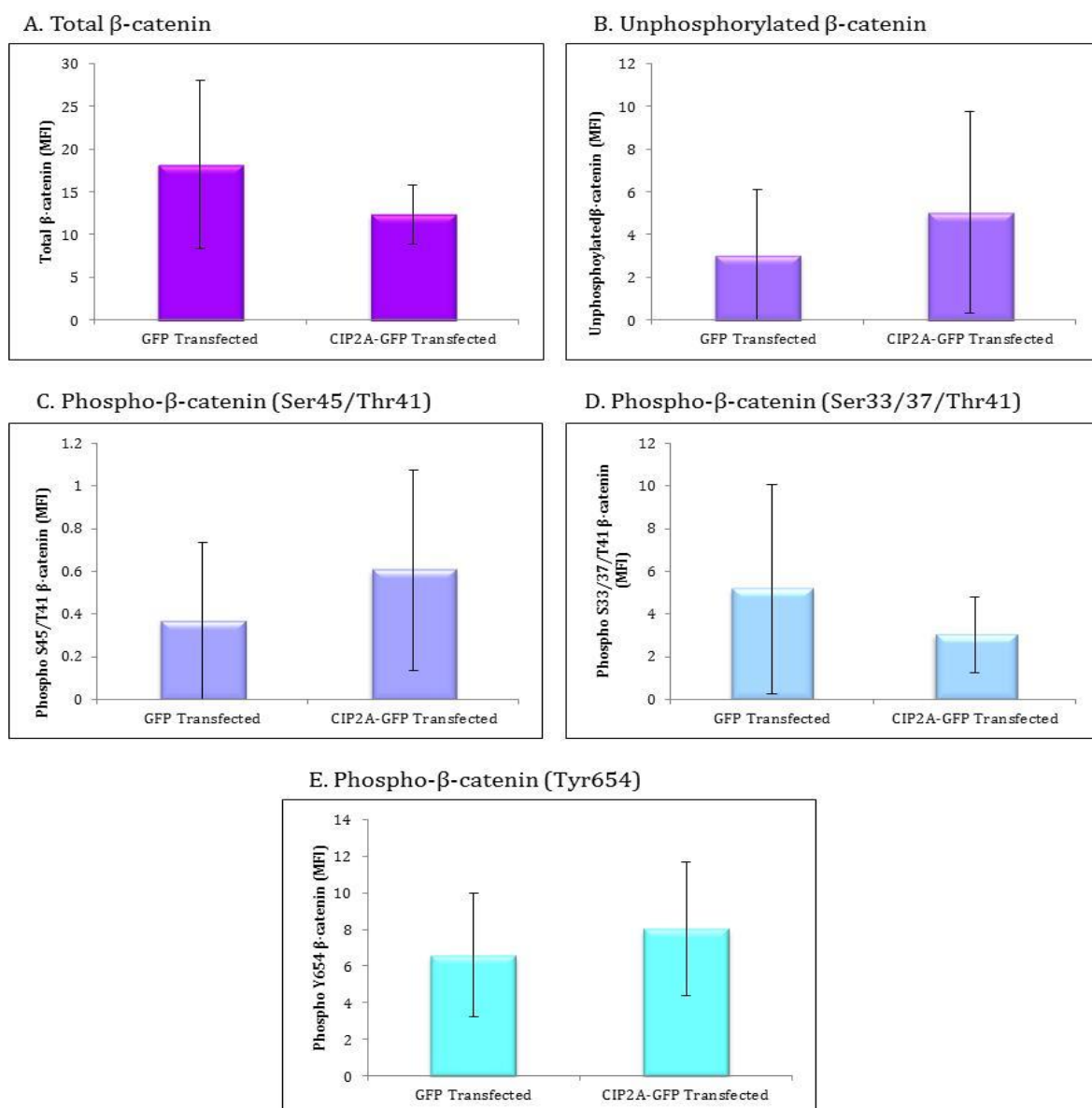
5.4.4.3 CIP2A may be acting through E2F1 to affect levels of β-catenin

CIP2A is known to regulate E2F1 [205], and E2F1 is known to correlate with increased levels of unphosphorylated β-catenin [206]. Therefore, to determine if the increase in unphosphorylated β-catenin is solely due to CIP2A or due to the process of transfection also increasing E2F1 levels which then subsequently act on β-catenin, the levels of E2F1 and phospho-E2F1 (Ser364) were measured by FACS analysis **(Methods section 2.7)** (N=3). Phospho-E2F1 (Ser364) was measured in addition to total E2F1 as this phosphorylation is known to stabilise the protein [210]. Results show that the CIP2A-GFP transfected cells have higher levels of total E2F1 compared to GFP-only transfected cells, and significantly higher levels of phospho-E2F1 (Ser364) (P=0.007) **(Figure 5.4.12)**, which suggests that the increase in unphosphorylated β-catenin could be due to E2F1 instead of a direct effect of CIP2A.

Figure 5.4.12 Transfection of CIP2A also increases E2F1 levels

Levels of total E2F1 and phospho-E2F1 (Ser364) were measured in the transfected cells. Results showed that cells transfected with CIP2A had higher levels of total E2F1 and significantly elevated levels of phospho-E2F1 (Ser364) (P=0.007) compared to GFP-only transfected cells.
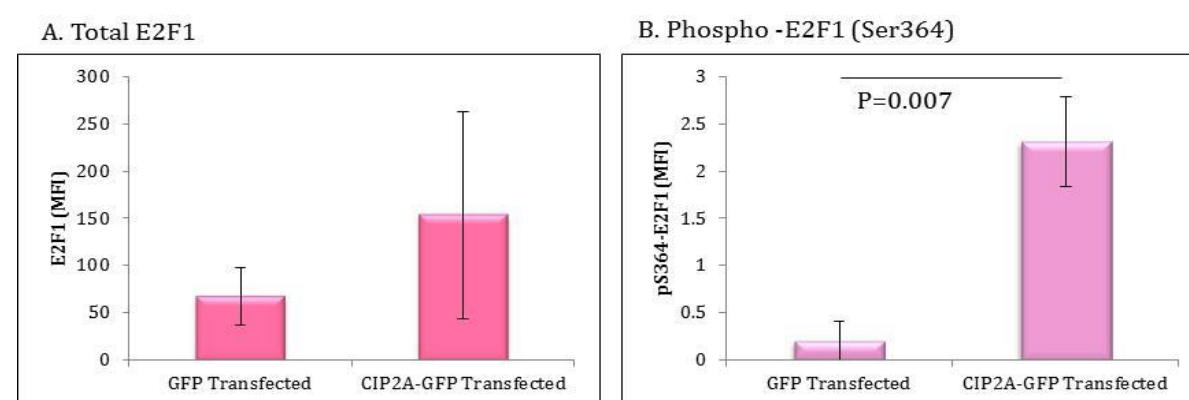
5.5 Main Conclusions

In the previous chapter it was discovered that patients in blast crisis had significantly less GSK3β activity compared to patients in chronic phase and that PP2A has a role in regulating the activity of GSK3β. As a consequence, it was relevant to try to further understand the relationship between GSK3β and PP2A.

From this investigation, the main conclusions found were that;

1. GSK3β shows a relationship with inactive PP2A (phosphorylated on Tyr307) and SET levels, with both increasing in patients who have transformed into blast crisis compared to chronic phase. This correlates with the decrease in GSK3β activity found in the previous chapter, suggesting a mechanism for GSK3β inhibition via SET inhibition of PP2A.

2. Levels of both phospho-GSK3β (Tyr216) and phospho-GSK3β (Ser9) are reduced in patients who have high levels of CIP2A, opposite to what would be predicted.

3. Inhibition of GSK3β by SB216763 and siRNA has opposite effects on the PP2A/CIP2A/SET pathway through different mechanisms of GSK3β inhibition. Inhibition with SB216763 causes an increase in Ser9 phosphorylation and subsequent decrease in Tyr307 phospho-PP2A levels observed, via dephosphorylation of PP2A by PTP1B. In contrast, knockdown of GSK3β by siRNA reduces the levels of Ser9 phosphorylation on GSK3β which results in an increase in

Tyr307 phosphorylation of PP2A, as GSK3β is unable to increase levels of PTP1B, preventing the dephosphorylation of PP2A at Tyr307. The results for CIP2A, SET and BCR-ABL1 activity (p-CrKL/CrKL ratio) are opposite to what would be predicted for the levels of PP2A shown, implying that PP2A may not be acting to down-regulate BCR-ABL1 activity in CML.

4. Inhibition of GSK3β reduces Thr58 phosphorylation of C-MYC, but does not have a significant influence on the expression of total C-MYC, further confirming results from the previous chapter that GSK3β is not the rate-limiting component of C-MYC degradation in CML.

5. Manipulation of CIP2A levels by siRNA and transient transfection does cause changes in the levels of GSK3β. However, these differences are not significant suggesting CIP2A is not a vital component in the regulation of GSK3β.

6. Higher levels of unphosphorylated β-catenin correlate with increased CIP2A, both in patient samples and manipulation of CIP2A levels by transient transfection in K562 cells. However, it is known that CIP2A regulates E2F1 [205], which in turn is known to correlate with increased levels of unphosphorylated β-catenin [206]. Increasing CIP2A levels by transient transfection consequently increased the levels of stabilised E2F1 (Ser365) (P=0.007), therefore CIP2A may not be having a direct effect on β-catenin but instead could be acting to increase unphosphorylated β-catenin levels indirectly through E2F1.

Chapter 6 – The role of the Wnt Transcription Factors as markers for disease progression

6.1 Introduction

Wnt/β-catenin signalling is crucial in maintaining the self-renewal of normal HSCs [143, 211] and when the signalling is disrupted, haematological malignancies may develop [150, 212, 213]. The first identification of deregulation of the Wnt/β-catenin pathway resulting in a haematological malignancy was described in CML, where it was found that increased Wnt/β-catenin pathway activation led to β-catenin accumulation. It was suggested that this contributed to disease progression [145].

Regulation of the Wnt/β-catenin signalling pathway is an extremely complex process, with multiple members of the pathway either up-regulating or down-regulating signal transduction through the cell. This is summarised in **section 1.7** of the introduction. In addition to the Wnt signal being regulated at the beginning of the pathway through secreted proteins, which either prevent the association between WNT ligands and the membrane receptors FZD and LRP5/6 (e.g. DKK, WIF, sFRP, CER) or bind to the receptors and activate the pathway (e.g. NORRIN, R-SPONDIN), the pathway can also be regulated further downstream, some mechanisms of which are described in **Table 6.1.1**.

Table 6.1.1 Summary of factors involved in the regulation of the Wnt signalling pathway

Antagonists	Agonists
DKK – inhibits signalling by blocking the LRP5/6 receptor, preventing Wnt ligand binding [85].	NORRIN – binds to the receptors (in particular Fz4) and activates the Wnt pathway [214, 215].
WIF - binds to the Wnt ligands to prevent the interaction with the Frizzled receptor [216].	R-SPONDIN - binds to the receptors (in particular Fz8 and LRP6) and activates the Wnt pathway [217, 218].
sFRP – bind to the Wnt ligands to prevent the interaction with the Frizzled receptor [216].	SKL2001 – activates β-catenin activity by competing with GSK3β through the prevention of β-catenin's interaction with Axin2 [219]
CER – binds to the Wnt ligands to prevent the interaction with the Frizzled receptor [85, 216].	APC – normally this functions as a tumour suppressor by being part of the destruction complex – however multiple mutations have been discovered which switch its role to enhancing the accumulation of β-catenin [220, 221].
KREMEN – involved with Dkk in the internalisation of LRP5/6 preventing association with Wnt ligands [85, 216].	DSH – prevents the degradation of β-catenin by recruiting GBP/Frat-1, which removes GSK3β from axin. Dsh can itself be regulated by PAR1, frodo, β-arrestin1 and Dapper [85].
CtBP – bind to the promoters of target genes to prevent transcriptional activation [222].	PYGO – involved in the activation of transcription by mediating the interaction of β-catenin or TCF with chromatin [222].
GROUCHO - bind to the promoters of target genes to prevent transcriptional activation [222].	LGS – links Pygopus to β-catenin in the nucleus [222].
NEMO-like kinase – phosphorylates the TCFs to prevent transcription [85].	
ICAT – Interacts with β-catenin to prevent binding with the transcription factors [85].	

The final stage at which Wnt/β-catenin signalling can be regulated is at the level of the transcription factors associated with the pathway. These are the TCF/LEF family of transcription factors which include TCF1, TCF3, TCF4, and LEF1. Their structure consists of a N-terminal β-catenin binding domain and a C-terminal high mobility group DNA binding domain [178] which assists their function by enabling the binding between β-catenin and the promoter region of the target genes including *CYCLIN D1* and *C-MYC* [122, 123]. The activity of the transcription factors themselves can be regulated by transcriptional co-activators and transcriptional co-repressors **(Table 6.1.1)**. Nuclear β-catenin functions by binding to these transcription factors and eliminates any inhibition by displacing the co-repressors from TCF/LEF, while the co-activators facilitate the association of β-catenin with the transcription factors and enhance transcriptional activation [122].

In addition to facilitating the signal transduction of the Wnt/β-catenin pathway, the TCF/LEF transcription factors may act independently of the pathway in haematological malignancies [178]. Grumolato *et al.*, [178] showed elevated levels of TCF/LEF transcriptional activity in CML cell lines and primary material, which did not correlate with an increase in nuclear β-catenin levels. They also showed that both *TCF1* and *LEF1* increased the level of *TCF/LEF* reporter activity in the 293T cell line, which is known to not have an active Wnt/β-catenin pathway. Additionally, mutation of *TCF1* which obstructed β-catenin's binding ability, or deletion of the binding site of β-catenin on *TCF1* had little effect on the transcriptional activity of *TCF1*. These data support the theory that *TCF1* can act independently of β-catenin and activate transcription [178].

To establish which aspects of the Wnt/β-catenin pathway are important in CML, it is of interest to see an overall view of the pathway to determine if there are any changes in correlation with the different patient responses. Furthermore, since the TCF/LEF transcription factors are involved in transcriptional activation, both via the Wnt/β-catenin pathway and independently, their influence on the disease may be substantial. Therefore, an investigation into their relationship with patient outcome is worthwhile.

6.2 Aims

The aims of this chapter are to;

1) Screen the components of the Wnt/β-catenin pathway in differing patient outcomes to determine if there is any difference in expression levels.

2) Analyse the genes which show the greatest difference between patient outcomes.

3) Investigate the transcription factors involved in the Wnt/β-catenin pathway to see if they are differentially expressed in the different patient cohorts.

4) Investigate any relation of the transcription factors with GSK3β or CIP2A.

6.3 Optimisation of techniques

All experimentation in this chapter was carried out according to manufacturer's recommendations. The list of primers used can be found in **Materials and Methods, Table 2.3**.

6.4 Results

6.4.1 Is there a difference in the Wnt pathway gene expression between differing patient responses?

Regulation of Wnt signalling can occur at various stages of the pathway. To establish an overall view of the differences in the Wnt pathway gene expression, a RT² Profiler PCR Array for the Human WNT Signalling Pathway (Qiagen) was carried out **(see Methods section 2.6.3)**. This permitted the assessment of changes in mRNA expression of the pathways components to visualise any upregulation or downregulation of genes. Initially, a diagnostic samples from an optimal responder (patient ID #29) was compared to a patient at diagnosis who later transformed into blast crisis (patient ID #115) to see if any resultant genetic differences could be used as a biomarker for disease progression **(Figure 6.4.1)**. Analysis was then undertaken on those genes which showed the largest differences to select which genes should be studied further **(Figures 6.4.2 and 6.4.3)**.

Figure 6.4.1 PCR screening of genes involved in the Wnt signalling pathway; optimal responder vs blast crisis at diagnosis

A PCR screening of all Wnt related genes was carried out looking at an optimal responder (green) and a patient who later transformed into blast crisis (red), each at original diagnosis of chronic phase to see if any genes showed a major difference between responses.
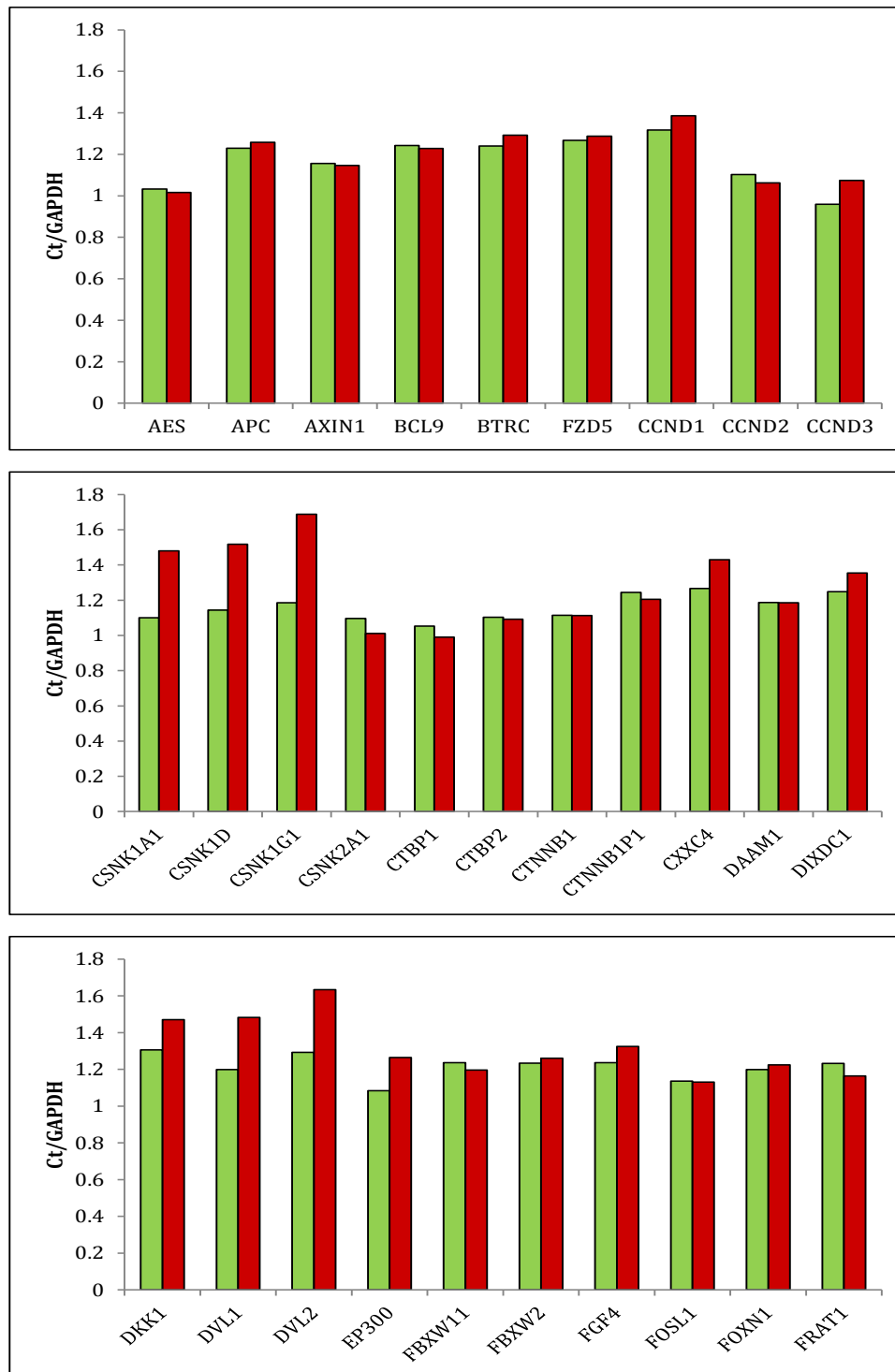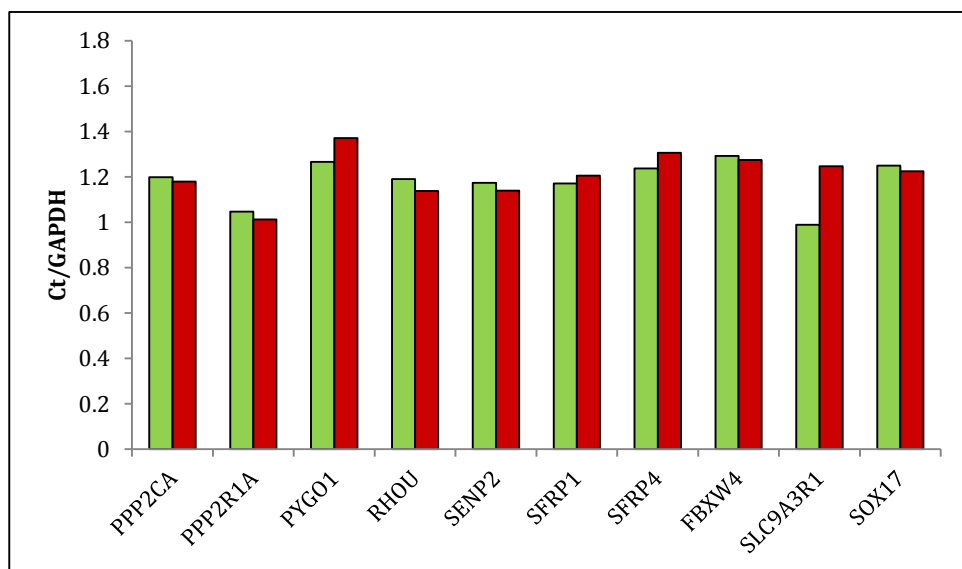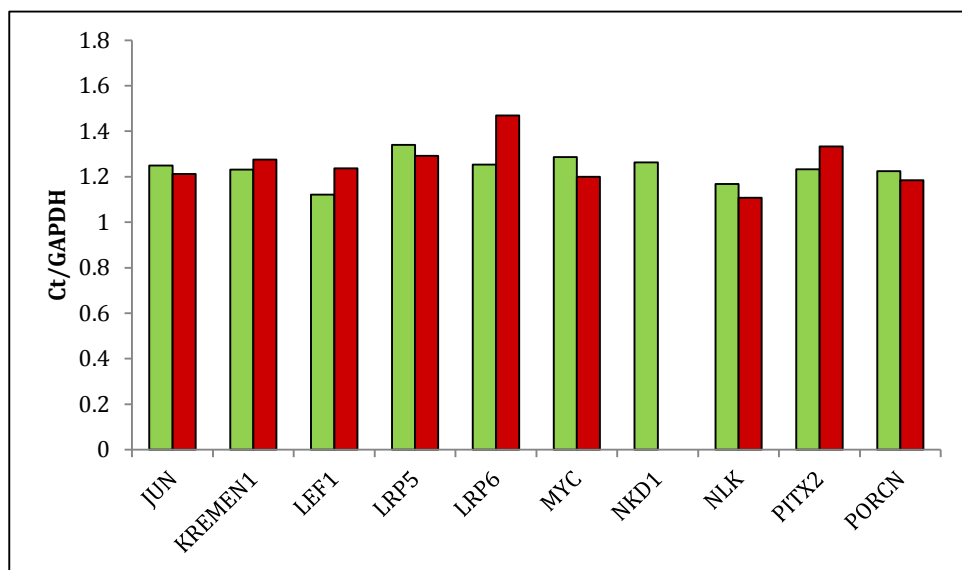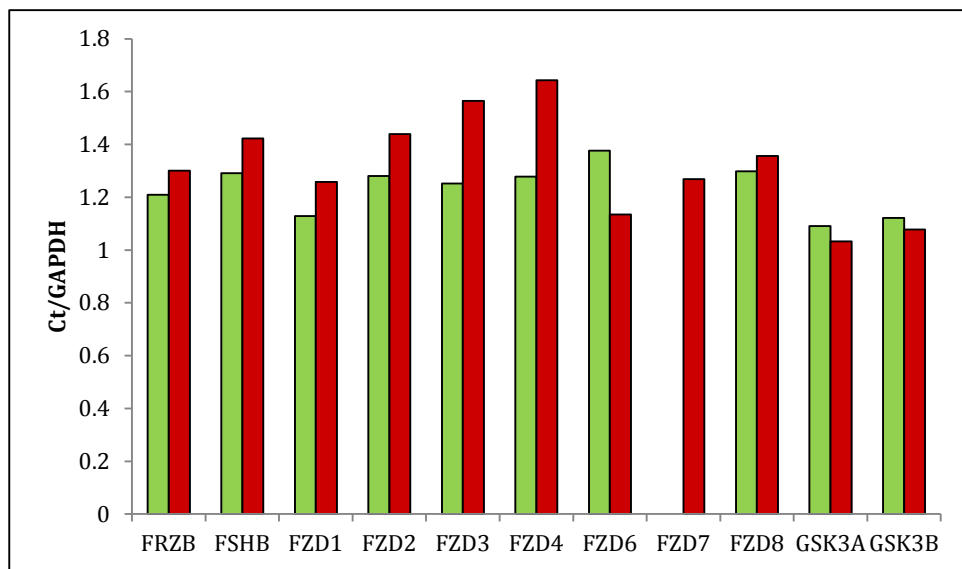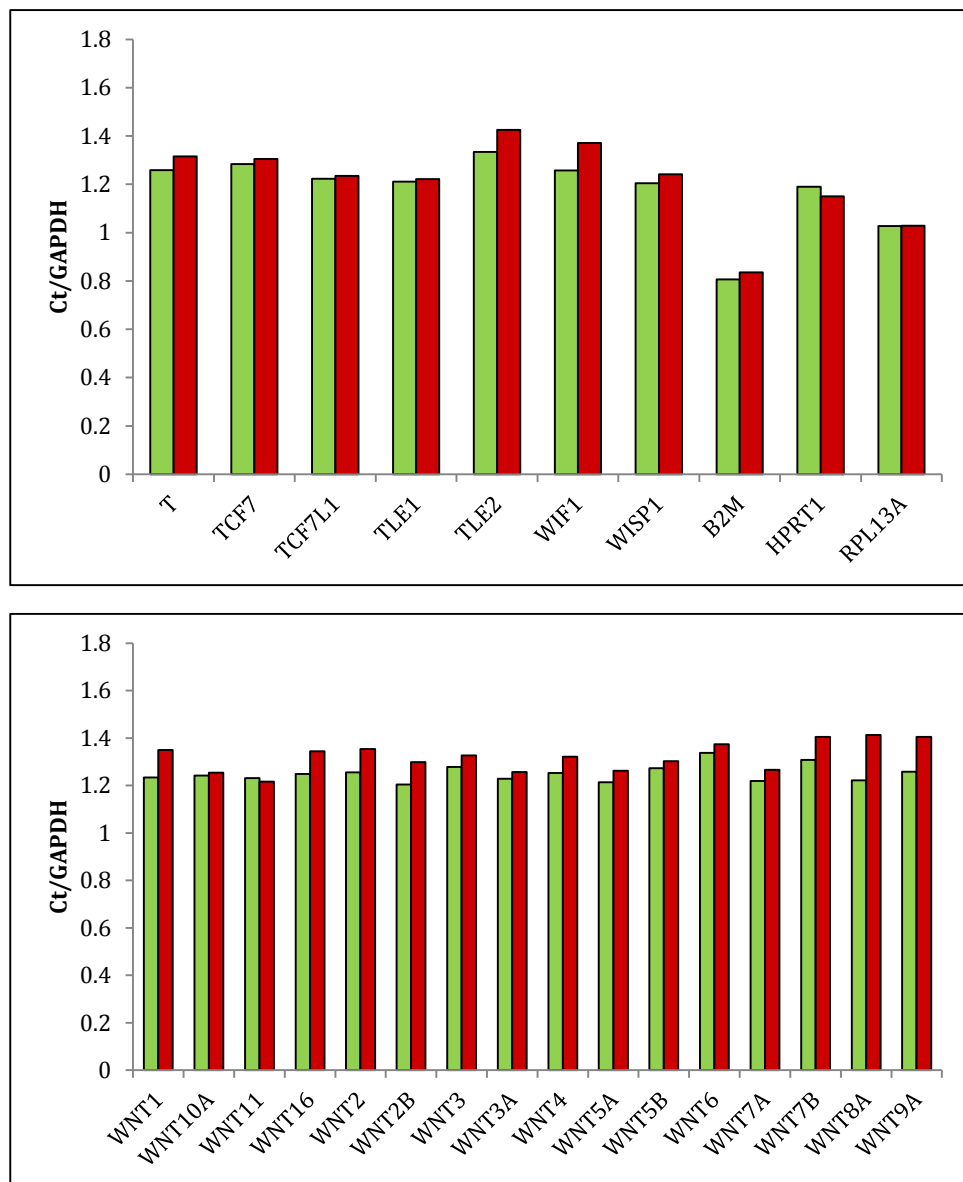
KEY:

AES: Amino-terminal enhancer of split

APC: Adenomatous polyposis coli

AXIN1: Axin 1

BCL9: B-cell CLL/lymphoma 9

BTRC: Beta-transducin repeat containing

FZD5: Frizzled homolog 5 (drosophila)

CCND1: Cyclin D1

CCND2: Cyclin D2

CCND3: Cyclin D3

CSNK1A1: Casein Kinase 1, alpha 1

CSNK1D: Casein kinase 1, delta

CSNK1G1: Casein kinase 1, gamma 1

CSNK2A1: Casein kinase 2, alpha 1 polypeptide

CTBP1: C-terminal binding protein 1

CTBP2: C-terminal binding protein 2

CTNNB1: Catenin (cadherin-associated protein), beta 1, 88kDa

CTNNB1P1: Catenin, beta interacting protein 1

CXXC4: CXXC finger 4

DAAM1: Dishevelled associated activator of morphogenesis 1

DIXDC1: DIX domain containing 1

DKK1: Dickkopf homolog 1 (Xenopus laevis)

DVL1: Dishevelled, dsh homolog 1 (Drosophila)

DVL2: Dishevelled, dsh homolog 2 (Drosophila)

EP300: E1A binding protein p300

FBXW11: F-box and WD repeat domain containing 11

FBXW2: F-box and WD repeat domain containing 2

FGF4: Fibroblast growth factor 4

FOSL1: FOS-like antigen 1

FOXN1: Forkhead box N1

FRAT1: Frequently rearranged in advanced T-cell lymphomas

FRZB: Frizzled-related protein

FSHB: Follicle stimulating hormone, beta polypeptide

FZD1: Frizzled homolog 1 (Drosophila)

FZD2: Frizzled homolog 2 (Drosophila)

FZD3: Frizzled homolog 3 (Drosophila)

FZD4: Frizzled homolog 4 (Drosophila)

FZD6: Frizzled homolog 6 (Drosophila)

FZD7: Frizzled homolog 7 (Drosophila)

FZD8: Frizzled homolog 8 (Drosophila)

GSK3A: Glycogen synthase kinase 3 alpha

GSK3B: Glycogen synthase kinase 3 beta

JUN: Jun oncogene

KREMEN1: Kringle containing transmembrane protein 1

LEF1: Lymphoid enhancer-binding factor 1

LRP5: Low density lipoprotein receptor-related protein 5

LRP6: Low density lipoprotein receptor -related protein 6

MYC : V-myc myelocytomatosis viral oncogene homolog (avian)

NKD1: Naked cuticle homolog 1 (Drosophila)

NLK: Nemo-like kinase

PITX2: Paired-like homeodomain 2

PORCN : Porcupine homolog (Drosophila)

PPP2CA: Protein phosphatase 2 (formerly 2A), catalytic subunit, alpha isoform

PPP2R1A: Protein phosphatase 2 (formerly 2A), regulatory subunit A, alpha isoform

PYGO1: Pygopus homolog 1 (Dosophila)

RHOU: Ras homolog gene family, member U

SENP2: SUMO1/sentrin/SMT3 specific peptidase 2

SFRP1: Secreted frizzled-related protein 1

SFRP4: Secreted frizzled-related protein 4

FBXW4: F-box and WD repeat domain containing 4

SLC9A3R1: Solute carrier family 9(sodium/hydrogen exchanger), member 3 regulator 1

SOX17: SRY (sex determining region Y)-box 17

T : T, brachyury homolog (mouse)

TCF7 : Transcription factor 7 (T-cell specific, HMG-box)

TCF7L1 : Transcription factor 7-like 1 (T-cell specific, HMG-box)

TLE1: Transducin-like enhancer of split 1 (E(sp1) homolog, Drosophila)

TLE2: Transducin-like enhancer of split 2 (E(sp1) homolog, Drosophila)

WIF1: WNT inhibitory factor 1

WISP1: WNT1 inducible signaling pathway protein

B2M: Beta-2-microglobulin

HPRT1: Hypoxanthine phosphoribosyltransferase 1

RPL13A: Ribosomal protein L13a

WNT1: Wingless-type MMTV integration site family member 1

WNT10A: Wingless-type MMTV integration site family member 10a

WNT11: Wingless-type MMTV integration site family member 11

WNT16: Wingless-type MMTV integration site family member 16

WNT2: Wingless-type MMTV integration site family member 2

WNT2B: Wingless-type MMTV integration site family member 2B

WNT3: Wingless-type MMTV integration site family member 3

WNT3A: Wingless-type MMTV integration site family member 3A

WNT4: Wingless-type MMTV integration site family member 4

WNT5A: Wingless-type MMTV integration site family member 5A

WNT5B: Wingless-type MMTV integration site family member 5B

WNT6: Wingless-type MMTV integration site family member 6

WNT7A: Wingless-type MMTV integration site family member 7A

WNT7B: Wingless-type MMTV integration site family member 7B

WNT8A: Wingless-type MMTV integration site family member 8A

WNT9A: Wingless-type MMTV integration site family member 9A

When analysing the results from this screening to determine which of the genes to investigate further, initially the WNT specific ligand genes were separated from the rest of the screening to establish whether there was an up regulation in any WNT ligands. Results from the optimal responder were subtracted from results from the blast crisis patient at diagnosis, to distinguish if any could be used as biomarkers of disease progression, and plotted with increasing difference **(Figure 6.4.2)**. This showed that *WNT1, WNT9A* and *WNT8A* had the largest difference between the two patients, and therefore these were followed up further in patient cohorts **(Section 6.4.1.1)**.

Figure 6.4.2 The difference in the WNT ligand mRNA expression between an optimal responder and a blast crisis patient at diagnosis

The difference in Wnt ligand mRNA expression in an optimal responder (patient ID #29) vs a blast crisis patient (patient ID #115) both at original diagnosis of chronic phase showed *WNT1, WNT9A* and *WNT8A* have the biggest difference in levels between patients.
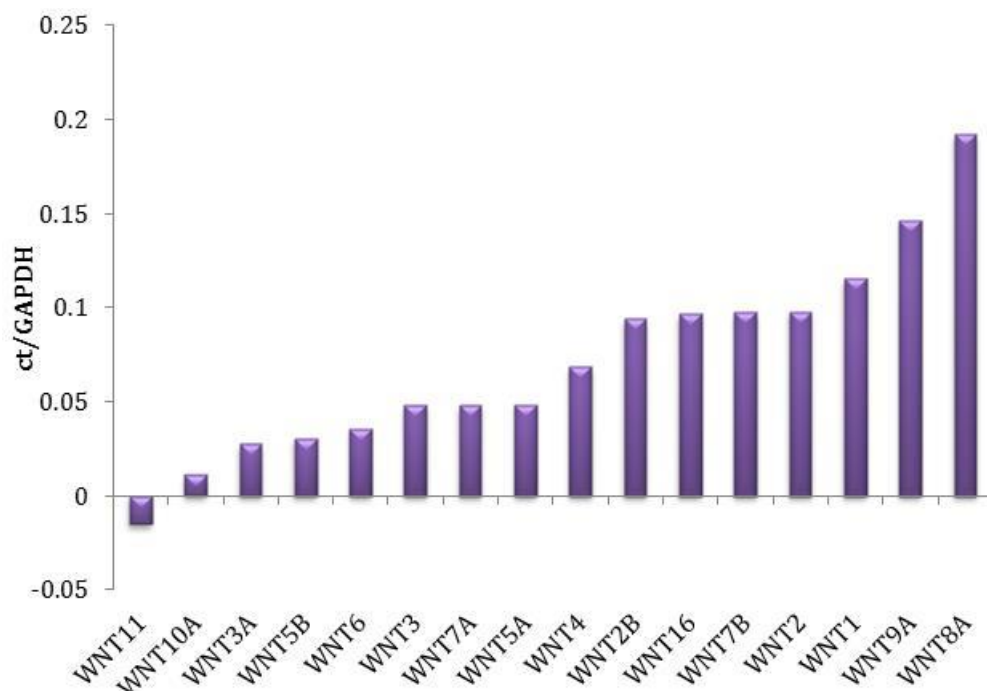
Separate to the WNT ligand genes, the other pathway components were analysed to investigate which differed the most between patients. Results from the optimal responder were again subtracted from results from the blast crisis patient at diagnosis, and the eight components with the largest difference are shown in **Figure 6.4.3**. Results showed *FZD7* and *NKD1* were both absent from one of the patients. *FZD7* was absent in the optimal responder at diagnosis, while *NKD1* was missing from the blast crisis patient at diagnosis; consequently both of these genes were taken on for further analysis **(Section 6.4.1.2 and 6.4.1.3)**.

Figure 6.4.3 The difference in Wnt pathway components mRNA expression between optimal responder and blast crisis patient at diagnosis

To determine the difference in the other components of the Wnt pathway, mRNA expression of the two patients in Figure 6.4.1 were analysed and the difference between patients was determined. Results showed that *FZD7* and *NKD1* had the largest difference between patient responses.
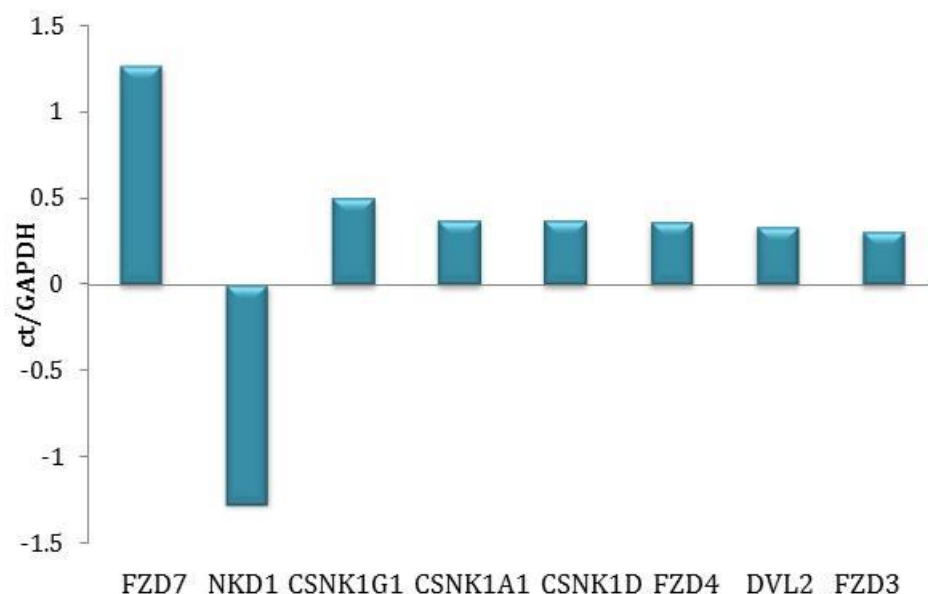
6.4.1.1 WNT ligands *1, 8A*, and *9A* are significantly higher in chronic phase compared to blast crisis

To further investigate the previously selected genes, they were examined in a larger cohort of patients. Patients again were initially split into the three patient outcomes in accordance with the ELN definitions (as described in the introduction **section 1.4**) optimal responders, failure patients and blast crisis patients. These were all analysed at original diagnosis of chronic phase, and those patients who had transformed into blast crisis were also studied after transformation.

Results for the *WNT* ligand genes showed that for *WNT1, WNT8A* and *WNT9A* there are higher mRNA levels in the diagnostic cohorts compared to those patients in blast crisis. Comparison between each of the groups however was not statistically significant **(Figure 6.4.4)**.

Figure 6.4.4. Levels of WNT ligand expression (*WNT1, WNT8A* and *WNT9A*) are lower in blast crisis compared to diagnostic samples from optimal, failure and blast crisis patients

Analysis of the WNT ligands in patient samples were grouped into optimal responders (N=9), failure patients (N=7) and blast crisis patients (N=4) all at original diagnosis of chronic phase, and patients who have transformed into blast crisis (N=4).
Results show levels of the WNT ligands to be higher in the optimal responders, failure patients and patients who later progressed to blast crisis at diagnosis compared to patients in blast crisis.
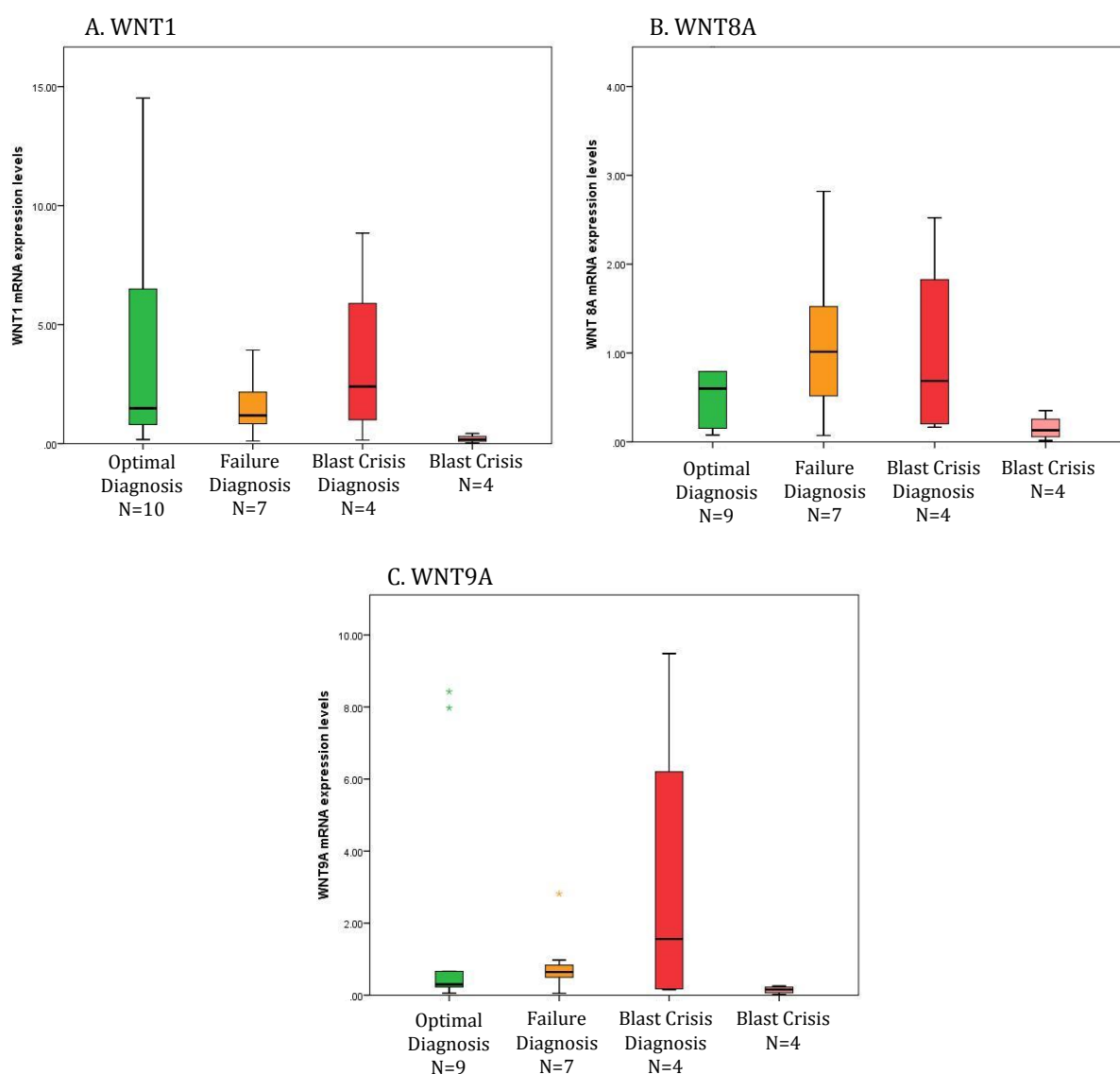
Alternatively, when data were analysed according to chronic phase vs blast crisis, the levels of all the three *WNT* ligands (*WNT1, WNT8A*, and *WNT9A*) were significantly higher in chronic phase compared to blast crisis (P=0.011, 0.045, and 0.037 respectively) **(Figure 6.4.5)**. In combination this could be indicating that activation of the Wnt/β-catenin pathway is occurring in chronic phase through the up-regulation of *WNT* ligand expression. This contradicts the literature where an activation of the Wnt/β-catenin pathway in progenitor cells is shown through an increase in the unphosphorylated form of β-catenin in blast crisis [150, 223]. However since no difference was found in the levels of β-catenin in MNCs between patient responses in my hands, this may suggest an alternative mechanism in these cells.

Figure 6.4.5 Levels of WNT ligand expression (*WNT1*, *WNT8A* and *WNT9A*) are significantly lower in blast crisis compared to chronic phase

Chronic phase samples (N=20) were compared to patients in blast crisis (N=4) for the three WNT ligands. Results showed all three have significantly higher mRNA levels in chronic phase cohort compared to blast crisis. P=0.011 for *WNT1* (A.), P=0.045 for *WNT8A* (B.), and P=0.037 for *WNT9A* (C.).
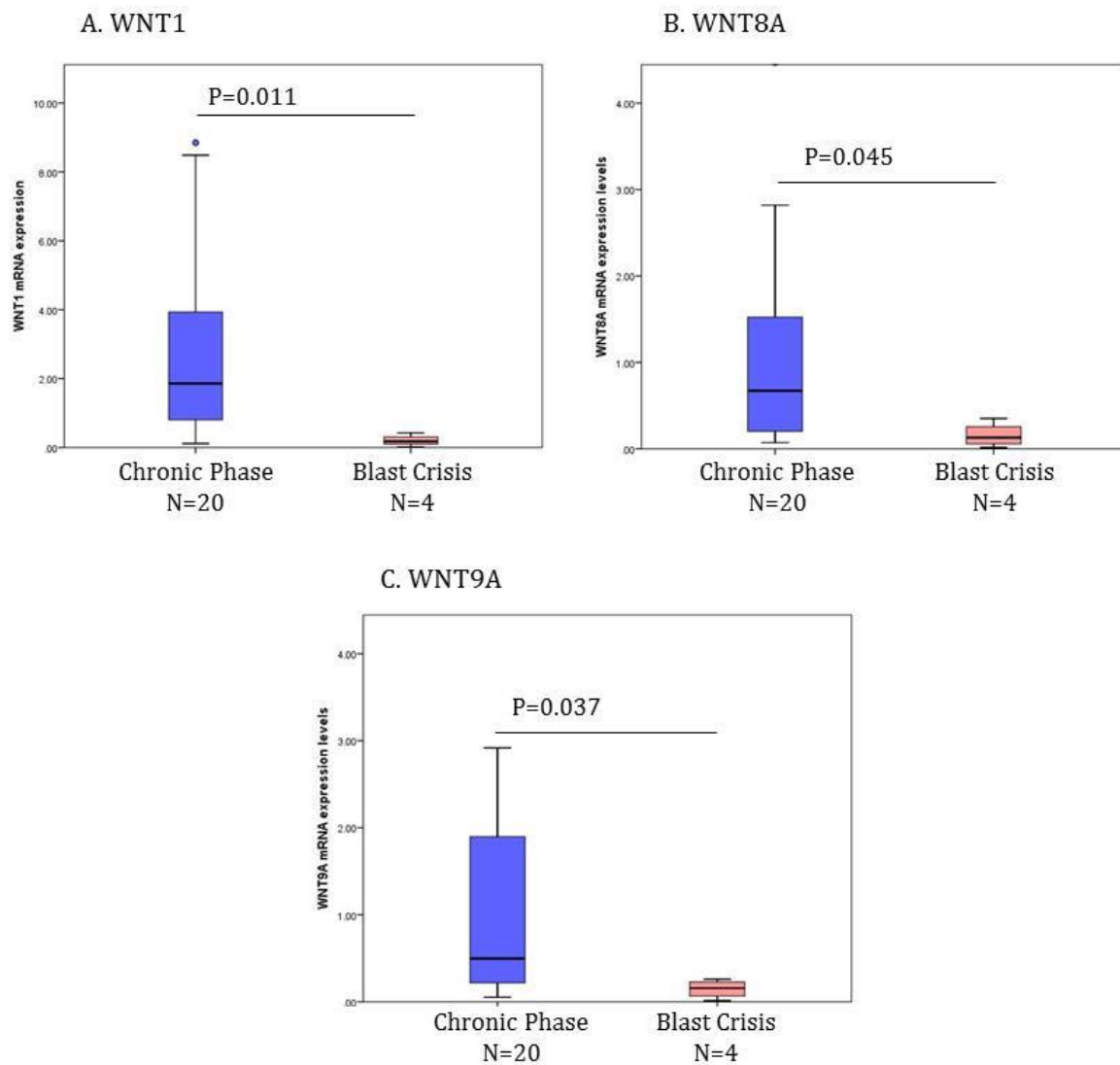
6.4.1.2 mRNA expression of *FZD7* is significantly higher in chronic phase compared to blast crisis

The *FZD7* gene encodes a member of the Frizzled family that is part of the 7-transmembrane protein which recognises the WNT ligands to transmit a signal intracellularly. It is reported to down regulate APC function while enhancing β-catenin mediated signals [224]. The screening showed it to be absent from the optimal responder patient **(Figure 6.4.3)**, however when analysed in a bigger cohort of patient samples, results revealed there are higher levels in the optimal responders, failure patients and patients who later progressed to blast crisis at diagnosis compared to patients in blast crisis **(Figure 6.4.6 A.)**. Levels of *FZD7* were significantly higher levels in the chronic phase cohort compared to blast crisis (P=0.037) **(Figure 6.4.6 B.)**. This increase in a member of the *FZD* receptors in chronic phase could contribute to an up-regulation of pathway activity correlating with the increase in *WNT* ligand expression seen in **Figure 6.4.5**.

Figure 6.4.6 mRNA levels of *FZD7* are significantly higher in chronic phase patients vs blast crisis patients

Patients were grouped as with the WNT ligands, and results showed that *FZD7* was higher in the diagnostic samples vs patients in blast crisis; however this result was not statistically significant (A.). Levels are significantly higher in chronic phase overall than in blast crisis (P=0.037) (B.)

A.

B.
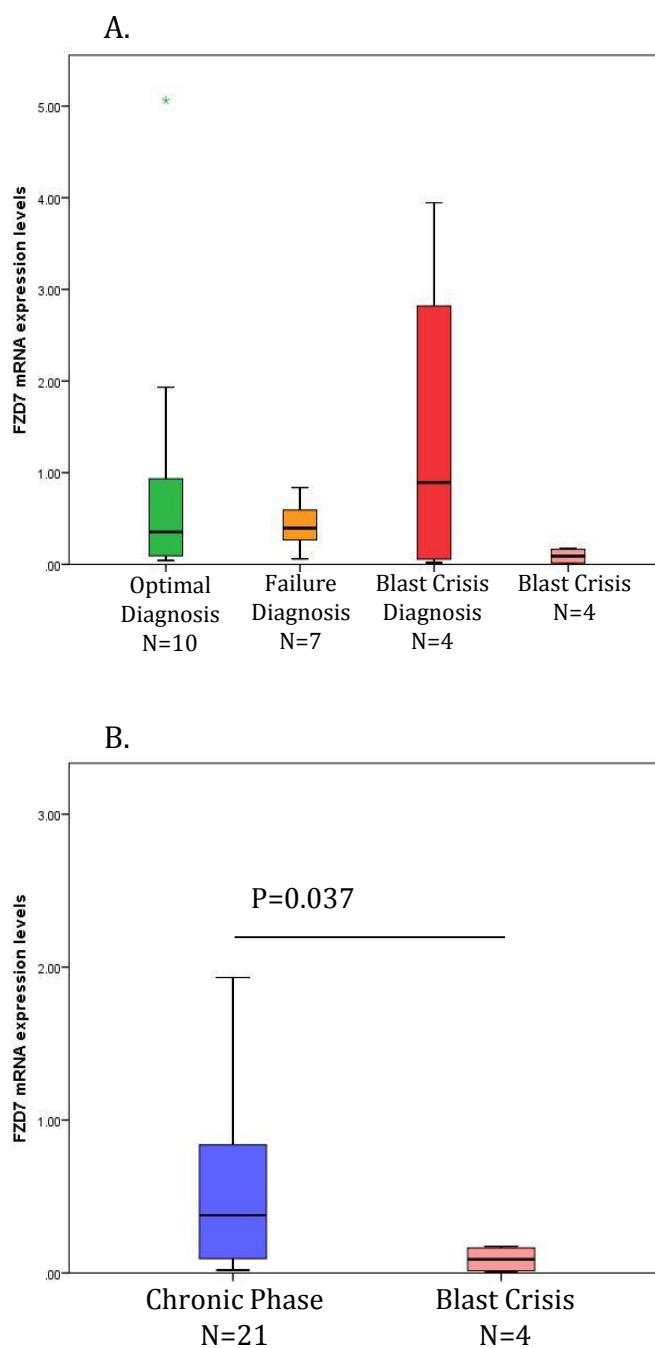
6.4.1.3 Levels of *NKD1* mRNA expression are significantly higher in chronic phase compared to blast crisis

Naked cuticle 1 (NKD1) is a member of the naked cuticle family whose purpose is to function as a negative regulator of the Wnt pathway by not only binding to DSH to impede the signal transmitting through to the other components of the pathway [225], but also by binding directly to β-catenin to inhibit the translocation of β-catenin into the nucleus [226]. When comparing an optimal responder patient to a blast crisis patient, both at diagnosis, it was absent in the patient's diagnostic sample who later progressed to blast crisis **(Figure 6.4.3)**. When levels of *NKD1* were measured in a bigger cohort of patient samples, a higher level of *NKD1* mRNA expression was seen in the optimal responders, failure patients and patients who later progressed to blast crisis at diagnosis compared to patients in blast crisis **(Figure 6.4.7 A.)**. This was shown to be statistically significant when the patients were grouped into chronic phase vs. blast crisis (P=0.013) **(Figure 6.4.7 B.)**. This implies that *NKD1* may be being used as a negative regulator to compensate for the enhanced expression of the *WNT* ligands and *FZD7* shown previously. It has been recently reported that NKD1 is a passive antagonist of the pathway that is only activated when there is a surplus of pathway activity [227]. This could be the mechanism occurring in chronic phase to stabilise an up-regulation of Wnt/β-catenin pathway activity.

Figure 6.4.7 mRNA levels of *NKD1* are significantly higher in chronic phase patients vs blast crisis patients

Patients were grouped as **Figure 6.4.6.** Results revealed that *NKD1* is higher in the optimal responders, failure patients and patients who later progressed to blast crisis at diagnosis vs patients in blast crisis (A.). This was statistically significant when chronic phase was compared to blast crisis (P=0.013) (B.)

A.

B.
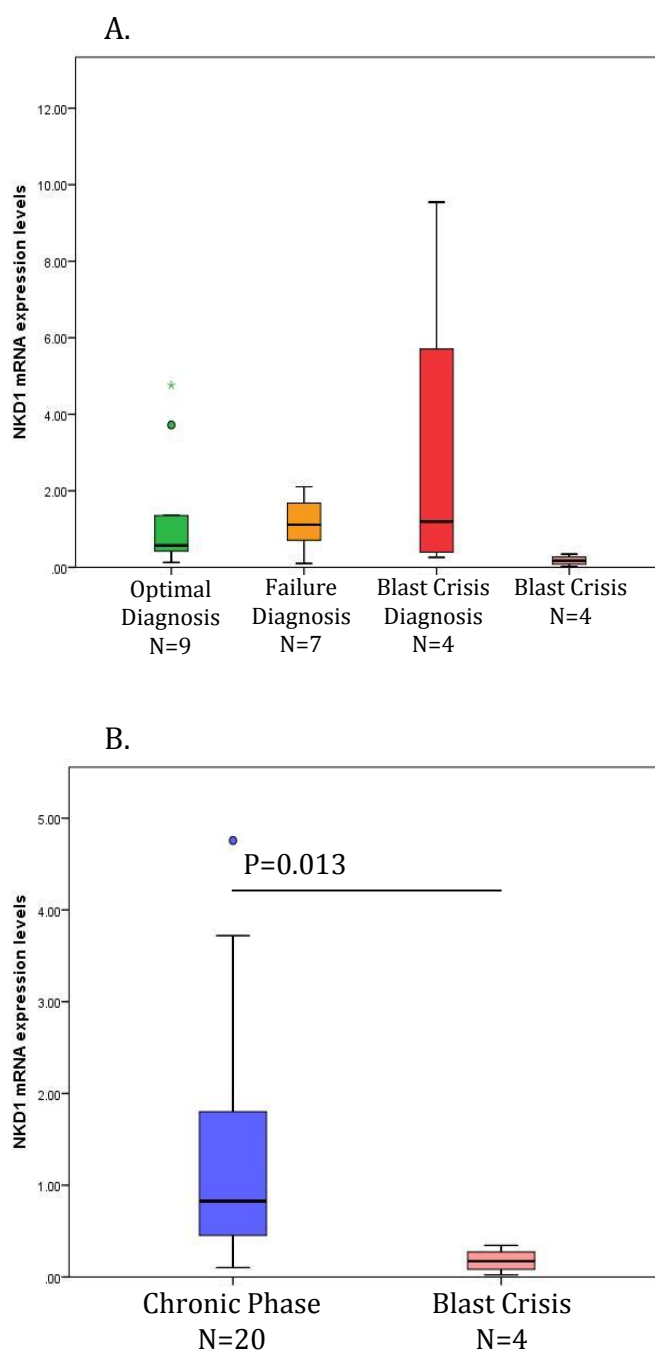
6.4.1.4 Levels of *APC* mRNA expression are significantly higher in blast crisis compared to chronic phase

Adenomatous polyposis coli (APC) is a component of the Wnt pathway which functions as a tumour suppressor by enhancing the phosphorylation and subsequent degradation of β-catenin [228] . It acts in the regulation of β-catenin and has been reported to play an important role in cancer progression, in particular in colon cancer whereby mutations in *APC* lead to disease progression [220, 221]. While the initial screening between two chronic phase diagnostic samples from an optimal responder and a blast crisis patient showed no difference in the levels of *APC*, its importance in malignancies [229] led to further investigation in a larger cohort of patients. When grouped according to patient outcome at diagnosis and when patients have transformed into blast crisis, results showed no significant difference between the cohorts **(Figure 6.4.8 A)**. However, when analysed as chronic phase vs blast crisis there are significantly higher levels of *APC* expression in the blast crisis patients compared to chronic phase (P=0.026) **(Figure 6.4.8 B)**.   This may be due to the significantly higher levels of *FZD7* found in chronic phase samples which is known to down-regulate APC [224].

Figure 6.4.8 mRNA levels of *APC* are significantly higher in blast crisis compared to chronic phase

Patients were grouped as **Figure 6.4.6** and results showed no significant difference in *APC* between patient cohorts. However when stratified by chronic phase vs blast crisis there are significantly higher levels of *APC* in blast crisis (P=0.026) (B.)
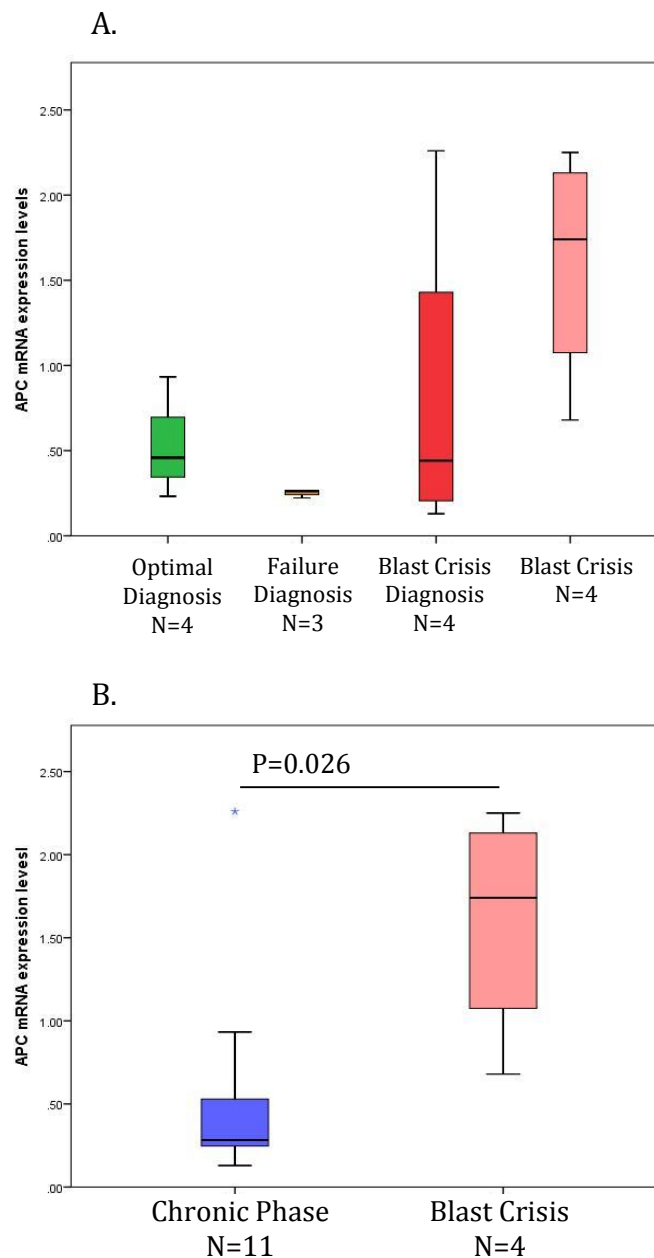
6.4.1.5 Re-screening of the Wnt/β-catenin pathway genes

To extend our knowledge of what was occurring in CML it was considered appropriate to further analyse these genes in a normal control, a failure patient at diagnosis (#9), and a patient in blast crisis (#115), alongside the previous optimal responder at diagnosis (#29) and the blast crisis patient at diagnosis (#115) **(data shown in Appendix Figure 8.6)**. This was intended to give a wider understanding of the regulation of the Wnt/β-catenin pathway in all the patient outcomes, however when processing the results limitations to this method arose. Firstly screening only one patient per cohort reduced the accuracy of this screening significantly. In addition to this it proved difficult to determine how much of a change per gene could result in a significant effect on the Wnt/β-catenin pathway and its signal transduction, as no statistical analysis could be carried out. Therefore, although this screening was a useful preliminary overview of what could be occurring to the Wnt/β-catenin pathway between different cohorts of patients, it was decided not to base further work on results from this screening.

6.4.2 Do the transcription factors involved in the Wnt/β-catenin pathway correlate with disease progression?

The last stage at which the Wnt/β-catenin pathway can be regulated is through the transcription factors which bind β-catenin to the promoter DNA of the targets genes and activate transcription [178]. Therefore, the decision was made to further investigate these transcription factors and whether they are differentially expressed in the various patient cohorts.

6.4.2.1 The transcription factors involved in the Wnt pathway are all higher in blast crisis, except *TCF3*

The transcription factors involved in the Wnt/β-catenin pathway include TCF1, TCF3, TCF4, and LEF1 [215]. These all play a significant role in the regulation of transcriptional activation, as without them β-catenin is unable to bind to the promoter of its target genes and activate their transcription **(Introduction section 1.10)**.

6.4.2.1.1 *TCF1*

TCF1 has been reported to function as both a tumour suppressor as well as an activator of transcription of target genes [215]. Its ability to function as a suppressor is due to a large amount of the isoform expressed being spliced leading to the loss of the β-catenin binding domain, enabling it to act as a competitor for fully functional isoforms [230]. Specifically in lymphomas, TCF1 acts as a repressor of LEF1, shown by both mRNA and

protein levels. Without the expression of *TCF1*, Wnt activity increases causing lymphoma progression [231].

TCF1 mRNA levels were analysed by RT-qPCR **(Materials and Methods section 2.6.3).** Results showed levels of *TCF1* mRNA are higher in the CML patients who had transformed into blast crisis compared to optimal responders, failure patients, and blast crisis patients all at original diagnosis of chronic phase **(Figure 6.4.12 A)**. This was shown to be a significant difference when stratified according to chronic phase vs blast crisis (P=0.001) **(Figure 6.4.12 B)**. These results indicate that elevated levels of *TCF1* correlate with blast crisis, but do not predict prognosis in chronic phase.

Figure 6.4.12 *TCF1* mRNA levels are significantly higher in patients who have transformed into blast crisis

Levels of *TCF1* were measured according to patient outcome (A.) and according to chronic phase vs blast crisis (B.) Results showed higher levels in the patients who have transformed into blast crisis compared to diagnostic chronic phase samples from optimal responders, failure patients, and patients who later progressed into blast crisis. Blast crisis had significantly elevated levels compared to diagnostic samples grouped into chronic phase (P=0.001).
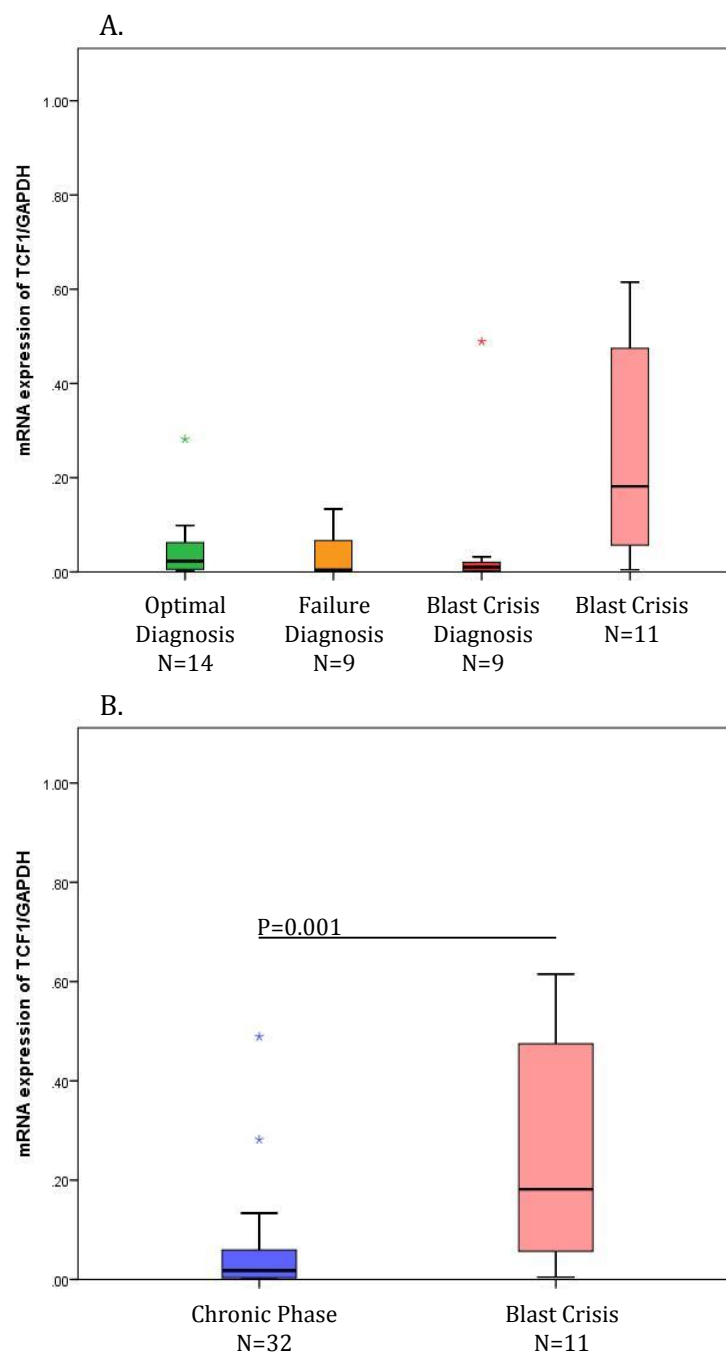
6.4.2.1.2 *TCF3*

There have been limited reports of TCF3 and its function in CML. It has been suggested that TCF3 functions mainly as a repressor of transcriptional activation [180]. Interestingly, *TCF3* and *TCF1* have been reported to have contrasting roles in the regulation of embryonic stem cell self-renewal, with *TCF3* suppressing it, while *TCF1* promotes it [232]. However, in breast cancer both mRNA and protein expression of TCF3 has been reported to be involved in the regulation of tumour development with over-expression correlating with poor differentiation of the disease. In addition, reducing *TCF3* levels diminished tumour formation [233].

When measuring the mRNA levels of *TCF3* in CML patients, results showed higher levels in the blast crisis patients compared to the optimal responders, failure patients and patients who later progressed to blast crisis at initial diagnosis, however these results were not statistically significant **(Figure 6.4.13 A)**. When comparing chronic phase overall to blast crisis there was again no statistical difference between the groups **(Figure 6.4.13 B)**. This may illustrate that *TCF3* is playing less of a role in blast crisis as a suppressor of transcription compared to the activational transcription factors.

6.4.2.1.3 *TCF4*

TCF4 is of particular interest as, within CML, TCF4 is known to specifically interact with β-catenin which has been directly phosphorylated by BCR-ABL at tyrosine residues Tyr86 and Tyr654, enabling activation of transcription [144]. Additionally it has been shown in B-cell CLL that levels of *TCF4* were elevated in conjunction with the Wnt target gene *CCND2*, demonstrating the possible importance of the Wnt/β-catenin pathway in CLL [234].

Expression levels of *TCF4* mRNA are higher in patients who had transformed into blast crisis compared to optimal responders, failure patients, and patients who later transformed into blast crisis at original diagnosis, however these results did not reach statistical significance **(Figure 6.4.14 A)**. When the results were re-stratified into chronic phase compared to blast crisis, *TCF4* mRNA levels were significantly higher in blast crisis (P=0.016) **(Figure 6.4.14 B)**. TCF4 has been shown to associate with the Tyr654 phosphorylated form of β-catenin to activate transcription [186]. Analysis of phospho-β-catenin (Tyr654) showed significantly lower levels in the blast crisis patients **(Chapter 3 - Figure 3.4.21)**. To determine if phospho-β-catenin (Tyr654) is still associating with TCF4, protein levels of TCF4 would need to be measured and immunoprecipitation carried out to ascertain the level of interaction TCF4 is having with phospho-β-catenin (Tyr654). It may be the case that, as phospho-β-catenin (Tyr654) levels are significantly reduced in patients that have elevated *TCF4* levels and vice versa, this is not a significant event in CML disease progression.

Figure 6.4.14 *TCF4* mRNA expression levels are significantly higher in blast crisis patients compared to chronic phase

Levels of *TCF4* were measured as before corresponding to patient outcome (A.) and according to chronic phase vs blast crisis (B.) Results showed higher levels in the patients in blast crisis compared to optimal responders, failure patients, and patients who later progressed into blast crisis at diagnosis . When re-stratified, blast crisis had significantly higher levels of *TCF4* in comparison to chronic phase (P=0.016).
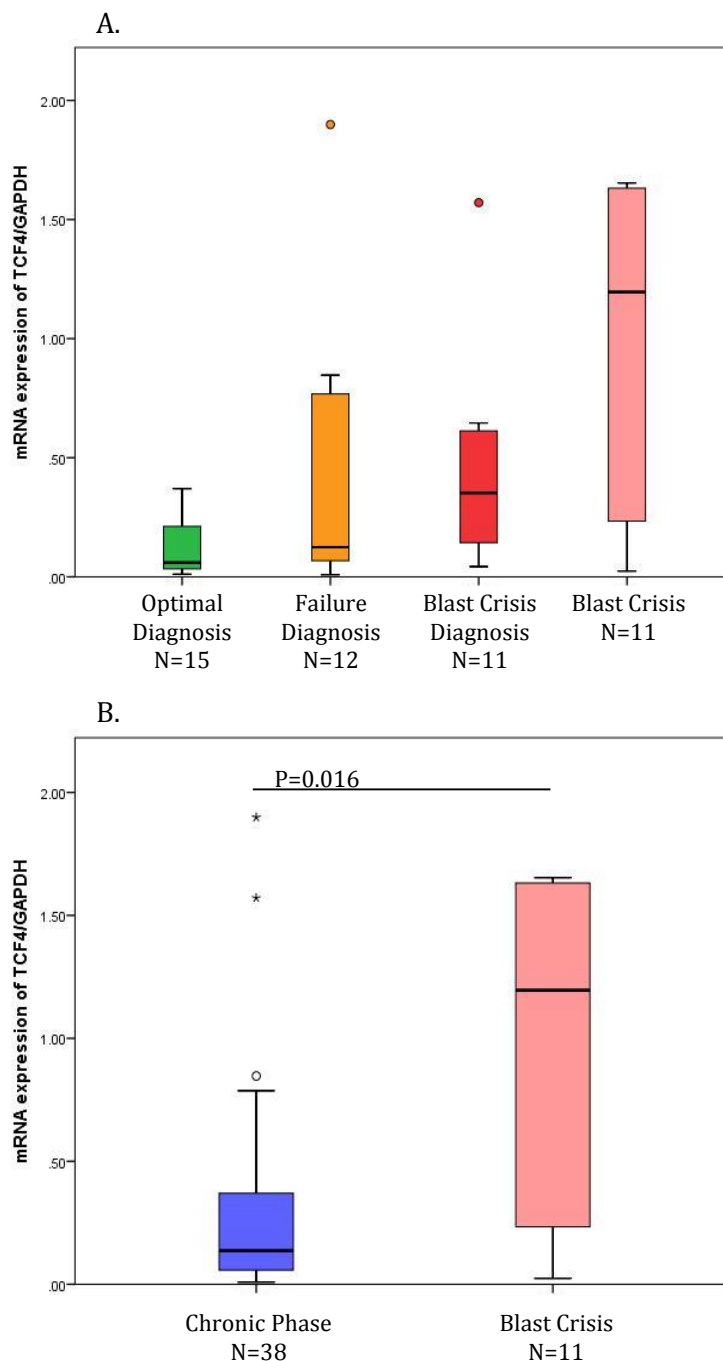
6.4.2.1.4 *LEF1*

There have been conflicting reports of whether LEF-1 is either an antagonist or agonist in the development of different leukaemias. It has been found in cytogenetically normal AML that an elevation in *LEF1* levels correlated with better cytogenetic response rate, overall survival, event-free survival and relapse-free survival. A decrease in *LEF1* levels conversely correlated with higher blast counts and disease progression [123]. These results contradict what has previously been shown with elevated levels of *LEF1* inducing the development of myeloid and lymphoid leukaemia. In B-cell CLL, LEF1 was found to be over-expressed and a reduction in the expression of LEF1 reduced the survival of CLL cells. This indicates that LEF1 is a pro-survival factor involved in the development of CLL [234]. Additionally there have been reports of mutations in *LEF1* taking place in T-cell ALL, and enhanced *LEF1* levels correlate with poor prognosis in B-cell ALL [123].

Investigation into the mRNA levels of *LEF1* in CML patients showed that patients in blast crisis have significantly higher levels than the optimal responders (P=0.002), failure patients (P=0.008), and blast crisis patients (P=0.008) all at diagnosis **(Figure 6.4.15 A)**. This result was validated when evaluating according to chronic phase vs blast crisis (P=0.003) **(Figure 6.4.15 B)**. This reveals that in CML enhanced *LEF1* levels correlate with blast crisis.

Figure 6.4.15 *LEF1* mRNA levels are significantly higher in blast crisis patients in comparison to chronic phase

mRNA levels of *LEF1* were measured according to patient outcome (A.) and according to chronic phase vs blast crisis (B.) Results for *LEF1* showed levels of patients in blast crisis being significantly higher than optimal responders, failure patients, and patients who progressed into blast crisis at diagnosis (P=0.002, 0.008, and 0.008 respectively). Additionally, levels in blast crisis were significantly higher compared to chronic phase (P=0.003).
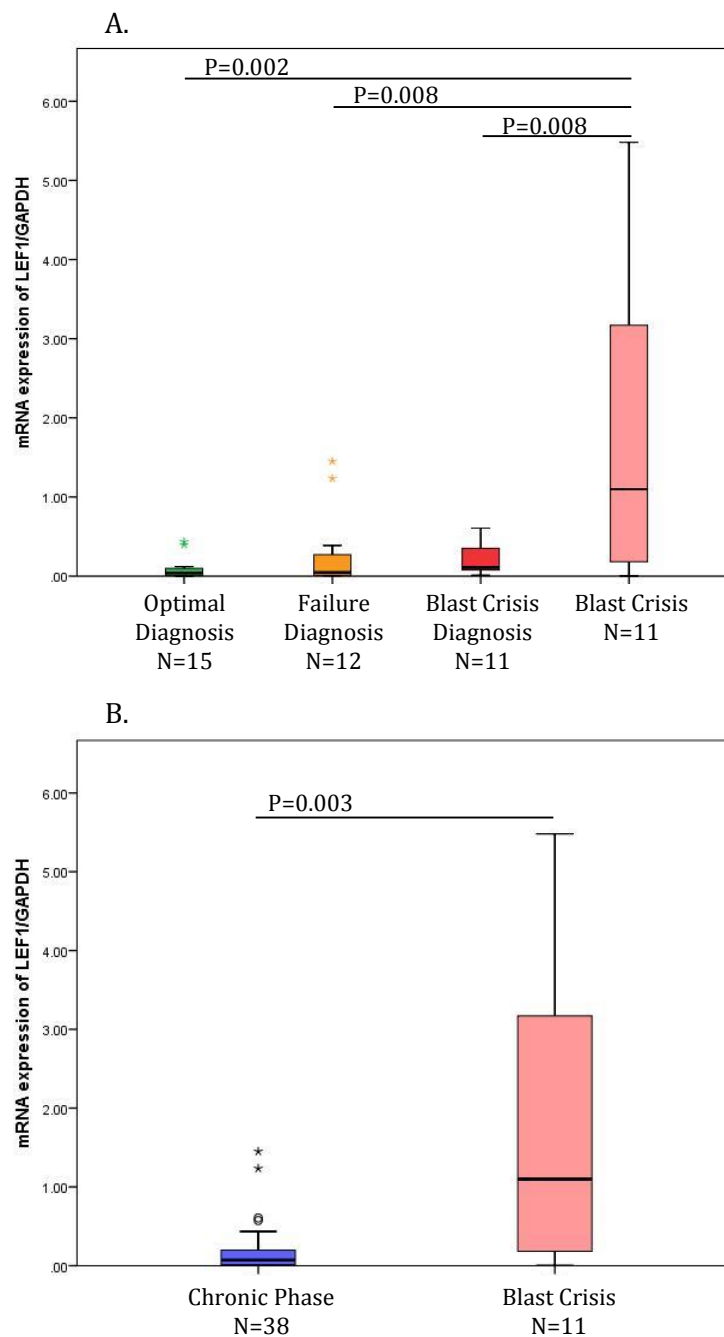
6.4.2.2 *C-MYC* mRNA levels are elevated in blast crisis

The mRNA expression levels of the TCF/LEF transcription factors correlate with poor prognosis in CML patients. However, to determine if this is due to enhanced transcriptional activation of Wnt target genes, the expression levels of known target genes of the Wnt/β-catenin pathway (*CYCLIN D1* and *C-MYC*) were investigated **(see Methods section 2.6)**. Results show that there is no significant difference between patient cohorts in *CYCLIN-D1* and *C-MYC* levels **(Figure 6.4.11 A. and B.)**. However, when comparing chronic phase to blast crisis, there are significantly elevated levels of *C-MYC* in blast crisis (P=0.038) **(Figure 6.4.11 D.)**. This activation of transcription of *C-MYC* in blast crisis correlates with significantly higher levels of C-MYC protein seen in **Chapter 4, Figure 4.4.14 C**. This implies that the transcription factors are functioning as transcriptional activators; however there are other factors which regulate the expression of *C-MYC* which could be contributing to the increase seen.

Figure 6.4.11 Blast crisis patients have significantly higher levels of *C-MYC* but not *CYCLIN D1* gene expression

Levels of *CYCLIN D1* and *C-MYC* were measured according to patient outcome (A. and B.) and according to chronic phase vs blast crisis (C. and D.) Results showed that there was no change in the levels of *CYCLIN D1* for either analysis, however for *C-MYC* there were significantly elevated levels in blast crisis compared to chronic phase (P=0.038) (D.).
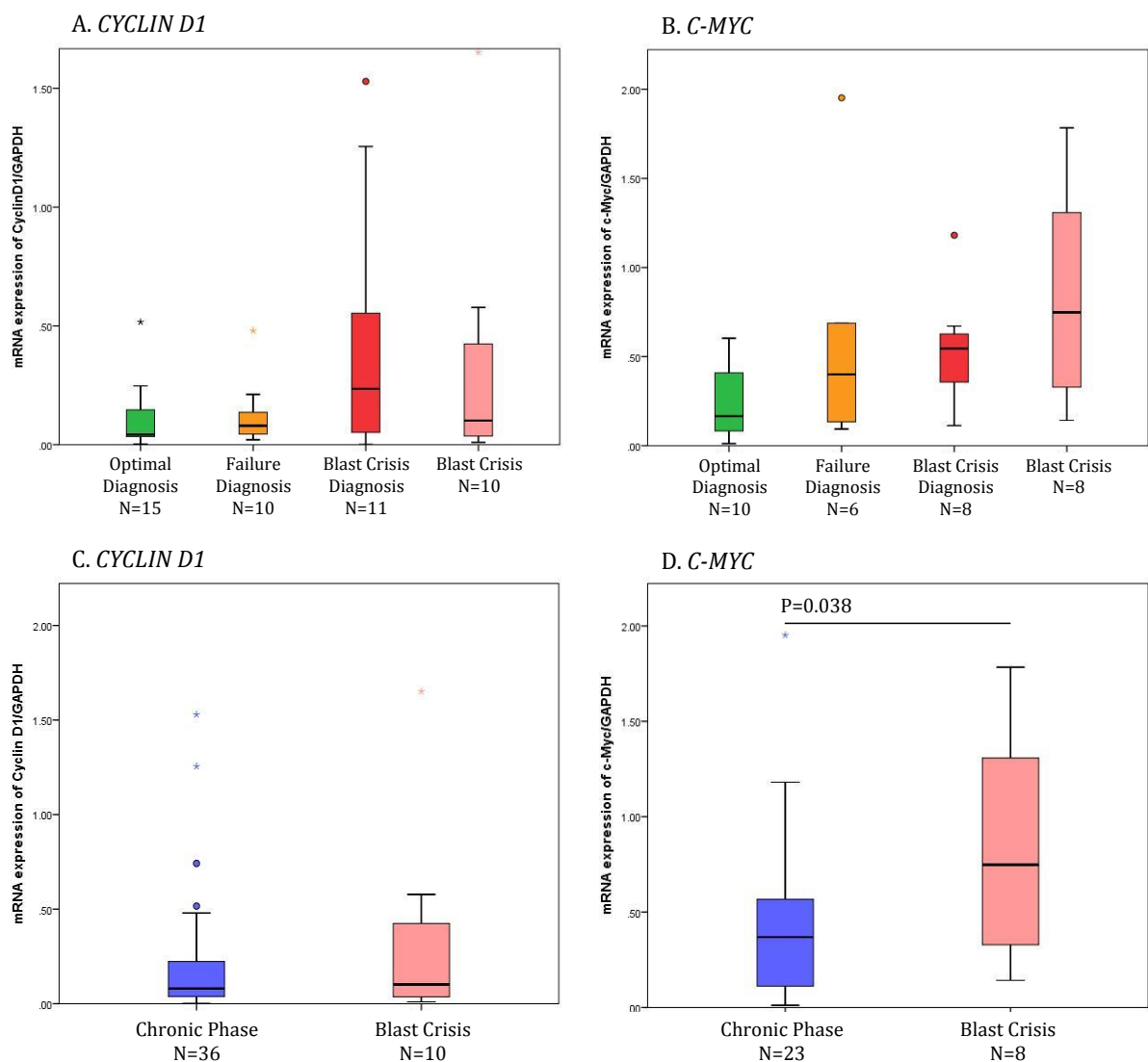
6.4.3 The Wnt transcription factors in relation to GSK3β and CIP2A

In this chapter it has been observed that in chronic phase there is a significant increase in Wnt/β-catenin pathway activation, seen through an up-regulation of the *WNT* ligands. This is contradictory to the observation of there being an up-regulation in the transcription factors in blast crisis. This, alongside the fact that it has been established that the transcription factors TCF1 and LEF1 can also function independently of the Wnt/β-catenin signalling pathway[178], instigated the investigation as to whether there is a relationship between the transcription factors and either GSK3β which was seen to have decreased activity in blast crisis, or CIP2A a predictive biomarker of disease progression.

6.4.3.1 GSK3β knockout does not significantly affect the mRNA levels of the Wnt transcription factors

To determine whether GSK3β had any effects on the expression of the Wnt transcription factors siRNA inhibition of GSK3β **(previously optimised in chapter 5, section 5.3.1)** was carried out in K562 cells and mRNA was extracted from the cultures to perform RT-qPCR (N=3) **(Materials and Methods section 2.6)**. Results showed that inhibition of GSK3β had no effect on the levels of *TCF1* expression. Meanwhile, there is a reduction in the expression of *TCF3, TCF4*, and *LEF1* when GSK3β has been knocked out **(Figure 6.4.17)** however these data did not reach statistical significance, indicating GSK3β does not play a significant role in the regulation of the transcription factors expression.

Figure 6.4.17 Knock out of GSK3β by siRNA does not significantly affect the mRNA expression levels of the Wnt transcription factors

siRNA was used to knock out GSK3β in K562 cells and then mRNA levels of *TCF1* (A.), *TCF3* (B.), *TCF4* (C.), and *LEF1* (D.) were measured. GSK3β knockout has no effect on the levels of *TCF1*. It does decrease the levels of *TCF3, TCF4*, and *LEF1* however this reduction is not significant.
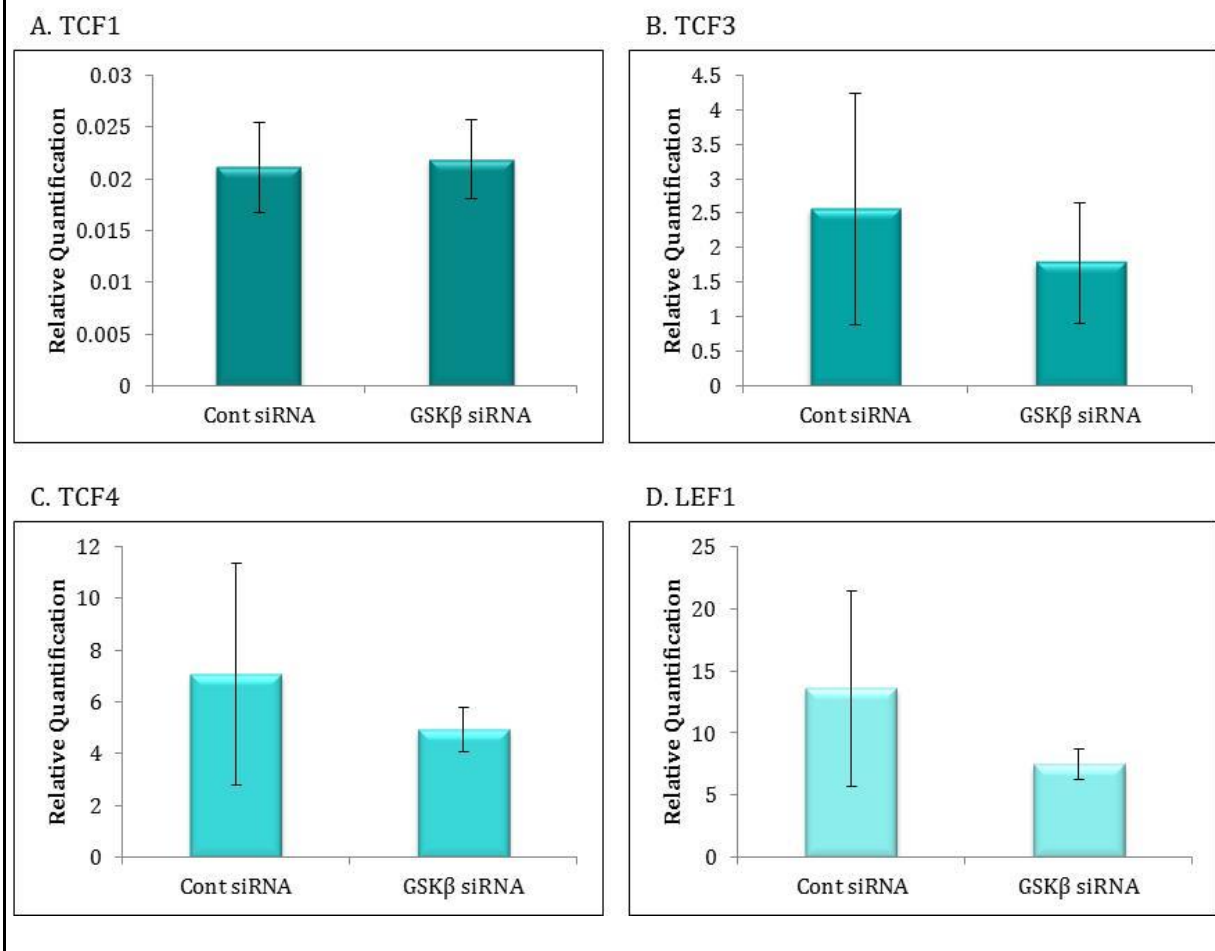
6.4.3.2 The mRNA expression of the transcription factors *TCF4* and *LEF1* are significantly higher in patients with high CIP2A

Next, to see any correlation of the Wnt transcription factors with CIP2A, the patients were stratified according to CIP2A protein levels (MFI >7 or < 7). Results showed higher *TCF4* and *LEF1* mRNA levels in high CIP2A patients (P=0.012 and 0.016 respectively) **(see Figure 6.4.19 C. and D.)**. There are no reports of CIP2A being linked with the WNT transcription factors, however these results show that patients with high CIP2A levels also have elevated levels of the transcription factors. The mechanism by which this occurs would need further investigation.

Figure 6.4.19 High CIP2A correlates with significantly higher levels of *TCF4* and *LEF1*

Patients were stratified into low CIP2A (MFI<7) (N=8) and high CIP2A (MFI>7) (N=5) groups and correlated with the mRNA levels of the *WNT* transcription factors. Results show high CIP2A correlates with increased levels of all the transcription factors. This was significant for *TCF4* (P=0.012) (C.) and *LEF1* (P=0.016) (D.).
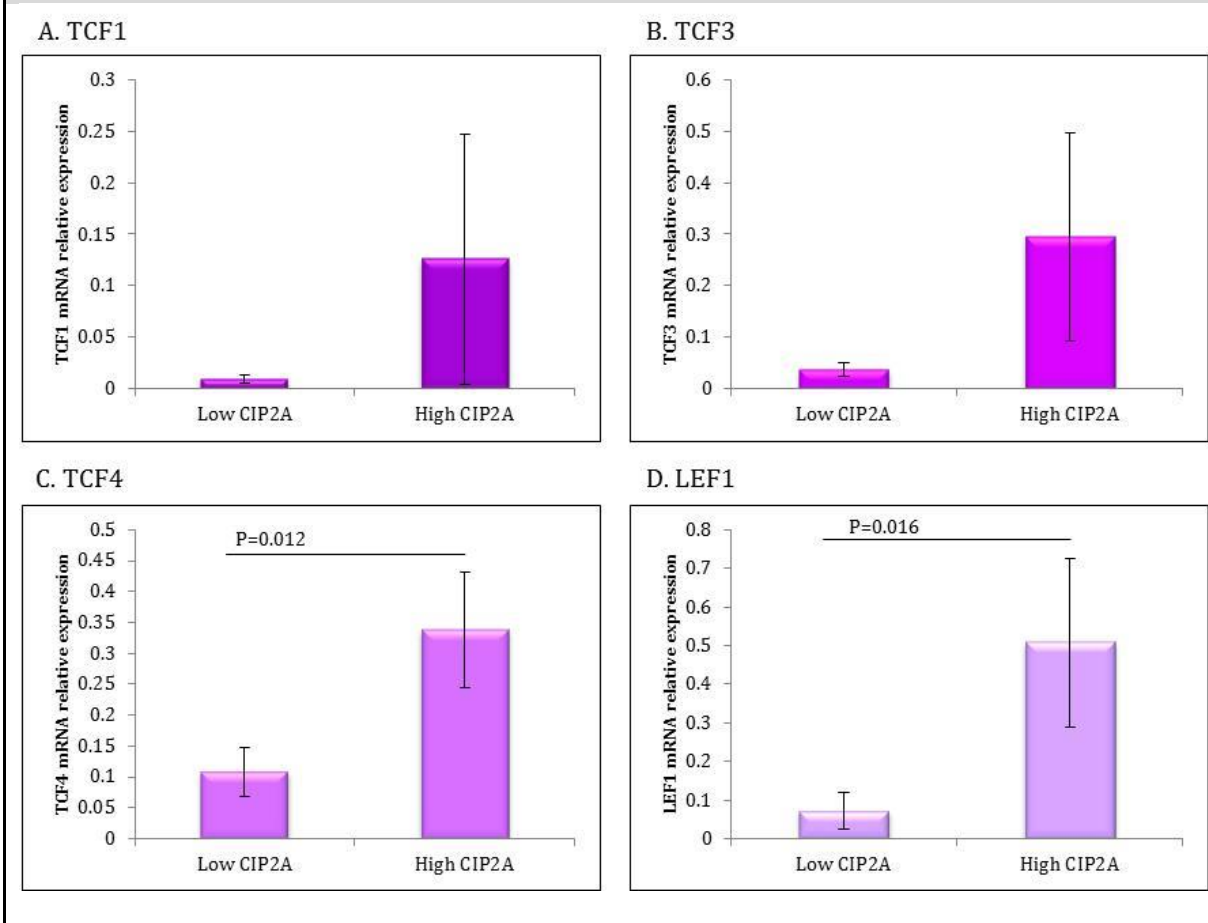
6.4.3.3 High CIP2A levels also correlate with increased expression of the Wnt target genes *CYCLIN D1* and *C-MYC*

The mRNA levels of *CYCLIN D1* and *C-MYC* were also stratified according to their CIP2A protein levels **(Figure 6.4.20)** and results showed that levels of both *CYCLIN D1* and *C-MYC* were elevated in patients with high CIP2A levels (P=0.06 and 0.28 respectively).

This correlates with increased expression of the *TCF/LEF* transcription factors shown in **Figure 6.4.19** and their association with poor prognosis.

Figure 6.4.20 High CIP2A correlates with elevated levels of both *CYCLIN D1* and *C-MYC*

Patients were separated into low CIP2A (MFI<7) and high CIP2A (MFI>7) and *CYCLIN D1* and *C-MYC* mRNA levels were measured. Results show high CIP2A protein levels correlate with increased (A.) *CYCLIN D1* levels (P=0.06) and (B.) *C-MYC* levels (P=0.28).
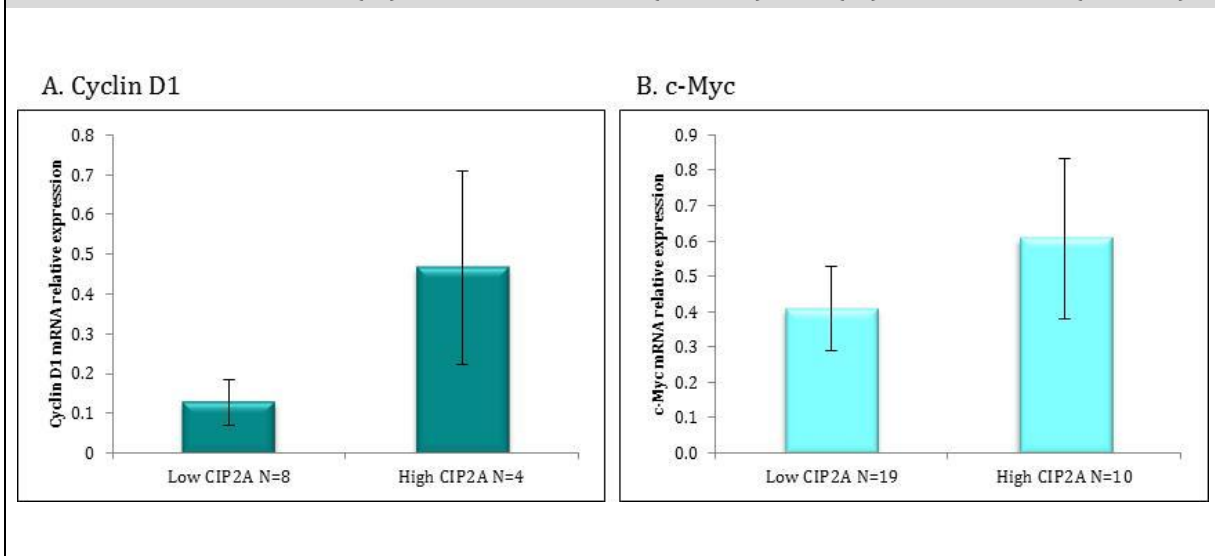
6.5 Main Conclusions

The Wnt pathway is known to play an important role in the development of several malignancies; however its regulation is very complex with numerous factors involved at different stages of the pathway, some of which were detailed in **Table 6.1.1**.

The main conclusions obtained from this chapter include;

1) The Wnt ligands *WNT1, WNT8A*, and *WNT9A* were significantly higher in chronic phase compared to blast crisis indicating an up-regulation of Wnt pathway activity in chronic phase MNCs.

2) *FZD7* is also significantly up-regulated in chronic phase patients, correlating with the elevated transcription of the Wnt ligands.

3) This apparent up-regulation in the Wnt/β-catenin pathway could be being modulated by NKD1 which acts as a negative regulator of the pathway. Significantly higher levels of *NKD1* were also found in chronic phase compared to blast crisis which could suggest a feedback mechanism of the pathway of intrinsic regulation when the pathway is activated. To determine if this is occurring, protein levels would need to be investigated to see if they correlate with what is seen in mRNA levels.

4) *APC* showed a significant increase in blast crisis compared to chronic phase. Ordinarily, it functions as part of the destruction complex to degrade β-catenin,

however mutations of *APC* have been implicated specifically in colon cancer to correlate with poor prognosis [220, 221]. To determine if this is occurring in CML, mutational analysis of *APC* would need to be carried out to determine its functionality in the disease. Interestingly, *FZD7* has also been reported to down-regulate APC function whilst enhancing β-catenin mediated signals [224]. This could be a reason why *APC* is low in the chronic phase patients when *FZD7* is significantly higher, and vice versa in blast crisis patients.

5) All four transcription factors show a significant difference between individual patient cohorts and *TCF1, TCF4* and *LEF1* have significantly higher expression levels in blast crisis compared to chronic phase. These results suggest their role as transcriptional activators within CML which correlates with blast crisis. *TCF3* is known to function mainly as a repressor of transcriptional activation [180] which could be why it is not significantly up-regulated in blast crisis similar to the other transcription factors.

6) Patients with high CIP2A protein levels have significantly increased mRNA levels of *TCF4* and *LEF1* which correlates with an increase in the target genes *CYCLIN D1* and *C-MYC*. This could suggest an alternative method of transcriptional activation through up-regulation of *TCF4* and *LEF1* either directly or indirectly through CIP2A. The mechanism by which this occurs needs investigating.

Chapter 7 – General Discussion and Future Work

The aim of this thesis was to obtain a better understanding of the effects and/or contribution of the Wnt/β-catenin signalling pathway in the development and progression of CML. Certain aspects of the pathway were prioritised following a review of the literature. The main objectives decided were to;

1) Determine if the levels of β-catenin and its phosphorylated forms in MNCs are predictive of clinical outcome in imatinib treated patients or differ in relation to patient treatment response groups.

2) Determine if BCR-ABL1 mediated β-catenin phosphorylation on Tyr654 correlates with disease progression.

3) Investigate phospho-GSK3β Ser9 and phospho-GSK3β Tyr216 to determine if GSK3β's activity differs in relation to patient outcome.

4) Examine what regulates GSK3β's activity in CML.

5) Determine if GSK3β activity correlates with C-MYC degradation.

6) Screen the Wnt/β-catenin pathway and analyse any of the genes which appear to be different between the response groups in a larger patient cohort.

7) Investigate the transcription factors involved in the Wnt/β-catenin pathway to see if they are differentially expressed in the various patient cohorts.

7.1 Levels of β-catenin do not correlate with patient outcome

Analysis of β-catenin was initially performed as it has previously been implicated in CML disease progression, with unphosphorylated levels having been reported to be up regulated in GMPs of blast crisis patients [150]. Investigation into whether this finding is also true in MNCs, and whether the phosphorylation status of β-catenin correlates with patient outcome, was undertaken to gain a better understanding of the role of β-catenin in CML.

After initial detection of elevated protein levels of β-catenin in primary CML MNCs at diagnosis, the question of whether β-catenin mRNA and/or total protein levels can be used to distinguish between the different patient cohorts and/or be used to differentiate between disease stages was addressed. Results from both mRNA expression and total protein levels, show that these levels cannot be used to distinguish between different patient response cohorts and do not differentiate between stages of disease progression using MNCs. It was considered that β-catenin (*CTNNB1*) mRNA levels may be important in response to treatment as levels reduced after 12 months imatinib treatment towards levels found in healthy donors due to the leukaemic cells being replaced with normal cells. . This was also shown in patients treated with the second generation TKIs (dasatinib and nilotinib), with a significant reduction in β-catenin mRNA levels seen in the optimal responders after 12 months treatment (P=0.05 and 0.001 respectively), suggesting that patients who respond well to treatment, irrespective of the drug they receive, have a significant reduction in β-catenin mRNA levels after 12 months treatment. Results for total β-catenin protein have not previously

been found to correlate with disease progression in CML, and considering the activity of β-catenin is regulated by its phosphorylation status this would explain why total levels are not providing insight into the role of β-catenin in CML.

To determine whether the activity and degradation of β-catenin differs in relation to patient outcome in MNCs, the phosphorylation status of β-catenin was investigated in the different patient cohorts. The levels of unphosphorylated β-catenin, used to represent the active form of β-catenin, and phospho-β-catenin (Ser45/Thr41), used to represent the form of β-catenin targeted for degradation, were measured. Analysis of unphosphorylated β-catenin showed no difference when investigating the various patient cohorts. When comparing chronic phase to blast crisis, levels were higher in blast crisis, correlating with what was seen in GMPs [150], however this difference was not statistically significant. Additionally, levels of phospho-β-catenin (Ser45/Thr41) were analysed, similarly results showed no variation between patient cohorts, however, levels decrease when patients have transformed into blast crisis compared to chronic phase. This correlates with the increase in unphosphorylated β-catenin shown. However, since neither of these trends reach a statistical significance, this suggests while β-catenin is important in achieving the full leukaemic potential of primitive leukaemic cells, as the cells progress to become more differentiated they are less dependent on β-catenin signalling for their survival, a finding that was also recently noted by Heidel *et al.*, [185]. This could explain why the results found for GMPs by Jamieson *et al.*,[150] were not reproducible in MNCs.

Subsequent analysis by nuclear and cytoplasmic extraction to investigate subcellular localisation of the various forms of β-catenin showed that phospho-β-catenin (Ser45/Thr41) is not solely found in the cytoplasm but it is also detected in the nucleus. Maher *et al.,* [149] also found this to be the case whereby β-catenin phosphorylated on Ser45/Thr41 can localise in the nucleus, unlike β-catenin phosphorylated on Ser33/37/Thr41. This suggests that phosphorylation of β-catenin by CK1 may have a dual effect on the activity and localisation of β-catenin, not only priming it for phosphorylation by GSK3β and subsequent degradation by the proteasome, but also by targeting it for nuclear import [149]. An additional question that this finding asks is that, if β-catenin phosphorylation on Ser45 by CK1 and Thr41 by GSK3β is occurring, what is preventing the phosphorylation on Ser37/33 by GSK3β that allows β-catenin to remain in the cytoplasm and degradation to occur instead of translocating to the nucleus? This rendered the use of phospho-β-catenin (Ser45/Thr41) unsuitable to assess β-catenin degradation and hence the Ser33/37/Thr41 phosphorylated form of β-catenin should be used as a marker of cytoplasmic β-catenin, and consequently, the form targeted for degradation.

Phospho-β-catenin (Ser33/37/Thr41) was therefore added to confocal microscopy analysis. From this evaluation a relationship was identified between the various forms of β-catenin in individual patients. This was shown by higher levels of unphosphorylated β-catenin correlating with low levels of phospho-β-catenin (both Ser45/Thr41 and Ser33/37/Thr41). Conversely, when levels of phospho-β-catenin (again, both Ser45/Thr41 and Ser33/37/Thr41) were elevated, the levels of unphosphorylated β-catenin were low. This shows that regulation of β-catenin by its

phosphorylation status is still functioning in CML MNCs, but β-catenin levels in MNCs cannot be used to distinguish between patient cohorts.

Due to results not showing a difference in the various forms of β-catenin between patient cohorts, CML cell lines were treated with bortezomib, WNT3A and WIF1 to address the question of what is happening to β-catenin in CML. Bortezomib (a proteasome inhibitor) increased the levels of total and unphosphorylated β-catenin, while decreasing phospho-β-catenin (Ser33/37/Thr41). This suggests that in the CML cell lines, β-catenin is being actively degraded by the cell and this could be why no difference is being detected in the levels of β-catenin. Meanwhile, results seen with WIF1 (Wnt pathway inhibitor) and Wnt3A (Wnt pathway activator) did not show the expected trend on β-catenin levels, suggesting that the Wnt pathway is not actively enhanced in CML MNCs. To substantiate this finding, the effects of bortezomib, Wnt3A, and WIF1 should be tested in patient samples to see if the results from cell lines are replicable. This would give a better understanding of what is happening to β-catenin in patient MNCs. However, as results were suggesting that β-catenin is not effective in differentiating between patient groups, it was decided to investigate whether any other aspects of the Wnt/β-catenin pathway are important in distinguishing between the response cohorts.

7.2 Levels of BCR-ABL1 mediated phosphorylation of β-catenin are significantly higher in chronic phase compared to blast crisis

BCR-ABL1 is known to be able to phosphorylate β-catenin directly on Tyr86 and Tyr654 to prevent the association of β-catenin with the destruction complex and target it to the nucleus to activate transcription [186], therefore in CML this could have a role in disease progression. Coluccia *et al*., [186] found that there was a correlation between BCR-ABL1 expression and nuclear localisation of tyrosine phosphorylated β-catenin in blast crisis patients. In this analysis, it was decided to investigate the Tyr654 phosphorylation of β-catenin as it is known to associate with the basal transcription factor TATA-binding protein to enhance transcription [235]. Analysis of this form of β-catenin showed no difference in the levels of Tyr654 phosphorylation between the patient cohorts at diagnosis. This is consistent with the view that BCR-ABL1 activity is similar in all patients at initial diagnosis as it will not yet have, in most cases, developed mutations or altered activity as a consequence of exposure to imatinib [190]. Levels showed a decrease after 12 months of imatinib treatment, which is anticipated as the BCR-ABL1 driven phosphorylation of β-catenin would be removed as leukaemic cells are replaced with normal cells. When comparing chronic phase to blast crisis there was a significant decrease in Tyr654 phosphorylation in patients in blast crisis (p=0.012). This could be representative of CML becoming BCR-ABL1 independent at disease transformation [191, 236]. Additionally, a further explanation for this could be that the evolution of kinase domain mutations in BCR-ABL1 at disease progression [60] could alter its ability to phosphorylate β-catenin on Tyr654. To examine if this is the case, patients with specific BCR-ABL1 mutations would need to be investigated for their levels of phospho-β-catenin (Tyr654), a line of investigation limited by the availability

of patient material. Alternatively, the various mutated forms of BCR-ABL1 could be transfected into an originally BCR-ABL1 negative cell line and its influence on the levels of phospho-β-catenin (Tyr654) measured. When analysing the localisation of phospho-β-catenin (Tyr654) in cell lines, levels were elevated in the nucleus compared to the cytoplasm, confirming the localisation of phospho-β-catenin (Tyr654) as found by Coluccia *et al.*, [186].

7.3 GSK3β's activity is significantly reduced in blast crisis by both increased phospho-GSK3β Ser9 and decreased phospho-GSK3β Tyr216

Abrahamsson *et al.*, [101] demonstrated a decrease in GSK3β protein expression as patients progress through the disease, however GSK3β protein overall does not reveal the kinase activity of GSK3β due to its regulation by its phosphorylation status. Consequently, it was of interest to examine phospho-GSK3β Ser9, which inhibits GSK3β, and phospho-GSK3β Tyr216, which enhances GSK3β activity [152, 155, 156], to determine if the activity of GSK3β differs in relation to patient outcome. Results showed there was a significant decrease in GSK3β activity in those patients who have transformed into blast crisis, which was demonstrated by opposing trends in Ser9 and Tyr216 phosphorylation. Elevated levels of phospho-GSK3β Ser9 were found in those patients who had transformed into blast crisis compared to those in chronic phase (P=0.026), which correlated to reduced levels of phospho-GSK3β Tyr216 in the patients who have transformed into blast crisis compared to the chronic phase patients (P<0.001). In addition significantly higher MCL-1 protein levels were found in patients in blast crisis (P<0.001 for both long and short forms), possibly due to the activity of

GSK3β being impaired in blast crisis and therefore it cannot act to phosphorylate and degrade MCL-1. The results, however, were not reflected in the levels of β-catenin as previously discussed **(section 7.1)**. A decrease in GSK3β activity would be predicted to increase unphosphorylated β-catenin, although as the Wnt/β-catenin pathway is not the only signalling pathway affecting GSK3β this may explain why no significant difference was seen in the levels of β-catenin between chronic phase and blast crisis. CML cell line material was incubated with the GSK3β inhibitor SB216763 and results confirmed that GSK3β is acting to degrade β-catenin in CML, with unphosphorylated (active) β-catenin increasing with inhibition by SB216763, while phospho-β-catenin (Ser33/37/Thr41) decreased with inhibition. This substantiates the question of whether the Wnt/β-catenin pathway is regulating the activity of GSK3β in CML, or whether it is functioning independently of β-catenin, a theory also stipulated by Reddiconto *et al*., [164]. Alternatively, the results could reflect that, while GSK3β is integral in the phosphorylation-dependent degradation of β-catenin, it is not the component of the destruction complex which is controlling the level at which β-catenin is degraded as it has been suggested that a decrease in GSK3β may be compensated by a replacement with GSK3α [152]. It is also considered that AXIN acts as a limiting factor in Wnt/β-catenin signalling due to lower quantities of the molecule being present in the cells compared to the other components of the degradation complex. This consequently means it could be a key factor in regulating the stability of β-catenin in the cell [88]. It is therefore of interest to determine what is impacting the activity of GSK3β, due to the significant change seen in disease progression, and whether this decrease in activity is in turn affecting other substrates which are central in CML development.

When investigating mRNA levels of *GSK3β*, results showed increased levels in patients who subsequently transformed into blast crisis, and patients in blast crisis, compared to optimal responders and failure patients at diagnosis. The decrease in GSK3β activity shown via protein levels could be a reason why message levels are elevated in those patients in blast crisis as a mechanism to compensate for the decrease in GSK3β activity.

7.4 PP2A acts as a regulator of GSK3β

As the activity of GSK3β was shown to correlate with patient outcome, it was of importance to determine what was regulating this activity. Initially three TKIs (imatinib, dasatinib and nilotinib) were tested *in vitro* to determine if GSK3β activity was under the control of BCR-ABL1. Reddiconto *et al.,* [164] showed that *in vitro* treatment with imatinib in CML chronic phase patients increased the levels of Tyr216 phosphorylation of GSK3β while dasatinib reduced it. The effects on Ser9 phosphorylation were not tested. My results showed there was no difference in the two forms of phospho-GSK3β on treatment with the TKIs. The results for Tyr216 phosphorylation may be contradictory due to the difference in material used to examine the effects of TKIs on GSK3β levels.

Next, the Wnt/β-catenin pathway was tested *in vitro* to see if it played a part in the regulation of GSK3β activity using Wnt3A as a pathway activator and WIF-1 as a pathway inhibitor. Results showed Wnt3A decreased Tyr216 phosphorylation of GSK3β, revealing that activation of the Wnt/β-catenin pathway causes inhibition of GSK3β. Results from WIF1 treatment showed no impact of GSK3β activity which implies the Wnt/β-catenin pathway may be maximally inhibited in cells. This correlates with the

results obtained from bortezomib incubation showing that β-catenin is being degraded by the cell. To determine if this is also the case between patient cohorts, samples from the different outcomes could be incubated with WIF1 and Wnt3A to determine if regulation of the Wnt/β-catenin pathway affects both GSK3β and β-catenin levels. If the Wnt/β-catenin pathway is inhibited in MNCs through all stages of the disease, this may be why a difference is not seen in the levels of β-catenin between cohorts.

Finally, the effects of PP2A activation and inhibition on the activity of GSK3β were investigated by incubation with FTY720 (a PP2A activator) and okadaic acid (a PP2A inhibitor). PP2A is a serine/threonine phosphatase which acts as part of the destruction complex in the Wnt pathway and is known to de-phosphorylate GSK3β on Ser9 [170]. Activation of PP2A via FTY720 reduces levels of phospho-GSK3β Ser9, while inhibition of PP2A via okadaic acid increases levels of phospho-GSK3β Ser9. These results show that PP2A can regulate the activity of GSK3β in CML via controlling its inhibition. Additionally, Lucas *et al*., [176] showed that PP2A has high importance in CML in correspondence with CIP2A [176], therefore the relationship between GSK3β and PP2A was examined further.

GSK3β is also known to influence PP2A indirectly through its phosphorylation status [202, 203]. To examine whether this is occurring in CML, GSK3β was inhibited by both SB216763 and siRNA and the effects on the PP2A pathway were measured. Results from the two forms of inhibition had contradictory outcomes. This is due to SB216763 and siRNA having opposite effects on Ser9 phosphorylation of GSK3β. Inhibition with SB216763 causes an increase in Ser9 phosphorylation which explains the decrease in Tyr307 phospho-PP2A levels observed via PTP1B, as inhibition of GSK3β increases

PTP1B and enables dephosphorylation of PP2A on Tyr307 to occur. In contrast, knockdown of GSK3β by siRNA reduced the levels of Ser9 phosphorylation on GSK3β which resulted in an increase in Tyr307 phosphorylation of PP2A shown, as GSK3β is unable to increase levels of PTP1B, preventing the dephosphorylation of PP2A at Tyr307. This difference in the effects of GSK3β inhibition by different methods suggests careful consideration if using GSK3β as a therapeutic target as considered by Reddiconto *et al.*, [164]. The results for CIP2A, SET and BCR-ABL1 activity (p-CrKL/CrKL ratio) are opposite to what would be predicted for the levels of PP2A shown, implying that although GSK3β can act to regulate PP2A, this effect does not translate to the inhibitors of PP2A. Additionally, although active PP2A has been reported to decrease BCR-ABL1 activity through the tyrosine phosphatase SHP-1 [173, 175], PP2A may not be acting to down-regulate BCR-ABL1 activity in CML.

Investigation into the levels of the PP2A pathway in primary CML MNCs showed that there was a trend for both phospho-PP2A (Tyr307) and the PP2A inhibitor SET to have higher levels in blast crisis compared to chronic phase, consistent with GSK3β activity being reduced in blast crisis. Elevation of SET (which correlates with a rise in inactive PP2A) suggests that PP2A is unable to dephosphorylate GSK3β on Ser9 in blast crisis, resulting in a decrease in GSK3β activity as observed. In relation to the alternative PP2A inhibitor CIP2A, patients who had high levels of CIP2A had a reduction in both forms of GSK3β. However, manipulation of CIP2A by both siRNA and transient transfection produced contradicting results to what was seen in patients. In K562 cells decreasing levels of CIP2A results in a decrease in phospho-GSK3β (Ser9), whereas increasing CIP2A levels increases phospho-GSK3β (Ser9). This correlates with the hypothesis of

PP2A regulating GSK3β activity by showing that increased levels of CIP2A result in an increase in GSK3β. This suggests that CIP2A is inhibiting PP2A, preventing its ability to de-phosphorylate GSK3β on Ser9. GSK3β may in turn feedback on itself to increase its activity by autophosphorylation of Tyr216. However, neither siRNA knockdown, nor transfectional upregulation of CIP2A showed a considerable effect on the levels of GSK3β, indicating that the inhibitory effect that CIP2A has on PP2A is not being translated to the levels of GSK3β.

It is known that CIP2A is able to regulate E2F1 [205], which in turn is known to correlate, alongside C-MYC, with increased levels of unphosphorylated β-catenin [206]. Therefore it was of interest to determine whether β-catenin correlates with CIP2A. Results from matched patient samples showed that there is an increase in unphosphorylated β-catenin in patients with high CIP2A levels. However whether this is directly due to CIP2A was questionable therefore transient transfection was used to increase CIP2A levels and investigate β-catenin levels. Results showed that increased CIP2A generated an increase in unphosphorylated β-catenin, which correlated with a decrease in phospho-β-catenin (Ser33/37/Thr41) to be targeted for degradation. This shows that CIP2A increases active β-catenin, enabling it to activate transcription of its target genes, at the same time as reducing β-catenin's degradation. This implies that CIP2A can regulate the levels of β-catenin but as results do not show a significant difference, it is not a vital component involved in its control. Unfortunately due to the transfection also increasing E2F1 levels, no conclusion can be made as to whether CIP2A is having a direct effect on β-catenin or whether it is acting indirectly through

E2F1. However, as CIP2A does not have a significant effect on β-catenin levels it was not deemed important to continue this line of investigation.

7.5 GSK3β is not the rate-limiting step of C-MYC degradation

GSK3β has a multitude of targets including C-MYC [152], a known oncogene which has been shown to be important in CML development [198]. Phosphorylation of C-MYC by GSK3β is relevant to C-MYC degradation. The protein kinase ERK initiates the sequence of events by the phosphorylation of C-MYC on Ser62. This activates C-MYC and if GSK3β is available this phosphorylation by ERK acts as a priming phosphorylation to allow C-MYC phosphorylation on Thr58. Once phosphorylated on Thr58, PP2A removes the Ser62 phosphorylation, allowing addition of an ubiquitin tag to C-MYC promoting its degradation by the proteasome **(Chapter 4, Figure 4.4.13)** [237]. Results showed that the activity of GSK3β is significantly reduced in blast crisis patients; therefore it was of interest to see whether this impacts on the degradation of C-MYC. In patient samples, levels of phospho- C-MYC (Thr58) did not change when comparing chronic phase to blast crisis, while levels of total C-MYC were significantly higher in blast crisis (P=0.024). In addition to this, inhibition of GSK3β by both SB216763 and siRNA reduced the levels of Thr58 phosphorylation but had no effect on total levels of C-MYC, corroborating with the results in patients, that GSK3β is not the rate limiting component in C-MYC degradation. Another stage at which C-MYC degradation could be regulated is by the removal of the Ser62 phosphorylation by PP2A. Total PP2A levels were significantly higher in blast crisis compared to chronic phase (P=0.013), with no significant rise in the levels of inactive PP2A. This contradicts what would be expected

as increased levels of active PP2A would correlate to increased removal of Ser62 phosphorylation, allowing C-MYC to be degraded in blast crisis. Instead there is a significantly higher level of total C-MYC seen in blast crisis compared to chronic phase. This suggests that neither GSK3β nor PP2A are controlling the rate of C-MYC degradation. While this study was being undertaken it was reported that FBXW7, an E3 ubiquitin ligase responsible for the ubiquitination of C-MYC, is an alternative mechanism by which C-MYC degradation can be regulated. FBXW7 has been shown to function by controlling the stability of C-MYC in haemopoietic stem cells. This was demonstrated by deletion of the FBXW7 gene causing elevated levels of C-MYC protein expression [198, 200, 201]. This, alongside the results showing that GSK3β and PP2A are not regulating C-MYC degradation, suggests that the ubiquitination of C-MYC by FBXW7 is a possible controlling factor of C-MYC degradation.

To develop this line of enquiry further the levels of FBXW7 would need to be investigated in the patient samples to determine if there was a difference between blast crisis and chronic phase which correlates to the difference in C-MYC levels. Additionally, it has been reported in T-cell ALLthat mutations have been found in FBXW7 which affect the ubiquitination and the half-life of C-MYC [238]. Consequently, mutational analysis of FBXW7 in CML patients could be carried out to determine if there is a difference between the patient responses.

7.6 Gene analysis of *WNT1, WNT8A, WNT9A, FZD7, NKD1* and *APC* showed significant differences between patient cohorts

The overall PCR screening of the Wnt/β-catenin pathway had limitations which prevented definitive conclusions being made. However, it did lead to the selection of a few genes to be investigated in a larger patient cohort. These were; *WNT1, WNT8A, WNT9A, FZD7*, and *NKD1*. In addition, *APC* was also examined due to it being implicated in other malignancies [220, 221]. Results show that the three *WNT* ligands, along with *FZD7* had significantly higher levels of mRNA expression in chronic phase compared to blast crisis (P=0.011, 0.045, 0.037 and 0.037 respectively), indicating an up-regulation of Wnt pathway activity in patients in chronic phase. This finding, however, is not consistent with elevated levels of β-catenin indicating that although there may be an elevation at the start of the pathway this is not transferred downstream to β-catenin. A reason for this could be that along with the *WNT* ligands and *FZD7, NKD1* is also significantly elevated in chronic phase (P=0.013). NKD1 acts as a negative regulator of the pathway and therefore could imply that there is a feedback mechanism of the pathway of intrinsic regulation when the pathway is activated [226]. This could be why this increase in pathway activity is not reflected in elevated levels of β-catenin. To determine if this is occurring, protein levels would need to be investigated to see if they correlate with what is seen in mRNA levels.

Figure 7.1 Potential mechanism to prevent an increase in unphosphorylated β-catenin in Chronic phase CML MNCs
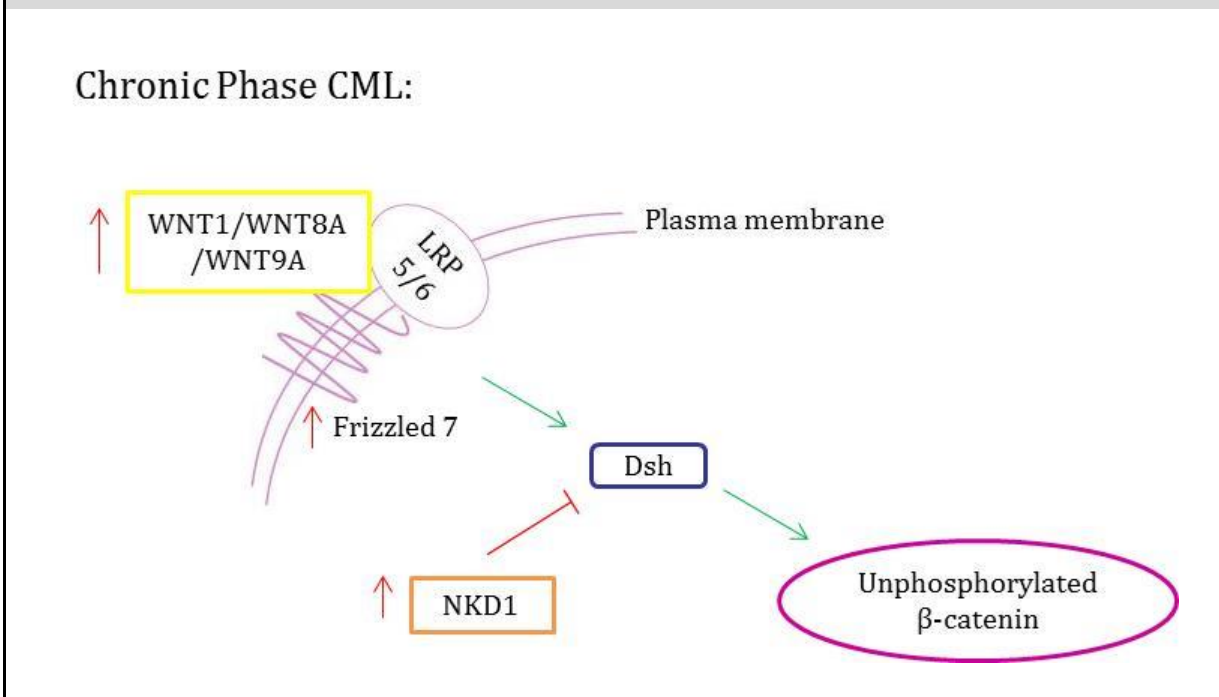
When examining *APC* mRNA, levels were significantly higher in blast crisis compared to chronic phase (P=0.026). APC is part of the destruction complex which acts to degrade β-catenin. Jamieson *et al.*, [150] previously showed that β-catenin is up-regulated in GMPs of blast crisis; however my analysis of MNCs showed that there was no significant difference between patient cohorts (optimal vs. failure vs. blast crisis, and chronic phase vs. blast crisis). This could be due to other aspects of the Wnt pathway, such as APC, being more active in differentiated cells than in earlier compartments, and down-regulating the Wnt pathway signal before it reaches β-catenin. An alternative explanation as to why *APC* is low in chronic phase and high in blast crisis could be due to FZD7. FZD7 has been reported to down regulate APC function [224] and the results for *FZD7* show the opposite trend to *APC* indicating that this could be occurring in CML cells. Mutations of *APC* have been implicated in other malignancies, the most common of

which is in colon cancer where they correlate with poor prognosis [220, 221]. To determine if this is also occurring in CML, mutational analysis of *APC* needs to be carried out to determine its functionality in the disease.

7.7 The transcription factors *TCF1, TCF4*, and *LEF1* are all significantly higher in blast crisis patients compared to chronic phase

The final stage at which regulation of the Wnt/β-catenin pathway can occur is via the transcription factors. They act as a binding site for both β-catenin and the promoter DNA of target genes to allow activation of transcription, and without them, β-catenin is unable to bind to DNA and transcription cannot occur [122, 123, 178]. Levels of mRNA were measured according to patient outcome, and comparing chronic phase to blast crisis. All four transcription factors show a significant difference between individual patient cohorts. *TCF1, TCF4* and *LEF1* have significantly higher levels of expression in blast crisis compared to chronic phase (P=0.001, 0.016, and 0.003 respectively). *TCF3* also has elevated levels but this is not statistically significant. These results suggest their role as transcriptional activators within CML which correlates with poor prognosis. TCF3 is known to function mainly as a repressor of transcriptional activation [180] which could be why it is not significantly up-regulated in blast crisis similar to the other transcription factors. In addition, as an upregulation of the Wnt/β-catenin pathway activity was not seen in blast crisis patients, this suggests that the reports of the transcription factors acting independently of the Wnt/β-catenin pathway in other haematological malignancies [178, 239, 240] may also be true for CML. It has been reported in haematological malignancies that the ATF2 transcription factors can

interact with TCF/LEF, resulting in enhanced transcription of target genes [178]. To investigate whether this is occurring in CML, the relationship between the ATF2 and TCF/LEF transcription factors would need to be studied further, potentially through manipulation of the ATF2 transcription factors by siRNA and transient transfection and measuring the effect on target genes, to determine if they are regulating the activity Wnt/β-catenin transcription factors.

Regulation of the TCF/LEF transcription factors not only occurs through their expression levels, but also through post-translational modifications which impact their activity status. These include phosphorylation, sumoylation, ubiquitination and acetylation, all of which can regulate the association of the transcription factors with co-activators, repressors or DNA [87, 95, 179, 180]. With this knowledge, to further progress this work it would be of interest to not only investigate whether this difference in mRNA levels translates also to protein levels, but also whether post-translational modifications are playing a role in the regulation of the transcription factors and whether there is a difference between the patient cohorts. Finally, the levels of the co-activators and co-repressors which act on the transcription factors should be analysed to see which, if any, correlate with disease progression.

From observations that there is an up-regulation in the transcription factors in blast crisis which does not correlate with other aspects of the Wnt/β-catenin pathway, alongside the fact that it has been established that the transcription factors TCF1 and LEF1 can also function independently of the Wnt signalling pathway[178], instigated

the investigation as to whether there is a relationship between the transcription factors and either GSK3β or CIP2A. Results showed that there are significantly higher levels of *TCF4* and *LEF1* in patients who have high CIP2A protein levels which correlated with an elevation in the levels of target genes *CYCLIN D1* and *C-MYC*. This could suggest an alternative method of transcriptional activation through up-regulation of *TCF4* and *LEF1* either directly or indirectly through CIP2A. CIP2A has not previously been linked with the Wnt/β-catenin transcription factors; however, a potential mechanism by which CIP2A could be regulating the TCF/LEF transcription factors may be through CYCLIN D1. It has been reported in ovarian cancer that a decrease in CIP2A correlated with a decrease in CYCLIN D1 levels [241]. This, alongside the increase in *CYCLIN D1* found in those CML patients with high CIP2A protein levels, suggests that CIP2A may be involved in regulating CYCLIN D1. Additionally both CIP2A [205] and CYCLIN D1 [242] are modulated by E2F1 further facilitating the mechanism by which CIP2A and CYCLIN D1 could interact. It has been detailed that CYCLIN D1 can act to regulate the activity of various transcription factors as well as transcriptional co-activators and co-repressors [243, 244], although the TCF/LEF transcription factors have not been specified. This could imply that CIP2A is regulating CYCLIN D1 levels, which is then adjusting the activity of the TCF/LEF transcription factors. To test whether this hypothesis is accurate, the first aspect which would need to be established is whether CYCLIN D1 is acting to regulate the TCF/LEF transcription factors. This could be done using an inhibitor of CYCLIN D1 to see its effects on the TCF/LEF levels. If this was confirmed, the levels of CIP2A could then be manipulated by siRNA and transient transfection to see the effects on CYCLIN D1 and the transcription factors.

7.8 Overall Conclusion

In conclusion, although β-catenin was previously shown in GMPs to be implicated in blast crisis, it is shown here to be less important in MNCs and therefore cannot be used to distinguish between patient response cohorts, or as a factor of disease progression. The BCR-ABL1 dependent Tyr654 phosphorylation of β-catenin is significantly decreased in blast crisis MNCs, potentially enhancing the theory that the disease can become BCR-ABL1 independent. GSK3β activity is significantly down-regulated in blast crisis, and appears to be being regulated through PP2A. Inhibition of GSK3β also affects the levels of PP2A, however, the mechanism of how GSK3β can be inhibited changes its effects on PP2A and its inhibitory Tyr307 phosphorylation. Neither GSK3β nor PP2A are the controlling factors of c-Myc degradation in CML. Additionally, up regulation of the Wnt pathway in chronic phase represented by the *WNT* ligands and *FZD7* does not translate through to β-catenin, possibly due to internal regulation of the pathway by *NKD1*. However, this needs to be tested in protein levels. Finally, the mRNA levels of the transcription factors are significantly overexpressed in blast crisis, but may be functioning independently from the Wnt/β-catenin pathway.

7.9 Future work

The main aspects of this work which would need further investigation, provided there were no limitations on patient material and time available, are the following;

1) Examine the effects of bortezomib and SB216763 on the levels of β-catenin, along with WNT3A and WIF1 on the levels of both β-catenin and GSK3β, in patient samples to distinguish if there is a difference in pathway inhibition between patient response cohorts.

2) Investigate whether inhibition of GSK3β by SB216367 also decreases the inhibited form of PP2A (Tyr307) in patient samples, as found in K562 cells, as this would enhance the use of the GSK3β inhibitor as a therapeutic drug, previously investigated by Reddiconto et al., [164] due to the implications of PP2A levels and disease progression [175, 176].

3) Determine whether the E3 ligase FBXW7 is controlling the rate of C-MYC degradation in CML by investigating the levels in patient samples to reveal if there is a difference between blast crisis and chronic phase which correlates with C-MYC levels. Additionally, carry out mutational analysis of FBXW7 in CML patients to determine if there is a difference between the patient responses which correlates with C-MYC levels.

4) Measure the protein levels of the WNT ligands, FZD7, and NKD1 to determine if the significant difference found in mRNA levels which implies a potential negative feedback mechanism in response to an elevation in pathway activity in chronic phase transcends to protein levels.

5) Undertake mutational analysis of *APC* to investigate whether the significant increase in *APC* mRNA levels found in blast crisis which correlates with poor prognosis is due to mutations which affect its function as a tumour suppressor.

6) Measure the protein levels of the Wnt/β-catenin transcription factors to ascertain whether there is still an upregulation of these factors in blast crisis. If this is the case, also investigate the ATF2 transcription factors and other co-activators and co-repressors which regulate the activity of the TCF/LEF transcription factors, alongside post translational modifications, to see if they correlate with their activity.

7) Determine whether CYCLIN D1 is acting as the link between CIP2A and the TCF/LEF transcription factors by using an inhibitor of CYCLIN D1 to see if it is involved in the regulation of TCF/LEF. Then, if this was confirmed, manipulate the levels of CIP2A by siRNA and transient transfection to see the effects on CYCLIN D1 and the transcription factors.

Chapter 8 - Appendix

Figure 8.1 Subcellular localisation of unphosphorylated β-catenin
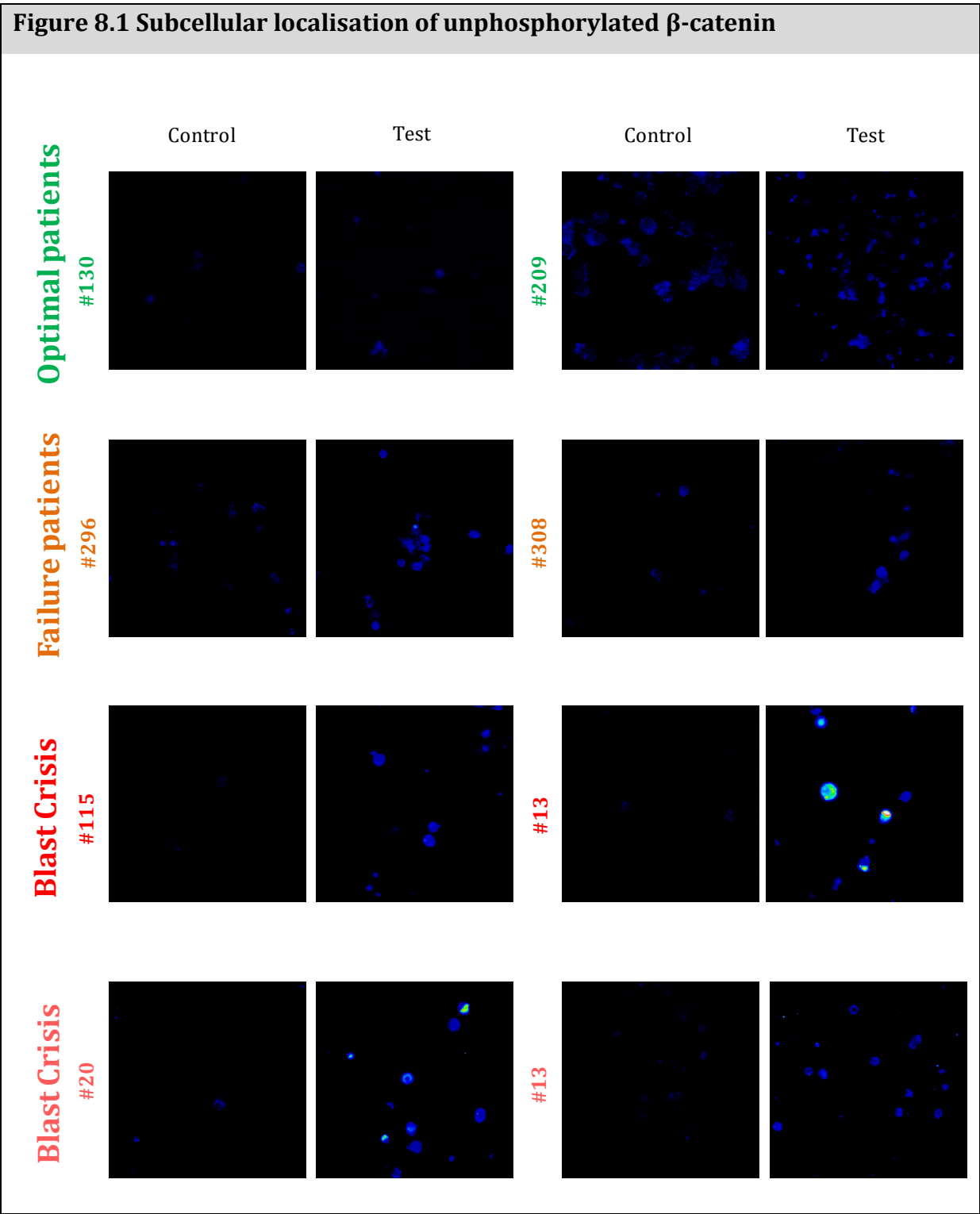
Figure 8.2 Subcellular localisation of phospho-β-catenin(Ser45/Thr41)
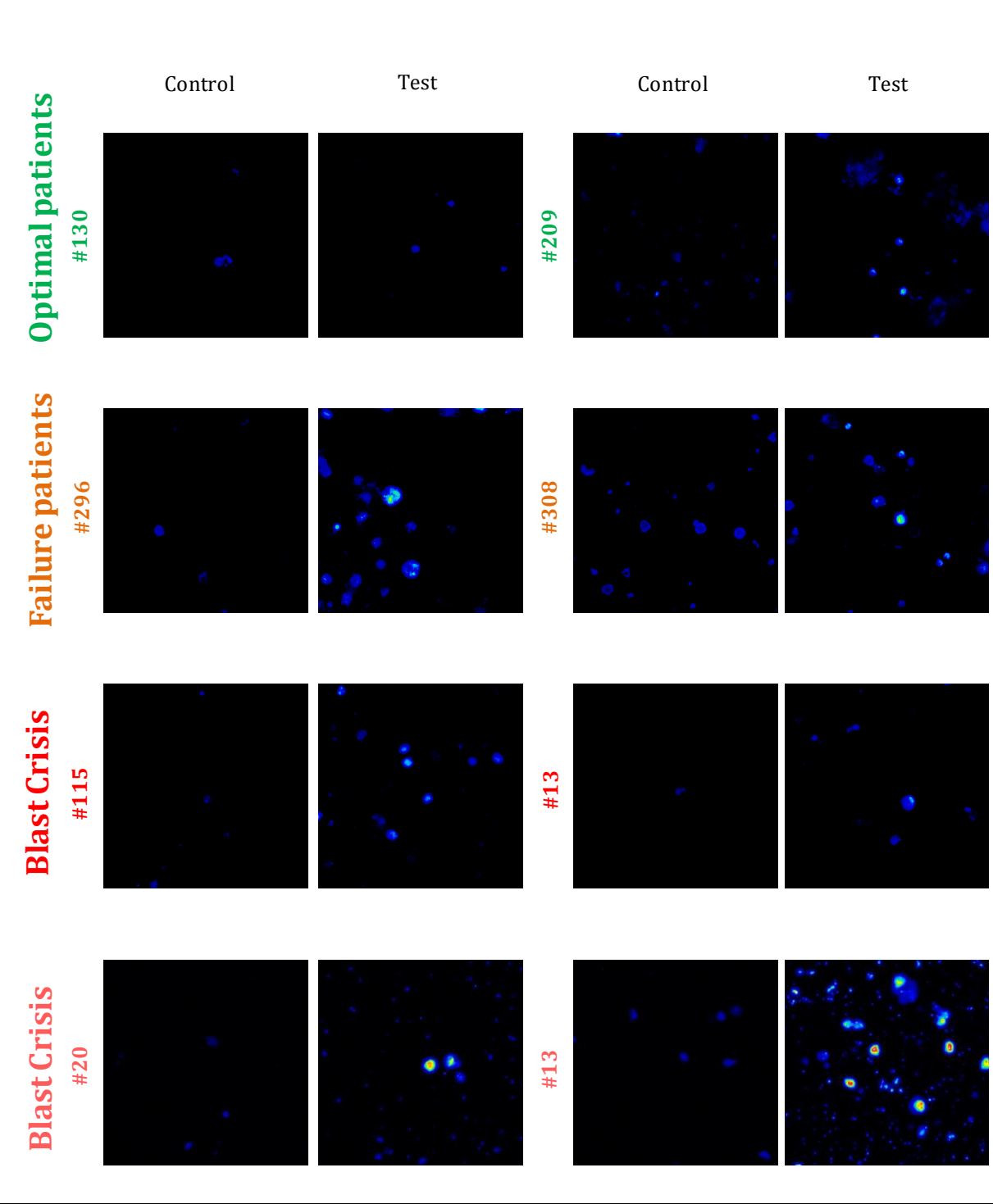
Figure 8.3 Subcellular localisation of phospho-β-catenin(Ser33/37/Thr41)
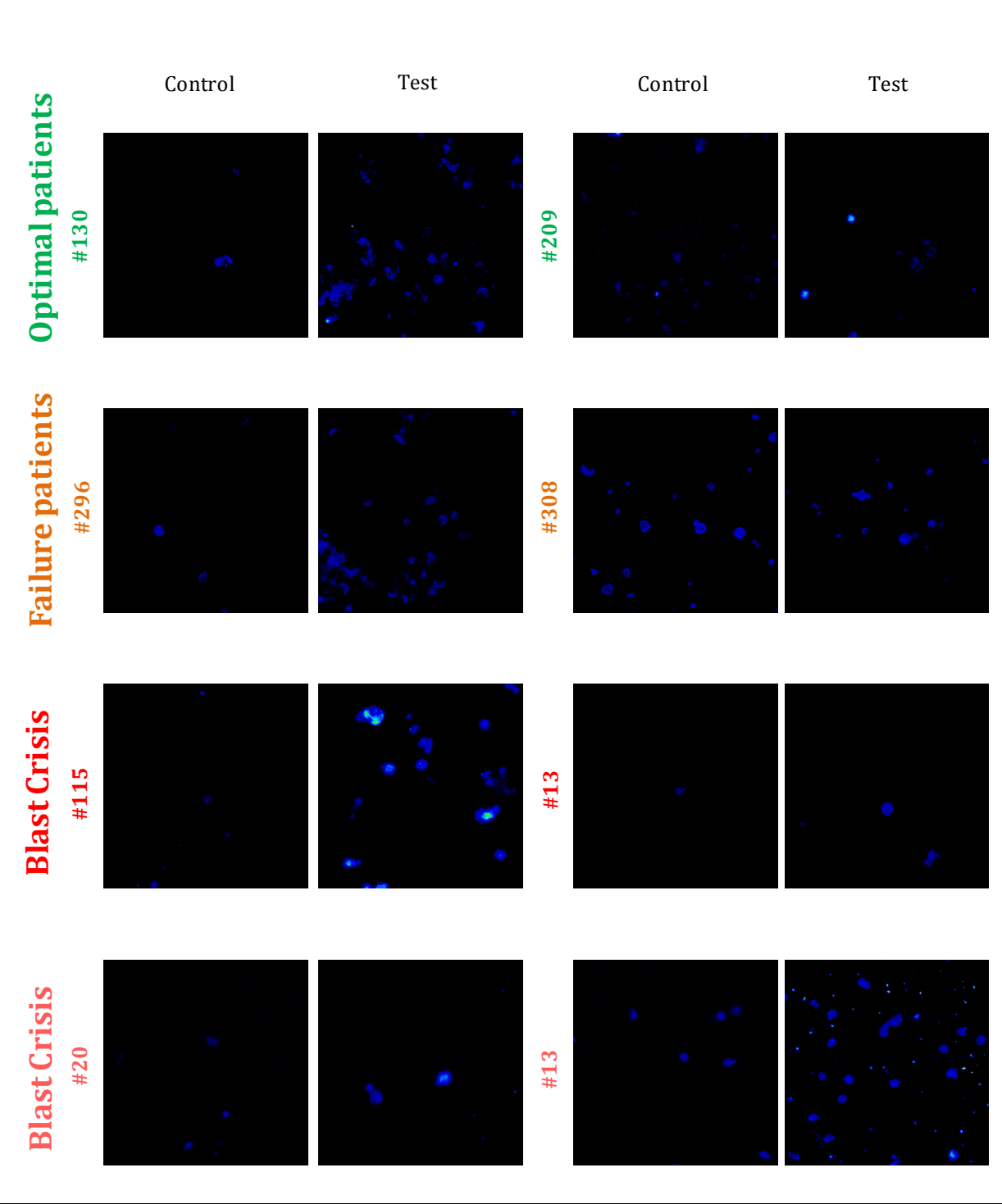
Figure 8.4 Subcellular localisation of phospho-β-catenin(Tyr654)
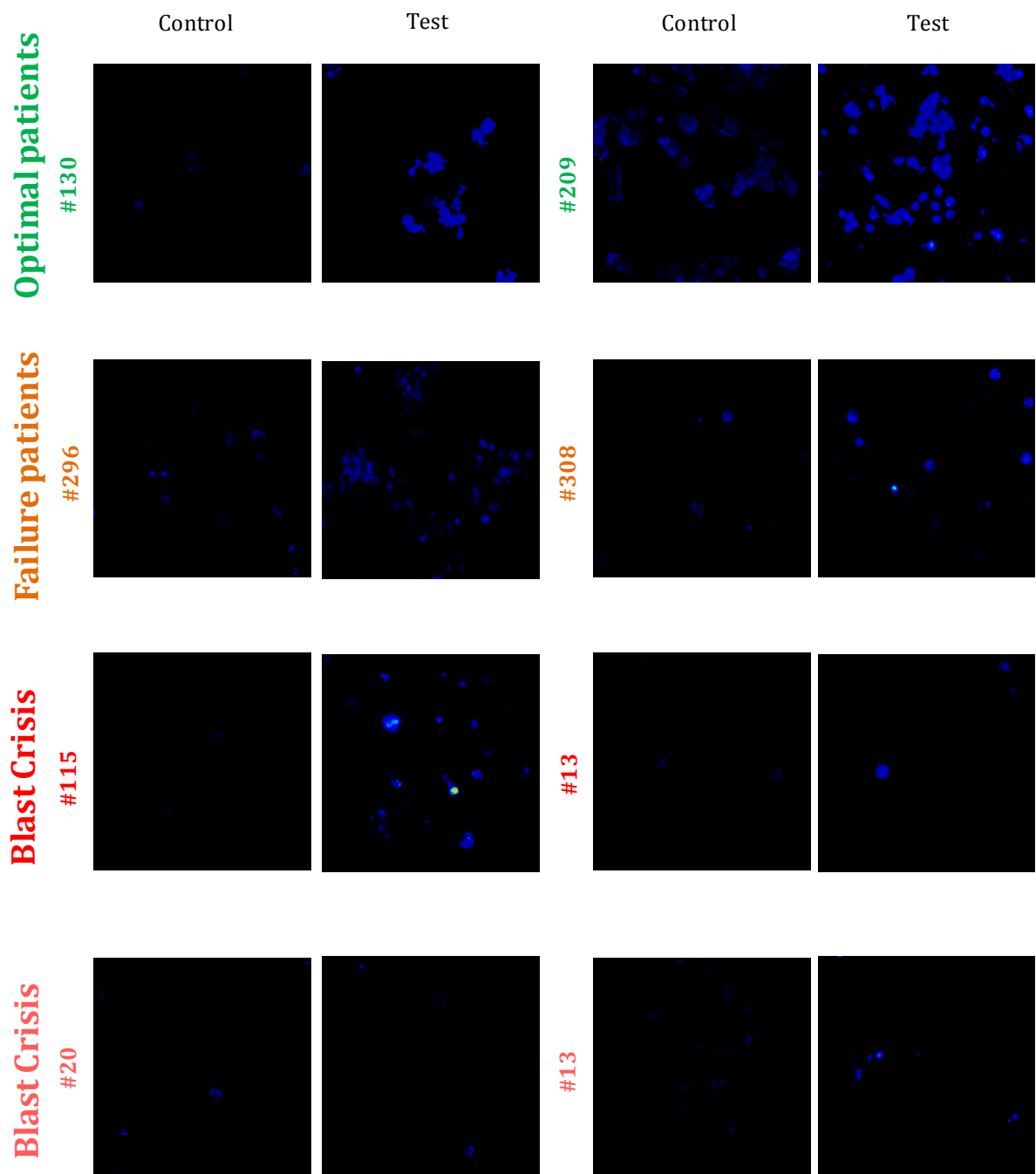
Figure 8.5 Key for Wnt genes re-screening

■ Normal
■ Optimal Diagnosis
■ Failure Diagnosis
■ BC Diagnosis
■ BC in BC

Figure 8.6 PCR re-screening of genes involved in the Wnt signalling pathway in a normal control, optimal responder, failure patient and blast crisis patient at diagnosis, and a patient transformed into blast crisis

Re-screening of all the Wnt related genes in a normal, an optimal responder at diagnosis, a failure patient at diagnosis, a diagnosis patient who later transformed into blast crisis, and a patient in blast crisis to see if any genes showed a major difference between cohorts.
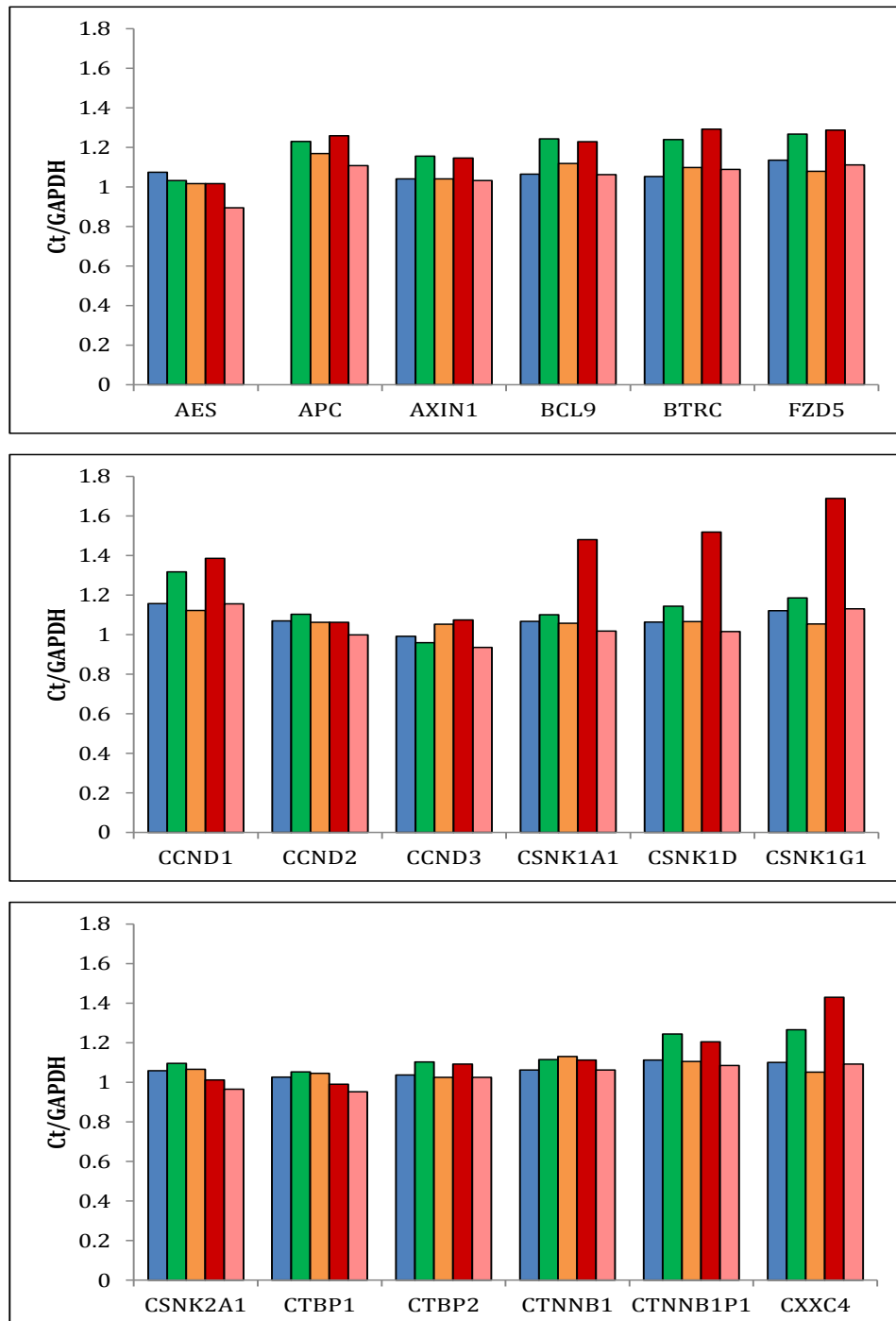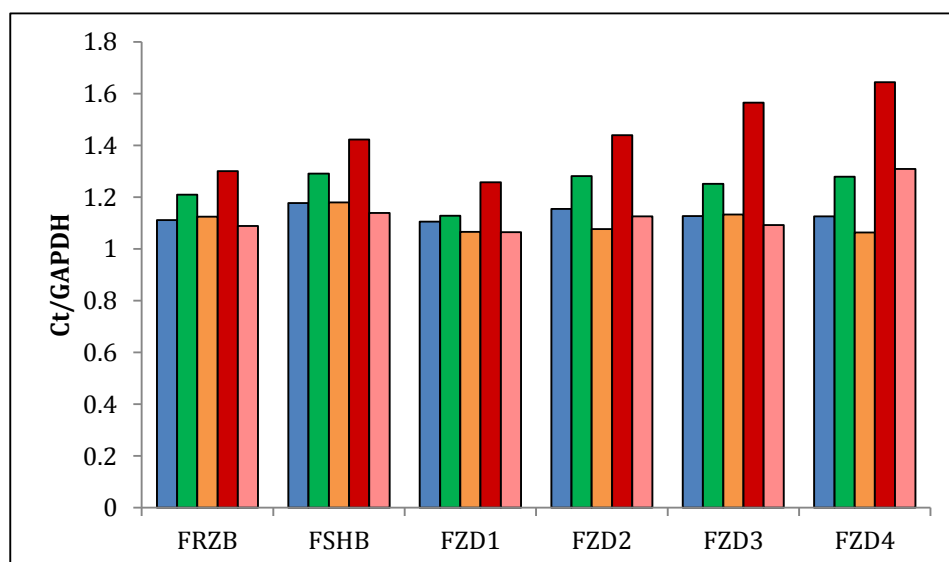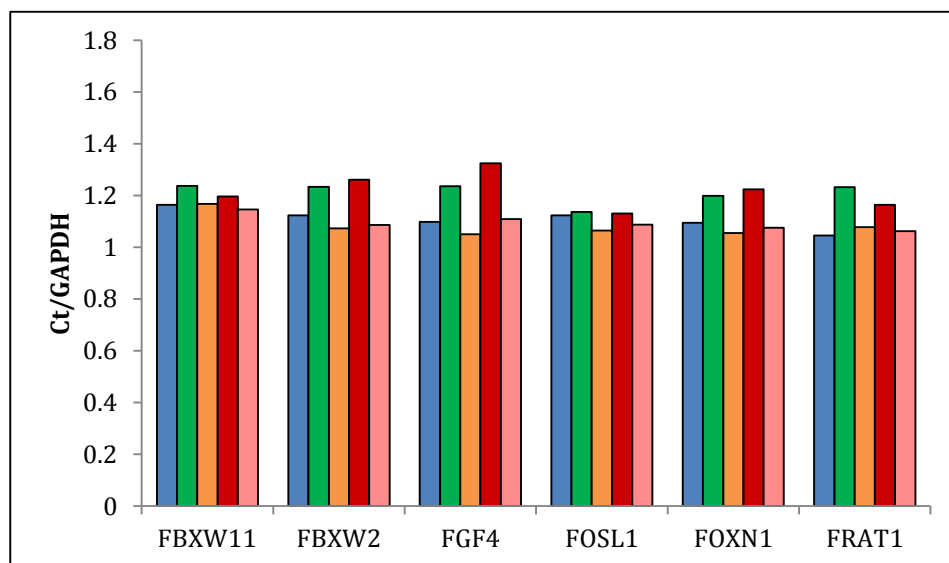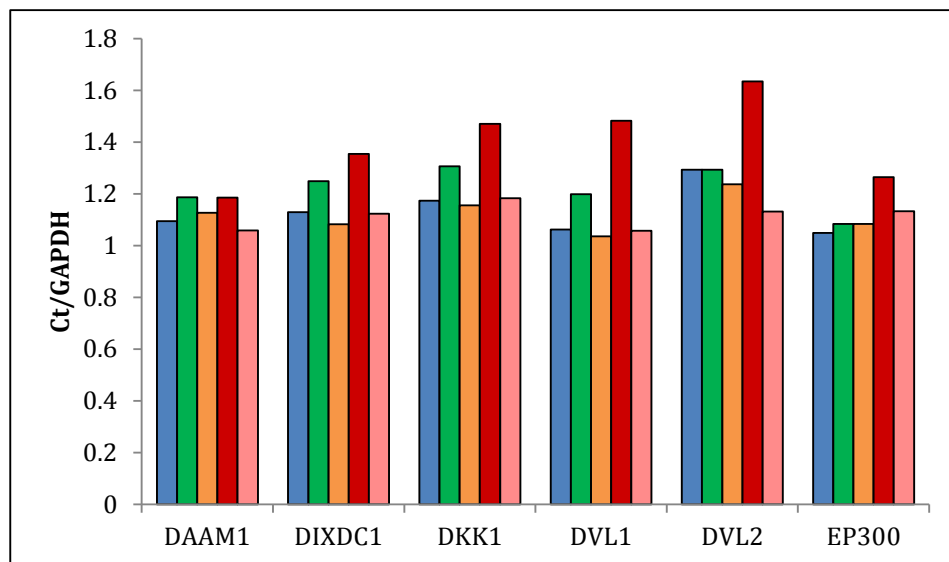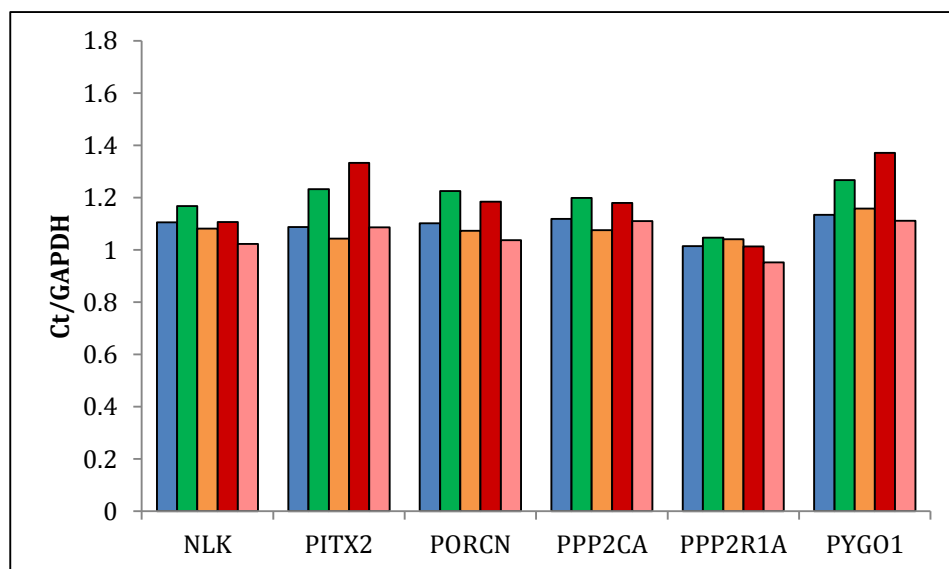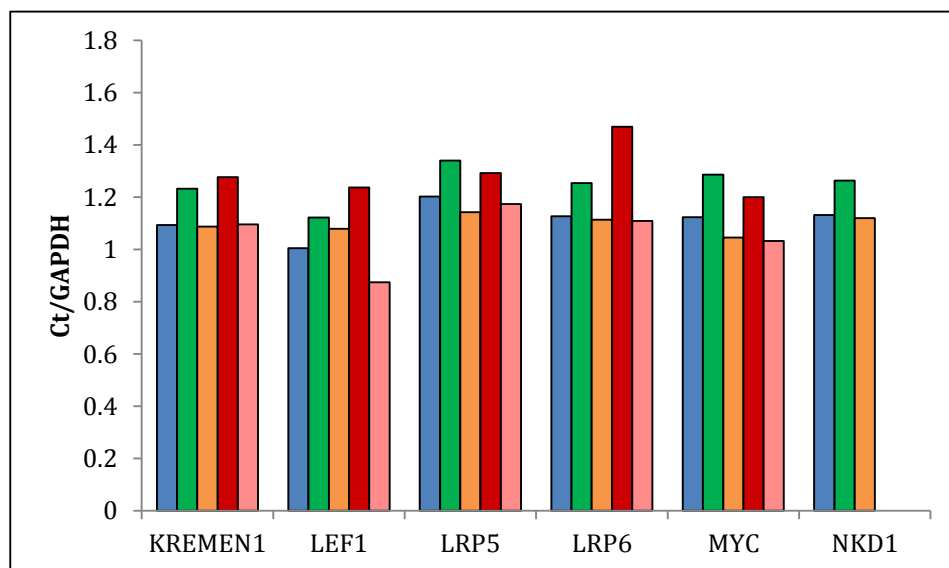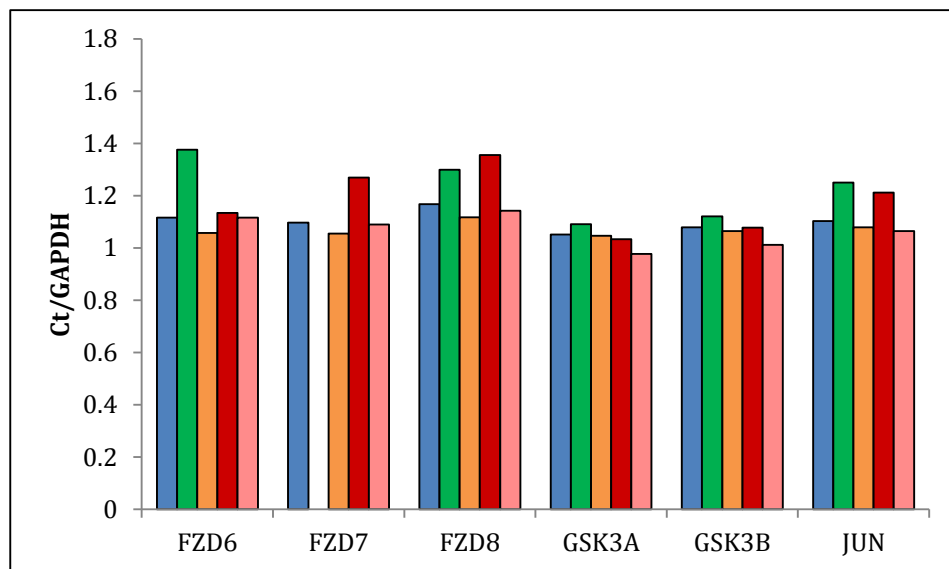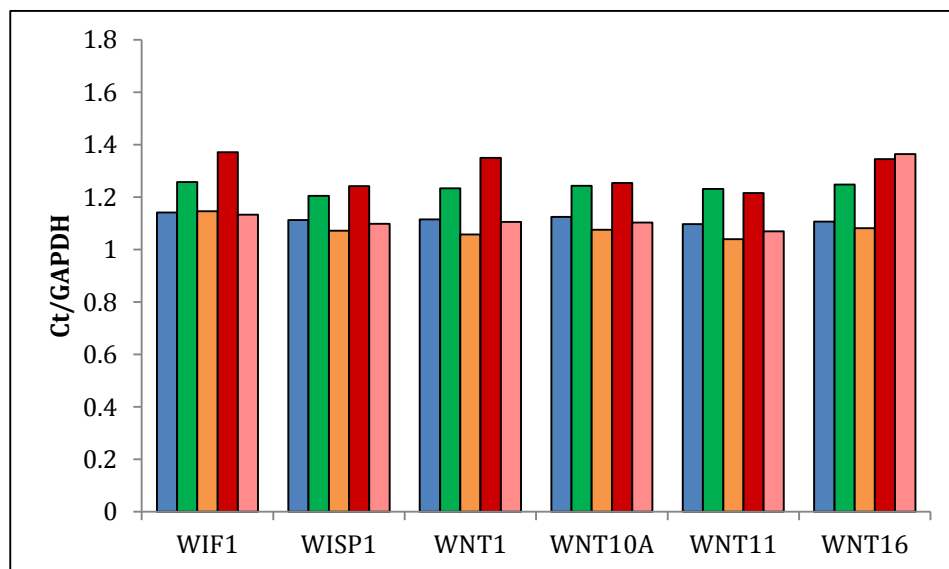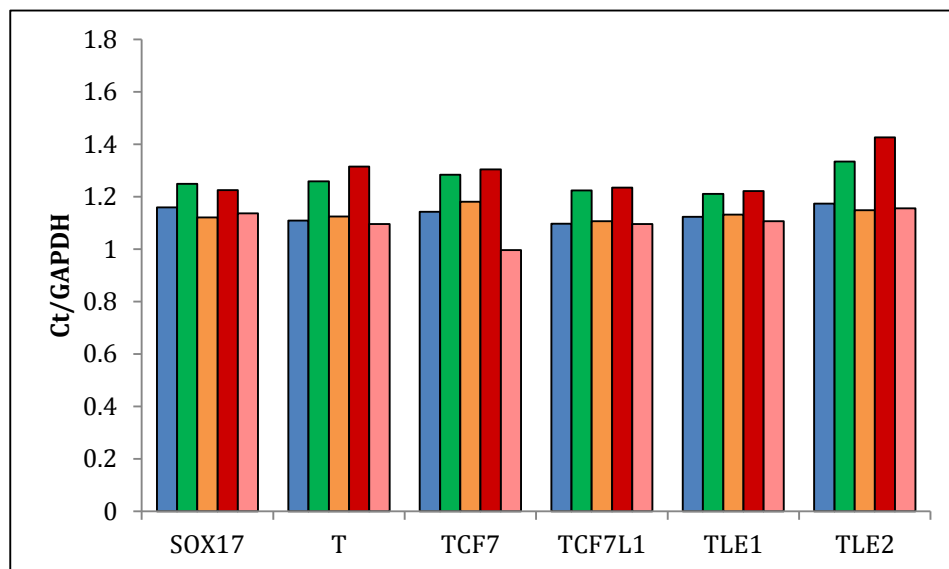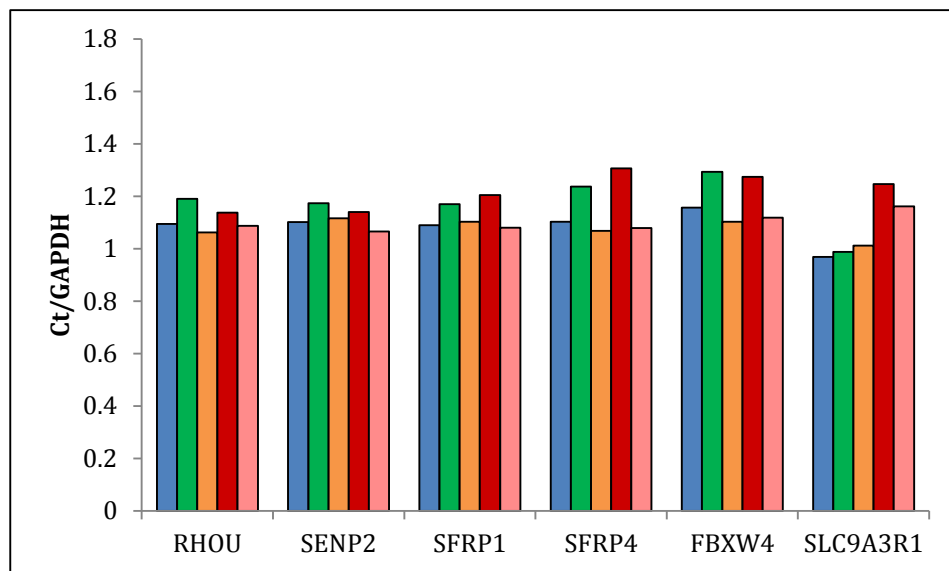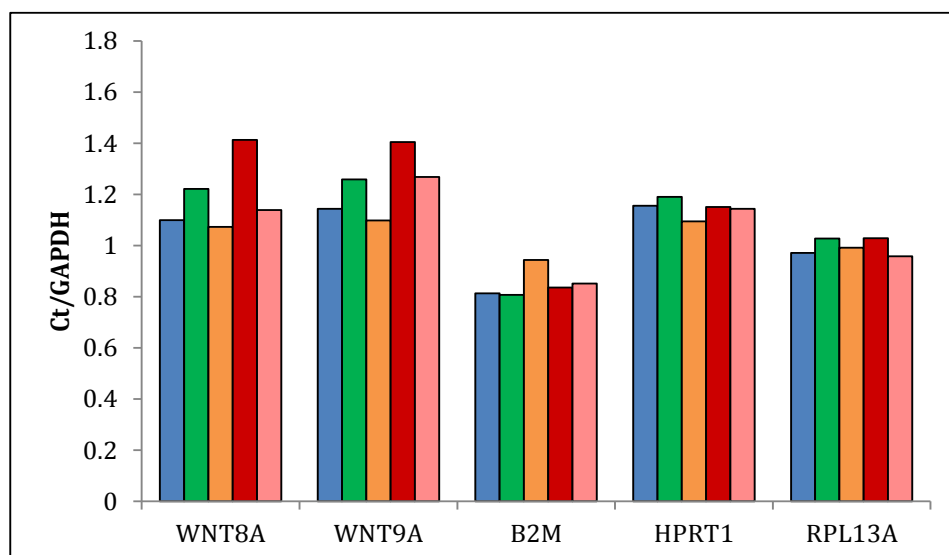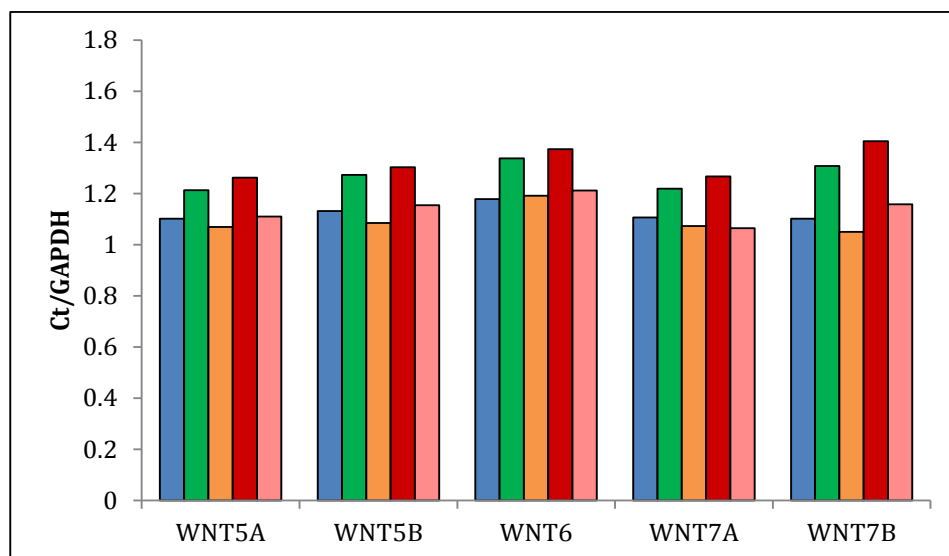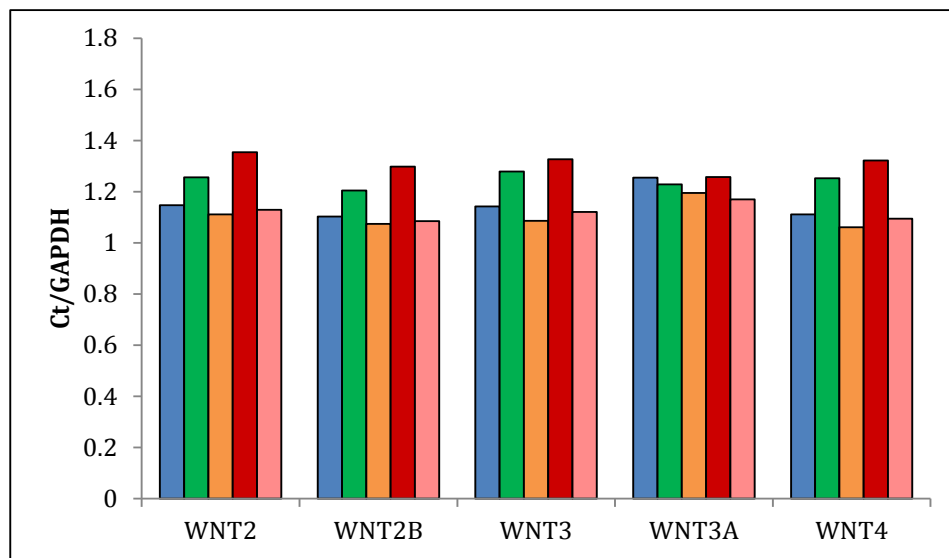
References

1. Bennett, J.H., *Case of hypertrophy of the spleen and liver in which death took place from suppuration of the blood.* Edinburgh Medical and Surgical Journal, 1845. **64**: p. 413-423.
2. Geary, C.G., *The story of chronic myeloid leukaemia.* British Journal of Haematology, 2000. **110**(1): p. 2-11.
3. Virchow, R., *Weisses Blut.* Frorieps Notizen, 1845. **36**: p. 151-156.
4. Goldman, J.M., *Chronic myeloid leukemia: a historical perspective.* Seminars in Hematology, 2010. **47**(4): p. 302-11.
5. Bennett, J.H., *Leucocythaemia, or White Cell Blood in Relation to the Physiology and Pathology of the Lymphatic Glandular System.* Edinburgh Medical and Surgical Journal, 1852. **72**: p. 7-82.
6. Virchow, R., *Weisses Blut und Milztumoren.* Medicale Zeitung., 1847. **16**: p. 9-15.
7. Neumann, E., *Ein Fall von Leukamie mit Erkrankungen des Knochenmarkes.* Archives Heilkunde, 1870.
8. Ehrlich, P., *Farbenanalystische Untersuchungen zur Histologie und Klinik des Blutes.* Hirschwald, Berlin, 1891.
9. Nowell, P.C. and D.A. Hungerford, *A minute chromosome in human chronic granulocytic leukaemia.* Science, 1960. **142**: p. p. 1497.
10. Rowley, J.D., *Letter: A new consistent chromosomal abnormality in chronic myelogenous leukaemia identified by quinacrine fluorescence and Giemsa staining.* Nature, 1973. **243**(5405): p. 290-3.
11. De Klein, A., et al., *bcr rearrangement and translocation of the c-abl oncogene in Philadelphia positive acute lymphoblastic leukemia.* Blood, 1986. **68**(6): p. 1369-75.
12. Bernards, A., et al., *The first intron in the human c-abl gene is at least 200 kilobases long and is a target for translocations in chronic myelogenous leukemia.* Molecular and Cellular Biology, 1987. **7**(9): p. 3231-6.
13. Groffen, J., et al., *Philadelphia chromosomal breakpoints are clustered within a limited region, bcr, on chromosome 22.* Cell, 1984. **36**(1): p. 93-9.
14. Konopka, J.B., S.M. Watanabe, and O.N. Witte, *An alteration of the human c-abl protein in K562 leukemia cells unmasks associated tyrosine kinase activity.* Cell, 1984. **37**(3): p. 1035-42.
15. Shtivelman, E., et al., *Fused transcript of abl and bcr genes in chronic myelogenous leukaemia.* Nature, 1985. **315**(6020): p. 550-4.
16. Suzuki, J. and T. Shishido, *Regulation of cellular transformation by oncogenic and normal Abl kinases.* Journal of Biochemistry, 2007. **141**(4): p. 453-8.
17. Quintás-Cardama, A. and J. Cortes, *Molecular biology of bcr-abl1-positive chronic myeloid leukemia.* Blood, 2009. **113**(8): p. 1619-1630.
18. Ren, R., *Mechanisms of BCR-ABL in the pathogenesis of chronic myelogenous leukaemia.* Nature Reviews Cancer, 2005. **5**(3): p. 172-83.
19. Hantschel, O. and G. Superti-Furga, *Regulation of the c-Abl and Bcr-Abl tyrosine kinases.* Nature Reviews Molecular Cell Biology, 2004. **5**(1): p. 33-44.
20. Rosee, P. and M. Deininger, *Cytogenetics and molecular biology of chronic myeloid leukemia*, in *Chronic Myeloproliferative Disorders*, T. Mughal and J. Goldman, Editors. 2008. p. 17-44.

21. Van Etten, R.A., P. Jackson, and D. Baltimore, *The mouse type IV c-abl gene product is a nuclear protein, and activation of transforming ability is associated with cytoplasmic localization.* Cell, 1989. **58**(4): p. 669-78.

22. Taagepera, S., et al., *Nuclear-cytoplasmic shuttling of C-ABL tyrosine kinase.* Proceedings of the National Academy of Sciences of the United States of America, 1998. **95**(13): p. 7457-62.

23. Tybulewicz, V.L., et al., *Neonatal lethality and lymphopenia in mice with a homozygous disruption of the c-abl proto-oncogene.* Cell, 1991. **65**(7): p. 1153-63.

24. Pluk, H., K. Dorey, and G. Superti-Furga, *Autoinhibition of c-Abl.* Cell, 2002. **108**(2): p. 247-59.

25. Maru, Y. and O.N. Witte, *The BCR gene encodes a novel serine/threonine kinase activity within a single exon.* Cell, 1991. **67**(3): p. 459-68.

26. Chuang, T.H., et al., *Abr and Bcr are multifunctional regulators of the Rho GTP-binding protein family.* Proceedings of the National Academy of Sciences of the United States of America, 1995. **92**(22): p. 10282-6.

27. Radziwill, G., et al., *The Bcr kinase downregulates Ras signaling by phosphorylating AF-6 and binding to its PDZ domain.* Molecular and Cellular Biology, 2003. **23**(13): p. 4663-72.

28. Ress, A. and K. Moelling, *Bcr is a negative regulator of the Wnt signalling pathway.* EMBO Reports, 2005. **6**(11): p. 1095-1100.

29. Melo, J., *The diversity of BCR-ABL fusion proteins and their relationship to leukemia phenotype* Vol. 88. 1996. 2375-2384.

30. Padron, E., J. Pinilla-Ibarz, and L. Hazlehurst, *Molecular pathogenesis of BCR-ABL in Chronic Myeloid Leukaemia*, in *Advances in Malignant haematology.* 2011, Chapter 4.

31. Pane, F., et al., *Neutrophilic-chronic myeloid leukemia: a distinct disease with a specific molecular marker (BCR/ABL with C3/A2 junction)* Vol. 88. 1996. p2410-2414. 2410-2414.

32. Bernt, K.M. and S.P. Hunger, *Current Concepts in Pediatric Philadelphia Chromosome-Positive Acute Lymphoblastic Leukemia.* Frontiers in Oncology, 2014. **4**: p. 54.

33. Hernandez, J.M., et al., *Clinical, hematological and cytogenetic characteristics of atypical chronic myeloid leukemia.* Annals of Oncology, 2000. **11**(4): p. 441-4.

34. Kurzrock, R., et al., *Philadelphia chromosome-negative chronic myelogenous leukemia without breakpoint cluster region rearrangement: a chronic myeloid leukemia with a distinct clinical course.* Blood, 1990. **75**(2): p. 445-52.

35. Mehta A and H. V, *Haematology at a Glance.* 2005: Blackwell Publishing Ltd.

36. Francis, S., et al., *A population study showing that the advent of second generation tyrosine kinase inhibitors has improved progression-free survival in chronic myeloid leukaemia.* Leukemia Research, 2013. **37**(7): p. 752-758.

37. Syed, N.N., et al., *Clinico-pathologic features of chronic myeloid leukemia and risk stratification according to sokal score.* Journal of the College of Physicians and Surgeons Pakistan, 2006. **16**(5): p. 336-339.

38. Cortes, J., et al. *Chronic Myeloid Leukemia*. 2014 08/06/14]; Available from: http://www.cancernetwork.com/cancer-management/CML.

39. Nikolas von Bubnoff, L.P., Daniel Neureiter, Victoria Faber, and Justus Duyster, *Chronic Myeloid Leukemia (CML). In: Chronic Myeloid Neoplasias and Clonal Overlap Syndromes*. 2010; p. 117-142.,

.

40. Heyssel, R., et al., *Leukemia in Hiroshima atomic bomb survivors.* Blood, 1960. **15**: p. 313-31.

41. Baccarani, M., et al., *European LeukemiaNet recommendations for the management of chronic myeloid leukemia: 2013.* Blood, 2013. **122**(6): p. 872-84.

42. Hehlmann, R., et al., *Randomized comparison of interferon-α with busulfan and hydroxyurea in chronic myelogenous leukemia.* Blood, 1994. **84**(12): p. 4064-4077.

43. Baccarani, M., et al., *Chronic myeloid leukemia: An update of concepts and management recommendations of European LeukemiaNet.* Journal of Clinical Oncology, 2009. **27**(35): p. 6041-6051.

44. Darkow, T., et al., *Treatment interruptions and non-adherence with imatinib and associated healthcare costs: a retrospective analysis among managed care patients with chronic myelogenous leukaemia.* Pharmacoeconomics, 2007. **25**(6): p. 481-96.

45. Hehlmann, R., et al., *Randomized comparison of busulfan and hydroxyurea in chronic myelogenous leukemia: prolongation of survival by hydroxyurea. The German CML Study Group.* Blood, 1993. **82**(2): p. 398-407.

46. *Long-term follow-Up of the italian trial of interferon-alpha versus conventional chemotherapy in chronic myeloid leukemia. The Italian Cooperative Study Group on Chronic Myeloid Leukemia.* Blood, 1998. **92**(5): p. 1541-8.

47. Ohnishi, K., et al., *A randomized trial comparing interferon-alpha with busulfan for newly diagnosed chronic myelogenous leukemia in chronic phase.* Blood, 1995. **86**(3): p. 906-16.

48. Allan, N.C., S.M. Richards, and P.C. Shepherd, *UK Medical Research Council randomised, multicentre trial of interferon-alpha n1 for chronic myeloid leukaemia: improved survival irrespective of cytogenetic response. The UK Medical Research Council's Working Parties for Therapeutic Trials in Adult Leukaemia.* Lancet Oncology, 1995. **345**(8962): p. 1392-7.

49. Bhattacharya, S., et al., *Bcr-abl signals to desensitize chronic myeloid leukemia cells to IFNα via accelerating the degradation of its receptor.* Blood, 2011. **118**(15): p. 4179-4187.

50. Jain, N. and K. van Besien, *Chronic Myelogenous Leukemia: Role of Stem Cell Transplant in the Imatinib Era.* Hematology/Oncology Clinics of North America, 2011. **25**(5): p. 1025-1048.

51. Gratwohl, A. and D. Heim, *Current role of stem cell transplantation in chronic myeloid leukaemia.* Best Practice & Research Clinical Haematology, 2009. **22**(3): p. 431-443.

52. Cortes, J.E., et al., *Pharmacokinetic/pharmacodynamic correlation and blood-level testing in imatinib therapy for chronic myeloid leukemia.* Leukemia 2009. **23**(9): p. 1537-1544.

53. Jabbour, E. and S. Soverini, *Understanding the Role of Mutations in Therapeutic Decision Making for Chronic Myeloid Leukemia.* Seminars in Hematology, 2009. **46**(SUPPL. 3): p. S22-S26.

54. Marcucci, G., D. Perrotti, and M.A. Caligiuri, *Understanding the molecular basis of imatinib mesylate therapy in chronic myelogenous leukemia and the related mechanisms of resistance. Commentary re: A. N. Mohamed et al., The effect of imatinib mesylate on patients with Philadelphia chromosome-positive chronic*

myeloid leukemia with secondary chromosomal aberrations. Clin. Cancer Res., 9: 1333-1337, 2003. Clinical Cancer Research, 2003. **9**(4): p. 1248-52.

55. Roy, L., et al., *Survival advantage from imatinib compared with the combination interferon-α plus cytarabine in chronic-phase chronic myelogenous leukemia: historical comparison between two phase 3 trials.* Blood, 2006. **108**(5): p. 1478-1484.

56. O'Brien, S.G., et al., *Imatinib compared with interferon and low-dose cytarabine for newly diagnosed chronic-phase chronic myeloid leukemia.* New England Journal of Medicine, 2003. **348**(11): p. 994-1004.

57. O'Dwyer, M. and E. Atallah, *Practical Considerations for the Management of Patients in the Tyrosine Kinase Inhibitor Era.* Seminars in Hematology, 2009. **46**(SUPPL. 3): p. S16-S21.

58. Gambacorti-Passerini, C.B., et al., *Molecular mechanisms of resistance to imatinib in Philadelphia-chromosome-positive leukaemias.* Lancet Oncology, 2003. **4**(2): p. 75-85.

59. Lucas, C.M., et al., *A population study of imatinib in chronic myeloid leukaemia demonstrates lower efficacy than in clinical trials.* Leukemia, 2008. **22**(10): p. 1963-1966.

60. O'Hare, T., C.A. Eide, and M.W.N. Deininger, *Bcr-Abl kinase domain mutations, drug resistance, and the road to a cure for chronic myeloid leukemia.* Blood, 2007. **110**(7): p. 2242-2249.

61. Weisberg, E., et al., *Second generation inhibitors of BCR-ABL for the treatment of imatinib-resistant chronic myeloid leukaemia.* Nature Reviews Cancer, 2007. **7**(5): p. 345-356.

62. Gorre, M.E., et al., *Clinical resistance to STI-571 cancer therapy caused by BCR-ABL gene mutation or amplification.* Science, 2001. **293**(5531): p. 876-80.

63. Thomas, J., et al., *Active transport of imatinib into and out of cells: implications for drug resistance.* Blood, 2004. **104**(12): p. 3739-45.

64. Wang, L., et al., *Expression of the uptake drug transporter hOCT1 is an important clinical determinant of the response to imatinib in chronic myeloid leukemia.* Clinical Pharmacology and Therapeutics, 2008. **83**(2): p. 258-64.

65. Weisberg, E., et al., *AMN107 (nilotinib): A novel and selective inhibitor of BCR-ABL.* British Journal of Cancer, 2006. **94**(12): p. 1765-1769.

66. Giles, F.J., *New Directions in the Treatment of Imatinib Failure and/or Resistance.* Seminars in Hematology, 2009. **46**(SUPPL. 3): p. S27-S33.

67. Quintas-Cardama A, et al., *Small Molecules in Oncology.* 2010. p. 103-117.: Springer Verlag Berlin Heidelberg.

68. Davies, A., et al., *Nilotinib concentration in cell lines and primary CD34(+) chronic myeloid leukemia cells is not mediated by active uptake or efflux by major drug transporters.* Leukemia, 2009. **23**(11): p. 1999-2006.

69. Jabbour, E., J.E. Cortes, and H. Kantarjian, *Second-line therapy and beyond resistance for the treatment of patients with chronic myeloid leukemia post imatinib failure.* Clinical lymphoma & myeloma, 2009. **9 Suppl 3**: p. S272-279.

70. Saglio, G., et al., *Nilotinib versus Imatinib for Newly Diagnosed Chronic Myeloid Leukemia.* New England Journal of Medicine, 2010. **362**(24): p. 2251-2259.

71. Larson, R.A., et al., *Nilotinib vs imatinib in patients with newly diagnosed Philadelphia chromosome-positive chronic myeloid leukemia in chronic phase: ENESTnd 3-year follow-up.* Leukemia, 2012. **26**(10): p. 2197-203.

72. Aichberger, K.J., et al., *Progressive peripheral arterial occlusive disease and other vascular events during nilotinib therapy in CML.* American Journal of Hematology, 2011. **86**(7): p. 533-9.

73. Quintas-Cardama, A., H. Kantarjian, and J. Cortes, *Nilotinib-associated vascular events.* Clinical lymphoma, myeloma & leukemia, 2012. **12**(5): p. 337-40.

74. Tefferi, A. and L. Letendre, *Nilotinib treatment-associated peripheral artery disease and sudden death: yet another reason to stick to imatinib as front-line therapy for chronic myelogenous leukemia.* American Journal of Hematology, 2011. **86**(7): p. 610-1.

75. Kim, T.D., et al., *Peripheral artery occlusive disease in chronic phase chronic myeloid leukemia patients treated with nilotinib or imatinib.* Leukemia, 2013. **27**(6): p. 1316-21.

76. Kantarjian, H., et al., *Dasatinib or high-dose imatinib for chronic-phase chronic myeloid leukemia resistant to imatinib at a dose of 400 to 600 milligrams daily: two-year follow-up of a randomized phase 2 study (START-R).* Cancer, 2009. **115**(18): p. 4136-47.

77. Keam, S.J., *Dasatinib: In chronic myeloid leukemia and Philadelphia chromosome-positive acute lymphoblastic leukemia.* BioDrugs, 2008. **22**(1): p. 59-69.

78. Giannoudis, A., et al., *Effective dasatinib uptake may occur without human organic cation transporter 1 (hOCT1): implications for the treatment of imatinib-resistant chronic myeloid leukemia.* Blood, 2008. **112**(8): p. 3348-54.

79. Khorashad, J.S., et al., *BCR-ABL1 compound mutations in tyrosine kinase inhibitor-resistant CML: frequency and clonal relationships.* Blood, 2013. **121**(3): p. 489-98.

80. Kantarjian, H.M., et al., *Dasatinib or imatinib in newly diagnosed chronic-phase chronic myeloid leukemia: 2-year follow-up from a randomized phase 3 trial (DASISION).* Blood, 2012. **119**(5): p. 1123-1129.

81. Konig, H., T.L. Holyoake, and R. Bhatia, *Effective and selective inhibition of chronic myeloid leukemia primitive hematopoietic progenitors by the dual Src/Abl kinase inhibitor SKI-606.* Blood, 2008. **111**(4): p. 2329-38.

82. Gambacorti-Passerini, C., et al., *Bosutinib efficacy and safety in chronic phase chronic myeloid leukemia after imatinib resistance or intolerance: Minimum 24-month follow-up.* American Journal of Hematology, 2014.

83. Stansfield, L., T.E. Hughes, and T.L. Walsh-Chocolaad, *Bosutinib: a second-generation tyrosine kinase inhibitor for chronic myelogenous leukemia.* Annals of Pharmacotherapy, 2013. **47**(12): p. 1703-11.

84. Cortes, J.E., et al., *A phase 2 trial of ponatinib in Philadelphia chromosome-positive leukemias.* New England Journal of Medicine, 2013. **369**(19): p. 1783-96.

85. Huelsken, J. and J. Behrens, *The Wnt signalling pathway.* Journal of Cell Science, 2002. **115**(21): p. 3977-3978.

86. Clevers, H., *Wnt/beta-catenin signaling in development and disease.* Cell, 2006. **127**(3): p. 469-80.

87. MacDonald, B.T., K. Tamai, and X. He, *Wnt/β-Catenin Signaling: Components, Mechanisms, and Diseases.* Developmental Cell, 2009. **17**(1): p. 9-26.

88. Logan, C.Y. and R. Nusse, *The Wnt signaling pathway in development and disease*. 2004. p. 781-810.

89. Huang, H.C. and P.S. Klein, *The Frizzled family: receptors for multiple signal transduction pathways.* Genome Biology, 2004. **5**(7): p. 234.

90. Bhanot, P., et al., *A new member of the frizzled family from Drosophila functions as a Wingless receptor.* Nature, 1996. **382**(6588): p. 225-30.

91.   He, X., et al., *LDL receptor-related proteins 5 and 6 in Wnt/beta-catenin signaling: arrows point the way.* Development, 2004. **131**(8): p. 1663-77.

92.   Niehrs, C., *Function and biological roles of the Dickkopf family of Wnt modulators.* Oncogene, 2006. **25**(57): p. 7469-81.

93.   Glinka, A., et al., *Dickkopf-1 is a member of a new family of secreted proteins and functions in head induction.* Nature, 1998. **391**(6665): p. 357-62.

94.   Mao, B., et al., *Kremen proteins are Dickkopf receptors that regulate Wnt/[beta]-catenin signalling.* Nature, 2002. **417**(6889): p. 664-667.

95.   Rao, T.P. and M. Kühl, *An updated overview on wnt signaling pathways: A prelude for more.* Circulation Research, 2010. **106**(12): p. 1798-1806.

96.   Yamamoto, H., et al., *Wnt3a and Dkk1 regulate distinct internalization pathways of LRP6 to tune the activation of beta-catenin signaling.* Developmental Cell, 2008. **15**(1): p. 37-48.

97.   Li, X., et al., *Sclerostin Binds to LRP5/6 and Antagonizes Canonical Wnt Signaling.* Journal of Biological Chemistry, 2005. **280**(20): p. 19883-19887.

98.   Semënov, M., K. Tamai, and X. He, *SOST Is a Ligand for LRP5/LRP6 and a Wnt Signaling Inhibitor.* Journal of Biological Chemistry, 2005. **280**(29): p. 26770-26775.

99.   Yamamoto, A., et al., *Shisa promotes head formation through the inhibition of receptor protein maturation for the caudalizing factors, Wnt and FGF.* Cell, 2005. **120**(2): p. 223-35.

100.   Polakis, P., *Wnt signaling and cancer.* Genes and Development, 2000. **14**(15): p. 1837-1851.

101.   Abrahamsson, A.E., et al., *Glycogen synthase kinase 3β missplicing contributes to leukemia stem cell generation.* Proceedings of the National Academy of Sciences of the United States of America, 2009. **106**(10): p. 3925-3929.

102.   Itoh, K., et al., *Interaction of dishevelled and Xenopus axin-related protein is required for wnt signal transduction.* Molecular and Cell Biology, 2000. **20**(6): p. 2228-38.

103.   Sun, T.Q., et al., *PAR-1 is a Dishevelled-associated kinase and a positive regulator of Wnt signalling.* Nature Cell Biology, 2001. **3**(7): p. 628-36.

104.   Kimelman, D. and W. Xu, *beta-catenin destruction complex: insights and questions from a structural perspective.* Oncogene, 2006. **25**(57): p. 7482-91.

105.   van Noort, M., et al., *Wnt signaling controls the phosphorylation status of beta-catenin.* Journal of Biological Chemistry, 2002. **277**(20): p. 17901-5.

106.   Staal, F.J., et al., *Wnt signals are transmitted through N-terminally dephosphorylated beta-catenin.* EMBO Reports, 2002. **3**(1): p. 63-8.

107.   Li, L., et al., *Axin and Frat1 interact with dvl and GSK, bridging Dvl to GSK in Wnt-mediated regulation of LEF-1.* EMBO Journal, 1999. **18**(15): p. 4233-40.

108.   Gloy, J., H. Hikasa, and S.Y. Sokol, *Frodo interacts with Dishevelled to transduce Wnt signals.* Nature Cell Biology, 2002. **4**(5): p. 351-7.

109.   Bryja, V., et al., *Beta-arrestin is a necessary component of Wnt/beta-catenin signaling in vitro and in vivo.* Proceedings of the National Academy of Sciences of the United States of America, 2007. **104**(16): p. 6690-5.

110.   Zhang, L., et al., *Dapper 1 antagonizes Wnt signaling by promoting dishevelled degradation.* Journal of Biological Chemistry, 2006. **281**(13): p. 8607-12.

111.   Davidson, G., et al., *Casein kinase 1 gamma couples Wnt receptor activation to cytoplasmic signal transduction.* Nature, 2005. **438**(7069): p. 867-72.

112. Zeng, X., et al., *A dual-kinase mechanism for Wnt co-receptor phosphorylation and activation.* Nature, 2005. **438**(7069): p. 873-7.
113. Polakis, P., *The many ways of Wnt in cancer.* Current Opinion in Genetics and Development, 2007. **17**(1): p. 45-51.
114. Behrens, J., et al., *Functional interaction of beta-catenin with the transcription factor LEF-1.* Nature, 1996. **382**(6592): p. 638-42.
115. Molenaar, M., et al., *XTcf-3 transcription factor mediates beta-catenin-induced axis formation in Xenopus embryos.* Cell, 1996. **86**(3): p. 391-9.
116. Wu, X., et al., *Rac1 activation controls nuclear localization of beta-catenin during canonical Wnt signaling.* Cell, 2008. **133**(2): p. 340-53.
117. Cong, F. and H. Varmus, *Nuclear-cytoplasmic shuttling of Axin regulates subcellular localization of β-catenin.* Proceedings of the National Academy of Sciences of the United States of America, 2004. **101**(9): p. 2882-2887.
118. Henderson, B.R., *Nuclear-cytoplasmic shuttling of APC regulates beta-catenin subcellular localization and turnover.* Nature Cell Biology, 2000. **2**(9): p. 653-60.
119. Kramps, T., et al., *Wnt/wingless signaling requires BCL9/legless-mediated recruitment of pygopus to the nuclear beta-catenin-TCF complex.* Cell, 2002. **109**(1): p. 47-60.
120. Krieghoff, E., J. Behrens, and B. Mayr, *Nucleo-cytoplasmic distribution of β-catenin is regulated by retention.* Journal of Cell Science, 2006. **119**(7): p. 1453-1463.
121. Mancini, M., et al., *Chibby drives beta catenin cytoplasmic accumulation leading to activation of the unfolded protein response in BCR-ABL1+ cells.* Cellular Signalling, 2013. **25**(9): p. 1820-7.
122. Cantu, C., T. Valenta, and K. Basler, *A RING finger to wed TCF and beta-catenin.* EMBO Reports, 2013. **14**(4): p. 295-6.
123. Metzeler, K.H., et al., *High expression of lymphoid enhancer-binding factor-1 (LEF1) is a novel favorable prognostic factor in cytogenetically normal acute myeloid leukemia.* Blood, 2012. **120**(10): p. 2118-26.
124. Barker, N., et al., *The chromatin remodelling factor Brg-1 interacts with beta-catenin to promote target gene activation.* EMBO Journal, 2001. **20**(17): p. 4935-43.
125. Takemaru, K.I. and R.T. Moon, *The transcriptional coactivator CBP interacts with beta-catenin to activate gene expression.* Journal of Cell Biology, 2000. **149**(2): p. 249-54.
126. Townsley, F.M., A. Cliffe, and M. Bienz, *Pygopus and Legless target Armadillo/[beta]-catenin to the nucleus to enable its transcriptional co-activator function.* Nature Cell Biology, 2004. **6**(7): p. 626-633.
127. Sustmann, C., et al., *Cell-Type-Specific Function of BCL9 Involves a Transcriptional Activation Domain That Synergizes with β-Catenin.* Molecular and Cellular Biology, 2008. **28**(10): p. 3526-3537.
128. Thompson, B., et al., *A new nuclear component of the Wnt signalling pathway.* Nature Cell Biology, 2002. **4**(5): p. 367-73.
129. Tago, K., et al., *Inhibition of Wnt signaling by ICAT, a novel beta-catenin-interacting protein.* Genes and Development, 2000. **14**(14): p. 1741-9.
130. Daniels, D.L. and W.I. Weis, *ICAT inhibits beta-catenin binding to Tcf/Lef-family transcription factors and the general coactivator p300 using independent structural modules.* Molecular Cell, 2002. **10**(3): p. 573-84.
131. Cavallo, R.A., et al., *Drosophila Tcf and Groucho interact to repress Wingless signalling activity.* Nature, 1998. **395**(6702): p. 604-8.

132. Daniels, D.L. and W.I. Weis, *[beta]-catenin directly displaces Groucho/TLE repressors from Tcf/Lef in Wnt-mediated transcription activation.* Nature Structural and Molecular Biology, 2005. **12**(4): p. 364-371.

133. Hart, M.J., et al., *Downregulation of beta-catenin by human Axin and its association with the APC tumor suppressor, beta-catenin and GSK3 beta.* Current Biology, 1998. **8**(10): p. 573-81.

134. Ikeda, S., et al., *Axin, a negative regulator of the Wnt signaling pathway, forms a complex with GSK-3beta and beta-catenin and promotes GSK-3beta-dependent phosphorylation of beta-catenin.* EMBO Journal, 1998. **17**(5): p. 1371-84.

135. Liu, C., et al., *Control of beta-catenin phosphorylation/degradation by a dual-kinase mechanism.* Cell, 2002. **108**(6): p. 837-47.

136. Amit, S., et al., *Axin-mediated CKI phosphorylation of beta-catenin at Ser 45: a molecular switch for the Wnt pathway.* Genes and Development, 2002. **16**(9): p. 1066-76.

137. Yamamoto, H., et al., *Phosphorylation of Axin, a Wnt Signal Negative Regulator, by Glycogen Synthase Kinase-3β Regulates Its Stability.* Journal of Biological Chemistry, 1999. **274**(16): p. 10681-10684.

138. Kikuchi, A., *Roles of Axin in the Wnt signalling pathway.* Cellular Signalling, 1999. **11**(11): p. 777-88.

139. Lee, E., et al., *The roles of APC and Axin derived from experimental and theoretical analysis of the Wnt pathway.* PLoS Biology, 2003. **1**(1): p. E10.

140. Orford, K., et al., *Serine Phosphorylation-regulated Ubiquitination and Degradation of β-Catenin.* Journal of Biological Chemistry, 1997. **272**(40): p. 24735-24738.

141. Aberle, H., et al., *beta-catenin is a target for the ubiquitin-proteasome pathway.* EMBO Journal, 1997. **16**(13): p. 3797-804.

142. Hart, M., et al., *The F-box protein beta-TrCP associates with phosphorylated beta-catenin and regulates its activity in the cell.* Current Biology, 1999. **9**(4): p. 207-10.

143. Reya, T., et al., *A role for Wnt signalling in self-renewal of haematopoietic stem cells.* Nature, 2003. **423**(6938): p. 409-14.

144. Coluccia, A.M.L., et al., *Bcr-Abl stabilizes [beta]-catenin in chronic myeloid leukemia through its tyrosine phosphorylation.* EMBO Journal, 2007. **26**(5): p. 1456-1466.

145. Pehlivan, M., Z. Sercan, and H.O. Sercan, *sFRP1 promoter methylation is associated with persistent Philadelphia chromosome in chronic myeloid leukemia.* Leukemia Research, 2009. **33**(8): p. 1062-1067.

146. Xing, Y., et al., *Crystal structure of a full-length beta-catenin.* Structure, 2008. **16**(3): p. 478-87.

147. Fang, D., et al., *Phosphorylation of beta-catenin by AKT promotes beta-catenin transcriptional activity.* Journal of Biological Chemistry, 2007. **282**(15): p. 11221-9.

148. Taurin, S., et al., *Phosphorylation of beta-catenin by cyclic AMP-dependent protein kinase.* Journal of Biological Chemistry, 2006. **281**(15): p. 9971-6.

149. Maher, M.T., et al., *Beta-catenin phosphorylated at serine 45 is spatially uncoupled from beta-catenin phosphorylated in the GSK3 domain: implications for signaling.* PLoS One, 2010. **5**(4): p. e10184.

150. Jamieson, C.H.M., et al., *Granulocyte-macrophage progenitors as candidate leukemic stem cells in blast-crisis CML.* New England Journal of Medicine, 2004. **351**(7): p. 657-667.

151. Hu, Y., et al., *β-Catenin is essential for survival of leukemic stem cells insensitive to kinase inhibition in mice with BCR-ABL-induced chronic myeloid leukemia.* Leukemia, 2009. **23**(1): p. 109-116.

152. Doble, B.W. and J.R. Woodgett, *GSK-3: tricks of the trade for a multi-tasking kinase.* Journal of Cell Science, 2003. **116**(Pt 7): p. 1175-86.

153. Medina, M. and F. Wandosell, *Deconstructing GSK-3: The Fine Regulation of Its Activity.* International journal of Alzheimer's disease, 2011. **2011**: p. 479249.

154. Woodgett, J., *Glycogen Synthase Kinase-3*, in *Encyclopedia of Signaling Molecules*, S. Choi, Editor. 2012, Springer New York. p. 799-805.

155. Hernandez, F. and J. Avila, *The role of glycogen synthase kinase 3 in the early stages of Alzheimers' disease.* FEBS Lett, 2008. **582**(28): p. 3848-54.

156. Harwood, A.J., *Regulation of GSK-3: a cellular multiprocessor.* Cell, 2001. **105**(7): p. 821-4.

157. Bhat, R.V., et al., *Regulation and localization of tyrosine216 phosphorylation of glycogen synthase kinase-3beta in cellular and animal models of neuronal degeneration.* Proceedings of the National Academy of Sciences of the United States of America, 2000. **97**(20): p. 11074-9.

158. Aichberger, K.J., et al., *Identification of mcl-1 as a BCR/ABL-dependent target in chronic myeloid leukemia (CML): evidence for cooperative antileukemic effects of imatinib and mcl-1 antisense oligonucleotides.* Blood, 2005. **105**(8): p. 3303-3311.

159. Michels, J., P.W.M. Johnson, and G. Packham, *Mcl-1.* The International Journal of Biochemistry and Cell Biology, 2005. **37**(2): p. 267-271.

160. Ruiz-Vela, A., et al., *Lentiviral (HIV)-based RNA interference screen in human B-cell receptor regulatory networks reveals MCL1-induced oncogenic pathways.* Blood, 2008. **111**(3): p. 1665-1676.

161. Miller, D.M., et al., *c-Myc and cancer metabolism.* Clinical Cancer Research, 2012. **18**(20): p. 5546-53.

162. Junttila, M.R. and J. Westermarck, *Mechanisms of MYC stabilization in human malignancies.* Cell Cycle, 2008. **7**(5): p. 592-6.

163. Kwok, J.B., et al., *GSK3B polymorphisms alter transcription and splicing in Parkinson's disease.* Annals of Neurology, 2005. **58**(6): p. 829-39.

164. Reddiconto, G., et al., *Targeting of GSK3β promotes imatinib-mediated apoptosis in quiescent CD34+ chronic myeloid leukemia progenitors, preserving normal stem cells.* Blood, 2012. **119**(10): p. 2335-2345.

165. Xu, Y., et al., *Structure of the protein phosphatase 2A holoenzyme.* Cell, 2006. **127**(6): p. 1239-51.

166. Mumby, M.C. and G. Walter, *Protein serine/threonine phosphatases: structure, regulation, and functions in cell growth.* Physiological Reviews, 1993. **73**(4): p. 673-99.

167. Lechward, K., et al., *Protein phosphatase 2A: variety of forms and diversity of functions.* Acta Biochimica Polonica, 2001. **48**(4): p. 921-33.

168. Ratcliffe, M.J., K. Itoh, and S.Y. Sokol, *A positive role for the PP2A catalytic subunit in Wnt signal transduction.* Journal of Biological Chemistry, 2000. **275**(46): p. 35680-3.

169. Hsu, W., L. Zeng, and F. Costantini, *Identification of a Domain of Axin That Binds to the Serine/Threonine Protein Phosphatase 2A and a Self-binding Domain.* Journal of Biological Chemistry, 1999. **274**(6): p. 3439-3445.

170. Seeling, J.M., et al., *Regulation of beta-catenin signaling by the B56 subunit of protein phosphatase 2A.* Science, 1999. **283**(5410): p. 2089-91.

171. Willert, K., S. Shibamoto, and R. Nusse, *Wnt-induced dephosphorylation of axin releases beta-catenin from the axin complex.* Genes and Development, 1999. **13**(14): p. 1768-73.

172. Ikeda, S., et al., *GSK-3beta-dependent phosphorylation of adenomatous polyposis coli gene product can be modulated by beta-catenin and protein phosphatase 2A complexed with Axin.* Oncogene, 2000. **19**(4): p. 537-45.

173. Neviani, P., et al., *The tumor suppressor PP2A is functionally inactivated in blast crisis CML through the inhibitory activity of the BCR/ABL-regulated SET protein.* Cancer Cell, 2005. **8**(5): p. 355-68.

174. Li, M., A. Makkinje, and Z. Damuni, *The myeloid leukemia-associated protein SET is a potent inhibitor of protein phosphatase 2A.* Journal of Biological Chemistry, 1996. **271**(19): p. 11059-62.

175. Perrotti, D. and P. Neviani, *ReSETting PP2A tumour suppressor activity in blast crisis and imatinib-resistant chronic myelogenous leukaemia.* British Journal of Cancer, 2006/09/05/online. **95**(7): p. 6.

176. Lucas, C.M., et al., *Cancerous inhibitor of PP2A (CIP2A) at diagnosis of chronic myeloid leukemia is a critical determinant of disease progression.* Blood, 2011. **117**(24): p. 6660-6668.

177. Samanta, A.K., et al., *Jak2 inhibition deactivates Lyn kinase through the SET-PP2A-SHP1 pathway, causing apoptosis in drug-resistant cells from chronic myelogenous leukemia patients.* Oncogene, 2009. **28**(14): p. 1669-81.

178. Grumolato, L., et al., *beta-Catenin-independent activation of TCF1/LEF1 in human hematopoietic tumor cells through interaction with ATF2 transcription factors.* PLoS Genetics, 2013. **9**(8): p. e1003603.

179. Kikuchi, A., S. Kishida, and H. Yamamoto, *Regulation of Wnt signaling by protein-protein interaction and post-translational modifications.* Experimental and Molecular Medicine, 2006. **38**(1): p. 1-10.

180. Arce, L., N.N. Yokoyama, and M.L. Waterman, *Diversity of LEF/TCF action in development and disease.* Oncogene, 2006. **25**(57): p. 7492-504.

181. Petropoulos, K., et al., *A novel role for Lef-1, a central transcription mediator of Wnt signaling, in leukemogenesis.* Journal of Experimental Medicine, 2008. **205**(3): p. 515-22.

182. Gujral, T.S. and G. MacBeath, *A system-wide investigation of the dynamics of Wnt signaling reveals novel phases of transcriptional regulation.* PLoS One, 2010. **5**(4): p. e10024.

183. Origene. 27/07/2014]; Available from: http://www.origene.com/destination_vector/PS100010.aspx.

184. Livak, K.J. and T.D. Schmittgen, *Analysis of Relative Gene Expression Data Using Real-Time Quantitative PCR and the 2-[Delta][Delta]CT Method.* Methods, 2001. **25**(4): p. 402-408.

185. Heidel, F.H., et al., *Genetic and pharmacologic inhibition of beta-catenin targets imatinib-resistant leukemia stem cells in CML.* Cell Stem Cell, 2012. **10**(4): p. 412-24.

186. Coluccia, A.M.L., et al., *Bcr-Abl stabilizes β-catenin in chronic myeloid leukemia through its tyrosine phosphorylation.* EMBO Journal, 2007. **26**(5): p. 1456-1466.

187. Holloway, K.R., et al., *SIRT1 regulates Dishevelled proteins and promotes transient and constitutive Wnt signaling.* Proceedings of the National Academy of Sciences of the United States of America, 2010. **107**(20): p. 9216-21.

188. Najdi, R., R.F. Holcombe, and M.L. Waterman, *Wnt signaling and colon carcinogenesis: beyond APC.* Journal of Carcinogenesis, 2011. **10**: p. 5.

189. Marcucci, G., D. Perrotti, and M.A. Caligiuri, *Understanding the Molecular Basis of Imatinib Mesylate Therapy in Chronic Myelogenous Leukemia and the Related Mechanisms of Resistance: Commentary re: A. N. Mohamed et al., The Effect of Imatinib Mesylate on Patients with Philadelphia Chromosome-positive Chronic Myeloid Leukemia with Secondary Chromosomal Aberrations. Clin. Cancer Res., 9: 1333–1337, 2003.* Clinical Cancer Research, 2003. **9**(4): p. 1248-1252.

190. Khorashad, J.S., et al., *The level of BCR-ABL1 kinase activity before treatment does not identify chronic myeloid leukemia patients who fail to achieve a complete cytogenetic response on imatinib.* Haematologica, 2009. **94**(6): p. 861-4.

191. Donato, N.J., et al., *Imatinib mesylate resistance through BCR-ABL independence in chronic myelogenous leukemia.* Cancer Research, 2004. **64**(2): p. 672-7.

192. Cruciat, C.M. and C. Niehrs, *Secreted and transmembrane wnt inhibitors and activators.* Cold Spring Harbor Perspectives in Biology, 2013. **5**(3): p. a015081.

193. Huang, J., et al., *Pivotal role for glycogen synthase kinase-3 in hematopoietic stem cell homeostasis in mice.* Journal of Clinical Investigation, 2009. **119**(12): p. 3519-29.

194. Trowbridge, J.J., et al., *Glycogen synthase kinase-3 is an in vivo regulator of hematopoietic stem cell repopulation.* Nature Medicine, 2006. **12**(1): p. 89-98.

195. Coghlan, M.P., et al., *Selective small molecule inhibitors of glycogen synthase kinase-3 modulate glycogen metabolism and gene transcription.* Chemistry and Biology, 2000. **7**(10): p. 793-803.

196. Maurer, U., et al., *Glycogen synthase kinase-3 regulates mitochondrial outer membrane permeabilization and apoptosis by destabilization of MCL-1.* Molecular Cell, 2006. **21**(6): p. 749-60.

197. Qian, W., et al., *PP2A regulates tau phosphorylation directly and also indirectly via activating GSK-3beta.* Journal of Alzheimer's disease, 2010. **19**(4): p. 1221-9.

198. Reavie, L., et al., *Regulation of c-Myc ubiquitination controls chronic myelogenous leukemia initiation and progression.* Cancer Cell, 2013. **23**(3): p. 362-75.

199. Luo, J., *Glycogen synthase kinase 3beta (GSK3beta) in tumorigenesis and cancer chemotherapy.* Cancer Letters, 2009. **273**(2): p. 194-200.

200. Reavie, L., et al., *Regulation of hematopoietic stem cell differentiation by a single ubiquitin ligase-substrate complex.* Nature Immunology, 2010. **11**(3): p. 207-15.

201. Takeishi, S., et al., *Ablation of Fbxw7 eliminates leukemia-initiating cells by preventing quiescence.* Cancer Cell, 2013. **23**(3): p. 347-61.

202. Yao, X.Q., et al., *Glycogen synthase kinase-3beta regulates Tyr307 phosphorylation of protein phosphatase-2A via protein tyrosine phosphatase 1B but not Src.* The Biochemical Journal, 2011. **437**(2): p. 335-44.

203. Liu, G.P., et al., *Activation of glycogen synthase kinase-3 inhibits protein phosphatase-2A and the underlying mechanisms.* Neurobiology of Aging, 2008. **29**(9): p. 1348-58.

204. Junttila, M.R., et al., *CIP2A inhibits PP2A in human malignancies.* Cell, 2007. **130**(1): p. 51-62.

205.   Laine, A., et al., *Senescence sensitivity of breast cancer cells is defined by positive feedback loop between CIP2A and E2F1.* Cancer Discovery, 2013. **3**(2): p. 182-97.

206.   Calvisi, D.F., et al., *Activation of the canonical Wnt/beta-catenin pathway confers growth advantages in c-Myc/E2F1 transgenic mouse model of liver cancer.* Journal of Hepatology, 2005. **42**(6): p. 842-9.

207.   Calvisi, D.F., et al., *Disruption of beta-catenin pathway or genomic instability define two distinct categories of liver cancer in transgenic mice.* Gastroenterology, 2004. **126**(5): p. 1374-86.

208.   Zhang, W., et al., *PR55 alpha, a regulatory subunit of PP2A, specifically regulates PP2A-mediated beta-catenin dephosphorylation.* Journal of Biological Chemistry, 2009. **284**(34): p. 22649-56.

209.   Li, X., et al., *Protein phosphatase 2A and its B56 regulatory subunit inhibit Wnt signaling in Xenopus.* EMBO Journal, 2001. **20**(15): p. 4122-31.

210.   Stevens, C., L. Smith, and N.B. La Thangue, *Chk2 activates E2F-1 in response to DNA damage.* Nature Cell Biology, 2003. **5**(5): p. 401-9.

211.   Willert, K., et al., *Wnt proteins are lipid-modified and can act as stem cell growth factors.* Nature, 2003. **423**(6938): p. 448-52.

212.   Staal, F.J., T.C. Luis, and M.M. Tiemessen, *WNT signalling in the immune system: WNT is spreading its wings.* Nature Reviews Immunology, 2008. **8**(8): p. 581-93.

213.   Lu, D., et al., *Activation of the Wnt signaling pathway in chronic lymphocytic leukemia.* Proceedings of the National Academy of Sciences of the United States of America, 2004. **101**(9): p. 3118-23.

214.   Xu, Q., et al., *Vascular development in the retina and inner ear: control by Norrin and Frizzled-4, a high-affinity ligand-receptor pair.* Cell, 2004. **116**(6): p. 883-95.

215.   MacDonald, B.T., K. Tamai, and X. He, *Wnt/beta-catenin signaling: components, mechanisms, and diseases.* Developmental Cell, 2009. **17**(1): p. 9-26.

216.   Kawano, Y. and R. Kypta, *Secreted antagonists of the Wnt signalling pathway.* Journal of Cell Science, 2003. **116**(Pt 13): p. 2627-34.

217.   Nam, J.S., et al., *Mouse cristin/R-spondin family proteins are novel ligands for the Frizzled 8 and LRP6 receptors and activate beta-catenin-dependent gene expression.* Journal of Biological Chemistry, 2006. **281**(19): p. 13247-57.

218.   Wei, Q., et al., *R-spondin1 is a high affinity ligand for LRP6 and induces LRP6 phosphorylation and beta-catenin signaling.* Journal of Biological Chemistry, 2007. **282**(21): p. 15903-11.

219.   Gwak, J., et al., *Small molecule-based disruption of the Axin/beta-catenin protein complex regulates mesenchymal stem cell differentiation.* Cell Research, 2012. **22**(1): p. 237-47.

220.   Rowan, A.J., et al., *APC mutations in sporadic colorectal tumors: A mutational "hotspot" and interdependence of the "two hits".* Proceedings of the National Academy of Sciences, 2000. **97**(7): p. 3352-3357.

221.   Segditsas, S. and I. Tomlinson, *Colorectal cancer and genetic alterations in the Wnt pathway.* Oncogene, 2006. **25**(57): p. 7531-7.

222.   van Es, J.H., N. Barker, and H. Clevers, *You Wnt some, you lose some: oncogenes in the Wnt signaling pathway.* Current opinion in genetics & development, 2003. **13**(1): p. 28-33.

223.   Schurch, C., et al., *CD27 signaling on chronic myelogenous leukemia stem cells activates Wnt target genes and promotes disease progression.* Journal of Clinical Investigation, 2012. **122**(2): p. 624-38.

224.   NCBI. *FZD7 frizzled class receptor 7 [Homo sapiens (human)]*. 2014 20/04/2014]; Available from: http://www.ncbi.nlm.nih.gov/gene/8324.

225.   Rousset, R., et al., *Naked cuticle targets dishevelled to antagonize Wnt signal transduction.* Genes and Development, 2001. **15**(6): p. 658-71.

226.   Van Raay, T.J., et al., *Naked1 antagonizes Wnt signaling by preventing nuclear accumulation of beta-catenin.* PLoS One, 2011. **6**(4): p. e18650.

227.   Angonin, D. and T.J. Van Raay, *Nkd1 functions as a passive antagonist of Wnt signaling.* PLoS One, 2013. **8**(8): p. e74666.

228.   Mendoza-Topaz, C., J. Mieszczanek, and M. Bienz, *The Adenomatous polyposis coli tumour suppressor is essential for Axin complex assembly and function and opposes Axin's interaction with Dishevelled.* Open Biology, 2011. **1**(3): p. 110013.

229.   Goss, K.H. and J. Groden, *Biology of the adenomatous polyposis coli tumor suppressor.* Journal of Clinical Oncology, 2000. **18**(9): p. 1967-79.

230.   *T-cell factors: turn-ons and turn-offs*, ed. A. Hurlstone and H. Clevers. Vol. 21. 2002. 2303-2311.

231.   Tiemessen, M.M., et al., *The nuclear effector of Wnt-signaling, Tcf1, functions as a T-cell-specific tumor suppressor for development of lymphomas.* PLoS Biology, 2012. **10**(11): p. e1001430.

232.   Yi, F., et al., *Opposing effects of Tcf3 and Tcf1 control Wnt stimulation of embryonic stem cell self-renewal.* Nature Cell Biology, 2011. **13**(7): p. 762-70.

233.   Slyper, M., et al., *Control of breast cancer growth and initiation by the stem cell-associated transcription factor TCF3.* Cancer Research, 2012. **72**(21): p. 5613-24.

234.   Gutierrez, A., Jr., et al., *LEF-1 is a prosurvival factor in chronic lymphocytic leukemia and is expressed in the preleukemic state of monoclonal B-cell lymphocytosis.* Blood, 2010. **116**(16): p. 2975-83.

235.   Piedra, J., et al., *Regulation of beta-catenin structure and activity by tyrosine phosphorylation.* Journal of Biological Chemistry, 2001. **276**(23): p. 20436-43.

236.   Hehlmann, R. and S. Saussele, *Treatment of chronic myeloid leukemia in blast crisis.* Haematologica, 2008. **93**(12): p. 1765-1769.

237.   Yeh, E., et al., *A signalling pathway controlling c-Myc degradation that impacts oncogenic transformation of human cells.* Nature Cell Biology, 2004. **6**(4): p. 308-18.

238.   King, B., et al., *The ubiquitin ligase FBXW7 modulates leukemia-initiating cell activity by regulating MYC stability.* Cell, 2013. **153**(7): p. 1552-66.

239.   Jeannet, G., et al., *Long-term, multilineage hematopoiesis occurs in the combined absence of beta-catenin and gamma-catenin.* Blood, 2008. **111**(1): p. 142-9.

240.   Cobas, M., et al., *Beta-catenin is dispensable for hematopoiesis and lymphopoiesis.* Journal of Experimental Medicine, 2004. **199**(2): p. 221-9.

241.   Fang, Y., et al., *CIP2A is overexpressed in human ovarian cancer and regulates cell proliferation and apoptosis.* Tumour Biology, 2012. **33**(6): p. 2299-306.

242.   Li, Q., et al., *Cloning of the rat beta-catenin gene (Ctnnb1) promoter and its functional analysis compared with the Catnb and CTNNB1 promoters.* Genomics, 2004. **83**(2): p. 231-42.

243.   Takahashi-Yanaga, F. and T. Sasaguri, *GSK-3beta regulates cyclin D1 expression: a new target for chemotherapy.* Cellular Signalling, 2008. **20**(4): p. 581-9.

244.   Coqueret, O., *Linking cyclins to transcriptional control.* Gene, 2002. **299**(1-2): p. 35-55.